



**Bournemouth
University**

**INTEGRATION OF A GENETIC OPTIMISATION ALGORITHM
IN A SIMULATION FRAMEWORK FOR OPTIMISING
FEMTOCELL NETWORKS**

Haseeb Ahmad Qureshi

Supervisory Team

Dr. David John

Dr. Simant Prakoonwit

The thesis is submitted in partial fulfilment of the requirements of Faculty of Science and Technology, Bournemouth University for the degree of Doctor of Philosophy

September 2021

Department of Computing and Informatics

Faculty of Science and Technology, Bournemouth University, UK

Copyright Statement

This copy of the thesis has been supplied on condition that anyone who consults it is understood to recognise that its copyright rests with its author and due acknowledgement must always be made of the use of any material contained in, or derived from, this thesis.

Abstract

The developments in mobile communication systems from 1G to 4G have increased demands on the network due to the increased number of devices and increasing volume of data and 5G is expected to significantly increase demands further. Therefore, networks need to be more efficient to deliver the expected increase in volume. An energy and cost efficient way to cope with such an anticipated increase in the demand of voice and data is the dense deployment of small cells i.e. femtocells. Femtocells are identified as a crucial way to the delivery of the increased demands for heterogeneous networks in which macrocells work in combination with femtocells to provide coverage to offices, homes and enterprise. A survey of the literature is conducted to examine the mechanisms and approaches different authors have used to optimise the network. One of the major activities in this project before the transfer was the identification of the parameters. The literature was analysed and key performance parameters were identified. Based on the identified key performance parameters, a simulation framework is used to perform the experiments and to analyse the performance of a two-tier LTE-A system having femtocell overlays. A comprehensive and easy to use graphical user interface has been set up with the desired two-tier network topologies. It estimates the throughput and path loss of all the femto and macro users for all the supported bandwidths of an LTE-A system using different modulation schemes. A series of tests are carried out using the described simulation framework for a range of scenarios. The modulation scheme that yield highest throughput for a femtocell user is identified, and path loss is found to be independent from the modulation scheme but is dependent on the distance from its base station. In another series of experiments, the effects that walls inside buildings have on connectivity are examined and positioning of the femtocells is changed for each scenario inside buildings to analyse the performance. These results are used to find the optimised location of femtocells in different room layouts of the building. The simulation framework is further developed to be able to optimise the whole femtocell network by finding the optimised positioning of femtocells using the genetic optimisation algorithm. The end user can provide the inputs of the desired network topology to the simulation framework through a graphical user interface. The throughput and path loss of all the femto users are calculated before and after optimisation. The simulation results are generated in the form of tables before and after optimisation for comparison and analysis. The layouts depicting the indoor environment of the building before and after optimisation can be seen and analysed through the graphical user interface developed as a part of this simulation framework. Two case studies are defined and described to test the capacity and capability of the developed simulation framework and to show how the simulation framework can be used to identify the optimum positions of the femtocells under different configurations of room designs and number of users that represent contrasting loads on the network. Any desired network topology can be created and analysed on the basis of throughput and path loss by using this simulation framework to optimise the femtocell networks in an indoor environment of the building. The results of the experiments are compared against the claims in other published research.

List of Publications

Journal Publication

1. Qureshi, H. A., John, D., and Prakoonwit, S., 2019. Performance analysis of LTE-A systems with femtocell overlays using different modulation techniques under different multipath fading. *International Journal of Soft Computing and Artificial Intelligence (IJSCAI)*, ISSN: 2321-404X, Volume-7, Issue-2, Nov-2019.

Poster Presentation

1. Qureshi, H. A., 2016. A Self Organising Network (SON) for 4G Mobile Communication System using Femto Cells. *The Faculty of Science and Technology's Second Annual PGR Conference*, Bournemouth University, United Kingdom, 18 May, 2016.

Table of Contents

Copyright Statement	II
Abstract	III
List of Publications	IV
Table of Contents.....	V
List of Figures	VIII
List of Tables	X
Acknowledgements	XI
Dedication	XII
Chapter 1: Introduction	1
1.1 Background.....	1
1.2 Aim of the Research	2
1.3 Objectives of the Research	2
1.4 Research Questions.....	2
1.5 Methodology of the Research.....	3
1.6 Contribution to Knowledge	3
1.7 Outline of the Thesis.....	4
Chapter 2: Literature Review	6
2.1 Evolution of Mobile Technology	6
2.2 Limitations of current mobile networks	10
2.3 Small Cells	12
2.4 Femtocells.....	13
2.4.1 Origin of Femtocells	15
2.4.2 Birth of Modern Femtocells	16
2.4.3 Femtocell Standardisation	17
2.4.4 Early Research on Femtocells	18
2.4.5 Modern Research on Femtocells	19
2.5 Summary	21
Chapter 3: Related Research Work.....	23

3.1 Two-Tier Architectures.....	23
3.2 Approaches used for Optimising Femtocell Networks	27
3.3 Selection of the Parameters to measure the performance of a Simulation Framework for Optimising Femtocell Networks	31
3.4 Summary	33
Chapter 4: Simulation Framework used to analyse the performance of LTE-A Systems with Femtocell Overlays	34
4.1 Requirements of the Simulation Framework	35
4.2 Numerical Modelling of the Simulation Framework.....	36
4.2.1 Path Loss Model.....	36
4.2.2 Throughput Computation	37
4.3 Architecture of the Simulation Framework	38
4.4 Implementation of the Simulation Framework	39
4.4.1 User Input Module	39
4.4.2 Path Loss Calculation Module	44
4.4.3 Capacity and Throughput Calculation Module	44
4.4.4 User Output Module	44
4.5 Simulation Results and Performance Analysis	48
4.5.1 Case Study 1	48
4.5.2 Case Study 2	51
4.5.3 Case Study 3	59
4.6 Conclusion	67
Chapter 5: Development of a Simulation Framework for Optimising Femtocell Networks	69
5.1 Genetic Algorithms (GAs)	69
5.2 Architecture of the Simulation Framework for Optimising Femtocell Networks.....	71
5.3 Simulation Results and Performance Analysis	77
5.3.1 Case Study 1	78
5.3.2 Case Study 2	96
5.4 Conclusion	115
Chapter 6: Conclusion of the Thesis	117

6.1 Summary of the findings of the Thesis	117
6.2 Comparison of the results with the Literature.....	120
6.3 Contribution to Knowledge	123
6.4 Limitations of the Work and Future Work.....	124
References.....	125
Appendix A.....	137
Appendix B	149

List of Figures

Figure 1: Outline of the PhD Thesis	5
Figure 2: Architecture of a basic mobile network (Gawas 2015).....	6
Figure 3: Wireless Standards Evolution, Roadmap to 5G (Soldani and Manzalini 2015)	10
Figure 4: Components of a heterogeneous network (dos Santos et al. 2020)	14
Figure 5: A Generic Femtocell (Ibrahim et al. 2019).....	14
Figure 6: Architecture of the simulation framework	39
Figure 7: User screen before inputs are fed in the GUI.....	41
Figure 8: User screen displaying the user defined network topology of buildings	42
Figure 9: User screen after inputs are fed in the GUI	43
Figure 10: User screen displaying simulation in progress.....	45
Figure 11: User screen displaying output after completion of simulation in the GUI	46
Figure 12: User screen displaying Coordinates and Unit Details of Femto User ID 1.....	47
Figure 13: Visual representation of the described scenario for Case Study 1.....	49
Figure 14: Throughput comparison of Femto U1 and Femto U2 for 64QAM, 16QAM and QPSK.....	52
Figure 15: Path Loss comparison of Femto U1 and Femto U2.....	53
Figure 16: Visual representation of the described scenario for Case Study 2.....	54
Figure 17: Throughput and Path Loss of the femto users with respect to the distance/0 wall....	57
Figure 18: Throughput and Path Loss of the femto users with respect to the distance/1 wall....	57
Figure 19: Throughput and Path Loss of the femto users with respect to the distance/2 walls ..	58
Figure 20: Throughput and Path Loss of the macro users with respect to the distance/2 walls ..	59
Figure 21: Throughput and Path Loss of the macro users with respect to the distance/4 walls ..	59
Figure 22: Visual representation of Scenario 1 for Case Study 3.....	60
Figure 23: Visual representation of Scenario 2 for Case Study 3.....	61
Figure 24: Visual representation of Scenario 3 for Case Study 3.....	62
Figure 25: Throughput of the femto Users with respect to the distance per number of walls for Scenario 1	63
Figure 26: Path Loss of the femto users with respect to the distance per number of walls Scenario 1	63
Figure 27: Throughput of the femto users with respect to the distance per number of walls for Scenario 2	64
Figure 28: Path Loss of the femto users with respect to the distance per number of walls for Scenario 2	65
Figure 29: Throughput of the femto users with respect to the distance per number of walls for Scenario 3	66

Figure 30: Path Loss of the femto users with respect to the distance per number of walls for Scenario 3	67
Figure 31: Flowchart of a genetic optimisation algorithm	70
Figure 32: Architecture of the simulation framework for optimising femtocell networks	76
Figure 33: User screen before inputs are fed in the Graphical User Interface	77
Figure 34: User screen once the inputs are fed in the Graphical User Interface for Case Study 1	78
Figure 35: Graphical User Interface displaying the indoor environment of the building before optimisation for Case Study 1	80
Figure 36: Layout of the building environment before optimisation for Case Study 1	81
Figure 37: Graphical User Interface showing the optimisation in progress for Case Study 1	84
Figure 38: Graphical User Interface showing the progress of optimisation in terms of Fitness value vs Generation for Case Study 1	85
Figure 39: Graphical User Interface displaying the output once the optimisation is terminated for Case Study 1	86
Figure 40: Layout of the building environment after optimisation for Case Study 1	87
Figure 41: Layout of the building environment before and after optimisation for Case Study 1	89
Figure 42: Throughput of the femto users before and after optimisation for Case Study 1	92
Figure 43: Path Loss of the femto users before and after optimisation for Case Study 1	94
Figure 44: Delta Throughput and Delta Path Loss of the femto users for Case Study 1	96
Figure 45: User screen once the inputs are fed in the Graphical User Interface for Case Study 2	97
Figure 46: Graphical User Interface displaying the indoor environment of the building before optimisation for Case Study 2	98
Figure 47: Layout of the building environment before optimisation for Case Study 2	99
Figure 48: Graphical User Interface showing the optimisation in progress for Case Study 2...102	
Figure 49: Graphical User Interface showing the progress of optimisation in terms of Fitness value vs Generation for Case Study 2	103
Figure 50: Graphical User Interface displaying the output once the optimisation is terminated for Case Study 2	104
Figure 51: Layout of the building environment after optimisation for Case Study 2	105
Figure 52: Layout of the building environment before and after optimisation for Case Study 2	107
Figure 53: Throughput of the femto users before and after optimisation for Case Study 2	111
Figure 54: Path Loss of the femto users before and after optimisation for Case Study 2	113
Figure 55: Delta Throughput and Delta Path Loss of the femto users for Case Study 2	115

List of Tables

Table 1: Classification of the Cells (Panwar et al. 2016)	12
Table 2: Comparison of Wi-Fi vs Picocell vs Femtocell.....	15
Table 3: Literature review of optimised femtocell networks	27
Table 4: Characteristics of different formats of QAM (Voudoukis 2017)	40
Table 5: Parameters of simulation framework for Case Study 1.....	49
Table 6: User inputs of simulation framework for Case Study 1	50
Table 7: Throughput and Path Loss of Femto Users 1 and 2 (Femto U1 and U2).....	51
Table 8: Parameters of simulation framework for Case Study 2.....	55
Table 9: User inputs of simulation framework for Case Study 2	55
Table 10: Throughput and Path Loss of the femto users with respect to the distance/number of walls	55
Table 11: Throughput and Path Loss of the macro users with respect to Distance/Number of Walls	58
Table 12: Parameters of simulation framework for Case Study 3.....	62
Table 13: User inputs of simulation framework for Case Study 3	62
Table 14: Throughput and Path Loss of the femto users with respect to the distance per number of walls for Scenario 1	63
Table 15: Throughput and Path Loss of the femto users with respect to the distance per number of walls for Scenario 2	64
Table 16: Throughput and Path Loss of the femto users with respect to the distance per number of walls for Scenario 3	66
Table 17: Throughput and Path Loss of the femto users with respect to their distance per number of walls before optimisation for Case Study 1	82
Table 18: Throughput and Path Loss of the femto users with respect to their distance per number of walls after optimisation for Case Study 1.....	88
Table 19: Throughput and Path Loss of the femto users before and after optimisation for Case Study 1.....	90
Table 20: Delta Throughput and Delta Path Loss of the femto users for Case Study 1.....	95
Table 21: Throughput and Path Loss of the femto users with respect to their distance per number of walls before optimisation for Case Study 2.....	100
Table 22: Throughput and Path Loss of the femto users with respect to their distance per number of walls after optimisation for Case Study 2.....	106
Table 23: Throughput and Path Loss of the femto users before and after optimisation for Case Study 2.....	109
Table 24: Delta Throughput and Delta Path Loss of the femto users for Case Study 2.....	114

Acknowledgements

I would like to thank ALLAH Almighty, the most merciful and compassionate, for the wisdom he bestowed upon me, the strength, peace of my mind and good health in order to finish this thesis.

I would like to extend my sincere gratitude to my respected supervisors, Dr. David John and Dr. Simant Prakoonwit for mentoring me. I am very thankful to them for their invaluable guidance and extreme patience they have shown throughout my research.

I would also like to thank my parents and family specially my brother Dr. Faisal Fayyaz Qureshi and cousin Abdul Rehman Chishti for their selfless support and motivating me to always aim high and work hard.

Last but not the least I appreciate the help of my friends and colleagues who contributed with their continuous support and encouragement.

Dedication

*This thesis is dedicated to my beloved father **Hafiz Fayyaz Ahmed Qureshi** and beloved mother **Razia Shehnaz Noor Chishti***

Chapter 1: Introduction

1.1 Background

This research is focused on examining the use and role of femtocells for analysing the network performance of a Long Term Evolution-Advanced (LTE-A) two-tier system and to identify how performance of the network having femtocells can be improved and optimised. There is a significant change in the mobile wireless technology in terms of reliable connectivity and fast data transmission with the advent of the fourth generation of mobile phone technology (4G) network in mobile communication system. 1G provided only voice calls. 2G, 2.5G and 2.75G have provided the voice and data services. 3G, 3.5G and 3.75G have allowed to make video calls in addition to data and voice services. 4G enables the users to enjoy services such as graphically intensive online gaming, streaming high definition videos, HDTV (high definition television) etc., in addition to voice, data and video calling facilities. The data rate has significantly increased from 64 Kbps in 2G GSM to 2 Mbps in 3G UMTS and 50 to 100 Mbps in 4G LTE as discussed in Chapter 2. A sudden upsurge in the usage of wireless network has been witnessed over the past few years. It has been estimated that in the coming 15-20 years the volume of the mobile data traffic will increase to 1000 times than the present volume (Chih-Lin 2021). A wide scale research and development is happening in the field of mobile networks to cope with the demands of such a large number of mobile users. The challenge is to achieve high data rates for the increased traffic.

The femtocells are launched in the present LTE 4G network. Femtocells are low power, less cost, short range and minimal effort cellular Base Stations (BSs) which are installed by consumers. They provide indoor as well as outdoor coverage (Wang et al. 2012). The advantages of deployment of femtocells are efficient spectrum use and high data rates (Wang and Zhang 2014a; Omar et al. 2021), energy saving (Ge et al. 2014b; Al-Khafaji and Majdi 2018), money saving (ElSawy et al. 2013; Bhushan et al. 2014a; Ravichandran et al. 2017), plug and play (Zhou et al. 2014; Alnoman et al. 2019), less congestion to a Main Base Station (MBS) (ElSawy et al. 2013) and easy handover (Bhushan et al. 2014a). They provide clear voice clarity and fast response data services. Femtocells increase the network capacity, for e.g., the materials used in the construction of large buildings resist wireless network signal access, however, femtocells can be placed within these locations (inside these buildings) to provide excellent coverage and signal reception. Femtocells are unique as they are largely deployed by private enterprises or customers in an ad hoc way without any requirement of radio frequency planning (Adi and Kitagawa 2019), maintenance and deployment by the operator, and site selection. These features enable the femtocells to support the plug and play functioning, with network adaptation and automatic configuration (Andrews et al. 2012). There are few drawbacks of

using femtocells, which include cost of operation and initial cost to infrastructure etc. (Panwar et al. 2016).

The substantial growth in the wireless communication networks results in a heterogeneous network with large macrocells in combination with small cells working together to provide the network coverage (Kazi and Wainer 2017; Malini and Babu 2017; Lai and Liu 2018). It allows the service providers to extend coverage indoors and achieve high capacity gain. It also helps to offload the data and reduce traffic on expensive macrocell networks (Bouras et al. 2012).

1.2 Aim of the Research

The aim of this research is to optimise femtocell networks for indoor communication. A simulation framework will be used and further developed to be able to optimise the femtocell networks by finding the optimised positioning of the femtocells using an optimisation algorithm on the basis of a unique mix of parameters to enhance the performance of existing networks.

1.3 Objectives of the Research

The objectives of the research are classified as:

- To review the literature of mobile standards, their related technologies and limitations
- To review the literature of femtocells including its origin and development over time
- To review the literature of algorithms and parameters for optimising femtocell networks
- To evaluate the existing algorithms and parameters for optimising femtocell networks
- To develop and integrate the algorithms to be able to optimise the femtocell networks for indoor communication
- To use and further develop a simulation framework to implement the algorithms developed for optimising femtocell networks
- To test the capacity and capability of the developed simulation framework for optimising femtocell networks

1.4 Research Questions

The research questions needed to be addressed are:

- How can a femtocell network be optimised?
- Can an optimised femtocell network improve the performance of existing networks?
- Can a simulation framework be developed to optimise the network of femtocells for indoor communication?
- How the results of the scenarios simulated for the developed simulation framework have improved on the performance of existing networks?

1.5 Methodology of the Research

The two main research methods identified in the literature are: Qualitative and Quantitative (Bryman 2017). Qualitative method of research includes Case Study, Phenomenology and Generic Qualitative Inquiry. Primary Data Collection and Secondary Data Analysis constitutes the Quantitative method of research. The method of research is informed by the research questions. According to Gartner (Iliashenko and Borremans 2015), it is no longer about how much information you have, it is about having the right insight. Based on this saying and the methodology best suited to find the solutions of the research questions identified above, this thesis methodology will follow the Case Study approach of Qualitative method of research as it is the most common approach for studying work environments. This research involves the use of multiple sources of data including journals, documents etc. Hence, the thesis methodology will be carried out as follows:

- The first step is to read the previously published works including research, projects and case studies from both academia and industries concerning cellular networks and femtocells, surveys and both proposed and deployed solutions
- The second step is to understand how important femtocells are in the upcoming mobile technology and what aspects of the femtocells need to be discussed and addressed to be able to improve the performance of mobile cellular networks. It also includes the review and evaluation of the existing algorithms and methodologies of femtocell networks focusing on a particular aspect identified in the literature
- The third step is to design and develop a simulation framework based on the previous research. The focus will only be on a certain proposed solution where the functionality of the simulation framework will be examined in order to discover its drawbacks. Then there will be an attempt to improve and refine the simulation framework. At this point, the project will concentrate on a certain level of the interoperability. The genetic optimisation algorithm used in this research will be defined in Chapter 5 and will also be examined to enable the simulation framework to find the optimal location of femtocells
- The fourth step is to test the capacity and capability of the simulation framework to be able to achieve the desired outcome of this research. The purpose is to slowly examine the outcome of different stages and gradually build up a workable framework to give the appropriate insight on how to implement the technique
- Finally, summarise the findings to complete the thesis writing

1.6 Contribution to Knowledge

The contributions to knowledge of the research are:

- The identification of the parameters most commonly used in published research to investigate the performance of a two-tier LTE-A system
- The development of a simulation framework with a graphical user interface that can be used to identify the optimised positioning of femtocells
- The analysis of results of series of case studies that used the simulation framework to identify the optimum positions of the femtocells under different configurations of room designs and contrasting loads on the network

1.7 Outline of the Thesis

This thesis is structured according to the Figure 1:

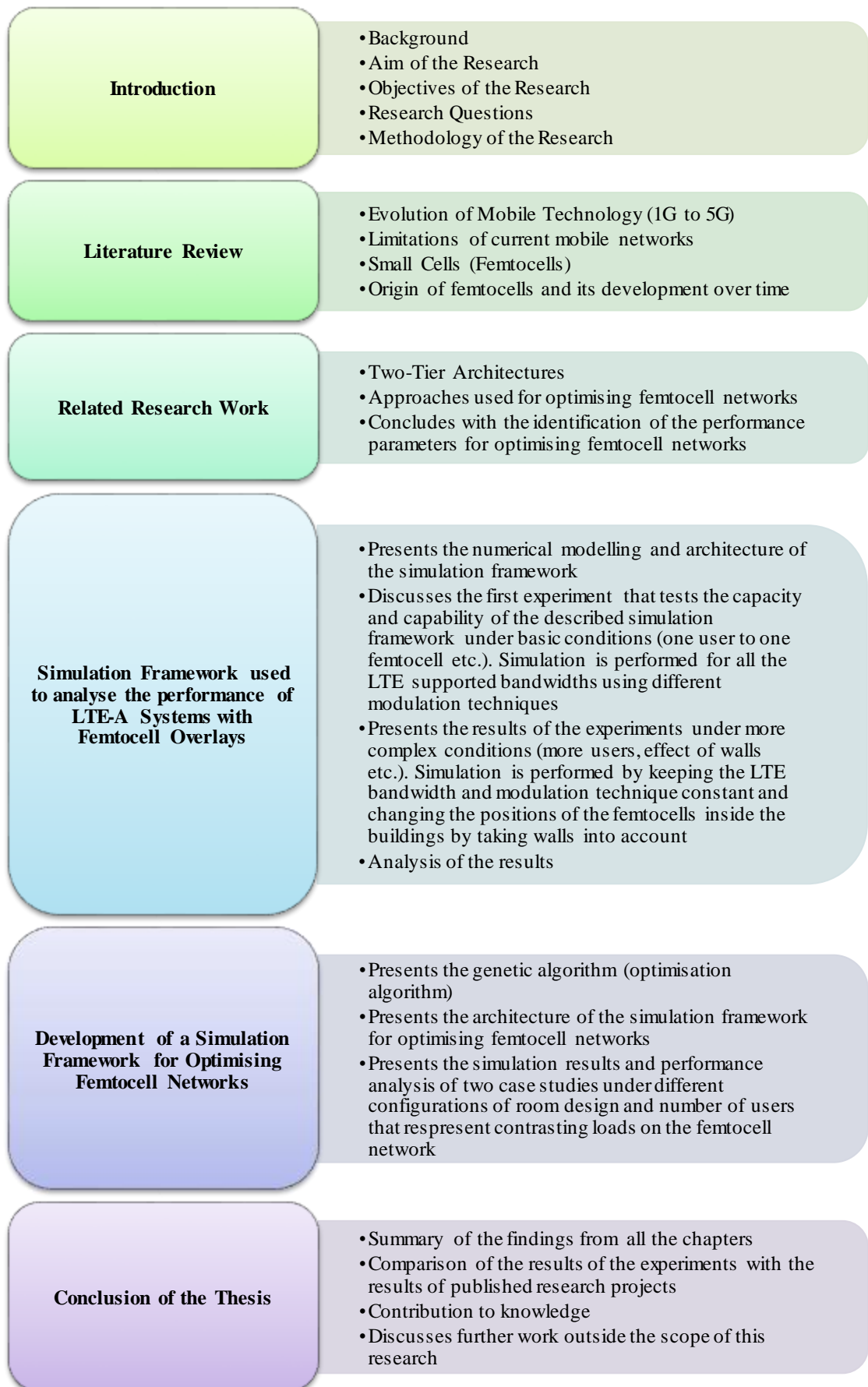


Figure 1: Outline of the PhD Thesis

Chapter 2: Literature Review

In order to achieve the research goals identified in Chapter 1, the areas that need to be researched are described in this Chapter 2. This chapter starts with an overview of the technical details and evolution of cellular mobile networks from 1G to 5G. This chapter then discusses the limitations of current mobile cellular networks in terms of coping up the demands of such a large number of users. It concludes with the role of small cells particularly femtocells as a potential solution to achieve high data rates for increased traffic.

2.1 Evolution of Mobile Technology

The mobile communication system keeps changing and evolving over the years according to the needs and requirements of the users across the world. Mobile networks are made up of a number of components including base stations, antennas and wireless access points. A mobile phone base station provides network coverage to a wide geographic area which is separated into a number of cells. To reduce black spots, each cell must fit closely together to form a continuous mobile network (Mahmoud et al. 2021). A network of antennas is needed to provide coverage for mobile services. The range of mobile base station is set according to the number of users subscribed in that area. When a user attempts to make a phone call, the user's mobile phone sends and receives signals called Radio Frequency (RF) signals (Adi and Kitagawa 2019). These radio signals are received by the antenna of the nearest base station which then forwards the signals to its respective exchange known as Mobile Telephone Switching Office (MTSO) (Sitorus et al. 2017). The MTSO consists of a Mobile Switching Centre (MSC) for routing mobile phone calls. This MSC then connects the call to its destination either through a mobile phone or a fixed line. The architecture of a basic mobile network is depicted in Figure 2.

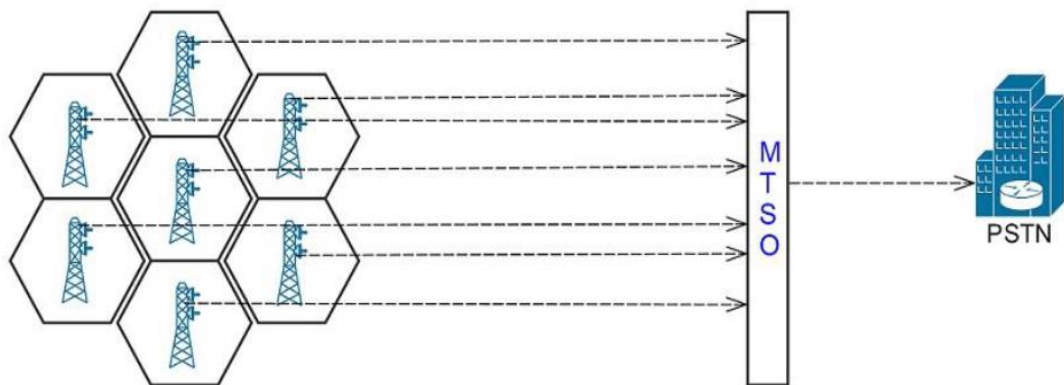


Figure 2: Architecture of a basic mobile network (Gawas 2015)

As mobile phone users change their physical locations, their connections need to change from one cell to another. MSC ensures that while moving from one cell to another, mobile phones

keep the connection with the network. The process of transferring of call by the network from one base station to another while moving is called handover (Saeed 2019). The caller is unaware of it and the handover is seamless. In order to provide good quality reception, the base stations need to be located in the close proximity of the mobile phone users. The coverage can be boosted outdoors via wireless access points in the streets by using small cell antennas or inside buildings using femtocells (as discussed in Section 2.4). A mobile cellular system acts as a duplex radio because two transmitters use different frequencies so both the mobile users are able to communicate at the same time (Liptak and Eren 2016). The evolution of mobile technology over the years has made more types of communication possible (e.g., voice, data, video etc.) which has attracted an increasing number of users. This has led to an exponential rise in demand for data and voice services. Therefore, there is a need for further network growth and evolution (Nguyen 2018; Chih-Lin 2021; Lal et al. 2021). The evolution of mobile networks is described in the following section.

The first cellular mobile network called the first generation (1G) was launched in 1979 and it was made operational in Japan by Nippon Telephone and Telegraph (NTT) (Valanarasu and Christy 2019). America then launched the cellular network called the Advanced Mobile Phone System (AMPS) approximately 2 years after that (Arshad et al. 2019). The technologies used to communicate 1G were Advanced Mobile Telephone System (AMTS), Mobile Telephone System (MTS), Push to Talk (PTT), Total Access Communications System (TACS) and Improved Mobile Telephone System (IMTS) etc. (Goyal et al. 2019). The main features of 1G were:

- It used analog radio signals for mobile calls using handsets
- It only provided analog voice services with no data services
- The sound quality was poor
- Large phone handset sizes
- Poor battery life for the handsets
- Frequent call drops
- Less secured (no encryption)
- Limited capacity
- Poor handover reliability
- It provided data rate up to 2.4 Kbps
- It used the circuit switching technology
- Frequency Division Multiple Access (FDMA) was used as a traffic multiplexer (Xu et al. 2017; Goyal et al. 2019).

The features of 1G such as poor service and limited capabilities were not able to provide adequate network service to the users. There was a need for improvements, and therefore, in 1991, the second generation, known as 2G, was launched in Finland to overcome some limitations of 1G, i.e., it provided the Short Messaging Service (SMS), enhanced privacy (comparatively secured), improved voice clarity and it made life healthier by omitting the radio power from handsets. 2G standard was based on the Global System for Mobile communication (GSM). GSM was the first digital cellular phone system. Time Division Multiple Access (TDMA) was used as a traffic multiplexer (Faruque 2019). 2G was not able to support complex data like video requiring high data rates. The speed could be up to 64 Kbps (Bulbul et al. 2017; Singh et al. 2017; Çakmak and Albayrak 2018; Kaur et al. 2020). The General Packet Radio Service (GPRS) was an intermediate technology between 2nd and 3rd generation of mobile technology. GPRS was able to support Multimedia Messaging Service (MMS) and Wireless Application Protocol (WAP). GPRS was the prime step in the development of 2G GSM networks towards 3G. 2.75G was the significant breakthrough prior to the evolution of 3G. The progress of GPRS towards Enhanced Data for GSM Evolution (EDGE) technology was the primary contribution of 2.75G (Dahiya 2017).

The 3rd generation cellular systems 3G were introduced in 2004-05 on the basis of International Telecommunication Union (ITU) standards. It provides services like real time multi-player gaming, video conferencing support, enhanced video and audio streaming, web browsing at a higher speed, IP TV support, Global Positioning System (GPS) etc. (Hegarty 2017). CDMA was the basic foundation of 3G. 3G satisfies the standards of International Mobile Telecommunication - 2000 (IMT - 2000) known as CDMA2000. The typical form of 3G known as Universal Mobile Telecommunications System (UMTS) uses Wideband Code Division Multiple Access (WCDMA) (SREELEKHA et al. 2017; Sivaganesan 2019). It can use data and audio services simultaneously and offers fast data rates of up to 2 Mbps in the local coverage areas and 144 Kbps to 384 Kbps in the wide coverage areas. 3.5G was the enhancement of the 3G UMTS technology. It has improved system capacity and introduced many new features like backward compatibility with 3G, fast scheduling, fast cell search, Adaptive Modulation and Coding (AMC) (Wang et al. 2020) and advance receiver design. HSPA improves and extends the working and performance of existing WCDMA protocols. It is an amalgamation of 2 mobile protocols, i.e., the High Speed Downlink Packet Access (HSDPA/3.5G) and the High Speed Uplink Packet Access (HSUPA/3.75G). It was evolved into High Speed Packet Access (HSPA+), that enabled data rates from 14.4 Mbps to 64 Mbps (Rathore 2020).

4G Long Term Evolution (LTE) is the 4th generation of cellular mobile networks. It is the standardisation of the 3rd Generation Partnership Project (3GPP). Numerous factors like Quality of Service (QoS), Operational Expenditure (OPEX) and less Capital Expenditure (CAPEX) has

led to the standardisation of LTE in order to cope the exponentially increasing demand of speed and data (Agiwal et al. 2021). The key features of LTE are as follows:

- Reduced delays on latency
- Increase in user data rates of up to 100 Mbps
- For even provision of services, increase in cell edge bit rate
- Improvement in spectral efficiency as a result of decrease in cost per bit
- A simpler and better network architecture
- Easy to access in terms of mobility
- The range of cell is increased to 5 km and the number of active users in a cell is 200
- Less power consumption by a mobile device (Verdugo et al. 2021)
- Multiple Input and Multi Output (MIMO) antennas are used in LTE communication system (Sivaraj and Mohapatra 2017)
- LTE can operate at the flexible bandwidths of 20, 15, 10, 5, 3 and 1.4 MHz
- Exponential increase in data rate. LTE provides peak rate of 100 Mbps for Downlink (DL) while peak rate of 50 Mbps for Uplink (UL) in 20 MHz channels
- The coverage radius of LTE provides excellent coverage up to 5 km. There is a slight degradation in performance from 5 km - 30 km and it can provide support for operation up until 100 km according to the standards set out for LTE (Agiwal et al. 2021)

The International Telecommunication Union - Radio Communication Sector (ITU - R) in 2008 has specified the International Mobile Telecommunications - Advanced (IMT - A) requirements for 4G standards. It sets the peak speed requirement of 100 Mbps for communication with high mobility like trains, cars etc. and 1 Gbps for communication with low mobility like pedestrians, stationary users etc. 4G is an entirely packet switched network. It has converged data and voice over Internet Protocol (IP). It provides facilities like IP telephony, HD mobile TV, ultra-broadband internet access, gaming services and streaming of multimedia services at a lower cost. MIMO replaced CDMA spread spectrum radio technology called Orthogonal Frequency Division Multiple Access (OFDMA) (Arshad et al. 2019; Goyal et al. 2019; Patra and Sharma 2020).

5G is being consolidated internationally and have features like providing 10's Mbps guaranteed with high reliability and availability, 1000 times more traffic volume and devices will have long battery life and low complexity. 1 Gbps will be achievable in extremely densely populated areas (Arshad et al. 2019; Alquhali et al. 2020). Many research groups have been working on 5G standards. Some of the key research groups working for 5G such as Mobile and wireless communications Enablers for the Twenty-twenty Information Society (METIS), 5G Infrastructure Public Private Partnership (5G - PPP), 5th Generation Non-Orthogonal

Waveforms (5GNOW), Enhanced Multicarrier technology for Professional Ad-Hoc and Cell-Based Communications (EMPhAtiC), Network of Excellence in Wireless Communications (NEWCOM), NYU WIRELESS, 5G Innovation Centre (5GIC), Electronics and Telecommunications Research Institute (ETRI), 5Gforum, 4G – Americas, other research groups such as TROPIC, MCN, MOTO, COMBO and PHYLAWS, several industries such as DOCOMO, Alcatel-Lucent, GSMA Intelligence, Nokia Siemens Networks, Huawei, Qualcomm, Samsung and Vodafone, and their achievements are mentioned in (Mitra and Agrawal 2015; Panwar et al. 2016; Verma 2018; Goyal and Sahoo 2019; Kaur et al. 2020). Figure 3 outlines the evolution of wireless technology from 1983 projected to 2041.

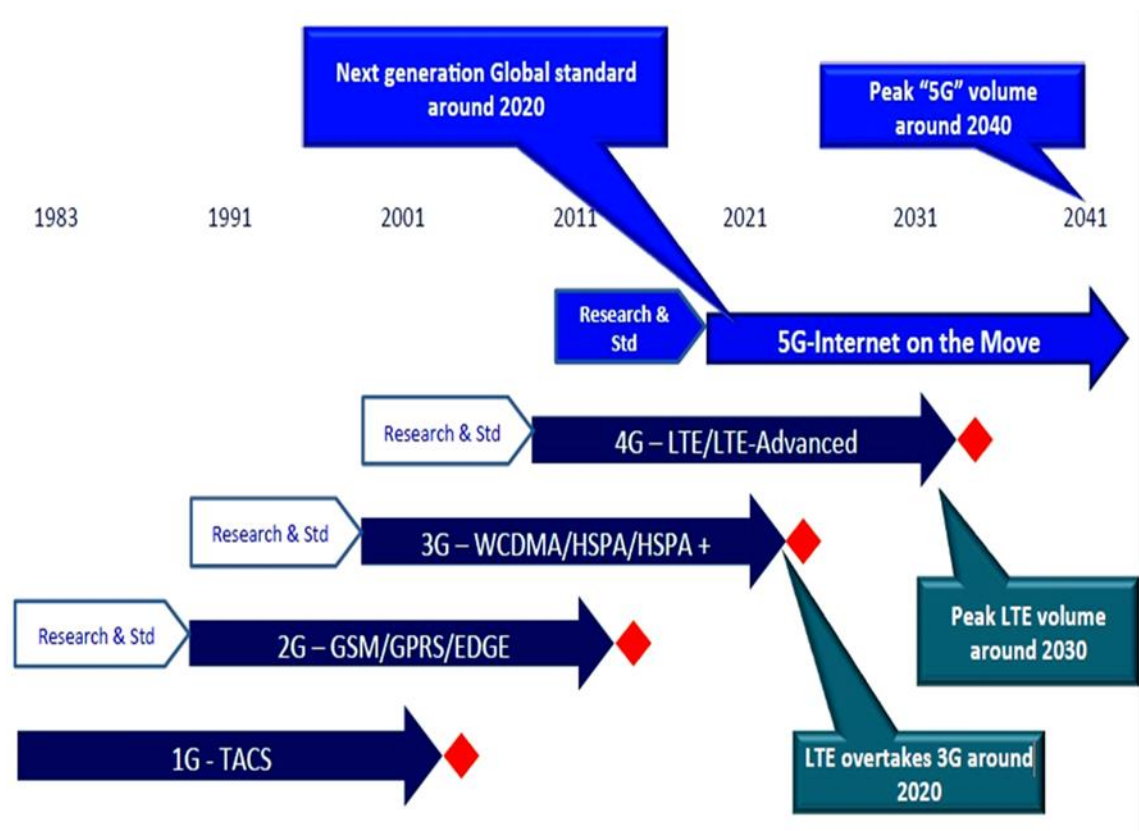


Figure 3: Wireless Standards Evolution, Roadmap to 5G (Soldani and Manzalini 2015)

2.2 Limitations of current mobile networks

Mobility, reliability and usability are the fundamental characteristics of mobile communication systems which make them more preferable to users. A tremendous rise is recorded in the number of users with the development of new technologies and recent advancements in communication. According to the Cisco Annual Internet Report (2018-2023) White Paper (Cisco 2020), almost 67% of the global population will have internet access by 2023. The total number of internet users are projected to increase from 3.9 billion in 2018 to 5.3 billion by 2023 (Cisco 2020). More resources are needed to provide communication services to such an expected increase in traffic and it will be a challenge for the existing communication systems.

Mobile systems require a suitable mechanism to cope with such a large volume of data and to manage complex systems. The installation, maintenance and operation of additional picocells, microcells and macrocells will result in heavy operational and capital expenditures (Jiang et al. 2017; Nguyen et al. 2017; Dhifallah et al. 2018). Therefore, it is imperative for mobile networks to provide seamless compatibility to meet the exponential rising demand of real-time traffic with dense heterogeneous networks, consequently providing smooth connectivity of the network to the end users (Gran et al. 2017; Williams 2018; Bojadzievski et al. 2020).

There has been a significant increase in the types and number of electronic devices and smart phones in the last decade. In addition, there has been a substantial rise in the usage of mobile devices to access the internet for activities such as browsing (websites, emails, web applications, social networking sites like Facebook, Twitter etc.), applications (Skype etc.), live streaming (BBC, CNN, live football, cricket and other games and news channels like Aljazeera etc.), VoIP, video and audio streaming, real time medical applications etc. that require internet connectivity with high speed. The number of Mobile to Mobile (M2M) connections, smart phones and tablets are expected to show a prominent increase over the next years (Goudar et al. 2017; Cisco 2020). Internet access, growing demand in the network traffic and availability of smart devices at affordable prices are the primary reasons for the popularity of 4G LTE networks.

According to the Ericsson Mobility Report of August 2015, there was a 55% growth in mobile data traffic between 2014 and 2015. 53 million new mobile users have subscribed globally in the Quarter 2 (Q2) in 2015 and the mobile broadband subscriptions have exceeded 3 billion in Q2 of 2015. According to the Ericsson Mobility Report of November 2016, there are 84 million new mobile subscriptions globally in Quarter 3 (Q3) of 2016 reaching a total of 5.1 billion subscribers globally. Ericsson predicted that by the end of 2022, 5G subscriptions will reach 550 million (Ericsson 2016). According to the latest Ericsson Mobility Report of November 2019, there are 61 million new subscribers during the quarter making the total number of mobile subscriptions around 8 billion in Quarter 3 (Q3) of 2019 (Jonsson et al. 2019). According to Cisco (2020), the mobile data traffic grew 17-fold from 2012 to 2017. There was a 71% increase in mobile data traffic in 2017 and it is expected to grow 46% from 2017 to 2022 reaching 77.5 Exabytes per month by 2022 (Cisco 2020). The Cisco and Ericsson forecasts and statistics are very alarming for the network service operators to accommodate the mobile users in the future. Therefore, researchers and service providers have to set their goals to meet the demands and fulfil users' requirements.

2.3 Small Cells

Small cells are characterised as low power access points for mobile phones. They operate in licensed spectrum. Small cells provide enhanced applications and capacity for enterprises and homes, and in addition to remote and metropolitan areas. Small cells include Microcells, Picocells and Femtocells (Panwar et al. 2016). The major mobile operators in the world such as AT & T (in US), Vodafone (in UK), DoCoMo (in Japan) and China Mobile are adopting the small cell's architecture to reduce the overall load on the macrocells and to increase the throughput of the network. The number of small cells is expected to exceed 70 million in 2025 and the number of 5G small cell deployments are expected to reach 5.2 million and consequently contribute to 62% of the network traffic in 2025 (Cisco 2020). Table 1 compares the characteristics of the large and small cells:

Table 1: Classification of the Cells (Panwar et al. 2016)

Cells	Range	Users
Macrocell	30 - 35 km	Many
Microcell	2 km	> 100
Picocell	200 m	20 - 40
Femtocell	10 – 20 m	A few users

Femtocells are more under the control of customers as compared to picocells. Femtocells are mainly used for private closed networks in homes and offices. Picocells are more appropriate for public networks as they are managed and controlled by the operator. Small cells are deployed because of the benefits they provide to the users and service providers. They are:

- **Coverage:** Small cells as compared to the Main Base Station (MBS, i.e., Macrocell) provides far better coverage within the homes in addition to the cost benefits of using the same number for both mobile and home applications (Panwar et al. 2016)
- **Efficient spectrum use and high data rate:** Since the Small Base Station (SBS, i.e., Femtocell) is located very close to the mobile devices, it provides much better indoor coverage and good signal reception which results in higher data rates. Since fewer mobile devices are in direct communication with the MBS due to the addition of small cells, it also increases the spectrum efficiency of the network (Wang and Zhang 2014a; Alnoman and Anpalagan 2017; Omar et al. 2021)
- **Energy saving:** The short distance between the users and small cells reduces the energy consumption of the mobile network and user equipments by not involving main base stations and the users are able to communicate at a much shorter distance with low signaling overhead (Ge et al. 2014b; Al-Khafaji and Majdi 2018)
- **Cost benefits:** Installation of a small base station is quite economical as it does not involve any cumbersome planning in comparison to a main base station, and its operational management cost is far less in contrast to the cost associated with a main base

station (ElSawy et al. 2013; Bhushan et al. 2014a; An et al. 2017; Ravichandran et al. 2017)

- **Plug-and-Play:** Since femtocells are auto configured and can be placed anywhere in the house, the usefulness of small cells enhance the on demand network capacity (Zhou et al. 2017; Bagwari et al. 2018; Alnoman et al. 2019)
- **Less congestion to a MBS:** Small cells offload mobile users from a main base station. As a result, main base station is less congested and lightly loaded. Hence, the system capacity is improved (ElSawy et al. 2013)
- **Easy handover:** Small cells provide an attractive solution for mobile users by decreasing their handover time overheads as a mobile small cell has the capability to do the handover on behalf of all related mobile devices by not involving MBS (Bhushan et al. 2014a)
- **Trade-off:** There are few realistic issues associated with the small cells like operational reliability and implementation cost along with the prominent benefits described above. The installation of small cells does impose an initial cost to the infrastructure but quite less than the budget associated with a main base station. In addition to that, a frequent authentication is required because of recurring handover operations (Panwar et al. 2016)

There is a substantial growth in the wireless communication networks. This results in a heterogeneous network in which large macrocells work together in combination with the small cells to provide network coverage. Some of the solutions mentioned below are proposed to satisfy the rapidly increasing user requirements (Kazi and Wainer 2017; Malini and Babu 2017; Lai and Liu 2018):

- Purchase of extra spectrum for the current network which will be very expensive
- Deployment of more macrocells for the existing networks which will increase capital expenditure cost
- Installation of small cells for the existing networks to reduce the burden on macrocells

Therefore, the deployment of small cells for the current mobile networks can provide the best possible solution to meet the future traffic demands for heterogeneous networks. Figure 4 shows the components of a heterogeneous network in which macrocells, femtocells and relays etc. can work in combination to provide coverage to homes, offices and enterprise.

2.4 Femtocells

A femtocell is an access point designed to support communication of mobile devices (i.e. phones, tablets etc.) that improves coverage and cellular reception within a home or inside an office building. Femtocell is a mobile phone base station for homes/offices and connects via broadband internet connection. Femtocell looks similar to a wireless router, 190 mm (h) x 150 mm (w) approx., see Figure 5. Femtocells can be installed by customers anywhere in their

homes or offices. A femtocell is inherently auto configured as no radio planning or frequency channel selection is required for it.

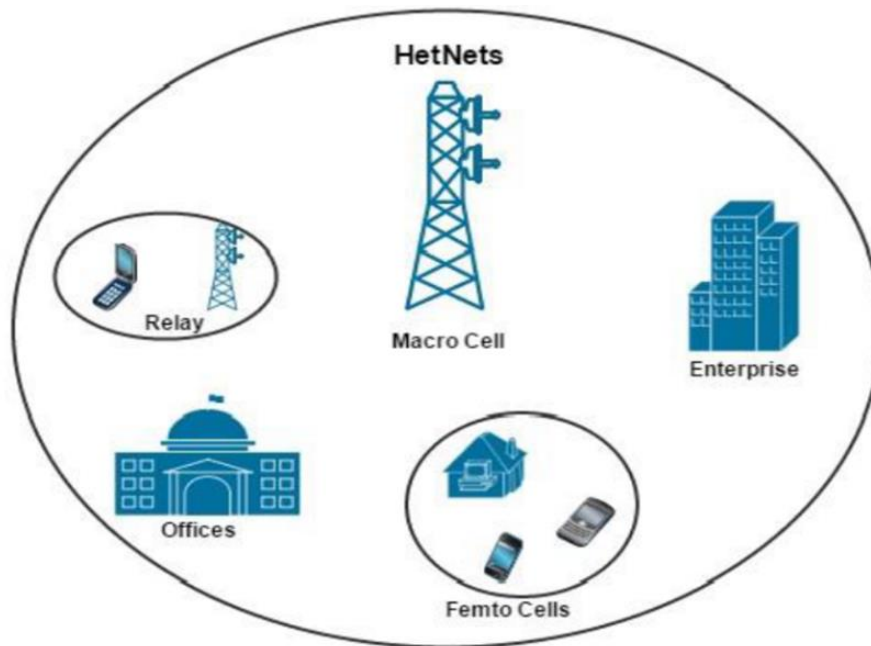


Figure 4: Components of a heterogeneous network (dos Santos et al. 2020)



Figure 5: A Generic Femtocell (Ibrahim et al. 2019)

Femtocells are inexpensive and low power small base stations. The femtocell does require a connection with the mobile network operator for backhaul. This can be achieved via a fixed or fibre optic cable line or a twisted pair telephone line. It enables the femtocell to interact with the operator's MBS and allow them to coordinate and perform operations such as handover between them. Femtocells are normally consumer deployed but unlike Wi-Fi they operate using the femtocell's provider own licensed spectrum. Since the femtocell operates on the same licensed frequency band allocated to the macrocell using the same overhead channels, it appears as a

normal traditional base station to a macrocell. Femtocells were initially intended to provide better signal reception inside homes as a result of poor coverage faced by many subscribers when they switched to different service providers, but are now considered as the potential cost-effective way of offloading the data and to ease the burden from the macrocells (Abbas and Hameed 2018; Ibrahim et al. 2018; Rehman and Safdar 2018). Table 2 provides the comparison of the properties of Wi-Fi, Picocell and Femtocell.

Table 2: Comparison of Wi-Fi vs Picocell vs Femtocell

	Wi-Fi	Picocell	Femtocell
Electricity Bill	customer	operator	customer
Installation	customer	operator	customer
Site Rental	customer	operator	customer
Macrocell Interaction	not applicable	yes	yes
Backhaul Connection	via customer	dedicated	via customer
Radio Planning	no (local)	yes (prior and global)	no
Handover	vertical	yes	possible
Access Rights	closed	public	mainly closed
Transmission Power	< 23 dBm	23 – 30 dBm	20 dBm

2.4.1 Origin of Femtocells

The idea of small cells was first discussed more than 3 decades ago in (Stocker 1984). At first, the term ‘small cells’ was used to describe the cell size in a metropolitan area, where a macrocell having diameter in kilometres would be split into a number of small cells. Today, these small cells with reduced transmit power are called metropolitan microcells or macrocells having radius of several hundred meters. Cellular repeaters called boosters were investigated simultaneously as a substitute of small base stations in (Drucker 1988). The purpose of these re-radiating boosters was to improve the quality of signals in areas of poor coverage. The aim was to reduce the cost as wireline backhaul was not required for these repeaters but the drawback of reusing the licensed spectrum did not achieve the desired throughput. In addition, these devices were not simple to deploy. Hence, these boosters did not help to improve the system capacity.

The predecessor of the picocells with cell sizes from a range of tens to around one hundred meters began to appear in the 1990s (Iyer et al. 1990). The situations where macrocell was overloaded or where the signals of macrocell were unable to provide a reliable connection, these traditional small cells were used to fill in the coverage and capacity gaps. Since they worked as a small version of the main base stations, therefore, these types of small cells required management, planning and network interfaces. In the early 90’s, an infamous industry project was led by Panasonic and Southwest Bell which was quite similar to the modern concept of today’s femtocells. They used wired backhaul, PSTN or T1, for the development of an indoor femtocell like solution and had re used the same spectrum as of macrocells (Brickhouse and Rappaport 1996). However, due to the lack of ubiquitous IP backhaul at that time, the level of integration failed to achieve the critical point where a base station possibly be accurately

miniaturised. They were technically ahead of other small cell technologies of that time but was not economically successful because the deployment and operational cost of a large number of small cells outweighed the benefits they offered at that time.

2.4.2 Birth of Modern Femtocells

The cost and operational aspects of small cell deployments were addressed in (Ho 2003; Claussen et al. 2006). These ideas proved successful in case of residential femtocells where cost issues were quite significant. The femtocells are fundamentally different from traditional small cells in their need to be self-adaptive and more autonomous. The backhaul interface of the femtocell which connects it back to the cellular network is IP based. Therefore, it supports higher latency and lower rate as compared to the standard X2 interface which connects picocells to the macrocell. It consequently allows the use of new network infrastructure along with femtocell gateways to serve and appropriately route the traffic.

The explosion of mobile data led to the development of a new cellular architecture with much higher capacity and is described in (Roth et al. 2010). The feasible way to meet such an unprecedented demand in speed and data is to decrease the cell size and consequently re use the spatial frequency (Dohler et al. 2011), unless the inexpensive frequencies available in tens of GHz could be harnessed for mobile broadband which is exceedingly challenging (Pi and Khan 2011). Societal trends and several technological aspects have also made femtocells feasible in addition to the escalating demands of data. The inherently IP based femtocell backhaul and the evolution of 4G mobile networks to OFDMA is a much better platform for femtocell overlays than 3G CDMA as it is predominantly a circuit switched technology. A fully functional femtocell communicating using the identical signalling protocols, the similar techniques and same frequencies as the main base stations and affordable around £100 range is foreseeable.

The small cell technology from cell splitting ideas presented in (Stocker 1984) has made remarkable advancements over the years. A significant increase in the number of publications in the IEEE database of the articles related to the femtocells has shown that small cells have been a hot topic for the researchers. For e.g., there were only 3 publications on the topics of femtocells in 2007 which had increased to 116 in 2010. The European Union also involved in funding femtocell projects, for example, ICT-4-248523 BeFEMTO project worked on the development and analysis of LTE and LTE-A compliant femtocell technologies (Andrews et al. 2012). In recent times, the auto configuration of the femtocell and its capacity to be optimised has enabled the end users to deploy small cells in a plug and play manner thereby integrating them into operational macro cellular networks. This proved to be a major step forward in the large-scale deployment of femtocells.

The successful commercial deployments of femtocells have been seen over the years. Spring Nextel initiated the deployment of femtocells in 2008 followed by Verizon and AT & T in 2009 and 2010 respectively in US. Vodafone was the first company in Europe to start deploying femtocells in 2009 in UK followed by other countries. In Asia, China Unicom, NTT DoCoMo and Softbank mobile were the companies to initiate femtocell services in 2009. Softbank in Japan, Vodafone in Europe, and Verizon, Sprint and AT & T in the United States have developed femtocells (Wang and Zhang 2014b). Big companies like Huawei, Alcatel-Lucent and Nokia Siemens Networks are also involved in developing plug-and-play small base stations (Ni et al. 2014; Mao et al. 2017).

2.4.3 Femtocell Standardisation

Femtocells are not only characterised by high throughput and short communication range, but they are also able to seamlessly coordinate with the traditional main base stations at all layers of network stack and perform operations like interference management, handovers, authentication and billing. Therefore, it was imperative for appropriate standard bodies to contribute to the development of femtocells.

Femto Forum, a non-profit organisation, established in 2007, contributed the most in promoting and enabling the femtocells and its technology worldwide in the early years. It had more than 70 providers of femtocell technology including software vendors, telecommunication hardware, mobile operators, start-ups and content providers. It had a significant impact on several standardisation bodies including 3rd Generation Partnership Project (3GPP) and European Telecommunications Standards Institute (ETSI) (Andrews et al. 2012). It played a major role in the development of a policy framework that derived and encouraged the standardisation of fundamental and technological aspects of the femtocells worldwide. Its two main contributing areas are: a) regulation, standardisation and interoperability; and b) promotion and marketing of femtocell solutions to analysts, journalists, regulators, standard bodies, special interest groups and across the industry. Femtocells fit into 3G CDMA and 4G LTE based networks as follows: Three main embodiments of UMTS brought forward by 3GPP and CDMA2000 brought forward by 3GPP2 have same frameworks and are based on CDMA. The performance of CDMA networks has a very limited dependence on power control. Since they use the identical band, the ‘near far effect’ causes the overwhelming of received power of farther users by nearby users without appropriate centralised power control. Such an accurate centralised power control is not possible to execute with femtocells as simultaneous equalisation of received power levels cannot be achieved at different points in space, for example, the transmit power level of an uplink macrocell mobile user may disable a large number of femtocells operating in the same band. In such circumstances, an addition of a few CDMA femtocells has profound effect as proved theoretically in (Chandrasekhar and Andrews 2009b).

The focus of 3GPP is now on LTE (3GPP Release 8 onwards) and LTE-A technologies (3GPP Release 10 onwards). The Media Access Control (MAC) and physical layer impact of femtocells on Worldwide Interoperability for Microwave Access (WiMAX) and LTE are somewhat alike because of their MAC and physical layer designs and both are based on OFDMA (Kim et al. 2009). The smooth integration of femtocells into LTE and LTE-A networks is very important and therefore is addressed by authors in (Solanki and Rafiq 2015). The femtocells can be assigned orthogonal resources, because of the attributes of OFDMA technology, to nearby macrocells and picocells. Theoretically, a complex network wide optimisation can be performed in which femtocells claim only the resources they need, and consequently macrocell avoids using those frequency and time slots (Arunabha et al. 2010). The drawback of this technique is that a significant amount of coordination is required for its execution. A compromise is discussed in (Boudreau et al. 2009) in which frequency or time resources can be assigned semi statically to edge, interior or small cell users with power control on top to reduce the throughput discrepancies in each of the scenarios, else, a semi static partition could be used between macrocells and femtocells. The simulated results of (Chandrasekhar and Andrews 2009a) indicated that most resources went to the macrocell, although femtocells were densely deployed, as little number of resources blocks was needed by each femtocell to provide high throughput to its users.

2.4.4 Early Research on Femtocells

H. Claussen and co-authors at Bell Labs in UK presented the early simulation results on femtocells in their work in (Claussen 2007; Ho and Claussen 2007; Claussen 2008). Their work was further extended to multiple antennas and optimisation techniques in (Claussen et al. 2008b; Claussen and Pivit 2009). Chandrasekhar and Andrews in the early work on femtocells introduced new mathematical models and analysis specifically focused on the uplink interference issue in Code Division Multiple Access based networks with closed access in (Chandrasekhar and Andrews 2007, 2009b). The approach and model used in their previous work was adapted later for downlink and with multiple antennas in (Chandrasekhar et al. 2009). The other early works related to the femtocells proposed an adaptive control access method to mitigate the problem of cross tier interference in (Choi et al. 2008) which was further addressed in (Lopez-Perez et al. 2009; Xia et al. 2010).

Das and Ramaswamy in (Das and Ramaswamy 2008; Ramaswamy and Das 2009) explored the reverse link capacity of the femtocells and modelled the inter cell interference as a Gaussian random variable. The model investigated by Das and Ramaswamy had compatibility issues with the current cellular networks. Regarding interference optimisation, the authors in (Schroder et al. 2009) explored the user assisted approaches. The authors introduced the techniques for interference management on High Speed Packet Access (HSPA) in (Yavuz et al. 2009) for both

uplink and downlink operation of femtocells. The authors in (Wang et al. 2010) extended the previous work and improved the optimisation of Wideband Code Division Multiple Access (WCDMA) femtocell networks by developing new analytical techniques. Other research works have contributed towards interference coordination including interference management (Garcia et al. 2009), co channel interference (Sahin et al. 2009) and strategies to avoid interference (Lopez-Perez et al. 2009) in OFDMA based networks. Access control and mobility management for femtocells was investigated in (Golaup et al. 2009; Joshi et al. 2009; Simeone et al. 2009) where access control was proved as an effective technique to avoid interference.

The standard bodies of 3GPP have focused on Self Organising Network (SON) characteristics in (Ahmad 2011; Network 2011a; Network 2011b; Ramiro and Hamied 2011) and defined procedures for authentication and automatic registration of femtocells, neighbour discovery, cell ID selection, provisioning and management, synchronisation and network optimisation. A considerable research has been carried out on power adjustment, automatic channel selection and frequency assignment for coverage optimisation and autonomous interference coordination. A number of algorithms are proposed in (Feng and Seidel 2008; López-Pérez et al. 2009a) for such problems formulated as mathematical optimisation problems. The two articles are particularly focused on adaptive interference coordination. (Cheung et al. 2012) is aimed at power control while (Garcia et al. 2012) is related to adaptive carrier selection. Since femtocells are mostly deployed in an unplanned manner, specifically in enterprise settings, placement of femtocells can be optimised for coverage and interference and is discussed in (Liu et al. 2012). The femtocell technology has built over time on the basis of this initial research and contributions.

2.4.5 Modern Research on Femtocells

The manner in which femtocells are deployed in an environment is very crucial and important. Therefore, in the recent research on femtocells, the authors in (Amine and Sylia 2017) proposed the mathematical model to optimise the positioning of femtocells in enterprise buildings. A Genetic Algorithm (GA) was used to address the problem of the placement of femtocells by maximising the indoor coverage while balancing the traffic load. The case study was defined and the proposed optimisation technique was able to improve the performance of network by 13.6% in terms of positioning of femtocells and providing the maximum coverage within the building as compared to the random placement of femtocells. Likewise, an efficient optimisation technique based on the genetic algorithm is applied on a large selection of sample buildings under various conditions for the joint optimisation of average downlink throughput and outage probability in (Badra and Figueras 2018). A set of applicable guidelines for the optimal deployment of femtocells is obtained as a result of this dual method technique focused on the indoor deployment of femtocells as part of the LTE-A heterogeneous network. The plan

to deploy the femtocells using cluster techniques is presented in (Ibrahim et al. 2018). The hierarchical agglomerative original algorithms were modified by taking into account the path loss influenced by various obstructions such as doors, windows and different types of walls to address the issue of indoor coverage. The simulated results have shown that the proposed algorithm is able to minimise the cost by maximising SINR and reducing the number of femtocells deployed in an indoor environment. To find the minimum number of femtocells required and their locations to achieve the full coverage in the building is a complicated issue. To address this, a novel approach on the placement of femtocells using genetic algorithm is described in (Nassiri and Borujeni 2020). The locations of the femtocells are computed on the basis that the number of handovers is minimal inside the commercial buildings. The concept of considering the assumptions and limitations to carry out the process of optimisation for this PhD work (as described in Section 5.2 of Chapter 5) is taken from (Nassiri and Borujeni 2020). The experimental results of (Nassiri and Borujeni 2020) have indicated the reduction in the number of handovers up to 30% with almost complete coverage.

The authors in (Deb et al. 2017) have discussed the different path loss computational models for indoor environment covered by femtocells. A comparative analysis was carried out and the performance of the path loss models (Cost 231 Model, WINNER II Model, Multi wall and Floor Model and ITU-R P Model) was analysed using vector signal analyser and vector signal generator. A case study was performed to illustrate how the most suitable model can be selected for an indoor scenario depending on the building structure, floor types, frequency range and wall types. To predict the number of femtocells required for successful deployment is described in (Alotaibi and Angelides 2017). The new deployment plan specified to provide coverage for indoor environment to determine the locations of the femtocells was based on factors such as measuring the path loss, predicting the received power from the femtocell and macrocell and estimating the coverage radii of the femtocells. In this research, to provide enhanced quality of service, the number of femtocells required was predicted on the basis of two factors: the femtocell access point radius in the target area and the area size. The indoor deployment plan described in this research outperformed its equivalent outdoor plan. Thus, femtocells are able to provide much higher high data rates in an indoor environment of the building. The authors in (Chen et al. 2020) have developed a tractable three-dimensional indoor multi story small cell network model in which small cells are distributed by using a 2D homogeneous Poisson point process on each story of the building. The results have shown that a higher penetration loss leads to a higher spectral efficiency and a higher coverage probability and certain values of base station density and story height should be avoided for better wireless indoor coverage.

All of the above works are mostly aimed at optimising the network in some way but none of the above have developed a simulation framework to optimise the network of femtocells to the best

of author's knowledge. This also forms the basis of this research project. The singularities of femtocells such as their unplanned deployment, short range and restricted number of users that a femtocell can accommodate etc., characteristics of an indoor environment such as multipath reflections, number of people etc., and the effect of walls pose different challenges. Such an environment demands the development of mechanisms for femtocell networks instead of using the same techniques to manage macrocell networks. Therefore, optimising the network of femtocells is desirable. The launch of femtocells for LTE and LTE-A 4G networks can be considered as the potential way to manage the complex heterogeneous mobile networks of 5G as shown in the above research projects. A number of papers mentioned above have shown improvements in network performance by optimising the location of femtocells that establishes this is a suitable area to research. The research conducted for this thesis will follow a similar approach. Femtocells can bridge the gap from operations, administration and maintenance to optimised networks. It has the potential to manage the demand of such a large number of users for future networks. It will increase the overall efficiency of networks thereby achieving high data rates and supporting the ever-increasing traffic. To develop a simulation framework to be able to find the optimised location of femtocells in an indoor environment by using an optimisation algorithm in order to optimise the whole femtocell network using a unique choice of parameters to analyse the performance will be a novel contribution. The plan to identify unique mix of parameters based on an analysis of related projects will be presented in the next Chapter 3.

2.5 Summary

The advancements in the mobile communication systems from 1G to 5G have been discussed in this chapter. 2G was the first digital mobile communication network planned for better coverage. 3G was planned for voice considering data and some multimedia. 4G truly constitutes mobile broadband allowing voice, data and video access wirelessly possible anywhere. To reduce the burden on main base stations due to the substantial increase in the number of users, small cells including femtocells have been introduced in the hierarchy of networks to provide coverage to homes, offices and metropolitan areas in a cost and energy efficient way. The literature review establishes that research into femtocells is an active research area and provides insights about the range of research activities involving femtocells. Femtocells operate in the licensed spectrum and act as a main base stations to the users they are connected. Femtocells are identified as a crucial way to the delivery of the increased demands. The history of femtocells is also discussed in this chapter including its origin and development over time. This chapter provides insights about the range of research activities involving femtocells and illustrates how femtocells fit in with the development of mobile networks. The research and recent advancements have shown that femtocells can manage the expected demand of real time traffic

with dense heterogeneous networks and enable the end users to experience uninterrupted connectivity to the network. This chapter gives some background and reviews literature that suggests optimising the location of femtocells will improve the efficiency of mobile networks. A survey of the literature is conducted in the next Chapter 3 to examine the parameters different authors have used to optimise the network.

Chapter 3: Related Research Work

Chapter 2 discussed the background to current mobile cellular networks and development of femtocells over time. This chapter focuses on the activities of researchers who are investigating areas related to the research questions for this research project. This chapter provides an inclusive discussion on the architectures, systems and methodologies followed by the other researchers described in the literature for cellular networks involving femtocells. A survey of the literature is conducted to examine the parameters different authors have used to optimise the network. Based on the survey, the key parameters are selected for the development of a proposed simulation framework and the methodology to be followed for conducting experiments are established. This chapter emphasises the architectures and networks proposed in the literature for small cell networks. To meet the research aim stated in Chapter 1, a simulation framework needs to be built to test the effect of changes in specific parameters. This review identifies the important parameters used by the other researchers in the literature. The choice of parameters for own simulation framework is made based on the analysis of the findings presented in this chapter. The simulation framework needs to be able to find the optimised positioning of the femtocells. Therefore, it is focused on the optimisation methods used in the networks involving femtocells and different approaches used in the optimisation of the femtocell indoor networks.

3.1 Two-Tier Architectures

The architectures where a main base station operates at the top tier while the small base stations operate under the supervisor of the main base station in the lower tier are referred to as two-tier architectures. A number of two-tier architectures have been discussed and proposed in the literature. A macrocell covers all types of small cells, e.g., microcells, picocells and femtocells (as shown in Table 1 of Section 2.3 of Chapter 2). Both the tiers share the same frequency bands. All small cells enhance the services, capacity and coverage of a macrocell. Cognitive Radio Network (CRN) based communication and Device-to-Device (D2D) communication can enhance two-tier architectures to multi-tier architectures (Panwar et al. 2016).

Femtocells can work with macrocell by using the same or different frequencies. However, the deployment of many femtocells within a macrocell overlay introduces new challenges in terms of efficient system operation and interference management thereby limiting system capacity. The initial research on femtocell networks while operating with macrocell was focused on the studies related to interference behaviour. The results of system level simulation are presented in (Claussen 2007) for possible uplink and downlink throughputs for both femtocells and macrocell at any location of the scenario. Different scenarios of femtocells deployment density are considered in this simulation. Key requirements are discussed for co channel operation of

femtocells, that is, auto configuration and public access. Femtocells, shown as circles, are randomly deployed within the coverage area and have reused the same frequency as the macrocells in hierarchical cell structure. Macrocells are shown as squares. The coverage area follows the hexagonal pattern. Hence, it is important to represent femtocells and macrocells by circles of different colours and sizes so that they can be easily distinguished from each other while deploying them in the coverage area. The co channel deployment of femtocells was achieved in this paper with a minor impact on the throughput of the macrocell. This resulted in a higher spectral efficiency per area because of efficient frequency reuse. (Guvenc et al. 2008) has described the interference in co-existing femtocell and macrocell networks, and provided simulation results for hybrid and co-channel frequency assignments. For picocells and microcells, due to their larger transmission powers and large cell sizes, co channel operation is not feasible resulting in severe interference issues. In case of femtocells, due to their low transmission powers, interference from femtocells to the macrocell closer to the cell edge is still limited that facilitates the working of femtocells and macrocell together as a two-tier architecture. The practicality of the propagation model is limited as it is not always feasible to know the exact number of walls between a femtocell and main base station. Furthermore, these simulation results are based on the standards prior to the 4G LTE-A. The utility based non-cooperative femtocell Signal to Interference Noise Ratio (SINR) adaptation is presented in several works such as (Altman et al. 2006). This work is associated to the existing literature on game theory related to non-cooperative cellular power control. The adaptation compels stronger femtocell interference to achieve their SINR equilibria closer to their minimum SINR targets, whereas femtocells creating trivial cross tier interference achieve higher SINR margins. This scheme is similar to Utility Based Power Control (UBPC) technique presented in (Xiao et al. 2001) in which users based on prevailing traffic conditions varied their target SINRs. The UBPC overcame the divergence problem and was flexible in achieving adaptiveness and fairness using different price coefficient settings and parameters.

Wang et al. (2014) has proposed a method for distinguishing between outdoor and indoor users with the help of a mobile small cell on a bus or a train. A main base station holds large antenna arrays for separating outdoor and indoor users with some antenna elements spread around the macrocell that are linked to the main base station using optical fibres. A small base station and large antenna arrays are installed in every building to communicate with the main base station. All the users inside a building can be connected with other users either through the small base station or by using mm wave, Wi-Fi or Visible Light Communication (VLC). Hence, the separation of outdoor and indoor users results in a less load on a main base station. (Wang et al. 2014) also proposed to utilise a mobile small cell that is installed inside a vehicle so that the internal mobile users can communicate with each other, whereas the large antenna arrays

located outside the vehicle can communicate with a main base station. In this way, all the internal users of a building or vehicle can act as a single unit to their corresponding main base station, and consequently, the small base station acts as a main base station to all these users. It improves the performance of the network by reducing the load on the main base station.

With respect to network densification, (Bhushan et al. 2014b) has deployed a two-tier architecture that is an amalgamation of a spectral aggregation (by using frequency bands higher than 3GHz) and spatial densification (by increasing the density of base stations, and also increasing the number of antennas per user and main base station). A trade-off between the coverage area of small cells and the transmission power of a macrocell is discussed in (Bhushan et al. 2014b). If a macrocell has a high transmission power, then a substantial number of users in the proximity of a small cell can find themselves in the coverage area of the macrocell, and consequently, it will decrease the coverage area of that small cell. If a macrocell has a low transmission power, then the small cell will have more coverage area accordingly. Hence, a cell range expansion, that is a biased handover towards small cells, is executed to accommodate more users by small cells to which they are closer. Furthermore, small base stations, installed in homes or offices, can be utilised to give services to outdoor users, such as low mobility vehicles and pedestrians, in their neighbourhoods, and this process is called indoor to outdoor user service (Bhushan et al. 2014b).

(Hossain et al. 2014) proposed a multi-tier architecture comprised of various types of small cells, D2D communication and relays to serve the users with discrete requirements of Quality of Service (QoS) in energy and spectrum efficient manners. In all of these architectures, it has been considered that the users spontaneously discover a small base station. A qualitative comparison and survey of the existing power control schemes and cell association was provided to illustrate their limitations to counter interference issues in current networks. It was suggested that objectives for future research should base on maximising system throughput while balancing traffic load for high priority users subject to a minimum SINR. (Zhang et al. 2015b) in their work has presented a centralised architecture in which key procedures were designed including synchronisation, small cell access and identification, small cell sleeping and handover. The simulations were carried out on the link and system level platform which was built according to the current 3GPP LTE standard. In this system, a main base station helps the users to connect to particular small base stations. As a result, the interference between users and small base stations is reduced. The simulation results showed the significant improvement in performance with the implementation of on-off strategy over the current networks. The results demonstrated the improvement in throughput by 17% with 90% gain in energy efficiency. This methodology, however, overburdens the main base station.

Two architectures presented by (Ge et al. 2014a) depend on the wireless Point to Multipoint (PTMP) approach. The first architecture is based on the centralised approach. In this architecture, all small base stations send their data to a main base station using mm wave. The received data is eventually aggregated and then forwarded to the core network by using fibre. The second architecture is based on the distributed approach. In this architecture, all small cells cooperatively forward their data by using mm wave to a specified small base station that eventually transfers the data without the explicit participation of a main base station to the core network using fibre. This article is focused on achieving high throughput for wireless backhaul networks. Two typical scenarios of small cells were configured and analysed to compare the energy efficiency of the networks. The radius of the small cell was taken as 50 m while coverage radius of the macrocell was considered as 500 m. The urban environment was considered for path loss. Numerical results implied that the distributed approach had higher energy efficiency as compared to the centralised approach.

(Ni et al. 2014) in their architecture have presented an adaptive backhaul approach. It is based on the wireless Point to Point (PTP) methodology and frequency division duplex for uplink and downlink channels. A tree like structure is proposed in this architecture in which the root node is associated with the core network by using fibre, the leaf nodes denote users while the other nodes are represented as small base stations. Data is transferred to the root node by the leaf nodes and the same data is transferred to the core network. According to the interference conditions, current bandwidth requirements and the network topology, for backhaul links, the bandwidth is dynamically selected. (Bhushan et al. 2014b) also used the similar approach in their work. (Wang and Zhang 2014b) have used three approaches namely centralised approach, distributed approach and hybrid or local cooperative approach in their contribution on three different densely deployed architectures presented in their work. These self-healing multi-tier architectures can automatically detect and recover a failed cell due to unexpected software or hardware failures in two steps: outage detection and compensation. The hybrid or local cooperative approach proved to be the most preferable solution for self-healing femtocell networks. The outage detection technique minimised the communication overhead by utilising the distributed trigger mechanism. It achieved the high detection accuracy by exploiting the spatial and temporal correlations in RSS measurements of the users.

The works described above demonstrate experimental results on the basis of theoretical models. The above authors created their theoretical models to show a wide variation in their approaches which makes direct comparisons of their results difficult. This leads to assertion that a user-friendly simulation framework would be beneficial for evaluating the two-tier model networks. Therefore, a simulation framework of a custom integrated macrocell and femtocells LTE-A network topology will be used for this research. The input parameters will be provided by the

user as in most cases of the works described above. The design of the simulation framework for optimising femtocell networks will be based on an analysis of the survey of literature in the following section to establish what approach to take and identify the parameters to use.

3.2 Approaches used for Optimising Femtocell Networks

A literature review on approaches used in the optimisation of femtocell networks is summarised in Table 3. A survey of the literature is conducted to examine the parameters different authors have used to optimise the network. Table 3 focuses on the parameters used to analyse the performance of the optimised femtocell networks in indoor environments. The parameters to be used in the simulation framework will be based on the analysis of this table in the next section.

Table 3: Literature review of optimised femtocell networks

Authors and Year	Research Objective and Methodology	Performance Parameters	Models, Protocols and Algorithms	Major Findings
(Claussen et al. 2008a)	<p>The proposed scheme optimised the current configuration formulated on statistics and measurements collected over time.</p> <p>Information on the number of mobility events and their time are gathered and utilised for additional refinement of the coverage.</p>	Femtocell Transmit Power and Coverage	<p>Propagation models for path loss, shadow fading and antenna gain for the macrocell sectors are used.</p> <p>An indoor user mobility model is used.</p> <p>The performance is analysed using system level simulations.</p>	The re-deployment of femtocells to a better location results in improved coverage.
(Hoydis et al. 2011)	<p>Macrocell base stations are unsuccessful in providing high data rate coverage to indoor environments and crowded metropolitan hotspots.</p> <p>Small cell networks are required to be reconfigured to be able to provide high data rate coverage according to the actual traffic situation using an energy follows load principle.</p>	Throughput and SINR	<p>Distributed resource allocation algorithms and protocols are developed.</p> <p>Ergodic mutual information versus the transmit signal to noise ratio is computed by Monte Carlo simulations and deterministic approximations.</p>	A novel and radically different small cell networks are designed to provide an energy and cost-efficient solution to cope with the forecast traffic growth.
(Hoadley and Maveddat 2012)	A wide scale deployment of femtocells is necessary to support the required capacity and offloading the traffic where small cells and macrocells work together to form heterogeneous networks.	Throughput and Latency	MIMO antenna technology is used.	A flexible deployment of small cells with associated Non-Line of Sight (NLOS) wireless backhaul has increased overall access capacity, eliminated coverage holes and increased

				subcarrier satisfaction.
(Liu et al. 2012)	<p>The issue of jointly optimising the placement of femtocell base station and power control in commercial building environments is addressed.</p> <p>Extensive numerical studies are conducted to demonstrate the efficiency of the algorithm.</p>	Femtocell Transmit Power and Path Loss	<p>A mathematical model with ability to capture the unique features of building (building size, structure, layout and floor/wall separation) is proposed.</p> <p>An effective global optimisation algorithm is suggested on the basis of convex relaxation of the formulated Mix Integer Convex Program (MICP) within a branch and bound framework.</p>	<p>The optimisation approach and proposed model has addressed the issues related to the deployment of femtocells in commercial buildings and resulted in prolong battery lives of mobile headsets.</p>
(Cheung et al. 2012)	<p>The effect of spectrum allocation is investigated in two-tier networks where the femtocells can operate in either closed or open access while the macrocells employ closed access policy.</p>	Throughput and Interference	<p>The probability of success for each tier under femtocell access policies and different spectrum allocation is derived by introducing a tractable model.</p>	<p>The optimised joint sub channel allocation has provided the highest possible throughput for all femtocell densities with open access femtocells.</p> <p>The optimised joint and disjoint sub channel allocations have provided the highest throughput in dense and sparse femtocell networks with closed access femtocells.</p>
(López-Pérez et al. 2009b)	<p>The femtocell is able to dynamically sense the air interface in an innovative manner and tune its sub channel allocation to enhance the system capacity and reduce the inter cell interference.</p> <p>A good solution for the frequency assignment problem is provided.</p>	Interference	<p>Mathematical optimisation problems are formulated.</p> <p>The proposed technique made use of either measurements reported by the users or messages broadcast by femtocells.</p>	<p>The results recommend to use the measurement reports i.e. the information collected at the user position when devising the algorithms for tuning the femtocell parameters.</p>

<p>(Wang et al. 2016)</p>	<p>The highly dense deployment of femtocells in an urban environment can result in serious inter femtocell interference.</p> <p>A distributed power optimisation technique is proposed for the downlink operation of dense femtocell networks.</p>	<p>Throughput and Femtocell Transmit Power</p>	<p>A unique convex pricing technique is proposed to price the transmit power of femtocells.</p> <p>A non-cooperative game framework is established based on the exact potential game theory which is demonstrated to converge to a novel and pure Nash equilibrium.</p> <p>An effective power optimisation algorithm combined with the firefly algorithm is finally presented with guaranteed convergence to obtain the Nash equilibrium of the presented game.</p>	<p>The simulation results have shown that the proposed game having mechanism of convex pricing increases the throughput of femtocell network by 7% and reduces the average transmit power of femtocells by 50%.</p>
<p>(Tsiropoulou et al. 2015)</p>	<p>A unique utility-based game framework is presented for a multi service two tier open access femtocell networks in which uplink transmission rate and power is simultaneously allocated to users.</p>	<p>Transmission Power and Transmission Data Rate</p>	<p>The uniqueness and existence of Utility-based uplink Power and Rate Allocation game in Multi-Service two-tier Femtocell networks (UPRA-MSF) games' Nash equilibrium with respect to both uplink transmission power and rate is analytically shown.</p> <p>A distributed algorithm is presented towards achieving the corresponding equilibrium point and its convergence is proven.</p>	<p>The operational effectiveness of the presented framework is evaluated through comparative simulation and modelling.</p> <p>The decision-making process and control intelligence lie at the macro and femto users in an automatic manner.</p>
<p>(Zhang et al. 2015a)</p>	<p>The femtocell base stations should have automatic parameter tuning, cognitive position awareness and learning abilities because of random positioning of the users.</p> <p>A unique joint dynamic power allocation and antenna pattern selection technique using the artificial neural network is presented.</p>	<p>Path Loss</p>	<p>A dynamic power allocation scheme for femtocell base station is analysed and designed by considering the path loss and different wall penetration conditions.</p> <p>Position awareness is employed for intelligent coverage optimisation.</p>	<p>The performance results demonstrate the accuracy and effectiveness of the presented coverage scheme for randomly deployed femtocell networks.</p>

				The optimal coverage radius of femtocell base station in centre, midpoint and corner positions is derived.
(Zhang et al. 2016)	A resilient optimised heterogeneous network is presented comprising of small cells in case of attacks, accidents and natural disasters.	Coverage and Handover	Coverage and Capacity Optimisation. Mobility Robustness Optimisation.	The simulation results have shown that the optimisation networking is an efficient tool to handle the deployment of additional small cells in disaster communication networks.
(Akinlabi and Joseph 2016)	The gains of deployment of femtocells and how femtocells can optimise the total capacity of the mobile network in areas of poor reception is presented.	Throughput, SINR and Bit Error Rate (BER)	MATLAB is used as a model of operation by the system to analyse the signal behaviour of femtocell in comparison to macrocell in indoor environment.	The results have demonstrated that the deployment of femtocells has resulted in better throughput, improved signal strength, lower bit error rate and improved voice calling over macrocell in an indoor environment.
(Aguilar-Garcia et al. 2016b)	The concept of context awareness is incorporated to optimise the small cell networks. Context information provides the important additional data to further enhance the optimisation mechanism.	Optimisation Time	A framework is described for context aware optimisation in small cell environments and a load balancing use case is used to evaluate the proposed approach.	The simulated results have shown that the presented context aware load balancing algorithm has increased the users' satisfaction while the optimisation time is reduced to 50%.
(Joseph and Akindeji 2016)	The challenge faced by the femtocells to cope with the interference that deteriorates the performance and capacity of the whole cellular network is	Throughput, Interference and BER	Bit Error Rate against signal behaviour and the power transmitted over signal for both femtocells and macrocell are	The proposed system has reduced the interference within the users.

	addressed.		simulated in the indoor environment.	
(Ho et al. 2016)	A technique to perform coverage optimisation, load balancing and manage sleep modes that utilises high level measurements is presented in a multi-vendor femtocell environment.	Coverage, Path Loss and Received Signal Strength (RSS)	The measurements are taken through the TR-069 device management protocol standard.	The proposed solution is able to effectively optimise the coverage by balancing load and managing sleep modes whilst ensuring that no coverage gap occurs.
(Aguilar-Garcia et al. 2016c)	A novel optimised mechanism is proposed to minimise congestion issues and prioritise voice traffic connections in indoor environments.	Throughput, Femtocell Transmit Power, Path Loss and RSS	The presented approach resizes femtocell coverage areas by tuning their transmission powers for the purpose of load balancing. Received signal level per user is evaluated.	Performance is analysed by simulation and real field trial. The proposed work is aimed for operators that prioritise users making phone calls over any other service in indoor femtocell scenarios.
(Aguilar-Garcia et al. 2016a)	An optimised system based on the coordination of Mobility Load Balancing and Energy Saving algorithms is described to enhance the performance of extremely congested indoor femtocell networks and to reduce the consumption of energy.	Femtocell Transmit Power and RSS	The proposed mechanism is supported by geo located measurement that automates the network operation, administration, management and provision procedures and provides the intelligence to network elements for a quick adaptation.	The performance of the system is analysed in a realistic simulated environment which shows the improvement in coverage, network capacity and efficient energy usage.

3.3 Selection of the Parameters to measure the performance of a Simulation Framework for Optimising Femtocell Networks

Throughput is the most frequently used parameter identified in the literature for optimisation of mobile networks involving femtocells. In most of these networks, femtocells work under the supervision of the macrocell whereas in some cases a group of femtocells work together to carry out the operations. Throughput is measured as a parameter in Hoydis et al. (2011), Hoadley and Maveddat (2012), Cheung et al. (2012), Wang et al. (2016), Akinlabi and Joseph (2016), (Joseph and Akindeji 2016) and Aguilar-Garcia et al. (2016c). Path Loss (PL) is used to measure the performance of optimised femtocell networks in Liu et al. (2012), Zhang et al.

(2015a), Ho et al. (2016) and Aguilar-Garcia et al. (2016c). Since femtocells can be deployed anywhere in the house, it encourages the users to change the position of the femtocells to achieve the highest coverage. Claussen et al. (2008) achieved the best results by deploying the femtocells in various places and the optimised positioning of the femtocells is found where the coverage is maximum. Claussen et al. (2008) used the propagation models for path loss and the performance was analysed using system level simulations. In extremely overloaded scenarios such as described in Aguilar-Garcia et al. (2016c) and Aguilar-Garcia et al. (2016a) and since the users constantly change their locations, the optimisation algorithm needs to be incorporated in the system to find the optimised positioning of the femtocells.

Hoydis et al. (2011) has shown that small cell networks need to adapt according to the traffic requirements to be able to provide high data rate coverage in an indoor environment while (Hoadley and Maveddat 2012) supported the wide scale deployment of femtocells to offload the traffic from heavy loaded macrocells to lightly loaded femtocells to support the required capacity. Both of them used throughput as one of the performance measuring parameters. Liu et al. (2012) addressed the issue of optimising the placement of femtocells in commercial buildings as they require the wide scale deployment of femtocells in different rooms of the building to accommodate a large number of users working in an indoor environment. Cheung et al. (2012) investigated two-tier networks in which macrocells employed closed access policy to avoid congestion while other users were accommodated by femtocells. Throughput was calculated for all femtocell densities. Wang et al. (2016) in its optimisation technique was able to increase the throughput of the femtocell network by 7%. Zhang et al. (2015a) designed a power allocation scheme for randomly deployed femtocells by considering the path loss and different wall penetration conditions. The work implemented in MATLAB showing the deployment of femtocells in an indoor environment resulted in better throughput and improved signal strength is presented by (Akinlabi and Joseph 2016). Path loss is used as a performance parameter in Ho et al. (2016) in which optimisation was performed on multi-vendor femtocells.

Based on the studies, findings and the frequency of the parameters (as identified in Table 3), the simulation framework used for this research will take into account the Throughput and Path Loss (PL) as the parameters to analyse the performance of the LTE-A two-tier system in which macrocell will stay in the top tier while femtocells will work in the lower tier of the network. A simulation environment will be used to test the effect of changing specific parameters. Based on the results and findings, the simulation framework will be refined and incorporate the optimisation algorithm to achieve the desired objectives of this research. The simulation framework will find the optimised positioning of the femtocells in an indoor environment on the basis of throughput and path loss.

3.4 Summary

In order to achieve the aim and objectives of the research, it is necessary to understand which specific set of parameters can be used together to carry out the allocation of resources in an efficient way and to offload the heavy traffic from already heavily loaded macrocells to lightly loaded femtocells. For this purpose, a survey of the literature was conducted to examine the parameters different authors have used to optimise the network. Methodologies and approaches used for optimising femtocell networks have been discussed. Based on the findings, throughput and path loss are selected as performance parameters for inclusion in a simulation framework developed for the optimisation of femtocell networks. The identification of the parameters to investigate the performance of a two-tier LTE-A system with femtocell overlays and then to find the optimised positioning of the femtocells by using the simulation framework is unique to this research. The comparison of approaches and the aspects they are trying to improve is discussed in Table 3. Chapter 3 draws attention to how the different themes and approaches (mixture of parameters) have developed and changed over time. The claimed improvement in the performances of the networks is compared with the emphasis on different parameters. Chapter 4 will present the results of experiments assessing the effect of these parameters for a two-tier LTE-A system having femtocell overlays.

Chapter 4: Simulation Framework used to analyse the performance of LTE-A Systems with Femtocell Overlays

This chapter presents the results of set of experiments performed to analyse the performance of LTE-A two-tier system in which macrocell remains in the top tier while femtocells work in the lower tier of the network as discussed in the two-tier architectures of Chapter 3. Since femtocells are identified as a crucial way to the delivery of the increased demands in the literature (as discussed in Chapter 2) for heterogeneous networks in which macrocells work in combination with femtocells to provide coverage to offices, homes and enterprise, therefore, a simulation framework is used to implement the LTE-A system of macrocell with femtocell overlays. The requirements, design and implementation of the simulation framework is discussed before it is used to perform the experiments. The algorithms are based on the set of formulae (as discussed in Section 4.2) using the key parameters identified in the literature (Throughput and Path Loss). The simulation framework is effectively utilised to test the operation and capability of the algorithms. The experiments performed in this chapter also establish the background to find the optimal positions of the femtocells on the basis of throughput and path loss in an indoor environment of the building (as discussed in Chapter 5). Since throughput and path loss are identified as potential parameters for modern networks (as discussed in Chapter 3), therefore, throughput and path loss are the parameters selected for this research to analyse the performance of networks having femtocells. An environment is defined to analyse various scenarios in which femtocells are working in conjunction with macrocell to create a two-tier mobile network. Multiple scenarios have been simulated using the Graphical User Interface (GUI) developed in MATLAB as part of the simulation framework to analyse the performance of the network. Initially, there is a minimal load on the network to analyse the change in throughput and path loss with respect to the change in modulation scheme for each LTE-A supported bandwidth. Then, the number of femtocells is increased and additional femto and macro users are added to the network to analyse the effect they have on the performance. The effect of the walls on the throughput and path loss of the users is also examined in this chapter. To conclude the set of experiments, the type of modulation scheme and LTE supported bandwidth is kept constant and positioning of the femtocells is changed for each scenario to analyse the performance of the network. Different case studies are proposed and implemented using the typical conditions defined in literature required for the operation of a two-tier LTE-A system with femtocell overlays. Each case study is implemented by utilising the simulation framework used for this research and the performance of each case study is analysed. The results of these case studies contribute to the development of set of recommendations for the placement of femtocells and consequently find the optimised positioning of the femtocells as discussed in detail in Chapter 5 thus achieving the aim and objectives of this research.

This chapter starts with the description of the requirements of the simulation framework followed by the numerical modelling of the simulation framework. The architecture of the simulation framework is explained in detail in the following section. The implementation of multiple scenarios and different case studies is then discussed followed by the comprehensive performance analysis. The chapter concludes with the summary of the key points derived as a result of the experiments.

4.1 Requirements of the Simulation Framework

Femtocells can work together with macrocells in LTE-A systems using the same or different frequencies. In this proposed two-tier system, femtocells work under the macrocell on the lower tier. To perform a set of experiments, a user friendly simulation framework is required as it allows the flexibility of choosing the desired environment. The simulator must have the capability to allow the operation of a macrocell and femtocells as a two-tier network to meet the aims of the experiments. Therefore, a simulation framework based on the numerical modelling described in the following section has been implemented integrating femtocell overlay in a macrocell environment to estimate the maximum throughput and calculate the path loss.

An easy to use and comprehensive Graphical User Interface (GUI) is required for this simulation framework to interact with users in terms of setting the inputs and analysing the output. The aim of using a user friendly GUI is to allow the random positioning of the femtocells, femto users and macro users. The GUI allows the flexibility of choosing the desired environment and running the simulation many times by only changing a few parameters and keeping the rest of the LTE-A environment constant to analyse the performance. The GUI must be able to calculate the throughput and path loss of all the femto and macro users to be able to analyse the output. There are other simulators available to carry out the experiments, but the simulation framework used for these experiments meets the requirements and aim of this PhD. There was an effort to use the Vienna LTE-A System Level Simulator but it does not allow the flexibility of using macrocell and femtocells together as a two-tier network. Full codes are not available and the lack of support from the technical team and developers of the simulator from the Institute of Telecommunications in Austria results in the rejection of this simulator. A dynamic system level simulator for LTE femtocell scenarios used in Aguilar-Garcia et al. (2016b) and Aguilar-Garcia et al. (2016c) is not available to use because of the copyright issues. The University of Malaga in Spain was contacted to use the simulator for research but only the students of their University are authorised to use the simulator. Some of the modules of the simulator used in Aguilar-Garcia et al. (2016a) for coordinated location based indoor femtocell networks are compatible with specific versions of software that are no longer available. Therefore, the desired topologies are executed in the simulation framework adapted from (Bouras et al. 2012) to create a two-tier LTE-A system to perform the experiments. The addition

of the genetic optimisation algorithm (as discussed in Section 5.1 of Chapter 5) in the simulation framework to be able to optimise the network of femtocells is the functionality that is the own development to the simulation framework. An environment is defined (as discussed in Section 4.3) to test different scenarios for this chapter in which femtocells are working in conjunction with a macrocell to create a two-tier mobile network. The simulation framework using the formulae discussed in the following section calculates the throughput and path loss of all the femto and macro users deployed in different scenarios. The simulation framework can calculate the throughput at every point in the working environment of LTE-A system having both the macrocell and femtocells working together. The simulation framework is implemented in MATLAB and can be further extended or modified. The code of the main layout file (mainlayout.m) of the whole simulation package is shared in the Appendix A of the thesis. The code is based on the previously existing framework described in (Bouras et al. 2012).

4.2 Numerical Modelling of the Simulation Framework

The following section explains and analyses how the throughput in every point of the LTE-A system integrating femtocells and macrocell is calculated. It also estimates the path loss of all the femto and macro users connected to their respective femtocells and macrocell. The model also takes into consideration the propagation models and losses caused due to attenuation and multipath fading. These are illustrated in the following sub sections.

4.2.1 Path Loss Model

Path loss significantly relies on the environment of the network (Bouras et al. 2016) and since urban environment is considered for this research as femtocells are mostly deployed in indoor environments, therefore, the chosen path loss model fulfils the desired objectives of the research. The path loss model used in this simulation framework also takes into account penetration losses because of the walls inside buildings unlike free space path loss and Friis' transmission equation which are mostly considered for outdoor environments. Free space path model is valid only in far field. Friis' transmission formula is mostly used to study communication links and involves the powers of the transmitter and receiver antennas and speed of light. Therefore, not suitable for the development of the simulation framework for optimising femtocell networks inside the buildings. In addition, the path loss model used in the development of this simulation framework for optimising femtocell networks is used by Bouras et al. (2012) in its framework and is also used in (Bouras et al. 2016) for transmission optimising on dense femtocell deployments. Hence, it has been used in the literature for the two-tier architectures and also for the dense deployment of femtocells. Since partitions in building environments vary drastically in their electrical and physical characteristics, it is very difficult to accurately derive and measure a general path loss model. Therefore, path loss model already exists in the literature is used in the simulation framework developed for this research to

find the optimised positioning of femtocells and described in the following section. The path loss between a macro user and macrocell and also between a femto user and femtocell in the same apartment needs to be calculated. The thickness of the walls within apartments is kept constant. The path loss of a macro user roaming in an outdoor urban area in dB is calculated as (Bouras et al. 2016):

$$PL (dB) = 37.6 \log_{10} R + 15.3 \quad (1)$$

while in comparison the path loss of an indoor macro user in dB is calculated as:

$$PL (dB) = 37.6 \log_{10} R + 15.3 + L_{ow} \quad (2)$$

In the above equations, R denotes the distance in meters between the transmitter and receiver while L_{ow} represents the penetration loss of an outdoor wall.

The path loss of a femto user to its femtocell in dB is calculated as (Ikuno et al. 2010):

$$PL (dB) = 20 \log_{10} R + 38.46 + 0.7d_{2D,indoor} + 18.3n^{((n+2)/(n+1)-0.46)} + L_{iw} * q \quad (3)$$

In the above equation, n denotes the number of penetrated floors. L_{iw} represents the penetration loss of the wall splitting the apartments. q denotes the number of walls dividing the apartments between the femto user and the femtocell. $0.7d_{2D,indoor}$ accounts for the penetration loss because of the walls inside an apartment calculated in meters.

In a case where an outdoor femto user connects to an indoor femtocell, the outdoor wall loss has to be considered. The path loss in dB will then be measured according to (Ikuno et al. 2010):

$$PL(dB) = \max(37.6 \log_{10} R, 38.46 + 15.3 + 20 \log_{10} R) + 0.7d_{2D,indoor} + L_{iw} * q + L_{ow} + 18.3n^{((n+2)/(n+1)-0.46)} \quad (4)$$

4.2.2 Throughput Computation

The total throughput of a serving macrocell M is calculated according to the following equation:

$$T_M = \sum_m \sum_k \beta_{m,k} C_{m,k} \quad (5)$$

where $\beta_{m,k}$ denotes the subcarrier assignment for macro users. $\beta_{m,k} = 1$ means the subcarrier k is allocated to the macro user m . Else $\beta_{m,k} = 0$. Each subcarrier is assigned to only one macro user at a time for every time slot in a macrocell, because of the attributes of OFDMA used in LTE-A technology. This results in the following equation:

$$\sum_{m=1}^{N_m} \beta_{m,k} = 1 \quad (6)$$

In the above equation, N_m represents the number of macro users in a macrocell. The throughput of the femto users is also calculated according to the above equations (5) and (6). The equations from (1) to (6) are used in accordance to the specifications set out in the Technical Specification Group Radio Access Network Release 9 technical report by 3rd Generation Partnership Project on Further Advancements for Evolved Universal Terrestrial Radio Access (E-UTRA) physical layer aspects (Bouras et al. 2016). The 3GPP in its deliverables (3GPP TR 36.814 V9.0.0) has set out the specifications for LTE-A networks. Based on this technical report, throughput and path loss being the key parameters identified in the literature, are calculated according to the equations (1) – (6) in the simulation framework used for this research.

4.3 Architecture of the Simulation Framework

The properties of a macrocell environment such as the positioning of the femtocells and the users attached to the femtocells, type of modulation scheme, transmission power of macrocell and femtocells and dimensions of buildings are fed as an input to the core component of the simulation framework. The core of the simulation framework calculates the power received from serving and interfering cells based on the transmission power of macrocell and femtocell and by taking into account the equations described in Section 4.2. By taking White Gaussian Noise (WGN) also used in (Bouras et al. 2016) into consideration and the values obtained from previous calculation, the core of the simulation framework is then able to calculate the throughput at any given position in the LTE-A network under examination. WGN is an additive noise. The signal received equals to the signal transmitted with the addition of a noise. WGN functions as a noise model to imitate the effect of various random processes happening in nature. Since the normal distribution of WGN in time domain has an average domain value equals to 0, it provides the equality to the LTE-A communication network. The White Noise Power Density is kept constant for this experiment to mitigate any random effects of noise in the simulation.

The internal architecture of the simulation framework is distributed in individual subunits called modules. These modules are responsible for executing a set of interdependent functions or a particular function. The architecture of this simulation framework is designed in a way that it can be extended or new functions can be added to it. The algorithm developed for this simulation framework is separated into two layers. All calculations of the simulation framework including penetration and path loss of macro or femto users takes place in the lower layer. Maximum throughput estimation by taking system defined parameters and input of the user into account also takes place in the lower layer. The user parameters are fed into this lower layer

where simulation based on the mathematical modelling as described in Section 4.2 takes place. Real time information is displayed in the lower layer. The higher layer consists of the graphical user interface. The purpose of the GUI is to visualise the input and output and hence no calculations take place at higher layer. The GUI enables the user to define the parameters, that is, positions of the femto and macro users, position of the femtocells, dimensions of the buildings and to visualise the output. Figure 6 depicts the architecture of the simulation framework.

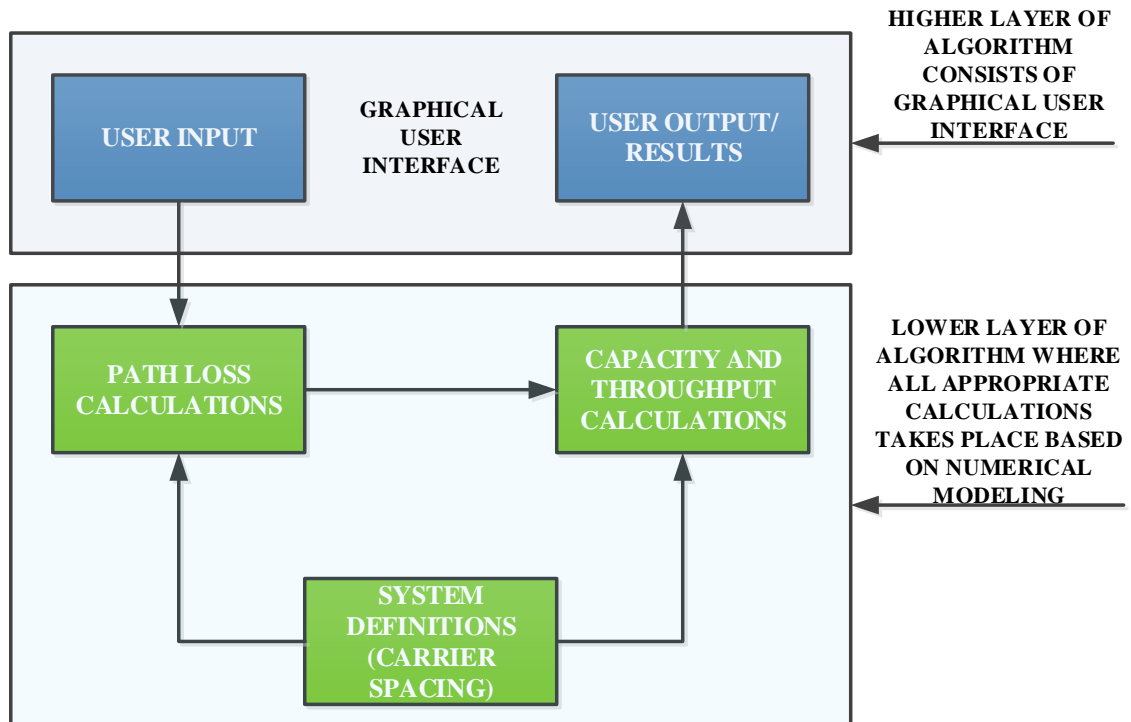


Figure 6: Architecture of the simulation framework

4.4 Implementation of the Simulation Framework

The simulation framework described above is implemented in MATLAB. The graphical user interface is also designed in MATLAB and integrated with the simulation framework. The whole package of the simulation framework runs on the MATLAB. The working of each module of the architecture to carry out the experiments is described in the following sub sections.

4.4.1 User Input Module

The graphical user interface of the simulation framework allows the end user to communicate with the system in terms of setting the inputs, visualising the network environment once the inputs are fed in the GUI, visualising and analysing the output. Figure 7 depicts the user screen of initial layout of the GUI before the inputs are fed in the GUI. The simulation framework needs inputs from the user to make the appropriate calculations i.e. the number of femtocells

and their precise location coordinates in the defined macrocell coverage area, the total number of femto users attached to particular femtocells and the number of macro users. Since LTE-A operates on multiple configuration modes, type of modulation scheme and bandwidth are also necessary parameters. The number of buildings along x and y axis are also required by the framework to generate the building map along with the width of the road. The GUI as shown in Figure 7 allows the end user to select the number of femtocells e.g. 3, the number of femto users e.g. 4, the number of macro users e.g. 2, modulation scheme e.g. 64QAM and preferred channel bandwidth e.g. 20MHz. The end user then has to select the number of buildings along x and y axis e.g. 3 and 2 respectively and define road width in meters e.g. 5 to generate an urban environment on the map. The end user can choose the number of femtocells, femto users and macro users of its choice to be deployed in the defined macrocell coverage area. Since 4G LTE-A uses Quadrature Amplitude Modulation (QAM) as modulation scheme for OFDMA and the current LTE standards for channel bandwidth are 1.4, 3, 5, 10, 15 and 20MHz, any Bandwidth/Modulation (BW/Modulation) combination can be selected by the end user through the GUI. They are 20MHz/64QAM, 20MHz/16QAM, 20MHz/QPSK, 15MHz/64QAM, 15MHz/16QAM, 15MHz/QPSK, 10MHz/64QAM, 10MHz/16QAM, 10MHz/QPSK, 5MHz/64QAM, 5MHz/16QAM, 5MHz/QPSK, 3MHz/64QAM, 3MHz/16QAM, 3MHz/QPSK, 1.4MHz/64QAM, 1.4MHz/16QAM and 1.4MHz/QPSK. The types of QAM include 2, 4, 8, 16, 32, 64, 128, 256 and 1024 QAM. The other forms include circular, rectangular etc. (Voudoukis 2017).

Table 4: Characteristics of different formats of QAM (Voudoukis 2017)

Multiplier	Modulation Scheme	Number of Bits	Bits per Symbol	Symbol Rate	Symbol Example
1x	On-Off Keying	2^1	1	1 x Bit Rate (BR)	0
2x	4QAM/QPSK/4PSK	2^2	2	$1/2$ x Bit Rate (BR)	01
4x	16QAM	2^3	4	$1/4$ x Bit Rate (BR)	0101
5x	32QAM	2^4	5	$1/5$ x Bit Rate (BR)	01010
6x	64QAM	2^5	6	$1/6$ x Bit Rate (BR)	010101
7x	128QAM	2^6	7	$1/7$ x Bit Rate (BR)	0101010
8x	256QAM	2^7	8	$1/8$ x Bit Rate (BR)	01010101
9x	512QAM	2^8	9	$1/9$ x Bit Rate (BR)	010101010
10x	1024QAM	2^9	10	$1/10$ x Bit Rate (BR)	0101010101

Considering the reliability and effectiveness of lower order QAM, QPSK, 16QAM and 64QAM are chosen for performance analysis and simulation of LTE-A systems as recommended by researchers such as (Frenzel 2013; Sood and Garg 2014; Soldani and Manzalini 2015) having femtocell overlays. Table 4 presents the recapitulation of the relation between the number of bits, symbol rate and bits per symbol of the different formats of QAM. From Table 4 it can be deduced that 64QAM provides 50% more bandwidth than 16QAM because it can transfer 6 bits per symbol whereas 16QAM can only transfer 4 bits per symbol. Similarly, 64QAM can

provide 3 times or 300% more bandwidth than QPSK while 16QAM can provide 2 times or 200% more bandwidth than QPSK. The simulation framework used for this research needs to provide the output results according to the modulation schemes and the bandwidths as stated in Table 4.

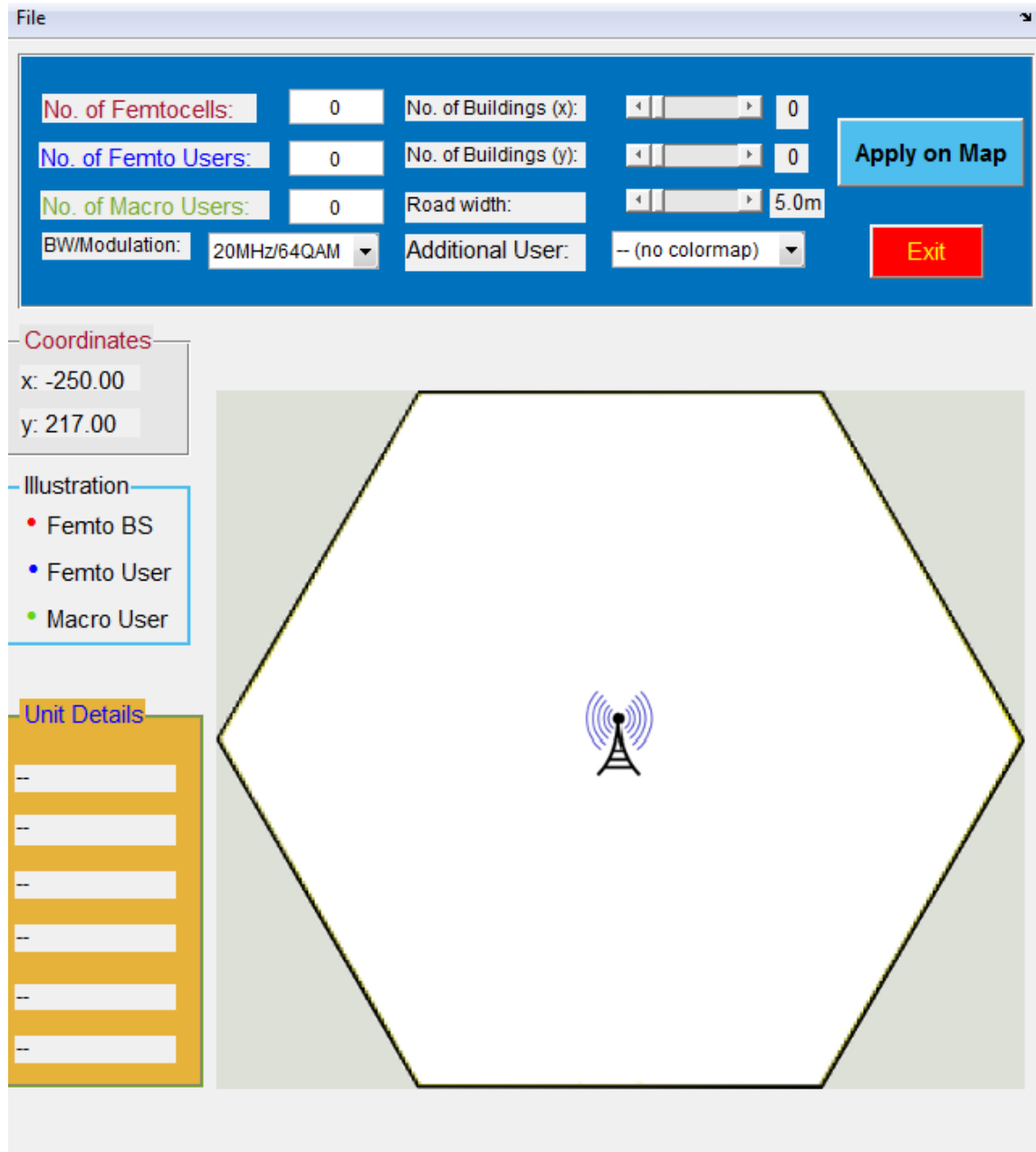


Figure 7: User screen before inputs are fed in the GUI

Taking as a reference from (Bouras et al. 2012), any value of the road width can be selected from a range of 5 to 15 meters. The number of buildings along x and y axis can be chosen up to a maximum of 15 each. Once the user inputs are fed in the GUI, the end user then has to press ‘Apply on Map’ as visible in light blue colour on top right corner of Figure 7 to display the user defined network topology of buildings as shown in Figure 8.

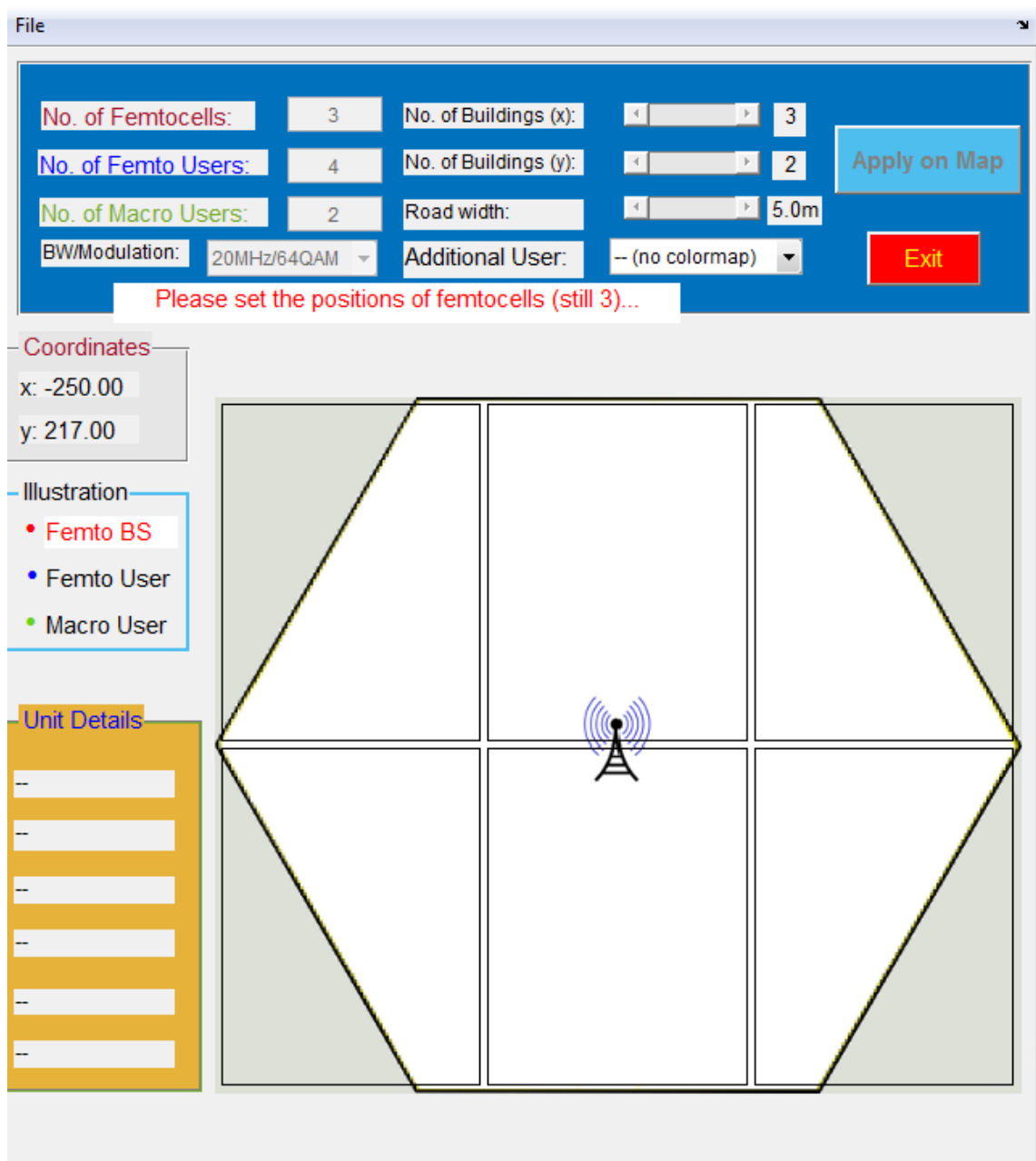


Figure 8: User screen displaying the user defined network topology of buildings

Once the buildings are displayed according to the inputs of the end user, a manual deployment of femtocells, femto users and macro users can take place according to the users' requirement by clicking on the desired locations in the available macrocell defined coverage area as shown in Figure 9. The distance between femto users to their respective femtocells, and macro users to the macrocell is calculated according to the Pythagoras Theorem based on the specified location coordinates. The deployment is considered to be complete once the last macro user is placed on the layout by the end user. Consequently, the tab on top right corner displaying 'Run Simulation' in Figure 9 turns red and can be pressed to run the simulation. This tab only turns

red and be ready to be pressed once all the femtocells, femto and macro users are successfully deployed in the defined coverage area.

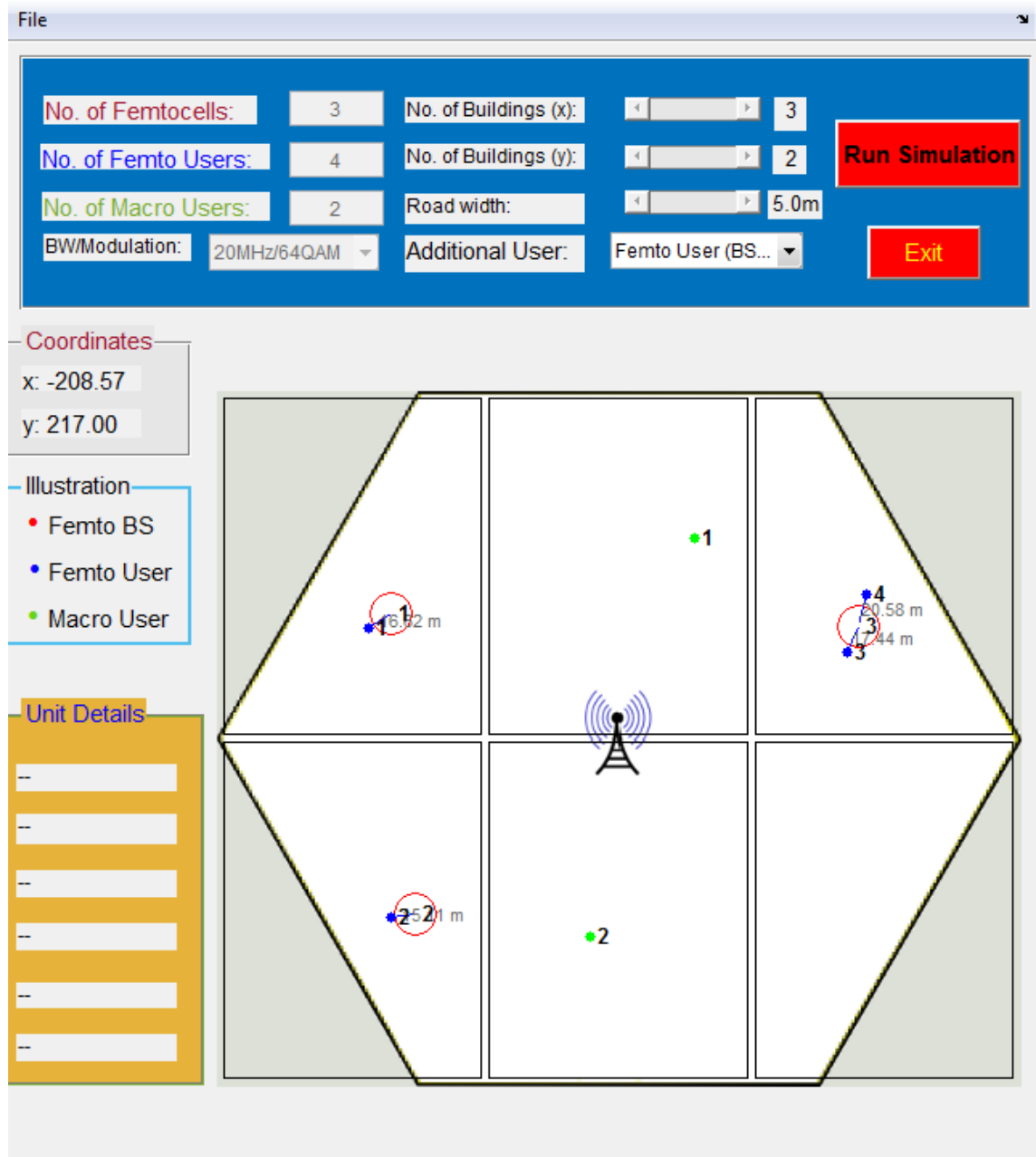


Figure 9: User screen after inputs are fed in the GUI

The macrocell antenna is located at the centre of layout. Since the antenna of a base station follows hexagonal coverage patterns to reduce black spots, the coverage area of this macrocell also displays hexagonal structure. It is surrounded by the femtocells deployed by the end user in their respective positions. Femto users are also seen to be attached to their respective base station antennas. Buildings along x and y axis are also displayed on the layout according to the user defined positions. The white area inside the hexagonal structure is the coverage area of the

LTE-A network in which macrocell and femtocells are working together to provide the coverage.

The small green circles represent the macro users whereas the small blue circles denote the femto users. The femtocells are represented by transparent large red circles. All the femto users (small blue circles) and macro users (small green circles) are represented by a number starting from 1 and rising in the order they are created. Femto users are connected to their specific femtocells through a solid blue line. Each blue line represents the distance of each femto user to its femtocell as seen in Figure 9. The distance calculated in meters is also displayed on the map in grey writing for each femto user. All macro users are connected to the macrocell antenna.

The location of macrocell and femtocells, macro and femto users, the structure of the map depicting the layout of the user defined topology and taking the interfering walls into account are the parameters required to calculate the path loss. Since the deployment of femtocells are mostly restricted to an indoor environment because of the need and population density in urban areas, therefore only the topology of an urban area was considered during the development of this graphical user interface.

4.4.2 Path Loss Calculation Module

The numerical modelling and analysis of the path loss estimation module is already described in Section 4.2.1. The numerical modelling implemented according to the Section 4.2.1 considers all possible intra tier and cross tier interferences that can occur in an urban scenario. The scenarios are:

- indoor macro user interfered by a femtocell
- outdoor macro user interfered by a femtocell
- indoor femto user interfered by a macrocell
- outdoor femto user interfered by a macrocell

Based on the input of the user from the previous module, an appropriate model is selected. The output of this module in dB acts as an input of the next module.

4.4.3 Capacity and Throughput Calculation Module

The capacity calculation module only implements the model of channel capacity estimation by taking into account the results from the previous module and carrier spacing known as system definition. The resulting matrix is then sent to the next module to be presented to the end user.

4.4.4 User Output Module

Once the inputs are fed in the graphical user interface, the end user has to press the Tab 'Run Simulation' as shown in Figure 9 to start the simulation. It will trigger the display of a progress

bar displaying the message “Simulating.....It will take a lot of time” as shown in Figure 10 keeping the end user informed about the progress of the simulation.

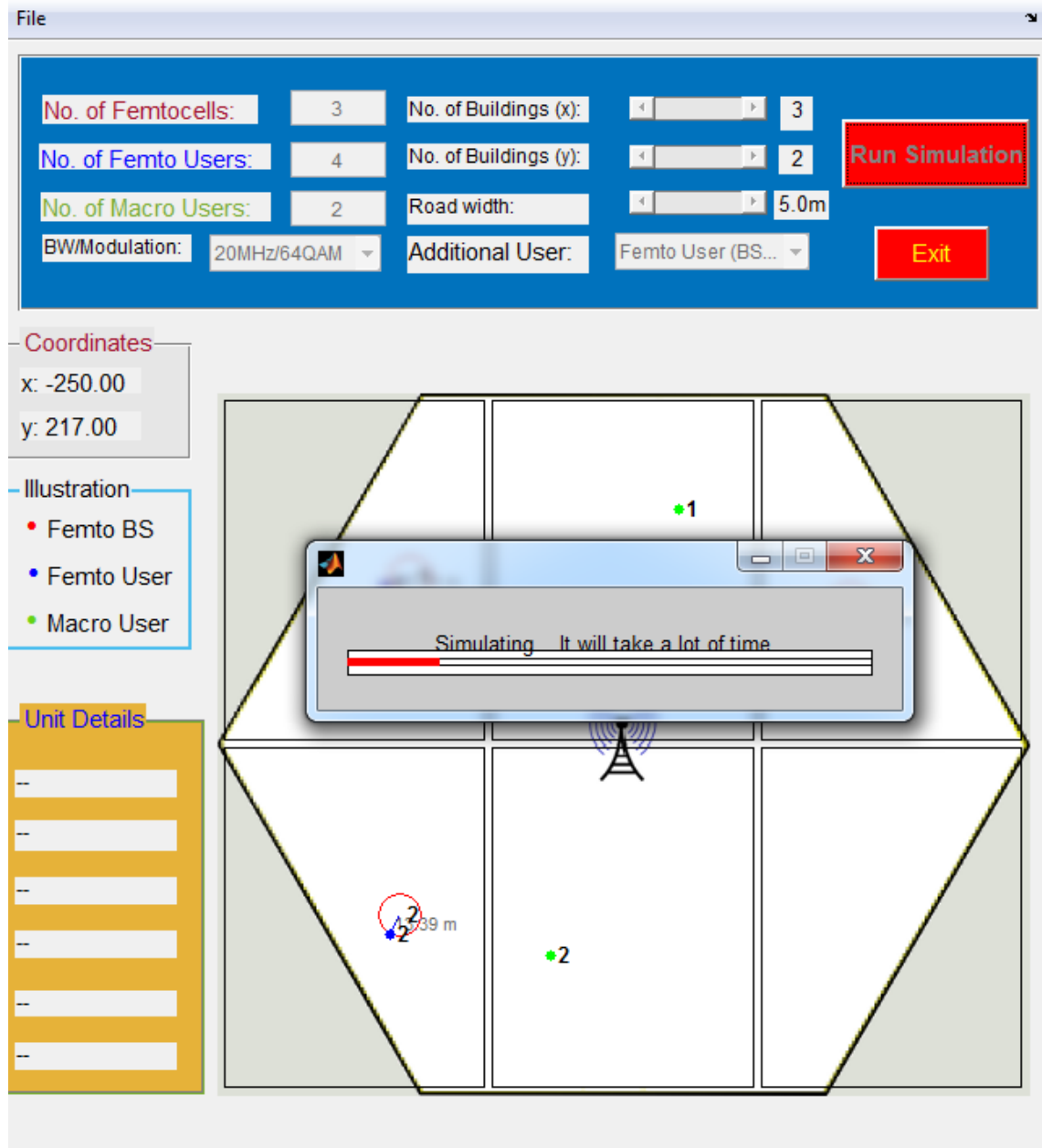


Figure 10: User screen displaying simulation in progress

Once the red line below the “Simulating.....It will take a lot of time” as shown in Figure 10 reaches the end point, the simulation completes and the final results can be visualised in a separate window, as shown in Figure 11.

The output of the user defined network topology can be seen and analysed through GUI as shown in Figure 11. The simulation framework has calculated the throughput and path loss of all the femto and macro users in the examined LTE-A network having femtocell overlays. By

hovering over the map, the coordinates of the current position are displayed on the map in the ‘Coordinates’ section of left side of the layout.

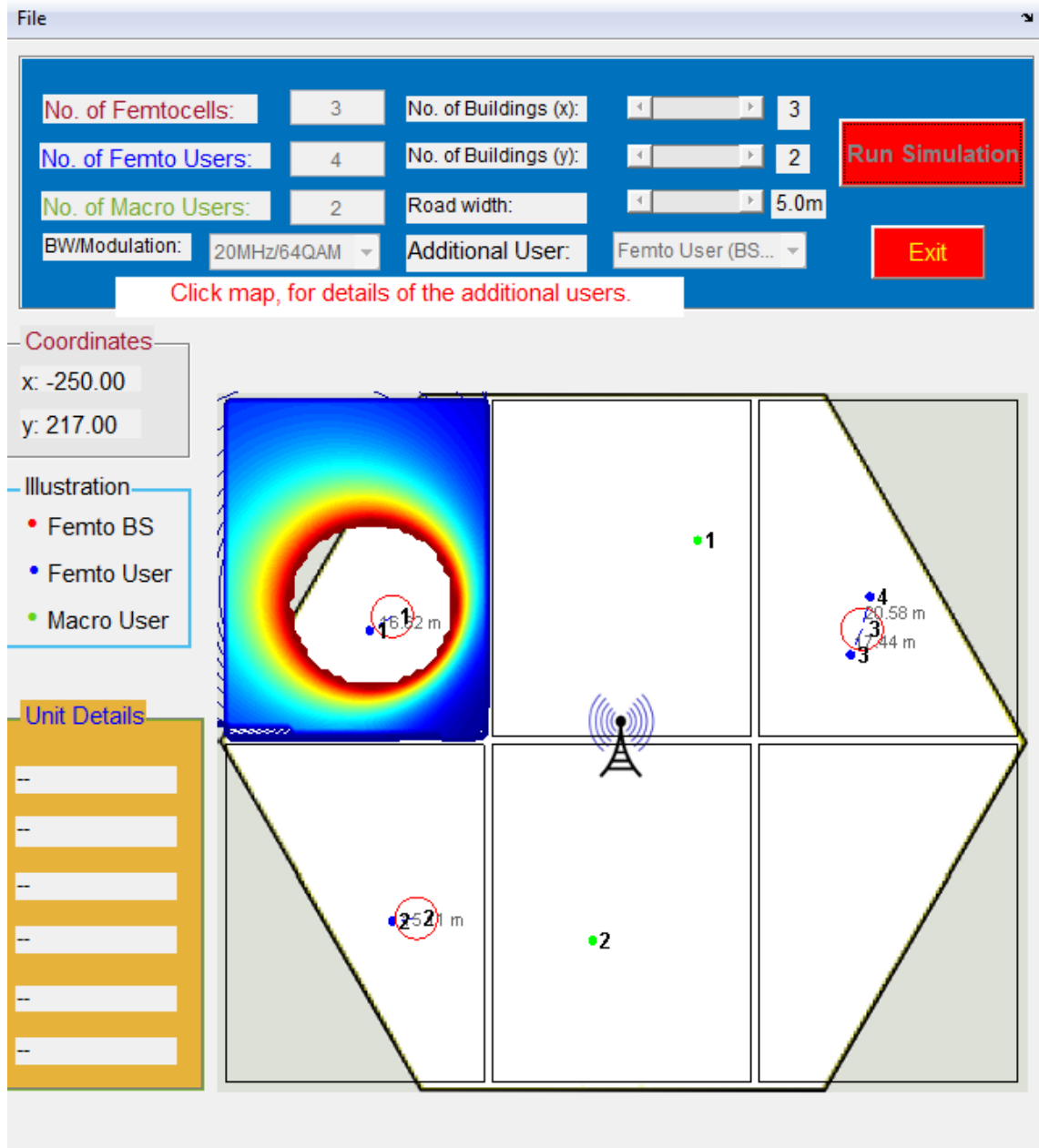


Figure 11: User screen displaying output after completion of simulation in the GUI

The ‘Unit Details’ section also on left side of the layout displays the ID number of femto or macro user under examination and whether the femto or macro user is roaming in an indoor or an outdoor location. It also displays the arithmetic values of throughput, SINR and path loss. It also shows the distance of femto or macro user from its base station and provides information about the number of walls between femto or macro user and its base station. Once clicked on the femto user ID 1, the ‘Coordinates’ and ‘Unit Details’ of the femto user ID 1 can be seen, as

shown in Figure 12. Similarly, coordinates and unit details of all the femto and macro users can be checked and analysed.

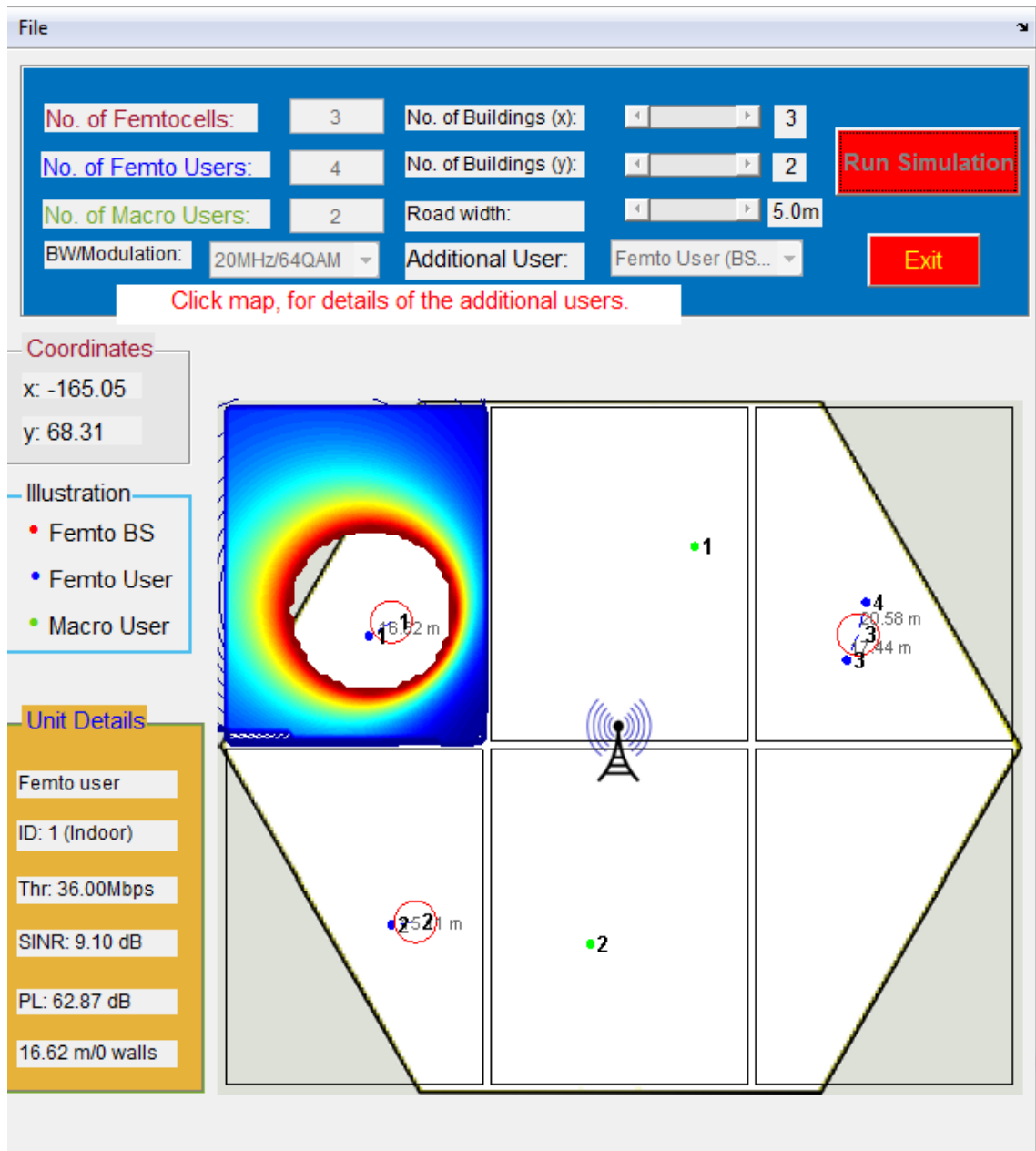


Figure 12: User screen displaying Coordinates and Unit Details of Femto User ID 1

The simulation framework implemented for this research has been described in detail in the above sections. The simulation framework was designed to be efficient and user friendly. The end user can easily provide the inputs of the network topology to the simulation framework through the graphical user interface. All the appropriate calculations of throughput and path loss are executed at the lower layer of the algorithm in a short time with just one click on the panel of the graphical user interface. The results are output graphically in real time. The end user can easily check the details of the femto and macro users' through graphical user interface.

4.5 Simulation Results and Performance Analysis

Different case studies are proposed and analysed to test the operation and capability of the simulation framework. Initially, all input parameters are kept constant except the type of modulation scheme and LTE supported bandwidth to analyse the performance of LTE-A system. In this case, there is a minimal load on the network as only one user is assigned to a femtocell, one user is assigned to a macrocell and two users are assigned to another femtocell. The aim is to analyse the change in throughput and path loss of the femto users with respect to the change in modulation scheme for each LTE-A supported bandwidth. This section builds on the results of first case study by adding a large number of femtocells, femto users and macro users in the system thereby increasing the load on the network. The effect of walls on the throughput of the users is also analysed in this section. A series of tests are then carried out using the simulation framework for the scenarios in which the type of modulation scheme and LTE supported bandwidth is kept constant and only positioning of the femtocells and femto users is changed inside the buildings to analyse the performance based on the throughput and path loss.

4.5.1 Case Study 1

For Case Study 1, the proposed scenario as shown in Figure 13 has been repeatedly simulated for all LTE supported bandwidths against each modulation scheme to analyse the performance of LTE-A systems with femtocell overlays. The proposed scenario is simulated for all the supported bandwidths of LTE-A systems (20, 15, 10, 5, 3 and 1.4 MHz) against each modulation scheme (64QAM, 16QAM and QPSK).

The metrics are calculated according to the numerical modelling described in Section 4.2 and outputted in real time. The values of the parameters used in the simulation framework for this scenario are stated in Table 5. Most of the values are typically used in LTE-A systems and are also based on (Bouras et al. 2016).

The inputs need to be fed in the graphical user interface manually to start the simulation. 2 femto base stations (femtocells), 1 macro user and 2 femto users are selected to be located within the macrocell coverage area. All the supported LTE bandwidths (20, 15, 10, 5, 3 and 1.4 MHz) are selected against each modulation scheme (64QAM, 16QAM and QPSK) one by one for simulation. 2 buildings are selected along x axis and 1 building is selected along y axis to generate the layout as shown in Figure 13. This layout allows the placement of 2 femtocells, 2 femto users and a macro user according to the desired location within the coverage area to produce the required scenario for analysis. A road width of 5 m is selected to create an urban environment in this simulation.

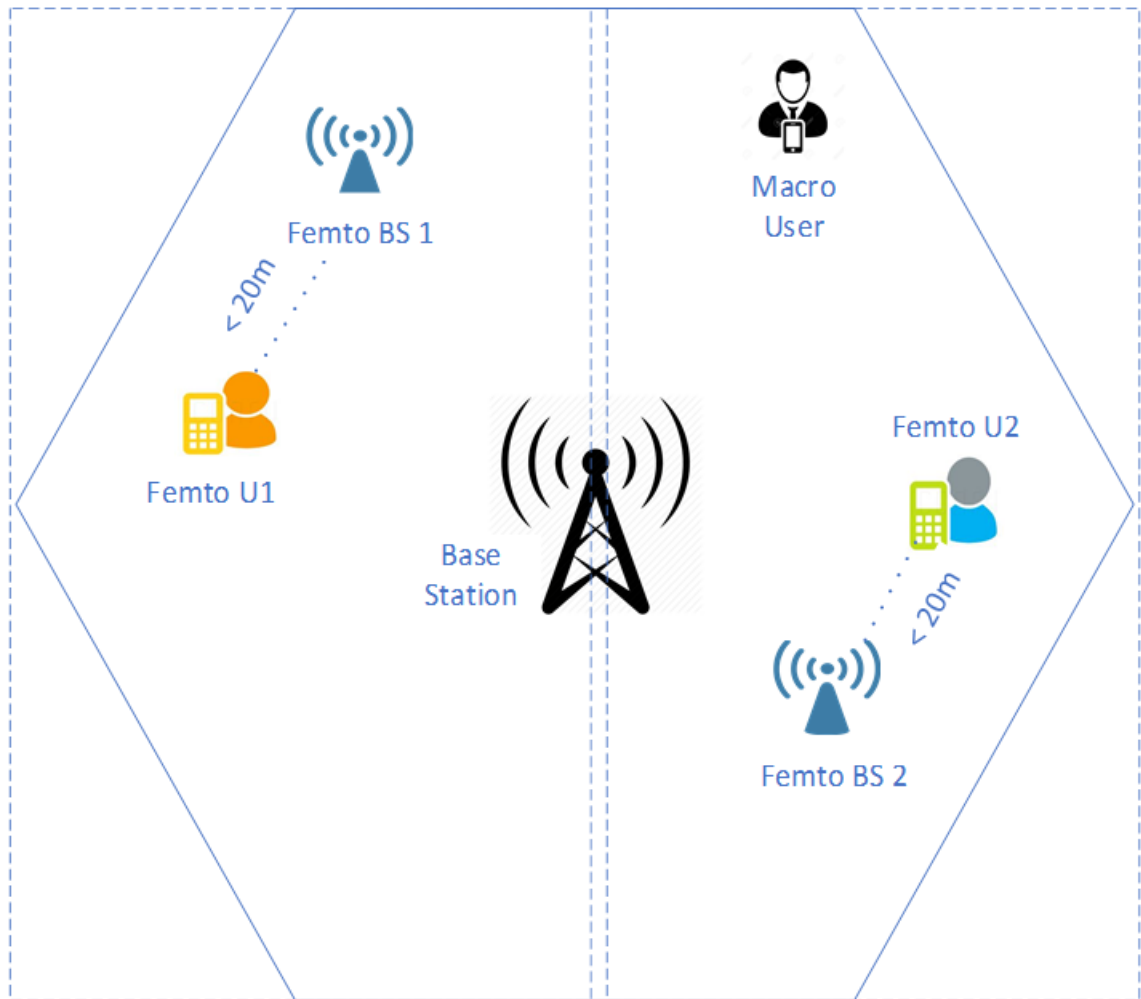


Figure 13: Visual representation of the described scenario for Case Study 1

Table 5: Parameters of simulation framework for Case Study 1

Parameter	Value
Femtocell Radius	20 m
Macrocell Radius	250 m
Frequency	2000 MHz
Femtocell Transmit Power	20 dBm
Macrocell Transmit Power	46 dBm
Indoor Wall Loss (L_{iw})	5 dB
Outdoor Wall Loss (L_{ow})	20 dB
White Noise Power Density	-174 dBm/Hz
Bandwidth (MHz)	1.4 3 5 10 15 20
Modulation Scheme	QPSK/4QAM/4PSK 16QAM 64QAM

The manual deployment of femtocells, femto users and a macro user takes place by clicking on the points of user choice (arbitrary positions) in the coverage area of macrocell within the hexagonal structure. As the last macro user is placed on the layout, the deployment is considered to be completed. Figure 13 represents the visual representation of the placement of femto base stations, femto users attached to their respective femto base stations (the distance should be less than 20 m as the femtocell radius is taken as 20 m in this scenario based on Table

5), a macro user and the macrocell antenna. The macrocell radius is taken as 250 m according to the requirement of the aim of this simulation. Since the LTE 4G operates on frequencies of 700 MHz, 1700-2100 MHz, 1900 MHz and 2500-2700 MHz in different parts of the world, the frequency of 2000 MHz is selected for this simulation and is also used in the simulation framework of (Bouras et al. 2012). For the transmission power of femtocell and macrocell antennas, typical values of 20 dBm and 46 dBm are used respectively (as mentioned in Table 5). A fixed value of -174 dBm/Hz is used for White Noise Power Density to mitigate any random effects of noise in the simulation. Based on the design, values of 5 dB and 20 dB are used for Indoor Wall Loss (L_{iw}) and Outdoor Wall Loss (L_{ow}) respectively. The framework also allows an end user to attach an additional macro or femto user to the already positioned macrocell or femtocells. For this particular scenario, an additional user is attached to the Femto Base Station 1. The purpose of connecting an additional user to the Femto BS 1 is to explore the effect adding an additional user has on the throughput and path loss. Table 6 provides the values of the user inputs used in the simulation framework for this scenario.

Table 6: User inputs of simulation framework for Case Study 1

User Input	Value
Number of Femtocells	2
Number of Femto Users	2
Number of Macro Users	1
Number of Buildings (x)	2
Number of Buildings (y)	1
Road Width	5 m
Additional User connected to	Femto BS 1

The described scenario is repeatedly simulated 18 times (one simulation for each combination of input) for all the supported bandwidths of LTE-A systems (20, 15, 10, 5, 3 and 1.4 MHz) against each modulation scheme (64QAM, 16QAM and QPSK). The estimated throughput and path loss of all the femto users and the distances of femto users from their corresponding femto base stations are mentioned in Table 7. Table 7 presents the results of the simulation based on the user defined topology of all the femto users for each combination of input.

The throughput and path loss are calculated for each femto user according to the mathematical modelling described in Section 4.2 and values are stated in Table 7. Since an additional user is also connected to Femto BS 1, therefore Femto BS 1 has to serve two users in its proximity whereas Femto BS 2 has to serve a single femto user. Therefore, calculated throughput of Femto U1 needs to be half than the throughput of Femto U2 for each scenario because only half bandwidth is available to Femto U1 in comparison to the bandwidth available to Femto U2 because of an additional user also served by the Femto BS 1. From the Table 7, it is evident that 64QAM provides 3 times more throughput as compared to QPSK against same bandwidth for each scenario. Table 7 also shows that 16QAM provides twice throughput as compared to

QPSK. 64QAM provides 1.5 times more throughput as compared to 16QAM as seen from the Table 7. Hence, the simulation framework is able to validate the expected outcomes as a result of these simulations. The comparison of throughputs of Femto Users 1 and 2 is shown in Figure 14 below. The throughput of Femto U1 is displayed by a blue line whereas the throughput of Femto U2 is shown by a red line to clearly show the comparison of obtained throughputs of both the users against each modulation scheme for all the supported bandwidths of LTE-A systems with femtocell overlays. Figure 14 shows that the values on the throughput axis for each graph has reduced from 64QAM to QPSK for each femto user.

Table 7: Throughput and Path Loss of Femto Users 1 and 2 (Femto U1 and U2)

Bandwidth (MHz)	Modulation Scheme	Femto User 1 (Femto U1)			Femto User 2 (Femto U2)		
		Throughput (Mbps)	Path Loss (dB)	Distance (m)	Throughput (Mbps)	Path Loss (dB)	Distance (m)
20	64QAM	54	62.82	16.52	108	63.29	17.43
20	16QAM	36	63.07	17	72	63.05	16.97
20	QPSK	18	62.61	16.12	36	61.98	15
15	64QAM	40.5	62.79	16.46	81	62.54	16
15	16QAM	27	62.42	15.78	54	63.1	17.05
15	QPSK	13.5	62.26	15.49	27	62.1	15.20
10	64QAM	27	62.87	16.61	54	63.55	17.96
10	16QAM	18	62.54	16	36	63.29	17.43
10	QPSK	9	62.12	15.23	18	63.56	17.99
5	64QAM	13.5	62.74	16.37	27	62.87	16.61
5	16QAM	9	62.33	15.62	18	63.11	17.08
5	QPSK	4.5	63.11	17.08	9	63.49	17.85
3	64QAM	8.1	62.59	16.09	16.2	61.96	14.97
3	16QAM	5.4	62.59	16.09	10.8	58.31	9.83
3	QPSK	2.7	57.58	9.04	5.4	57.08	8.53
1.4	64QAM	3.24	52.59	5.09	6.48	52.42	4.99
1.4	16QAM	2.16	55.69	7.27	4.32	52.42	4.99
1.4	QPSK	1.08	41.45	1.41	2.16	50.75	4.11

The path loss increases as the distance of femto users from their femtocells increase. The path loss does not have a linear relationship with the distance because of the logarithm function involved in the equations of Section 4.2.1 used to compute the path loss. Table 7 also confirms that the path loss is independent of the type of modulation scheme. Figure 15 shows the comparison of path loss (in dB) of Femto U1 and Femto U2 against their distances (in meters) from their femtocells.

4.5.2 Case Study 2

For Case Study 2, the scenario shown in Figure 16 has been run and simulated. In Case Study 1, the emphasis was to analyse the performance of all LTE supported bandwidths against different modulation schemes. In Case Study 2, the aim is to increase the load on the network and then to analyse the throughput and path loss of the femto and macro users while keeping the modulation scheme and LTE supported bandwidth constant.

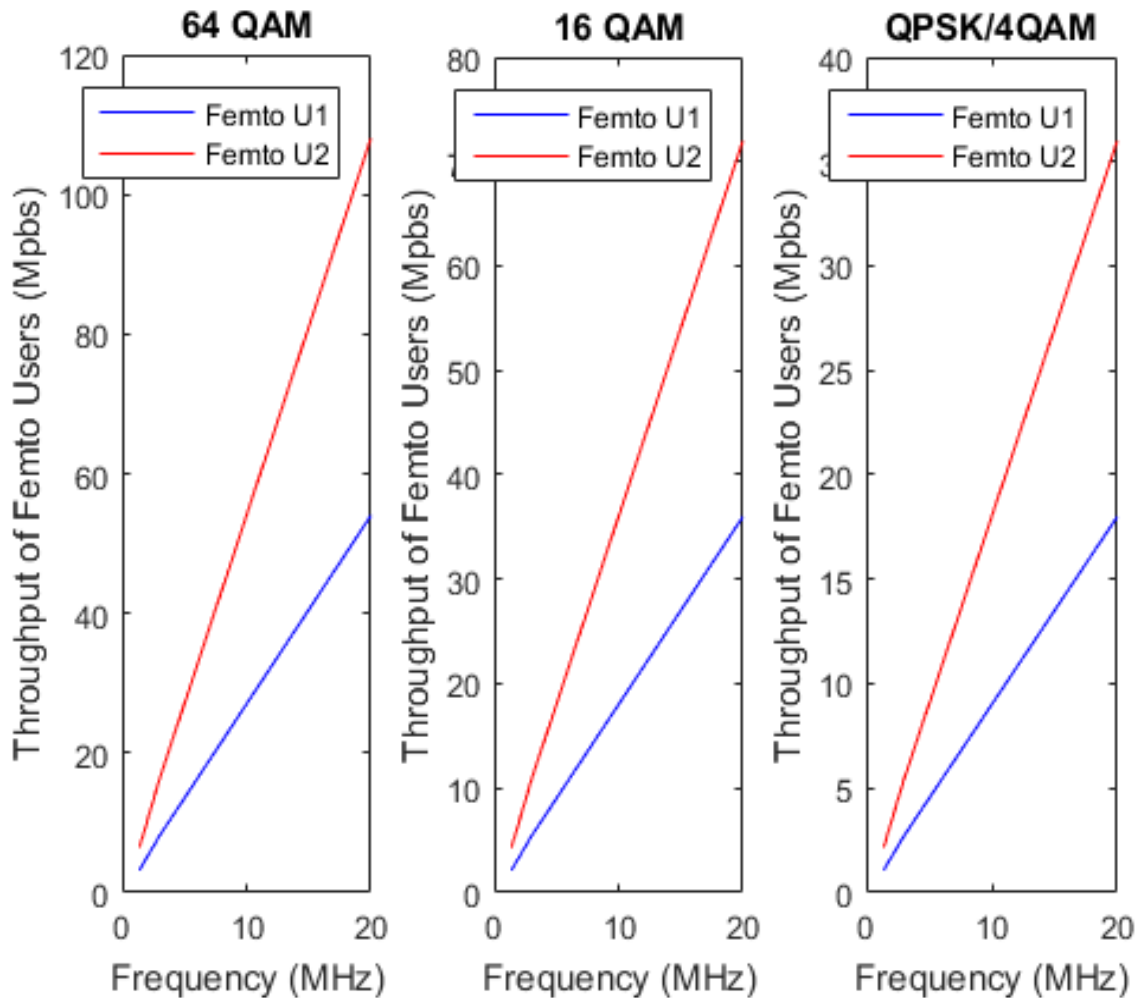


Figure 14: Throughput comparison of Femto U1 and Femto U2 for 64QAM, 16QAM and QPSK

The throughput and path loss are calculated according to the mathematical modelling illustrated in Section 4.2. The values of the parameters used in the simulation framework for this scenario are stated in Table 8. To start with, 15 femtocells are selected to be placed within the coverage area of macrocell. Only 2 femtocells were selected in the scenario of Case Study 1. Since the aim is to increase the load on the network, therefore, a large number of femtocells are placed in different apartments of the buildings to have a wide range of scenarios for comprehensive analysis. Similarly, 25 femto users are selected for this scenario to be placed in distinct locations of the coverage area. The aim is to create a range of scenarios in which femto users are connected to femtocells under different conditions e.g. some of the femto users are located close to the femtocells with a single or double wall in between while some of the femto users are located further away from the femtocells without any wall in between.

6 macro users are selected to be placed within the defined macrocell coverage area unlike a single macro user in the scenario of the previous Case Study. Macro users are placed in random positions to analyse the effect of the number of walls on the throughput of the macro users.

These settings give a variety of scenarios to have a more realistic and detail analysis of the LTE-A system. The supported bandwidths of LTE-A system are 20, 15, 10, 5, 3 and 1.4 MHz. 20 MHz is selected for this simulation (any bandwidth can be chosen as all bandwidths are already analysed in Case Study 1). Similarly, the most common types of modulation schemes used in 4G LTE are QPSK, 16QAM and 64QAM. 64QAM is selected for this simulation (any modulation scheme can be chosen as all modulation schemes are already analysed in Case Study 1). 5 buildings are selected along the x axis and 3 buildings are selected along the y axis to produce the layout as shown in Figure 16. This layout allows the placement of femtocells, femto users and macro users in different locations within the macrocell coverage area to produce a range of scenarios for comprehensive analysis in an urban environment. A road width of 6 m is chosen to create an urban environment in this simulation.

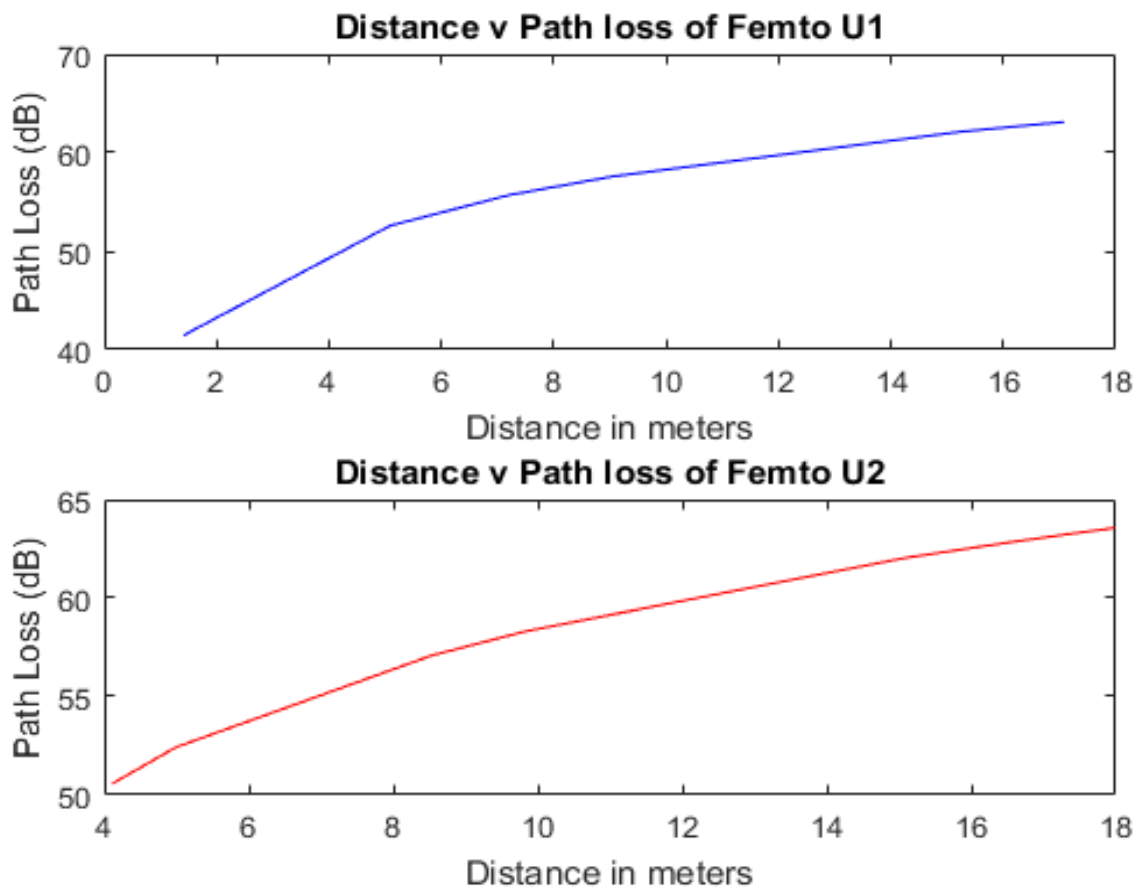


Figure 15: Path Loss comparison of Femto U1 and Femto U2

The manual deployment of femtocells, femto users and macro users takes place by clicking on the points of user choice in the coverage area of macrocell within the hexagonal structure. As the last macro user is placed on the layout, the deployment is considered to be completed. Figure 16 represents the visual representation of the placement of femtocells, femto users attached to their respective femtocells (the femtocell radius is taken as 30 m in this scenario to give better comparison of the effect of walls on the throughput of the femto users) along with

their distances from their respective femtocells, macro users and the macrocell antenna. The macrocell radius, frequency, transmission power of femtocell and macrocell, White Noise Power Density and values of Indoor and Outdoor Wall Losses are same as in Case Study 1 to mitigate any other effects on simulation. An additional user is attached to the Femtocell 1. Table 9 provides information of the user inputs and their values used in the simulation framework for the described scenario.

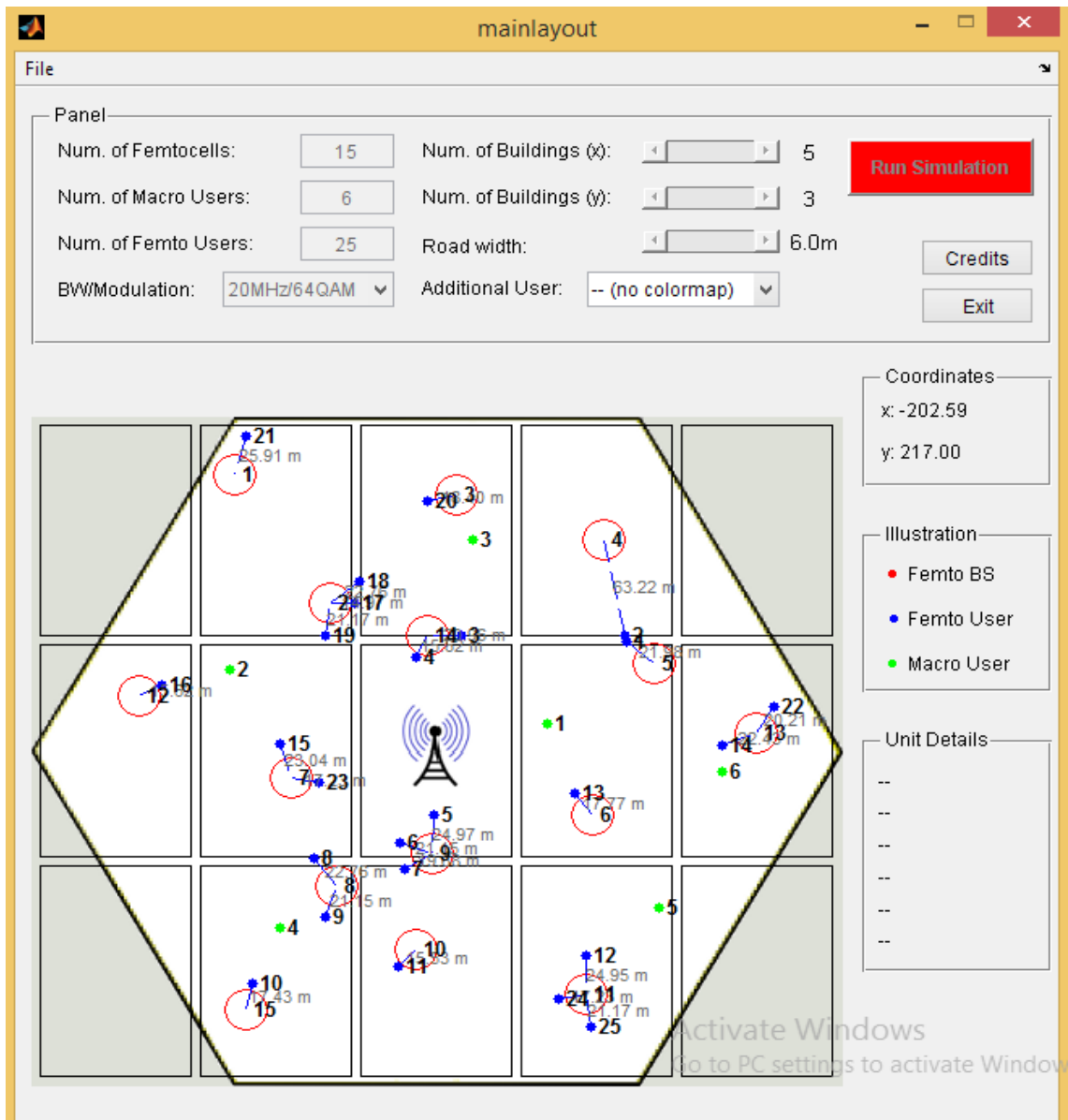


Figure 16: Visual representation of the described scenario for Case Study 2

The simulation is run for the user inputs mentioned in Table 9 at the LTE supported bandwidth of 20 MHz and modulation scheme of 64QAM. The throughput and path loss of all the femto and macro users are calculated and the distances of femto and macro users from their

corresponding femtocells and macrocell are also measured. Table 10 represents the results of the simulation based on the user defined topology of all the femto users.

Table 8: Parameters of simulation framework for Case Study 2

Parameter	Value
Femtocell Radius	30 m
Macrocell Radius	250 m
Frequency	2100 MHz
Femtocell Transmit Power	20 dBm
Macrocell Transmit Power	46 dBm
Indoor Wall Loss (L_{iw})	5 dB
Outdoor Wall Loss (L_{ow})	20 dB
White Noise Power Density	-174 dBm/Hz
Bandwidth	20 MHz
Modulation Scheme	64QAM

Table 9: User inputs of simulation framework for Case Study 2

User Input	Value
Number of Femtocells	15
Number of Femto Users	25
Number of Macro Users	6
Number of Buildings (x)	5
Number of Buildings (y)	3
Road Width	6 m
Additional User connected to	Femtocell 1

Table 10: Throughput and Path Loss of the femto users with respect to the distance/number of walls

Femtocell Number	Femto User Number	Throughput (Mbps)	Path Loss (dB)	Distance (m) /Number of Walls
1	21	36	68.45	25.91/0
2	19	24	65.15	21.17/0
2	17	3.1	81.96	14.97/1
2	18	1.67	86.33	22.76/1
3	20	72	63.76	18.40/0
4	2	46.9	83.01	63.22/0
5	1	9.2	85.76	21.98/1
6	13	72	63.45	17.77/0
7	15	36	66.53	23.04/0
7	23	36	63.18	17.23/0
8	8	1.4	86.33	22.76/1
8	9	36	65.13	21.15/1
9	5	0.07	67.84	24.97/0
9	6	0.63	65.13	21.15/0
9	7	0	104.34	19.68/2
10	11	72	62.28	15.53/0
11	12	24	67.83	24.95/0
11	24	24	63.18	17.23/0
11	25	24	65.15	21.17/0
12	16	72	62.33	15.62/0
13	14	36	66.09	22.43/0
13	22	36	64.57	20.21/0
14	4	0	102.33	15.62/2
14	3	17.4	64.98	20.96/0
15	10	72	63.29	17.43/0

Since an additional user is also connected to the Femtocell 1 as stated in Table 9, the Femtocell 1 has to serve two users in its proximity. As a result, the calculated throughput of the Femto User 21 is 36 Mbps which is also equal to the throughput of additional user as available bandwidth is shared between the two users. Three Femto Users 19, 17 and 18 are connected to the Femtocell 2. The Femto User 19 has a throughput of 24 Mbps as there is no wall between the user and the femtocell, whereas the Femto User 17 although located only 14.97 m away from the Femtocell 2, has a throughput of only 3.1 Mbps. This clearly shows that if a user is in a close proximity of the femtocell but if there is a wall in between, the signal strength reduces to a great extent and consequently the user suffers low bandwidth. The Femto User 18 has a throughput of only 1.67 Mbps because of the effect of the wall and being farther away from the Femtocell 2 in comparison to the other 2 users attached to the same femtocell. The Femto Users 20, 13, 11, 16 and 10 all have a maximum throughput of 72 Mbps as they are the only users in the close proximity of their femtocells and have no wall in between them and their corresponding femtocells. The Femto User 2 is the only user attached to the Femtocell 4 with no wall in between but since it is 63.22 m away from the Femtocell 2, the throughput is degraded to 46.9 Mbps. This shows the user without any obstacles in between still suffers degradation of signal if it moves away from its femtocell. Since the Femto User 1 is located in between the walls, despite being the only user connected to Femtocell 5 has a throughput of only 9.2 Mbps. The Femto Users 5 and 6 being so close to the macrocell suffer cross tier interference and therefore have an extremely low throughput of 0.07 and 0.63 Mbps respectively. The Femto User 7 although located only 19.68 m away from the Femtocell 9, has two walls in between them and consequently results in 0 throughput. This indicates that even if the users are in close proximity of the femtocells but there are walls in between in places like corridor etc., they might end up having 0 throughput. Therefore, femtocells should be placed separately in corridors to mitigate the effect of walls preventing degradation of the signals. The bandwidth is shared equally amongst the Femto Users 12, 24 and 25 as they all are connected to the Femtocell 11 with no wall in between them. This same applies to Femto Users 14 and 22 that are both connected to the Femtocell 13, and Femto Users 15 and 23 that are both connected to the Femtocell 7 and therefore all have a throughput of 36 Mbps each. Although the Femto Users 3 and 4 are both connected to the same Femtocell 14, they have quite different throughputs. Femto User 4 because of two walls in between itself and the femtocell has a throughput of 0 while Femto User 3 has a throughput of only 17.4 Mbps as it suffers from cross tier interference because of being so close to the macrocell.

The path loss increases as the distance of femto users from their femtocells increase. The path loss does not have a linear relationship with the distance because of the logarithm function involved in the equations of Section 4.2.1 used to compute path loss as seen clearly in the

Figures 17-19. The path loss further increases if there are any obstacles e.g. walls in between the femto user and its femtocell as evident from the simulation results of Table 10. According to Table 10, the path loss of the Femto User 21 is 68.45 dB with a distance of 25.91 m from its femtocell. In contrast, the path loss of the Femto User 17 is 81.96 dB, although it is only 14.97 m away from its femtocell but has a wall in between. Similarly, the path loss of the Femto User 7 is 104.34 dB because of two walls in between the user and its femtocell. Hence, it is shown from the simulation results that the path loss has further increased as the number of walls between the user and its femtocell increase.

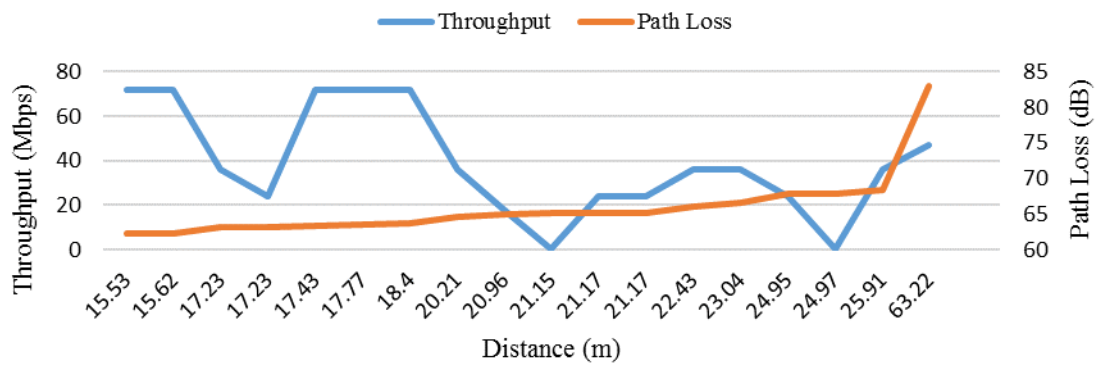


Figure 17: Throughput and Path Loss of the femto users with respect to the distance/0 wall

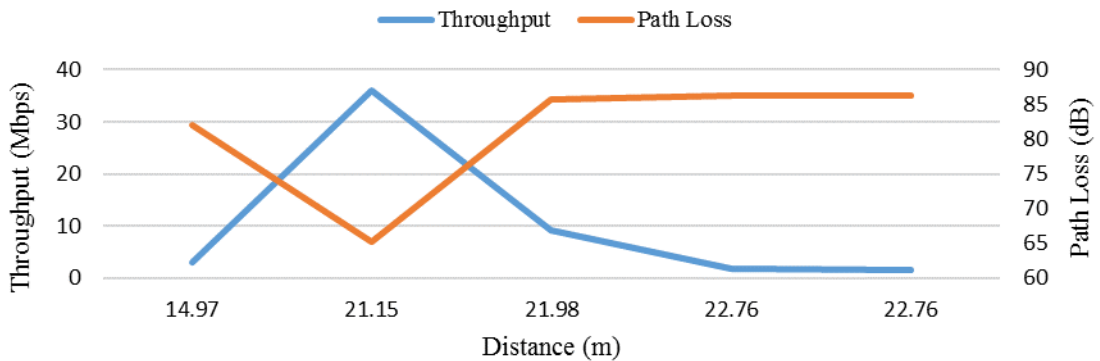


Figure 18: Throughput and Path Loss of the femto users with respect to the distance/1 wall

In Case Study 1, the performance was analysed for all LTE supported bandwidths against each modulation scheme. In Case Study 2, the results are analysed in terms of increasing the load on the network and the effect that the walls have on the throughput and path loss of the femto users. Therefore, the results are also presented in a different way. For Case Study 2, the throughput and path loss of the femto users are graphically represented with respect to their distances from their corresponding femtocells and the number of walls in between them. The graphs showing the comparison of throughput and path loss against the distance per number of walls of all the femto users are shown in Figures 17-19. Throughput is shown by a solid blue

line whereas a solid orange line represents the path loss. Throughput axes are shown on left side of the figures along the vertical axes. Path loss axes are shown on right side of the figures along the vertical axes. Both sides of vertical axis are utilised so that both the throughput and path loss can be plotted together with respect to the distance per number of walls. The distance is shown along the horizontal x axis. The values along the axis of throughput, path loss and distance are varied in each figure according to the simulation values of Table 10.

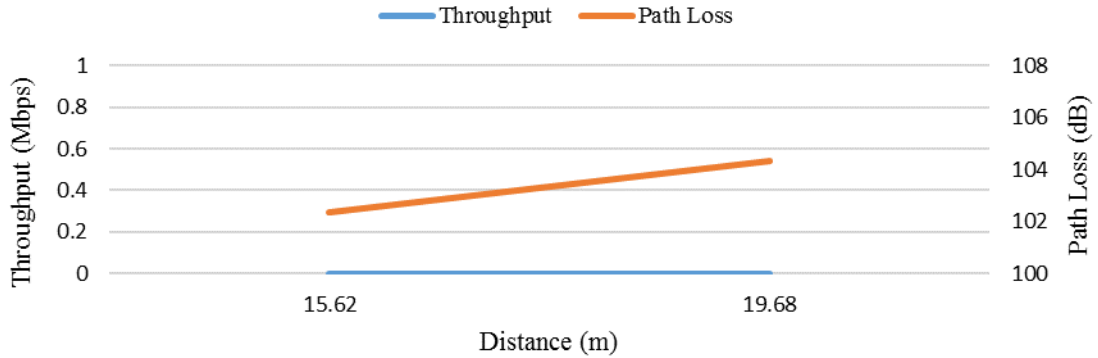


Figure 19: Throughput and Path Loss of the femto users with respect to the distance/2 walls

Similarly, Table 11 represents the results of the simulation based on the user defined topology of all the macro users.

Table 11: Throughput and Path Loss of the macro users with respect to Distance/Number of Walls

Macro User Number	Location	Throughput (Mbps)	Path Loss (dB)	Distance (m) /Number of Walls
1	Indoor	12	94.74	70.29/2
2	Indoor	8.25	105.81	138.39/2
3	Indoor	0.27	105.86	138.82/2
4	Indoor	0.06	117.02	149.12/4
5	Indoor	0.33	119.13	169.66/4
6	Indoor	0.01	119.74	176.10/4

The throughput of the Macro User 1 is 12 Mbps as it is 70.92 m away from the macrocell with two walls in between them. The throughput of the Macro Users 2 and 3 are further reduced to 8.25 and 0.27 Mbps respectively as their distances from the macrocell are significantly increased with two walls each in between them. The Macro Users 4, 5 and 6 have almost negligible throughputs of 0.06, 0.33 and 0.01 Mbps respectively because of being farther away from macrocell and 4 walls each between them and the macrocell.

In case of path loss, the Macro User 1 has a path loss of 94.74 dB with a distance of 70.29 m from the macrocell and two walls in between them. Likewise, the Macro Users 2 and 3 have a path loss of 105.81 dB and 105.86 dB with distances of 138.39 m and 138.82 m respectively and two walls in between them and the macrocell. This proves that although number of walls

are same, but path loss of one macro user is more than the other because of being farther away from the macrocell. The path loss of the Macro Users 4, 5 and 6 is further increased to 117.02 dB, 119.13 dB and 119.74 dB because they are located at a larger distance of 149.12 m, 169.66 m and 176.10 m respectively from the macrocell with each having 4 walls in between them and the macrocell.

The graphs showing the comparison of throughput and path loss against the distance per number of walls of all the macro users are shown in Figures 20 and 21. Throughput is shown by a solid blue line whereas a solid orange line represents the path loss. The distance is shown along the horizontal x axis. The values along the axis of throughput, path loss and distance are varied in each figure according to the simulation values of Table 11.

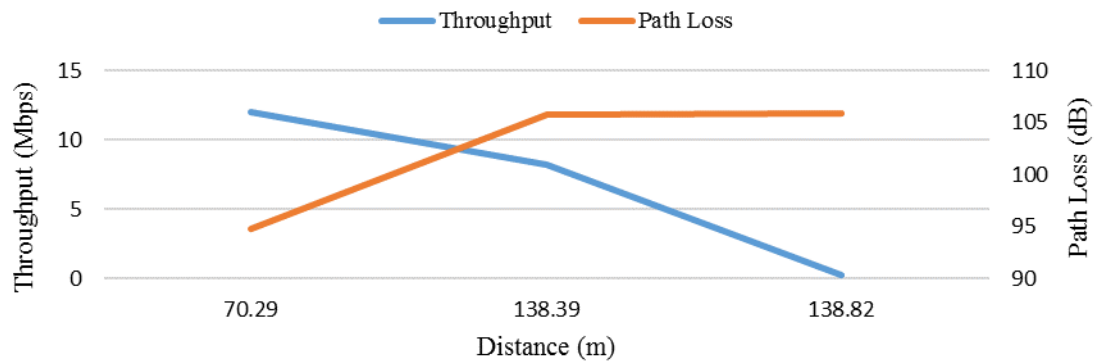


Figure 20: Throughput and Path Loss of the macro users with respect to the distance/2 walls

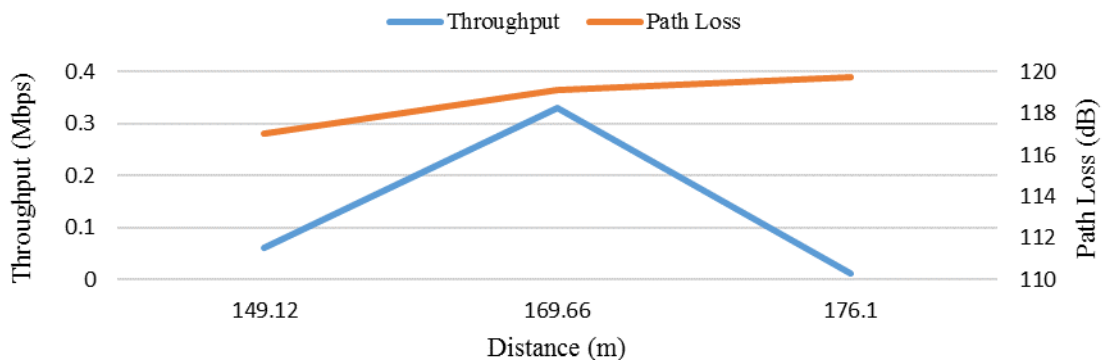


Figure 21: Throughput and Path Loss of the macro users with respect to the distance/4 walls

4.5.3 Case Study 3

For Case Study 3, three different scenarios have been run and simulated. In Case Study 1, the emphasis was to analyse the performance of all LTE supported bandwidths against different modulation schemes. In Case Study 2, the aim was to increase the load on the network and then to analyse the throughput and path loss of all the femto and macro users by taking the effect

walls into account. In this Case Study, three different scenarios are simulated by keeping the parameters of the simulation framework and the user inputs for the simulation framework constant. Only the positioning of the femtocells and the femto users are varied in each scenario to analyse the performance of LTE-A system with femtocell overlays on the basis of throughput and path loss. The visual representation of three scenarios are shown in Figures 22-24.

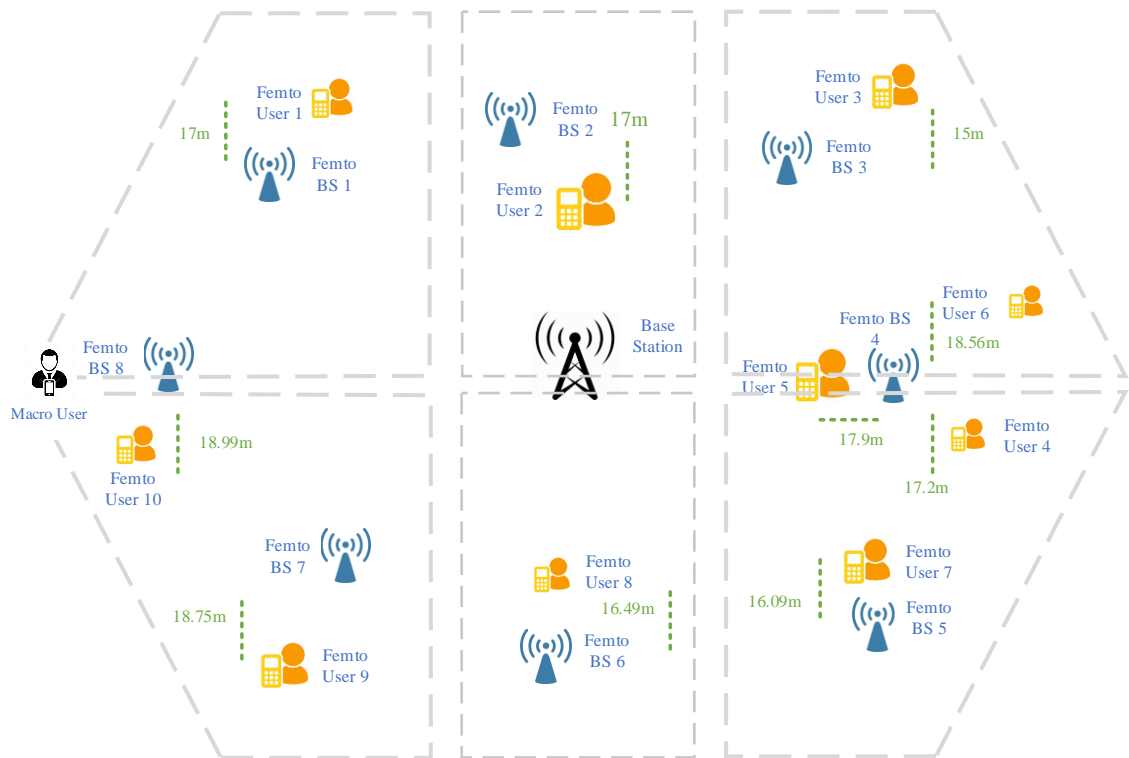


Figure 22: Visual representation of Scenario 1 for Case Study 3

The throughput and path loss are calculated according to the mathematical modelling outlined in Section 4.2. The values of the parameters used in the simulation framework for these scenarios are shown in Table 12. Table 13 provides the values of the user inputs for three different scenarios used in the simulation framework. The simulation is run for each scenario for the user inputs mentioned in Table 13 at the LTE supported bandwidth of 20 MHz and the modulation scheme of 64QAM. In each of the scenarios, only the positions of the femtocells and the femto users along with their distances from their corresponding femtocells are altered. The throughput and path loss of all the femto users are calculated with respect to their distances per number of walls from their corresponding femtocells for each scenario.

For Scenario 1, the maximum throughput achieved by most of the femto users is 72 Mbps since they are the only users in the coverage area of their femtocells (all femto users are located within 20 m proximity of their corresponding femtocells) with no wall in between them and their femto base stations. Although it is at a distance of 17.9 m with no wall in between from its femtocell, the throughput of the Femto User 5 is 22.6 Mbps because two other femto users are

connected to the same femtocell. The achieved throughputs are considerably decreased to 30.78, 13.53 and 10.81 Mbps for the femto users having a wall in between them and their corresponding femtocells. The Femto User 4 has a throughput of only 10.81 Mbps because of a wall and presence of other femto users in the proximity of the same femtocell. The throughputs of all the femto users in Scenario 1 can be seen in Table 14. Figure 25 shows a considerable increase in throughput of the femto users with no wall as compared to those femto users having a wall in between them and their corresponding femtocells. Throughput is shown by a solid blue line. Throughput calculated in Mbps along vertical axis is shown against the number of walls along the horizontal axis.

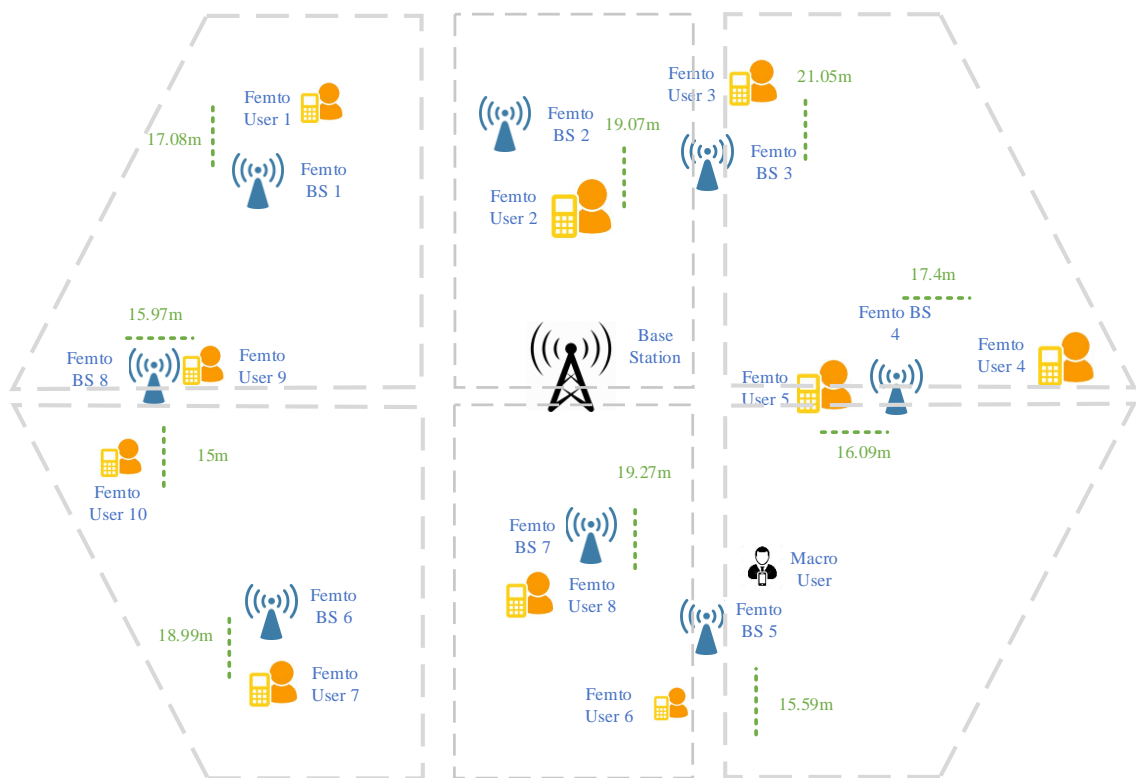


Figure 23: Visual representation of Scenario 2 for Case Study 3

For Scenario 1, it is evident from Table 14 that the path loss of a femto user increases with the increase of distance from its femtocell. The path loss further increases if there are any obstacles e.g. walls in between the femto user and its femtocell. For example, the path loss of the Femto User 9 is 63.92 dB with a distance of 18.75 m from its femtocell. In contrast, the path loss of the Femto User 4 is 83 dB, although it is only 17.2 m away from its base station but has a wall in between. Hence, the path loss has further increased with the increase in number of walls between the user and its femtocell as seen in the simulation results of Table 14. Figure 26 shows a decrease in path loss of the femto users with no wall as compared to having a wall in between them and their corresponding femtocells. Path loss is represented by a solid orange line. Path

loss in dB along vertical axis is shown against the number of walls along the horizontal axis in Figure 26.

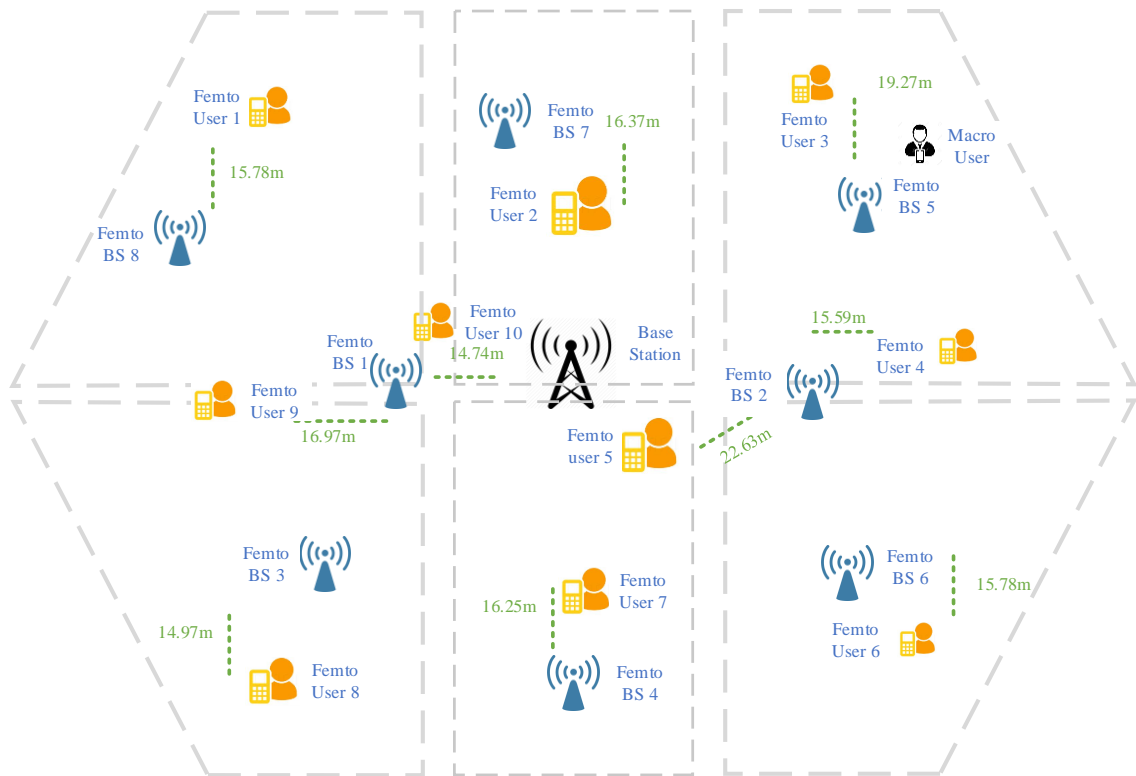


Figure 24: Visual representation of Scenario 3 for Case Study 3

Table 12: Parameters of simulation framework for Case Study 3

Parameter	Value
Femtocell Radius	20 m
Macrocell Radius	250 m
Frequency	2000 MHz
Femtocell Transmit Power	20 dBm
Macrocell Transmit Power	46 dBm
Indoor Wall Loss (L_{iw})	5 dB
Outdoor Wall Loss (L_{ow})	20 dB
White Noise Power Density	-174 dBm/Hz
Bandwidth	20 MHz
Modulation Scheme	64QAM

Table 13: User inputs of simulation framework for Case Study 3

User Input	Value
Number of Femtocells	8
Number of Femto Users	10
Number of Macro Users	1
Number of Buildings (x)	3
Number of Buildings (y)	2
Road Width	5 m

Table 14: Throughput and Path Loss of the femto users with respect to the distance per number of walls for Scenario 1

Femto User ID	Throughput (Mbps)	Path Loss (dB)	Distance (m)	/Number of Walls
1	72	63	17	0
2	72	63	17	0
3	72	63.56	15	0
4	10.81	83	17.2	1
5	22.6	62.59	17.9	0
6	13.53	83.8	18.56	1
7	72	62.59	16.09	0
8	72	62.79	16.49	0
9	72	63.92	18.75	0
10	30.78	84.03	18.99	1

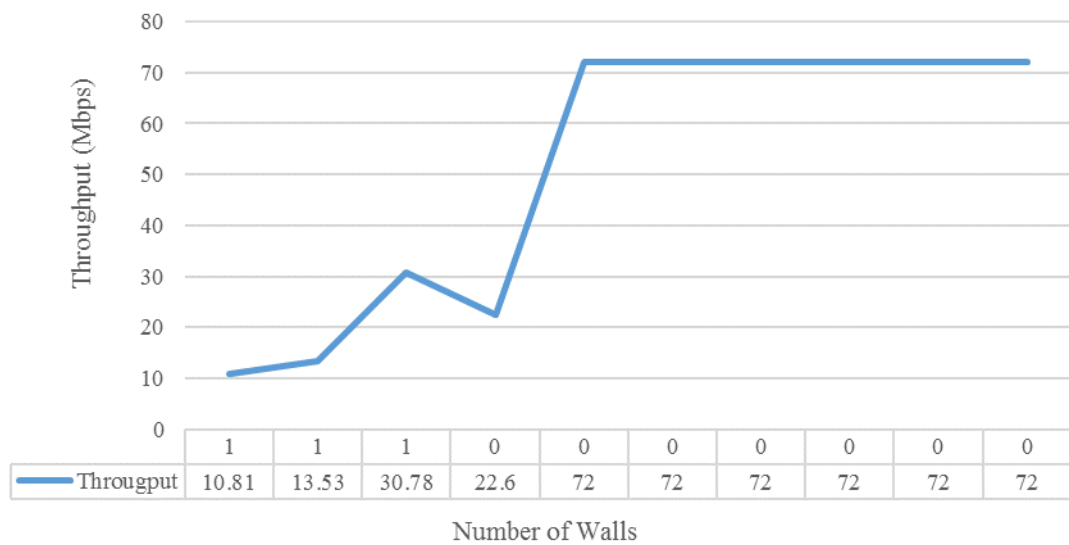


Figure 25: Throughput of the femto Users with respect to the distance per number of walls for Scenario 1

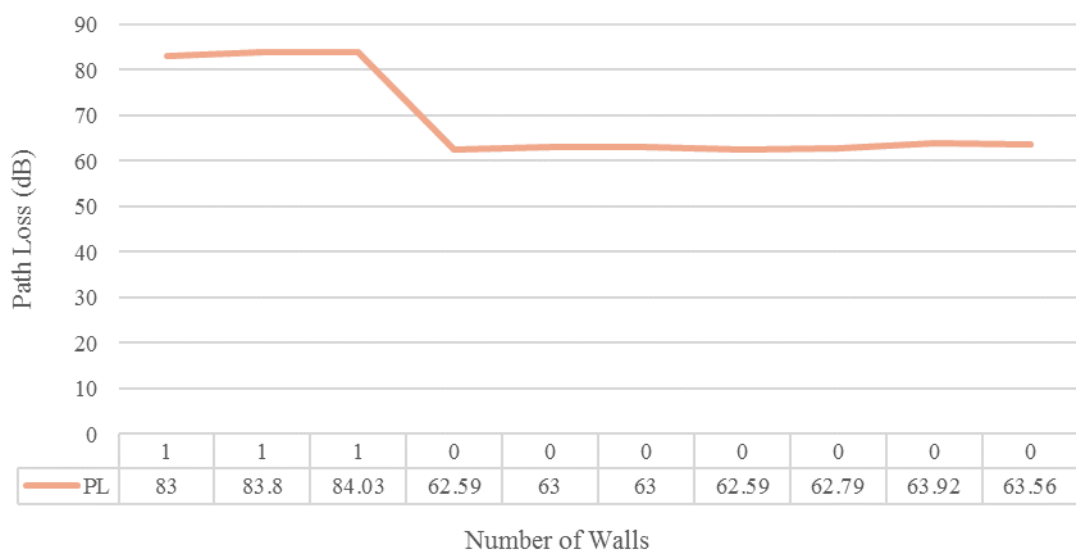


Figure 26: Path Loss of the femto users with respect to the distance per number of walls Scenario 1

For Scenario 2, the maximum throughput achieved by most of the femto users is 72 Mbps since they are the only users in the coverage region of their femtocells. Although it is at a distance of 15.97 m with no wall in between from its femtocell, the throughput of the Femto User 9 is 36 Mbps because bandwidth is shared with other femto user connected to the same femtocell. The estimated throughputs are substantially reduced to 18.18, 10.1, 2.34 and 1.86 Mbps for the femto users having a wall in between them and their corresponding femtocells. The Femto User 10 has a throughput of only 1.86 Mbps because of a wall and presence of other femto user in the proximity of the same femtocell. The throughputs of all the femto users in Scenario 2 can be seen in Table 15. Figure 27 shows a considerable increase in throughput of the femto users with no wall as compared to those femto users having a wall in between them and their corresponding femtocells. Throughput is shown by a solid blue line. Throughput calculated in Mbps along vertical axis is shown against the number of walls along the horizontal axis.

Table 15: Throughput and Path Loss of the femto users with respect to the distance per number of walls for Scenario 2

Femto User ID	Throughput (Mbps)	Path Loss (dB)	Distance (m)	/Number of Walls
1	72	63.1	17.08	0
2	66.2	64.07	19.07	0
3	10.1	85	21.05	1
4	18.18	83.29	17.4	1
5	28.26	62.59	16.09	0
6	2.34	82.32	15.59	1
7	72	64	18.99	0
8	72	64.16	19.27	0
9	36	62.53	15.97	0
10	1.86	81.98	15	1

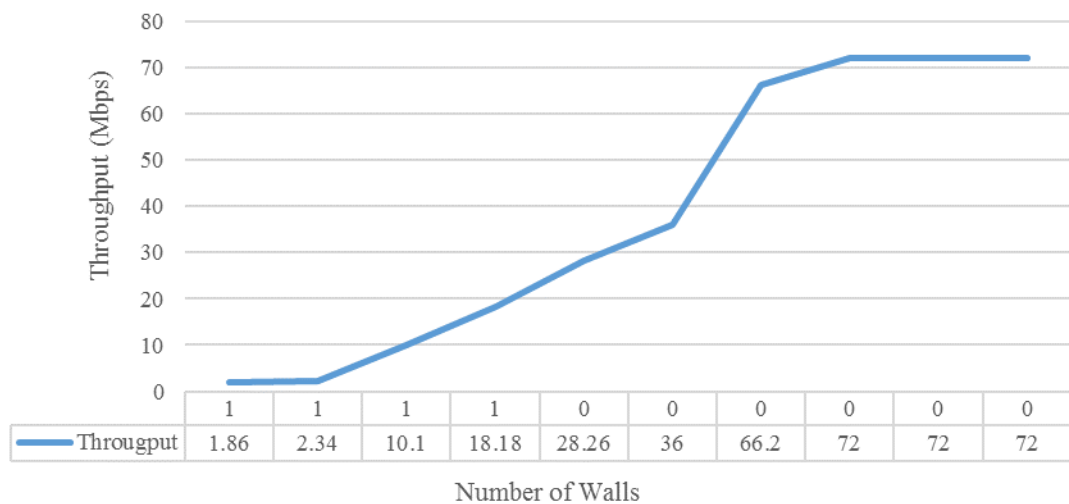


Figure 27: Throughput of the femto users with respect to the distance per number of walls for Scenario 2

For Scenario 2, it can be clearly seen in Table 15 that the path loss of a femto user increases with the increase of distance from its femtocell. The path loss further increases if there are any

obstacles e.g. walls in between the femto user and its femtocell. For example, the path loss of the Femto User 7 is 64 dB with a distance of 18.99 m from its femtocell. In contrast, the path loss of the Femto User 10 is 81.98 dB, although it is only 15 m away from its base station but has a wall in between. Hence, the path loss has further increased with the increase in number of walls between the user and its femtocell as can be seen in Table 15. Figure 28 shows a decrease in path loss of the femto users with no wall as compared to having a wall in between them and their corresponding femtocells. Path loss is represented by a solid orange line. Path loss in dB along vertical axis is shown against the number of walls along the horizontal axis in Figure 28.



Figure 28: Path Loss of the femto users with respect to the distance per number of walls for Scenario 2

For Scenario 3, the estimated throughput calculated for most of the femto users is 72 Mbps since they are the only users in the coverage region of their femtocells. Although it is at a distance of 16.97 m with no wall in between from its femtocell, the throughput of the Femto User 9 is 8.42 Mbps because bandwidth is shared with other femto user connected to the same femtocell. The calculated throughputs are significantly decreased to 2.61, 0.15 and 0.03 Mbps for the femto users having a wall in between them and their corresponding femtocells. The Femto Users 4 and 5 have throughputs of only 2.61 and 0.03 Mbps respectively because of a wall in between them and their corresponding femtocell and both are connected to the same femtocell thereby sharing bandwidth between them. The throughputs of all the femto users in Scenario 3 can be seen in Table 16. Figure 29 shows a considerable increase in throughput of the femto users with no wall as compared to those femto users having a wall in between them and their corresponding femtocells. Throughput is shown by a solid blue line. Throughput calculated in Mbps along vertical axis is shown against the number of walls along the horizontal axis.

For Scenario 3, the simulated results of Table 16 show that the path loss of a femto user increases with the increase of distance from its femtocell. The path loss further increases if there are any obstacles e.g. walls in between the femto user and its femtocell. For example, the path loss of the Femto User 3 is 64.1 dB with a distance of 19.27 m from its femtocell. In contrast, the path loss of the Femto User 4 is 82.32 dB, although it is only 15.59 m away from its base station but has a wall in between. Hence, the path loss has further increased with the increase in number of walls between the user and its femtocell and can be seen in Table 16. Figure 30 shows a decrease in path loss of the femto users with no wall as compared to having a wall in between them and their corresponding femtocells. Path loss is represented by a solid orange line. Path loss in dB along vertical axis is shown against the number of walls along the horizontal axis in Figure 30.

Table 16: Throughput and Path Loss of the femto users with respect to the distance per number of walls for Scenario 3

Femto User ID	Throughput (Mbps)	Path Loss (dB)	Distance (m)	/Number of Walls
1	72	62.42	15.78	0
2	72	62.74	16.37	0
3	72	64.1	19.27	0
4	2.61	82.32	15.59	1
5	0.03	86.23	22.63	1
6	72	62.42	15.78	0
7	72	62.68	16.25	0
8	72	61.66	14.97	0
9	8.42	63.1	16.97	0
10	0.15	81.83	14.74	1

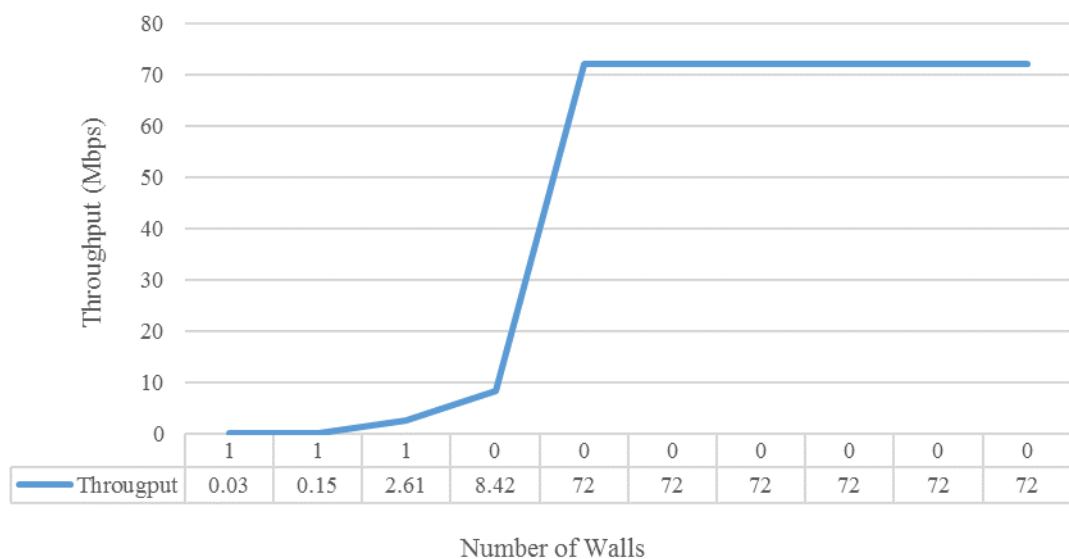


Figure 29: Throughput of the femto users with respect to the distance per number of walls for Scenario 3



Figure 30: Path Loss of the femto users with respect to the distance per number of walls for Scenario 3

4.6 Conclusion

The graphical user interface of the simulation framework allows the flexibility to set up the desired two-tier network topology. The framework is effectively utilised to set up the simulations according to the desired parameters. It calculates the throughput and path loss of all the femto and macro users for all the supported bandwidths of an LTE-A system using different modulation schemes. A series of tests are carried out to calculate the maximum throughput and path loss for the described scenarios. An environment is defined to analyse various scenarios in which femtocells are working in conjunction with a macrocell to create a two-tier mobile network. The experiments are run several times for different values and the simulation results are evaluated in terms of throughput and path loss. The bandwidth and modulation schemes are varied initially for simulation in Case Study 1 to analyse the effect they have on the throughput and path loss of the femto users. The simulation framework was able to analyse the performance and showed that for any bandwidth of an LTE-A system with femtocell overlays, the throughput of a femto user was increased two times for 16QAM modulation scheme as compared to QPSK. The throughput was increased to three times for 64QAM as compared to QPSK. The simulation results also confirmed that the path loss is independent of the modulation scheme. Case Study 1 used minimal load on the network because the aim was to analyse the change in throughput and path loss with respect to the change in modulation scheme for each LTE-A supported bandwidth. In Case Study 2, the load on the network was increased to test the capacity and capability of the simulation framework as the number of femtocells were increased and additional femto and macro users were added to the network. The aim was to examine the effect of walls on the throughput and path loss of the users and the effect of additional users on the throughput and path loss of the users connected to the same femtocells. In Case Study 3, the type of modulation scheme and LTE supported bandwidth was kept constant and positioning of

the femtocells was changed for each scenario inside the buildings to analyse the performance. The aim was to analyse the effect of changing the positions of the femtocells only on the throughput and path loss of the femto users if all other parameters are kept constant. This simulation framework is able to identify the extent to which the signal strength is reduced. It is shown that if a user is located in the close proximity of a femtocell but there is a wall in between, the signal strength reduces to a great extent and consequently the user suffers low bandwidth. In places such as corridors etc., users sometime end up with almost no connectivity. Therefore, it is important to make sure that femtocells are placed separately in corridors to mitigate the effect of walls thus preventing the degradation of signals for the users. The bandwidth is shared amongst femto users if they all are connected to the same femtocell. Hence, the optimised location is placing the femtocell in the middle of a room or office so that the users in the corner still have reasonable throughput. The simulation framework incorporating two-tier mobile network is able to verify that the simulations accurately result in what is expected as a result of testing various scenarios in different case studies. In places like offices etc. with large number of people and where number of users also change constantly, the optimisation algorithm needs to be incorporated in this simulation framework to find the optimised positioning of the femtocells to maintain quality of service. These results will be used and the simulation framework will be further developed to find the optimised positioning of the femtocells in different room layouts unlike frameworks proposed in the previous works which could only be used to analyse the performance of LTE-A two-tier systems. It will be discussed in detail in Chapter 5.

Chapter 5: Development of a Simulation Framework for Optimising Femtocell Networks

This chapter is an extension of the previous work described in Chapter 4. In Chapter 4, the aim was to analyse the change in throughput and path loss of the femto and macro users with respect to the change in modulation scheme for each LTE-A supported bandwidth. Then, the number of femtocells were increased and additional femto and macro users were added to the network to analyse the performance in terms of throughput and path loss of the femto and macro users. The effect of walls on the throughput of the users was also examined in Chapter 4. In this chapter, an optimisation algorithm is integrated to the simulation framework discussed in Chapter 4 to find the optimal positions of the femtocells on the basis of throughput and path loss in an indoor environment. This simulation framework is unique as a user friendly simulation framework integrating optimisation algorithm to find the optimised positioning of the femtocells on the basis of throughput and path loss is not implemented in the literature to the best of the knowledge of the author. In addition, the mix of algorithms integrated in this simulation framework to find the optimised positioning of the femtocells are not used in the literature before and hence form the contribution to knowledge of this research. The type of modulation scheme and LTE supported bandwidth of the femtocells are kept constant and only positioning of the femtocells are optimised inside the building to analyse the performance. The singularities of femtocells such as their unplanned deployment, short range and restricted number of users that a femtocell can accommodate etc., characteristics of an indoor environment such as multipath reflections, number of people etc., and the effect of walls pose different challenges (Aguilar-Garcia et al. 2016a). In such an environment, the optimised positioning of the femtocells is determined based on the genetic optimisation algorithm discussed below.

5.1 Genetic Algorithms (GAs)

Genetic Algorithms were introduced by John Henry Holland in 1975 (Goldberg and Holland 1988). They are one of the most robust type of global search algorithms for finding the optimum solution based on natural selection from population to population. Decision variables are encoded into chromosomes which are represented by a binary string of finite length i.e. the string of ones and zeros in this algorithm. Each chromosome consists of bits called genes and their values are defined as alleles (Johnson and Rahmat-Samii 1997). The presence of a certain measure is necessary for selecting the best solutions to implement the natural evolution. An objective function represented by a mathematical model of the fitness evaluation criteria could be a measure. Genetic algorithms are distinct from other search algorithms because of their initialisation of random solutions called population and each individual in a population represents the solution to the problem called chromosome. Chromosomes are then evolved iteratively known as generations. The chromosomes with the best fitness are selected while the

fragile individuals are rejected from the population in each generation. The best individuals are generated called off-springs by the application of the genetic algorithm operators namely selection, crossover and mutation. A careful use of a selection operator is important as it controls the preference of the individuals for producing off-springs for next generation. In case of a strong selection, most fit suboptimal solutions may take charge of population thereby reducing diversity. If the selection is weak, it results in slow convergence (Arora et al. 2018).

Genetic algorithms unlike conventional search methods depend on their population. The user defines the size of population which affects the scalability and performance of the genetic algorithms. Small sizes of population often result in premature convergence while large sizes of population may take unnecessary computational time (Mitchell 1998). The crucial part of a genetic algorithm is the selection of the stopping criteria. The stopping criteria is responsible for the convergence of the fitness towards the desired limit. The algorithm stops when the fitness value does not change for the defined number of generations (Harada and Alba 2020; Koohestani 2020). Figure 31 depicts the operation of a genetic optimisation algorithm.

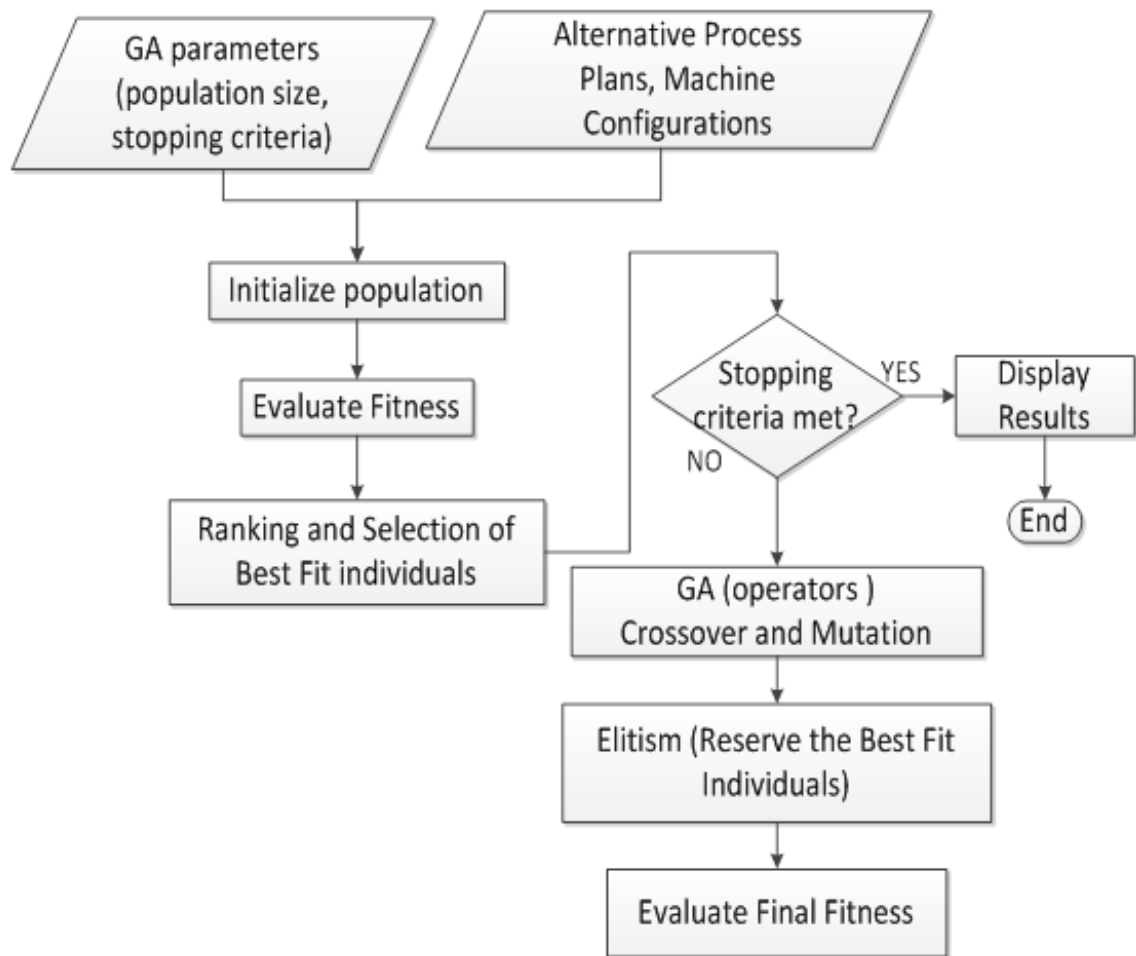


Figure 31: Flowchart of a genetic optimisation algorithm

Genetic algorithms aim to achieve the optimum solutions by starting with the randomly selected design variables. These design variables are then evaluated based on the fitness criteria called the objective function. The set of design variables is selected at random which is a subset of the whole region. This selected subset of design variables is called the population size. These design variables go through the selection method, cross over and mutation where best individuals are segregated and generated because of which the fitness starts converging towards the best fit solution and this algorithm is repeated until some stopping criteria is achieved thus giving the global best optimum or near optimum solution. These best fit individuals are the off-springs for the current generation but parents for the next successive iteration. In this way the evolution cycle continues till the stopping criteria is achieved. The considerable advantage of using the genetic algorithm over the other optimisation techniques is that it does not have intense mathematical requirements. Genetic algorithms have the ability and capacity of handling any type of objective function and constraints. Other evolutionary algorithms lack the diversity of solutions which is better in a genetic algorithm because of its operators. It is least likely to happen in a genetic algorithm that it leaves behind the global solution due to premature or early convergence (Bodenhofer 2003; Arora 2004). To identify the optimum position of a femtocell, there is a need to add the functionality of optimisation in the simulation framework discussed in Chapter 4. Therefore, a genetic optimisation algorithm is incorporated in the simulation framework discussed in Chapter 4 and is the own development to the simulation framework to be able to optimise the network of femtocells.

5.2 Architecture of the Simulation Framework for Optimising Femtocell Networks

Since the femtocells are user deployed, issues such as poor connectivity, low data rate, bad signal reception, insufficient quality of service due to lack of coverage etc. can arise if the femtocells are not placed in optimal positions. The inappropriate deployment of femtocells may result in a decreased network capacity. Therefore, the simulation framework described in detail in Chapter 4 is further developed and enhanced to be able to optimise the femtocell networks. The aim of the further development of this simulation framework is to optimise the femtocell networks in an indoor environment. Since the deployment of femtocells is mostly restricted to an indoor environment because of their range and the need and population density in urban areas, therefore, the graphical user interface is also developed further accordingly for this simulation framework. The designed simulation framework needs to be flexible so that any desired environment can be defined to perform a set of experiments. The simulation framework must have the capacity and capability to optimise any network of femtocells on the basis of throughput and path loss to meet the aim and objectives of this research. The simulation framework calculates the throughput and path loss of all the femto users connected to their respective femtocells according to the numerical modelling already described in detail in

Section 4.2 of Chapter 4. An indoor environment of the building needs to be defined to test the scenarios in which a number of femtocells are deployed in different locations of the rooms inside the building. The number of femtocells and femto users are fed as an input to the simulation framework through graphical user interface. The femto users are randomly deployed inside the building. Since the users working in an office or building are randomly distributed, therefore the algorithm developed for this simulation framework also distributes the femto users randomly inside the building.

The femtocells are categorised into distributed and additional femtocells. The distributed and additional femtocells are represented by different colours on graphical user interface (similar to the graphical user interface discussed in Chapter 4) so that they can be easily distinguished from each other. The purpose of using two different femtocells is that the distributed femtocells are deployed uniformly inside the building whereas the additional femtocells are deployed randomly inside the building. The algorithms developed to carry out the simulations deploy the distributed femtocells in a uniform way that at least one distributed femtocell must be deployed in each room initially, for example, if the building layout has 4 rooms and the number of distributed femtocells to be deployed is also 4, then the algorithm must ensure that each room has a distributed femtocell. If the number of distributed femtocells to be deployed are selected as 5, then 5th distributed femtocell would be allocated to any of the 4 rooms before a distributed femtocell is assigned to each room at first instance. This is to ensure that each room has at least one distributed femtocell, else the users in that room will try to connect to other femtocells outside the room and consequently the signal strength will reduce to a great extent as evident from the simulation results of Chapter 4. The algorithm also ensures that no room in the building has a difference of more than one to any other room all the time while deploying the distributed femtocells inside the building. For example, if the building layout has 4 rooms and the number of distributed femtocells to be deployed is 10, then third distributed femtocell would not be allocated to any room until 2 distributed femtocells are allocated to each room. It means 2 rooms would have 3 distributed femtocells while 2 rooms would have 2 distributed femtocells. The additional femtocells are deployed randomly inside the building to counter the increase in the number of users and to ease the burden on the already serving femtocells.

Once the user inputs i.e. the number of distributed femtocells, the number of femto users, the number of additional femtocells and the number of rooms along x and y axis to generate the building layout are fed to the simulation framework, the indoor environment of the building layout is generated and displayed. All femto users are connected either to the distributed femtocells or additional femtocells. The simulation framework is able to calculate the throughput and path loss of all the femto users with respect to their distance per number of walls from their corresponding femtocells. The algorithm is able to generate the simulation results in

the form of a table so that the results can later be compared once optimisation is performed. After that, optimisation is performed based on the genetic algorithm as described in Section 5.1. The optimisation is carried out according to the following criteria:

1. The positions (x and y coordinates) of the distributed and additional femtocells that can be relocated are taken as variables for optimisation.
2. On the basis of the throughput received by each femto user, the objective (penalty) function is computed. According to the results of extensive simulations carried out in Chapter 4, following are the basis taken for anticipated throughput of each femto user.
 - a. In a case where only one femto user was connected to a femtocell in a close proximity with no wall in between, the maximum throughput received by a femto user was 72 Mbps (as shown in the simulated results of Table 10 of Case Study 2 and simulated results of Tables 14, 15 and 16 of Case Study 3 in Chapter 4).
 - b. In a case where four femto users were located in the close proximity of the femtocell with no wall in between, the maximum value of the estimated throughput received by a femto user was 18 Mbps (since bandwidth was equally shared amongst the femto users as shown in the simulated results of Table 10 of Case Study 2). Since the femto users are randomly deployed inside the building, the location of the femto users remain constant i.e. they remain stationary once deployed. In a case where users are mobile and moving around the environment is outside the scope of these scenarios. This could be done as part of the future work.

The cellular signal strength has a typical range from -50 dB to -110 dB. Since the minimum signal strength needed for data exchange and holding a conversation is at least -100 dB for LTE-A, users experience significant deterioration in signal strength past -100 dB (1 bar reception) till dead zone (0 connectivity) of -120 dB. Therefore, the minimum throughput received by each femto user should be at least 25% of the maximum throughput received by each femto user before optimisation to maintain the quality of service as a result of this optimisation. Consequently, in the above case, the minimum throughput of each femto user must not fall below 4.5 Mbps as a result of optimisation. The limit of the minimum throughput received by each femto user during optimisation can be set to another value and optimisation can be carried out accordingly by using this simulation framework.

3. Objective Function (Penalty Function):

- a. Based on the simulation results and the criteria defined above, the objective function for each femto user is defined as:

$$J = \max\left(\frac{18E6}{\text{number of sharing users}} - \theta, \quad 4.5E6 - \theta\right) \quad (7)$$

where θ is the throughput received by each femto user

- b. If J is negative, the minimum requirement is fulfilled. So comprehensive objective function is defined as:

$$\sum_{i=1}^n J_i \quad \text{if} \quad J_i \text{ is positive} \quad (8)$$

where $i = 1, 2, 3, \dots, n$ (total number of femto users)

4. The bounds of the variables i.e. the positions of the distributed and additional femtocells are defined as:
- a. For each distributed femtocell, the boundary of the walls of the room is set as a bound.
 - b. For each additional femtocell, the boundary of the entire building is set as a bound.

The distributed femtocell must find the optimal position within the same room during optimisation. It must not leave the room, else the users might end up with 0 connectivity if it is the only femtocell providing connectivity to the users in that room. The additional femtocell can move to any room inside the building to ease the burden on the already overloaded distributed femtocells.

5. **Choosing Best Femtocell:** The femto user follows the following criteria during optimisation to connect to a femtocell:
- a. The user first finds the closest femtocell for connection.
 - b. If the femtocell is serving up to 4 users, then no user must leave that femtocell unless the estimated throughput of the femto user is below the desired level before optimisation. This condition is selected on that fact that a typical femtocell can serve 4 users at a time while maintaining quality of service according to the literature review.
 - c. If the femtocell is serving more than 4 users, then to ease the burden on that particular femtocell during optimisation:
 - i. The farthest user connected to that particular femtocell leaves the femtocell first if requires. For example, if 5 users are connected to a particular femtocell, then the user with the maximum distance of all the users from that femtocell tries to leave that femtocell first and connects

to another femtocell. This process continues until the minimum fitness limit is reached and optimisation is terminated.

- ii. In order for the user to be able to connect to another femtocell during optimisation while the simulation is running, the other femtocell must fulfil following conditions:
 - a) The other femtocell must be within the same room.
 - b) The user must not leave its current femtocell if the number of users connected to the other femtocell are more in numbers.
 - c) The difference in the number of users connected to the other femtocell user is trying to connect and the femtocell user is trying to leave must be at least 3. For example, if a user is trying to leave the femtocell serving 11 users and the other femtocell user wants to connect is serving only 1 user, then a user can leave the femtocell serving 11 users and can connect to the other femtocell serving only 1 user. The updated number of users connected to both femtocells will then be 10 and 2 respectively. This process will stop until the femtocell initially serving 12 users will now be serving 7 users and the femtocell initially serving only 1 user will now be serving 5 users.
 - d) One of the coordinates (x or y) of the user must fall in between the two femtocells i.e. the femtocell user is trying to leave and the femtocell user is trying to connect. This is because if the user moves from the other side of the femtocell to a side lies between the two femtocells, regardless of meeting all the previous criteria, the user will not be able to achieve the optimum throughput because of the interference between the two femtocells as seen in some cases of the simulation results of Chapter 4.

The Genetic Algorithm is implemented in MATLAB (codes for performing optimisation and .m file containing optimisation code that needs to run in MATLAB are shown in Appendix B) as an optimisation technique to carry out the simulations according to the criteria mentioned above. The optimisation is terminated as the minimum fitness level is reached. The objective is to achieve the maximum throughput and keep the path loss as minimum as possible for each femto user during optimisation. Since the throughput and path loss are interdependent on each other, the objective function defined on the basis of throughput will consequently adjust the path loss to provide the optimised positioning of the distributed and additional femtocells.

As the process of optimisation completes, a message is displayed in the command window of the MATLAB ‘Optimization terminated: minimum fitness limit reached’. The indoor environment of the building layout is generated and displayed showing the optimised positioning of the distributed and additional femtocells. Since the femto users were already randomly distributed, their positions are not changed. All femto users are now connected either to an optimised positioned distributed femtocell or to an optimised positioned additional femtocell. The simulation framework again calculates the throughput and path loss of all the femto users with respect to their distance per number of walls from their corresponding optimised positioned femtocells. The algorithm is also able to generate the simulation results in the form of a table so that the results achieved after optimisation can be compared with the results before optimisation for comparison and analysis. Figure 32 depicts the architecture of the designed simulation framework for optimising femtocell networks.

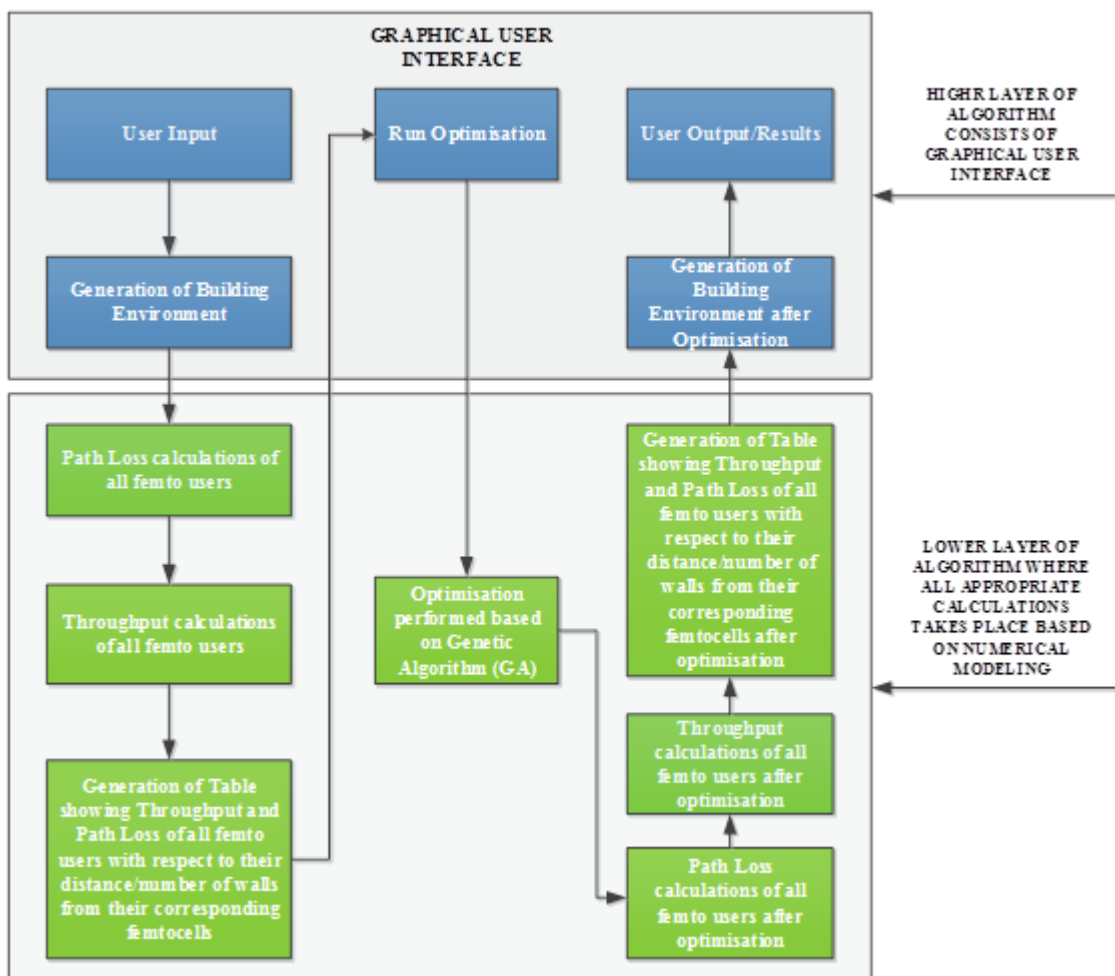


Figure 32: Architecture of the simulation framework for optimising femtocell networks

This simulation framework can also be used to implement other optimisation techniques such as Particle Swarm Optimisation, Fmincon Optimisation etc., but due its ability of fast convergence and to stick on local and global optimum points, a genetic algorithm is implemented as an optimisation technique for this research.

5.3 Simulation Results and Performance Analysis

Two case studies are proposed and analysed by using the simulation framework developed for optimising the femtocell networks. The aim is to find the optimised positioning of the distributed and additional femtocells on the basis of throughput and path loss. The number of distributed and additional femtocells, the number of femto users and the number of rooms along x and y axis are varied in both case studies and the results are analysed in terms of how much the genetic algorithm is able to optimise the whole femtocell network in an indoor environment of the building.

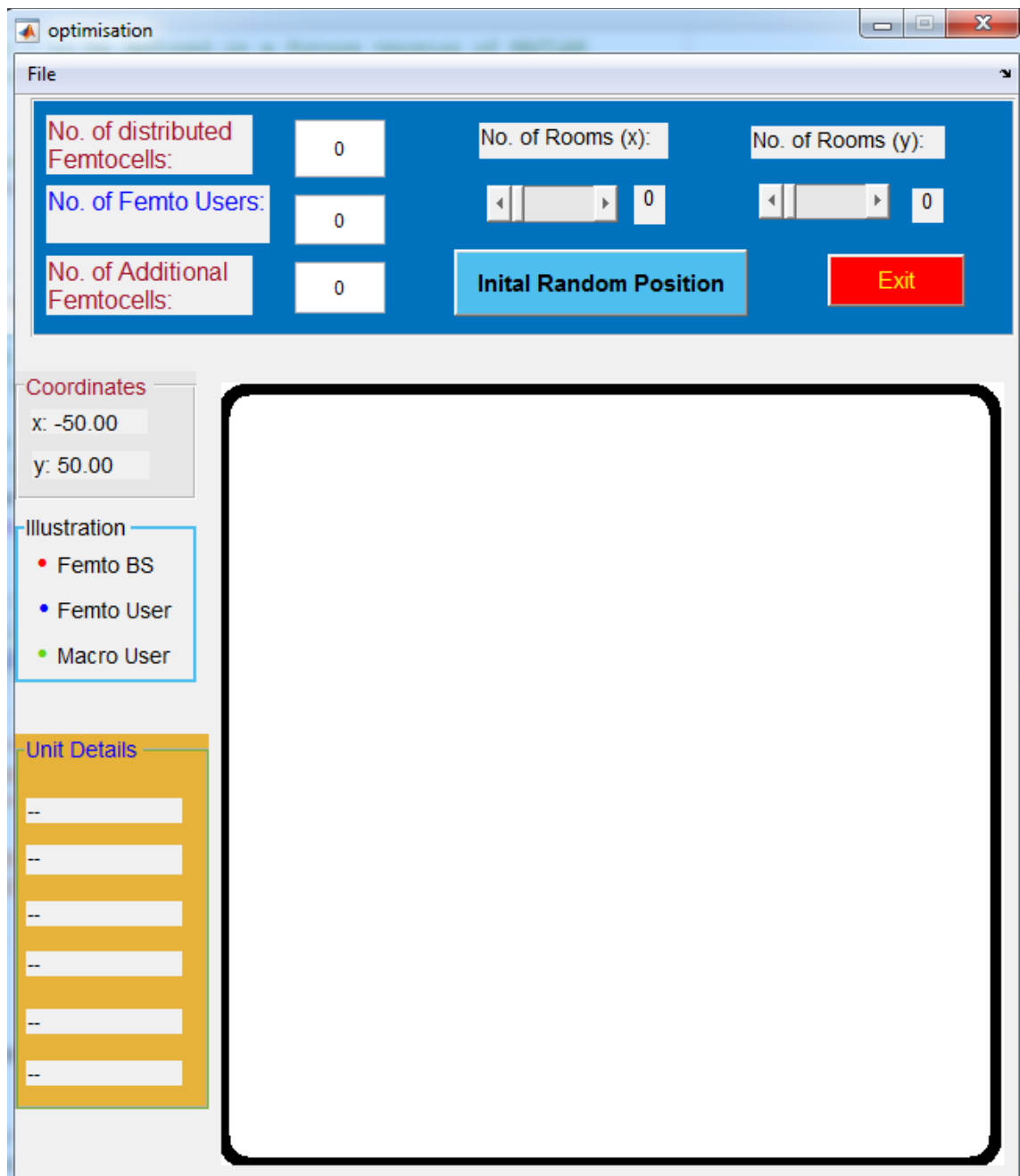


Figure 33: User screen before inputs are fed in the Graphical User Interface

5.3.1 Case Study 1

The graphical user interface developed for this simulation framework allows the end user to communicate with the system in terms of setting the inputs, visualising the network topology once the inputs are fed in the GUI, visualising the optimisation in progress, visualising the building layout before and after optimisation and analysing the output once the optimisation is terminated and minimum fitness level is achieved. Figure 33 depicts the user screen of initial layout of the GUI before the inputs are fed in the GUI.

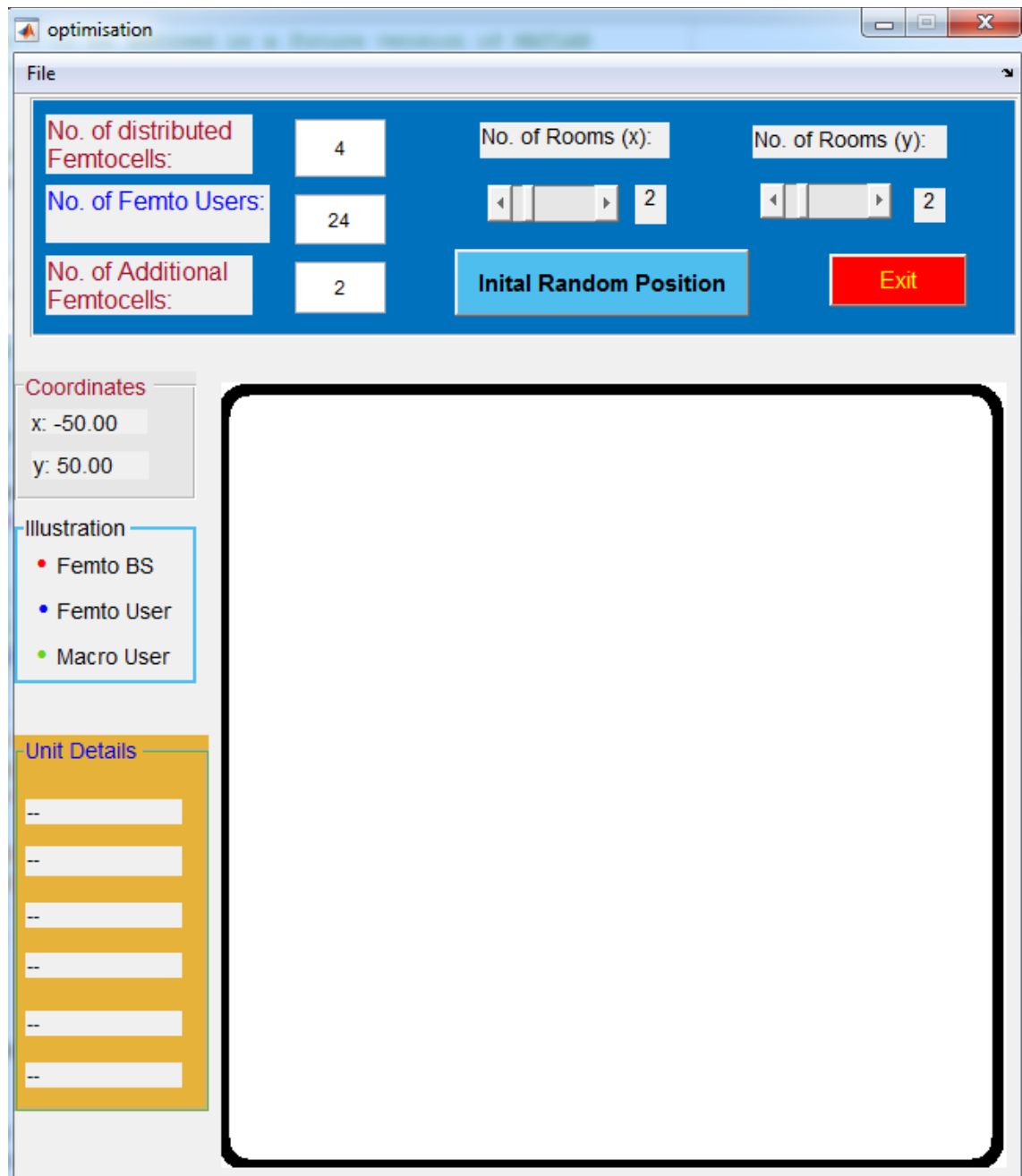


Figure 34: User screen once the inputs are fed in the Graphical User Interface for Case Study 1

The simulation framework needs inputs from the end user to start the simulation i.e. the number of distributed femtocells, the number of femto users and the number of additional femtocells. The number of rooms along x and y axis are also required by the simulation framework to generate the building layout. The GUI shown in Figure 33 allows the end user to select the number of distributed femtocells i.e. 4, the number of femto users i.e. 24 and the number of additional femtocells i.e. 2 in this Case Study. The end user then has to select the number of rooms along x and y axis i.e. 2 and 2 respectively to generate an indoor environment of the building. The user screen once the inputs are fed in the GUI is shown in Figure 34.

The simulation framework developed for this research must allow the flexibility of choosing the desired environment for optimising femtocell networks. Therefore, the end user can choose the number of distributed femtocells, the number of femto users and the number of additional femtocells of its choice to be deployed in the defined layout of the building. Since 4G LTE-A uses quadrature amplitude modulation as modulation scheme for OFDMA as described earlier in Section 4.1 and the current LTE standards for channel bandwidth are 1.4, 3, 5, 10, 15 and 20MHz, any combination of bandwidth and modulation scheme can be selected by the end user. The available combinations (as discussed in Chapter 4) are 20MHz/64QAM, 20MHz/16QAM, 20MHz/QPSK, 15MHz/64QAM, 15MHz/16QAM, 15MHz/QPSK, 10MHz/64QAM, 10MHz/16QAM, 10MHz/QPSK, 5MHz/64QAM, 5MHz/16QAM, 5MHz/QPSK, 3MHz/64QAM, 3MHz/16QAM, 3MHz/QPSK, 1.4MHz/64QAM, 1.4MHz/16QAM and 1.4MHz/QPSK. All femtocell base stations operate at 20MHz/64QAM to perform optimisation in this simulation framework.

Keeping in mind the typical sizes of the buildings in urban areas, any value of the rooms can be selected from a range of 0 to 15 along x and y axis each to generate a building layout. Once all the user inputs are fed in the GUI, the end user then has to press ‘Initial Random Position’ as visible in light blue colour located in the top section of the GUI of Figure 34 to display the user defined network topology in an indoor environment of the building comprising of femtocells and femto users as shown in Figure 35.

The layout of the building environment before optimisation is also generated separately as shown in Figure 36 according to the criteria described in Section 5.2 once the user has clicked the ‘Initial Random Position’.

The red circles represent the distributed femtocells. The algorithm developed for this optimisation deploys the distributed femtocells uniformly. Since the above building layout has 4 rooms and the number of distributed femtocells selected for this Case Study is also 4, therefore, each room has a distributed femtocell. The additional femtocells are represented by pink circles so that they can be easily distinguished from uniformly distributed femtocells. The algorithm

developed for this optimisation deploys the additional femtocells randomly inside the building. The aim of the random distribution of additional femtocells is to counter the condition when there is a sudden increase in the number of users in a certain area. These additional femtocells can move anywhere inside the whole building to accommodate the users during optimisation. Consequently, they will decrease the load on the overloaded distributed femtocells and hence will optimise the whole network.

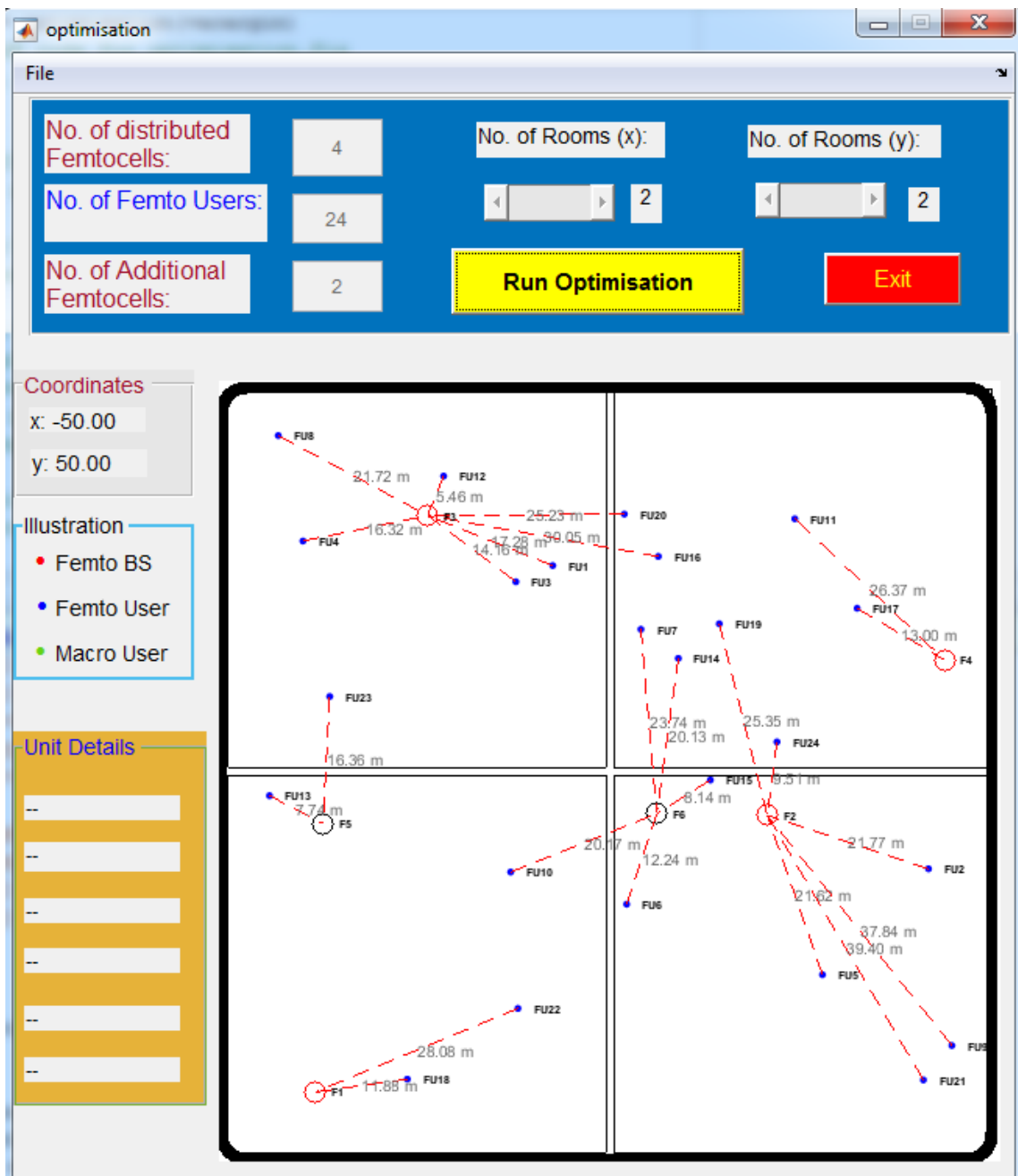


Figure 35: Graphical User Interface displaying the indoor environment of the building before optimisation for Case Study 1

The blue dots represent the users connected to the femtocells. The users are randomly distributed in different rooms of the building. The femto users connected to their nearest distributed and additional femtocells are seen in Figure 36. All the femto users and the distributed and additional femtocells are represented by an ID number. The femto users are represented by numbers FU1 to FU24. The distributed femtocells are represented by numbers F1 to F4 whereas additional femtocells are represented by numbers F5 and F6. The connection of a femto user to its corresponding femtocell is shown by a dotted red line. The distance of each femto user to its femtocell is also shown in meters in grey writing and can be seen in Figure 36. The distance of each femto user to its corresponding femtocell is calculated according to the Pythagoras Theorem. The layout of the building environment displaying rooms along x and y axis according to the user defined inputs is also seen in Figure 36. The layout of the building is taken as 100 x 100 meters and the rooms are uniformly distributed in this layout. Since there are 4 rooms in the building, each room has a size of 50 x 50 m.

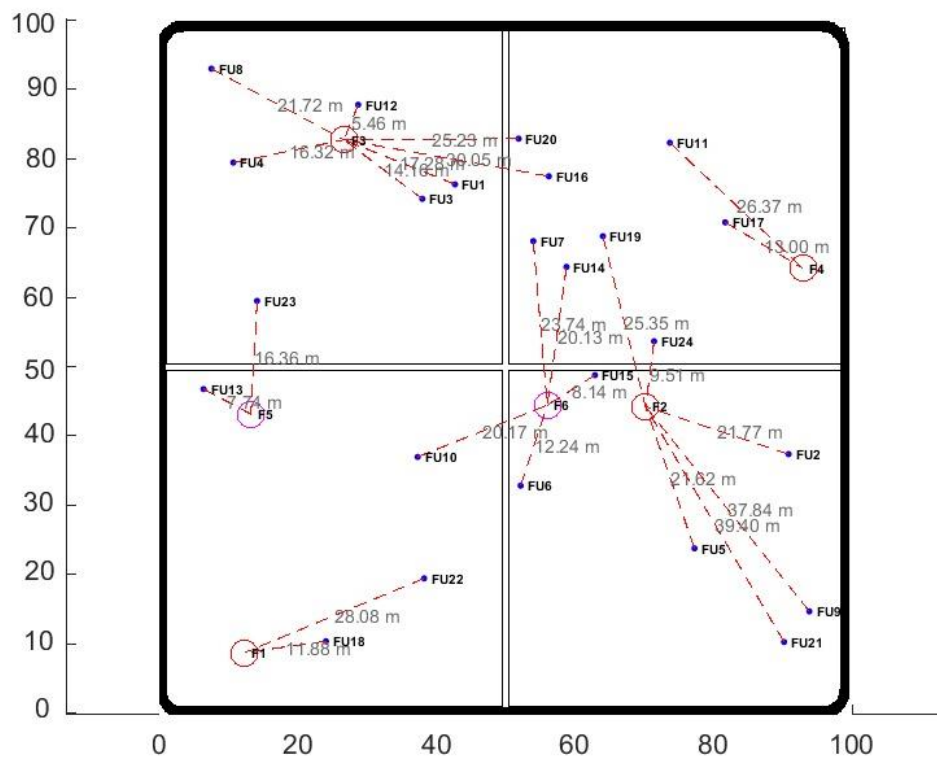


Figure 36: Layout of the building environment before optimisation for Case Study 1

The location of the distributed and additional femtocells, femto users, structure of the building depicting the layout of the user defined topology and taking interfering walls into account are sufficient parameters to calculate the path loss of all the femto users. The simulation framework calculates the path loss and throughput of all the femto users according to the numerical

modelling described in detail in Section 4.2.1. The algorithms are developed in a way that the simulation framework automatically generates the Table 17 representing the results of the simulation before optimisation is performed. Table 17 represents the throughput and path loss of all the femto users with respect to their distance per number of walls from their corresponding femtocells.

Two Femto Users FU13 and FU23 are connected to the additional Femtocell F5. The Femto User FU13 has a throughput of 36 Mbps as there is no wall between the user and the femtocell, whereas the Femto User FU23 has a throughput of only 0.0026 Mbps because of being farther away and significantly because of two walls in between the user and the femtocell. In contrast, two Femto Users FU11 and FU17 connected to the distributed Femtocell F4 as seen in Figure 36 have throughputs of 36 Mbps each because of no wall in between the users and their corresponding femtocell. 7 Femto Users FU1, FU3, FU4, FU8, FU12, FU16 and FU20 are connected to the distributed Femtocell F3. 5 Femto Users FU1, FU3, FU4, FU8 and FU12 have throughputs of 10.29 Mbps each because they all are located in the close proximity of Femtocell F5 having no wall in between them.

Table 17: Throughput and Path Loss of the femto users with respect to their distance per number of walls before optimisation for Case Study 1

Femtocell Number	Femto User Number	Throughput (Mbps)	Path Loss (dB)	Distance (m) /Number of Walls
3	1	10.29	63.21	17.28/0
2	2	9.07	65.60	21.77/0
3	3	10.29	61.48	14.16/0
3	4	10.29	62.71	16.32/0
2	5	5.56	65.49	21.62/0
6	6	6.83	60.21	12.24/0
6	7	0.0016	107.02	23.74/2
3	8	10.29	65.57	21.72/0
2	9	3.10	74.63	37.84/0
6	10	0.00044	104.55	20.17/2
4	11	36	68.73	26.37/0
3	12	10.29	53.20	5.46/0
5	13	36	56.24	7.74/0
6	14	0.0018	104.54	20.13/2
6	15	2.67	56.67	8.14/0
3	16	0.00048	110.87	30.05/2
4	17	36	60.74	13/0
1	18	36	59.96	11.88/0
2	19	0.00036	108.09	25.35/2
3	20	0.0016	108.01	25.23/2
2	21	2.72	75.29	39.40/0
1	22	12.13	69.76	28.08/0
5	23	0.0026	102.73	16.36/2
2	24	0.0017	98.02	9.51/2

Two Femto Users FU16 and FU20 located in one room are connected to the distributed Femtocell F3 located in a different room have throughputs of only 0.00048 Mbps and 0.0016

Mbps respectively because signals degrade significantly while connecting through walls. Similarly, the Femto Users FU19 and FU24 are connected to the distributed Femtocell F2 placed in a different room as seen in Figure 37 have very low throughputs of 0.00036 Mbps and 0.0017 Mbps respectively.

The simulation results of Table 17 confirm that the path loss increases as the distance of femto user from its corresponding femtocell increase and significantly increases if there are any walls in between the femto user and its femtocell. The path loss does not have a linear relationship with the distance because of the logarithm function involved in the equations of Section 4.2.1 used to compute path loss. According to Table 17, the path loss of the Femto User FU11 is 68.73 dB with a distance of 26.37 m from its distributed Femtocell F4. In contrast, the path loss of the Femto User FU19 is 108.09 dB, although it is only 25.35 m away from its connected distributed Femtocell F2 but has walls in between as they are located in different rooms of the building. The path loss of the Femto User FU7 is 107.02 dB because it is connected to an additional Femtocell F6 located in a different room and consequently path loss increases because of penetration losses due to walls.

Once the simulation framework has calculated the throughput and path loss of all the femto users and the results are generated in the form of Table 17, the Tab 'Initial Random Position' located in the top section of the GUI of Figure 34 changes to a yellow Tab of 'Run Optimisation' as seen in Figure 35. The end user then has to click 'Run Optimisation' to start the optimisation process based on the genetic algorithm. The popping up of a progress bar 'Running optimisation...' as seen in Figure 37 shows the optimisation process has started and it keeps the user informed about the progress of simulation.

As the process of optimisation continues, a new Genetic Algorithm screen appears showing the Fitness Value along vertical axis against the Generation along horizontal axis. This can be seen in Figure 38.

As the process of optimisation completes, a message is displayed in the command window of MATLAB 'Optimization terminated: minimum fitness limit reached'. The output can be visualised in Figure 39. It takes around 10 min to complete the whole process and find the optimised positioning of the distributed and additional femtocells. The simulation time also depends on the processing speed of the machine (PC or Laptop) and the number of femtocells and femto users deployed in the building layout.

The layout of the building environment once the optimisation is completed is also generated separately as shown in Figure 40 according to the criteria described in Section 5.2. Figure 40 depicts the optimised positioning of the distributed and additional femtocells.

Once the optimisation process is completed and the distributed and additional femtocells have switched to their new optimised positions as depicted in Figure 40, the simulation framework again calculates the throughput and path loss of all the femto users. The algorithms are developed in a way that the simulation framework automatically generates Table 18 representing the results of the simulation after optimisation is carried out according to the criteria described in Section 5.2. Table 18 represents the throughput and path loss of all the femto users with respect to their distance per number of walls from their corresponding optimised positioned femtocells.

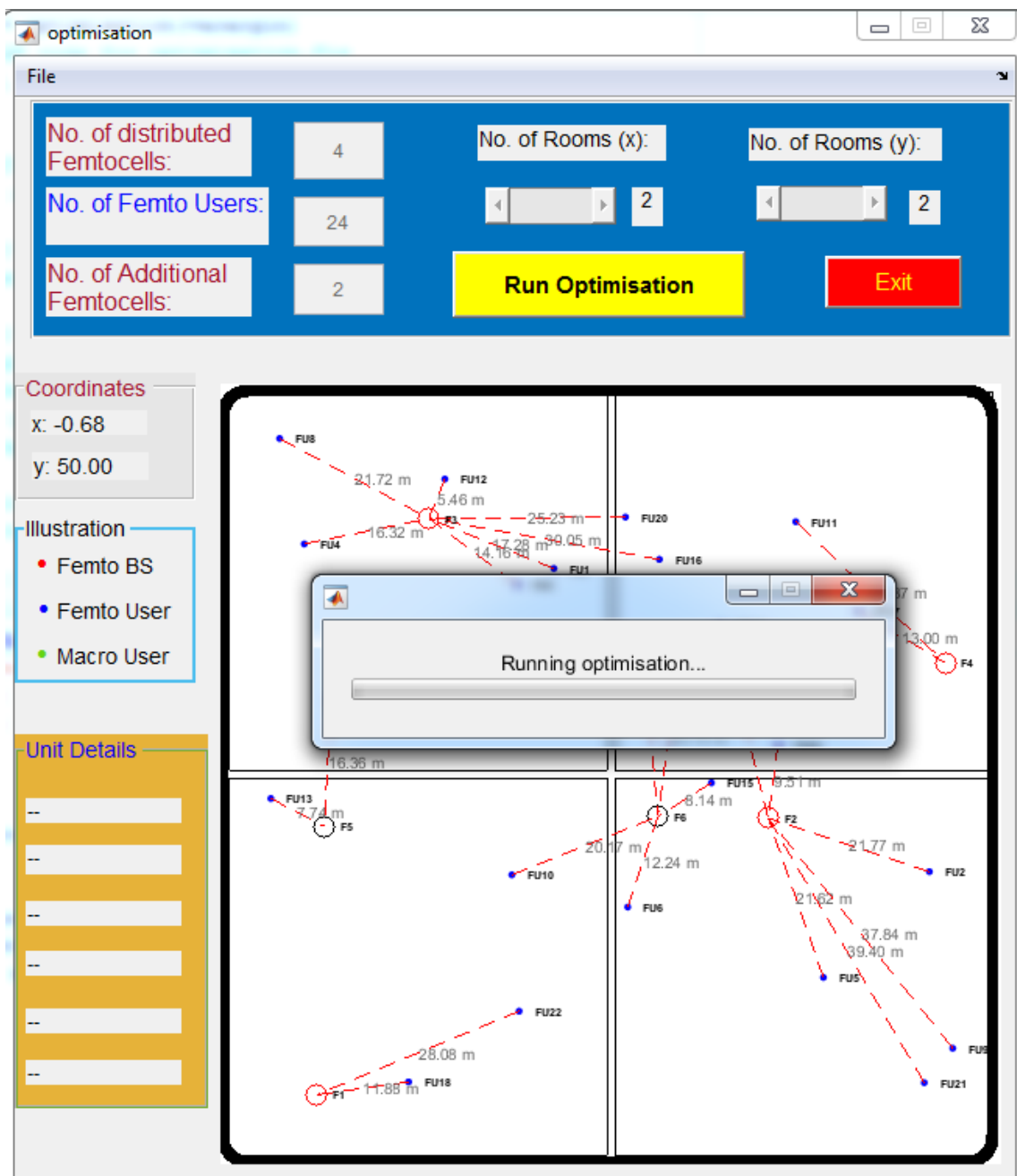


Figure 37: Graphical User Interface showing the optimisation in progress for Case Study 1

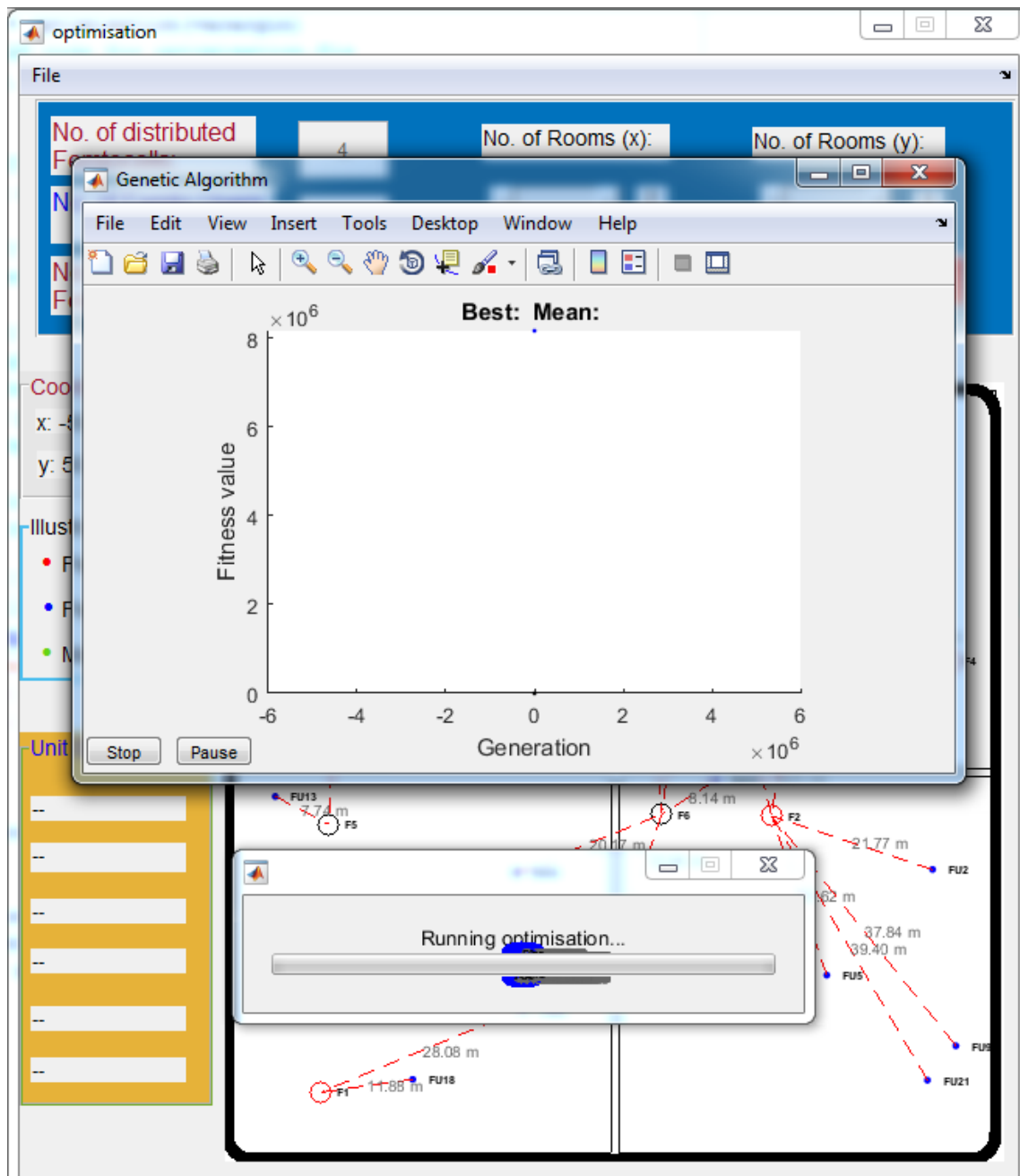


Figure 38: Graphical User Interface showing the progress of optimisation in terms of Fitness value vs Generation for Case Study 1

Two Femto Users FU6 and FU15 connected to the distributed Femtocell F5 as seen in Figure 40 have throughputs of 36 Mbps each because of no wall in between the users and their corresponding femtocell. 8 Femto Users FU7, FU11, FU14, FU16, FU17, FU19, FU20 and FU24 are connected to the distributed Femtocell F4. There is no wall in between and bandwidth is shared amongst all the femto users. Therefore, achieved throughputs of all the Femto Users FU7, FU11, FU14, FU16, FU17, FU19, FU20 and FU24 are 9 Mbps each. Similarly, all 6 Femto Users FU1, FU3, FU4, FU8, FU12 and FU23 connected to the same distributed

Femtocell F3 have throughputs of 12 Mbps each as there is no wall in between and available bandwidth is equally shared amongst all the femto users.

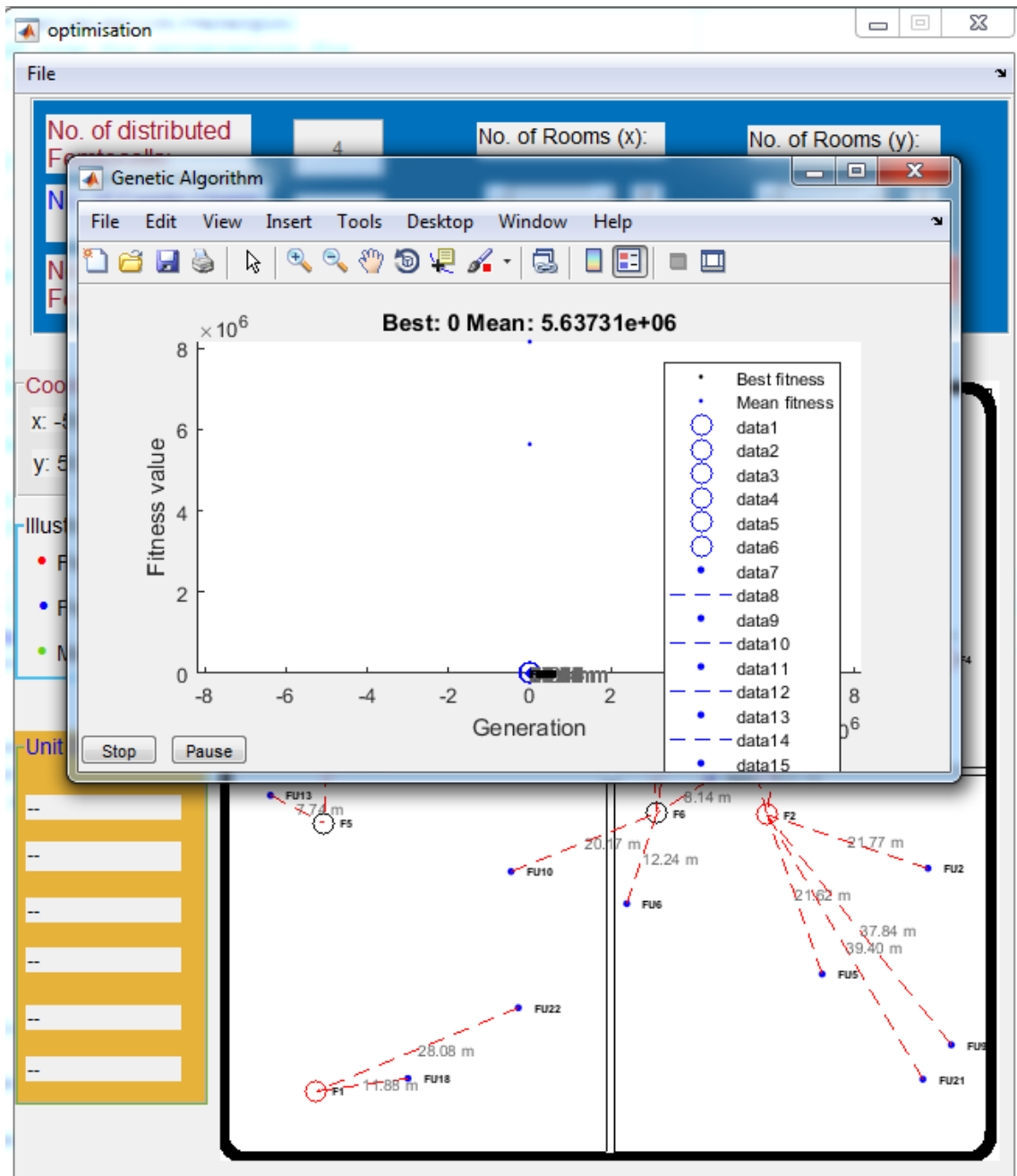


Figure 39: Graphical User Interface displaying the output once the optimisation is terminated for Case Study 1

The path loss of the Femto User FU11 is 71.60 dB with a distance of 31.44 m from its distributed Femtocell F4 whereas the path loss of the Femto User FU6 is 53 dB and it is only 5.33 m away from its connected additional Femtocell F5. This decrease in path loss is due to the decrease in distance of femto user from its femtocell.

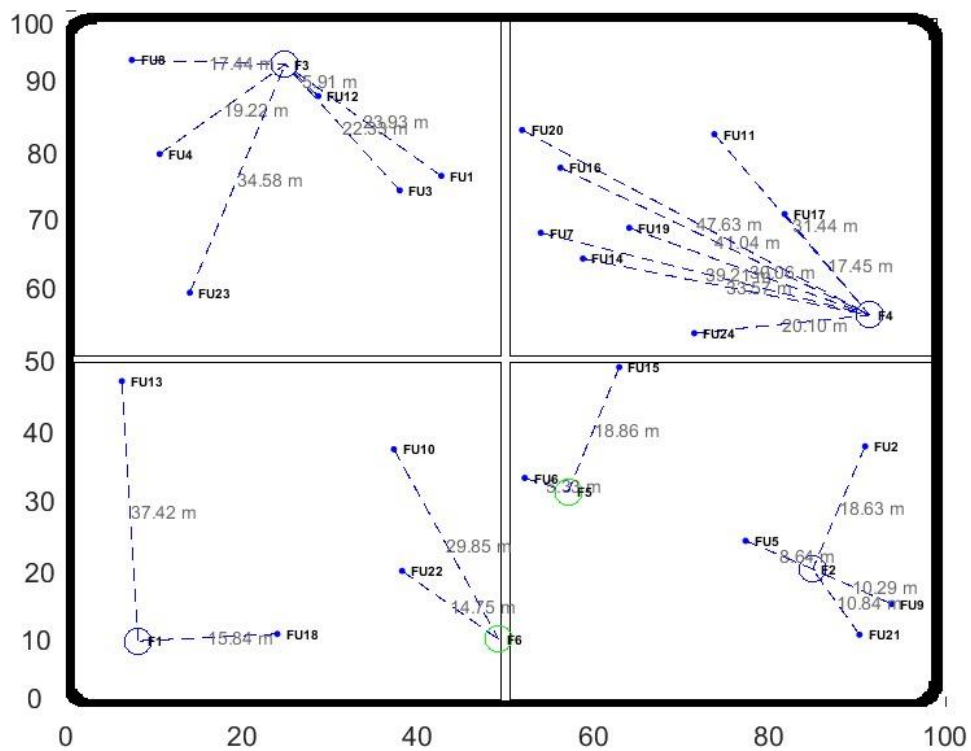


Figure 40: Layout of the building environment after optimisation for Case Study 1

The blue circles represent the new optimised positioning of the distributed femtocells unlike before optimisation where they were represented by red circles. Since boundary of the walls of each room was set as a bound for each distributed femtocell, the genetic algorithm developed for this optimisation has made sure that each distributed femtocell has found the new optimised position in the same room as seen clearly in Figure 40. Figure 41 shows the layouts of the building environment before and after optimisation together for comparative analysis. It is clearly seen in Figure 41 that the distributed femtocells represented by numbers F1 to F4 shown in red before optimisation have switched to new positions after optimisation shown in blue.

The new optimised positioning of the additional femtocells is represented by green circles unlike before optimisation where they were represented by pink circles as shown in Figure 41. Different colours are used to represent optimised additional femtocells so that they can be easily distinguished from optimised distributed femtocells. Since additional femtocells were deployed randomly inside the building, the boundary of the entire building was set as a bound for each additional femtocell. As the purpose of additional femtocells is to ease the burden on the already serving overloaded femtocells, therefore they can move in any room of the building to accommodate the users, thereby increasing the overall throughput of the whole femtocell network. It is clearly seen in Figure 41 that the additional femtocells F5 and F6 have switched to

the new positions after optimisation shown in green from their previous positions before optimisation shown in pink.

Table 18: Throughput and Path Loss of the femto users with respect to their distance per number of walls after optimisation for Case Study 1

Femtocell Number	Femto User Number	Throughput (Mbps)	Path Loss (dB)	Distance (m) /Number of Walls
3	1	12	67.15	23.93/0
2	2	16.92	63.86	18.63/0
3	3	12	66.02	22.33/0
3	4	12	64.14	19.22/0
2	5	14.98	57.19	8.64/0
5	6	36	53	5.33/0
4	7	9	75.21	39.21/0
3	8	12	63.29	17.44/0
2	9	18	58.71	10.29/0
6	10	16.26	70.76	29.85/0
4	11	9	71.60	31.44/0
3	12	12	53.90	5.91/0
1	13	23.47	74.45	37.42/0
4	14	9	72.68	33.57/0
5	15	36	63.97	18.86/0
4	16	9	75.95	41.04/0
4	17	9	63.30	17.45/0
1	18	18.56	62.46	15.84/0
4	19	9	70.87	30.06/0
4	20	9	78.39	47.63/0
2	21	18	59.16	10.84/0
6	22	36	61.84	14.75/0
3	23	12	73.16	34.58/0
4	24	9	64.52	20.10/0

Since the users were already randomly distributed, their positions are not changed as the objective function taken to optimise this femtocell network is the positioning of the femtocells. They are represented by same blue dots but are now connected to their nearest optimised femtocells as shown in Figure 41. For example, the Femto User FU22 was connected to the distributed Femtocell F1 shown in red before optimisation while it is now connected to the additional Femtocell F6 shown in green after optimisation. It can also be seen clearly in Figure 41 that the Femto Users FU13 and FU23 were corresponding with the additional Femtocell F5 shown in pink before optimisation while they are now corresponding with the distributed Femtocells F1 and F3 respectively shown in blue after optimisation.

The connection of a femto user to its corresponding femtocell after optimisation is shown by a dotted blue line unlike before optimisation where it was represented by dotted red line. The optimised distance of each femto user to its corresponding femtocell is again displayed in grey writing. The layout of the building environment displaying rooms along x and y axis and the positioning of the distributed and additional femtocells before and after optimisation can be visualised in Figure 41.

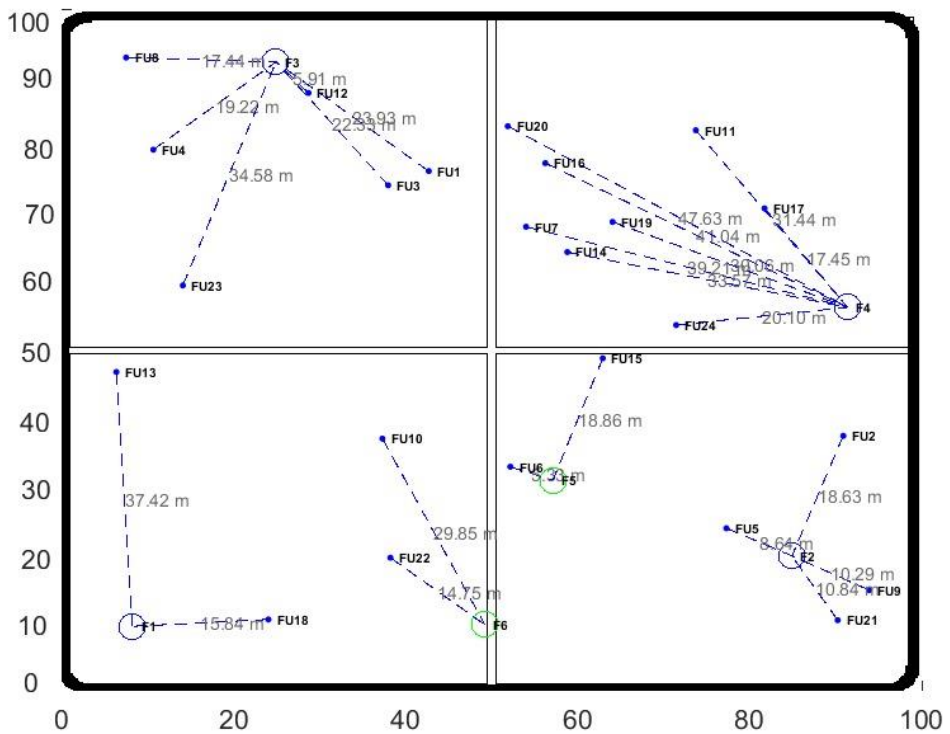
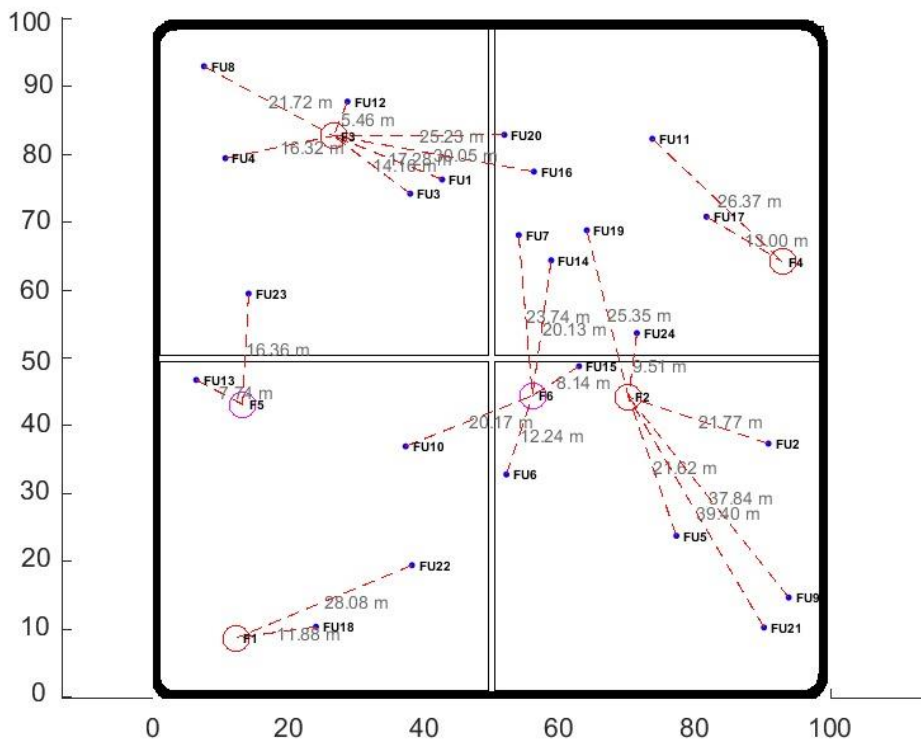


Figure 41: Layout of the building environment before and after optimisation for Case Study 1

Table 19 shows the comparison of the throughput and path loss of all the femto users before and after optimisation for comparative analysis. The simulation results of Table 19 shows that the objective to increase the throughput while keeping the path loss as minimum as possible for most of the femto users is achieved during this optimisation based on the genetic algorithm.

Table 19: Throughput and Path Loss of the femto users before and after optimisation for Case Study 1

Femto User Number	Throughput before Optimisation (Mbps)	Throughput after Optimisation (Mbps)	Path Loss before Optimisation (dB)	Path Loss after Optimisation (dB)
1	10.29	12.00	63.21	67.15
2	9.07	16.92	65.60	63.86
3	10.29	12.00	61.48	66.02
4	10.29	12.00	62.71	64.14
5	5.56	14.98	65.49	57.19
6	6.83	36.00	60.21	53.00
7	0.0016	9.00	107.02	75.21
8	10.29	12.00	65.57	63.29
9	3.1	18.00	74.63	58.71
10	0.00044	16.26	104.55	70.76
11	36	9.00	68.73	71.60
12	10.29	12.00	53.20	53.90
13	36	23.47	56.24	74.45
14	0.0018	9.00	104.54	72.68
15	2.67	36.00	56.67	63.97
16	0.00048	9.00	110.87	75.95
17	36	9.00	60.74	63.30
18	36	18.56	59.96	62.46
19	0.00036	9.00	108.09	70.87
20	0.0016	9.00	108.01	78.39
21	2.72	18.00	75.29	59.16
22	12.13	36.00	69.76	61.84
23	0.0026	12.00	102.73	73.16
24	0.0017	9.00	98.02	64.52
Sum	237.54058	378.19	1863.32	1585.58
% Change		59.21		-14.90

There is a minimal increase of 1.71 Mbps in the throughputs of the Femto Users FU1, FU3, FU4, FU8 and FU12 each. The throughput received by each of these femto users before optimisation was 10.29 Mbps while throughput received by each of these femto users after optimisation is 12 Mbps each. A slightly higher increase of 7.85, 9.42, 8.9984, 8.9982, 8.99952, 8.99964, 8.9984 and 8.9983 Mbps each in throughputs is observed for the Femto Users FU2, FU5, FU7, FU14, FU16, FU19, FU20 and FU24 respectively. The throughputs received by the Femto Users FU2 and FU5 before optimisation were 9.07 Mbps and 5.56 Mbps respectively whereas after optimisation their received throughputs are 16.92 Mbps and 14.98 Mbps respectively. The Femto Users FU7, FU14, FU16, FU19, FU20 and FU24 have very negligible throughputs of 0.0016, 0.0018, 0.00048, 0.00036, 0.0016 and 0.0017 Mbps each respectively before optimisation while they all have achieved throughputs of 9 Mbps each after optimisation.

These femto users were scarcely receiving any connectivity before optimisation while optimised positioning of the femtocells has enabled these femto users to receive reasonable throughputs.

The Femto Users FU9, FU10, FU21 and FU23 have a substantial increase in their throughputs of 14.9, 16.25956, 15.28 and 11.9974 Mbps each respectively. The throughputs received by the Femto Users FU9 and FU21 before optimisation were 3.1 Mbps and 2.72 Mbps respectively whereas after optimisation the received throughputs of both these Femto Users are 18 Mbps each. Hence, the signal reception has substantially increased for the Femto Users FU9 and FU21. The Femto Users FU10 and FU23 have extremely low throughputs of 0.00044 and 0.0026 Mbps each respectively before optimisation whereas they have considerable throughputs of 18 and 12 Mbps each respectively after optimisation. The Femto Users FU10 and FU23 are now able to communicate with the femtocell base station antennas while before optimisation they were barely receiving any signal. A very significant increase of 29.17, 33.33 and 23.87 Mbps each can be seen in the throughputs of the Femto Users FU6, FU15 and FU22 respectively. The throughputs received by the Femto Users FU6, FU15 and FU22 before optimisation were 6.83 2.67 and 12.13 Mbps each respectively whereas after optimisation their received throughputs have considerably increased to 36 Mbps each respectively. 36 Mbps is the maximum estimated throughput received by any femto user after optimisation. Thus, the Femto Users FU6, FU15 and FU22 are receiving maximum throughputs as a result of the optimised positioning of the distributed and additional femtocells.

In contrast, some of the Femto Users FU11, FU13, FU17 and FU18 have received a decrement in their throughputs. Their throughputs have decreased to a minimum value of 9 Mbps which is still a reasonable throughput considering that some of the femto users have negligible throughputs before optimisation. The throughputs of only 4 of the total 24 femto users have decreased as a result of this optimisation. Most of the femto users i.e. 20 of the total 24 femto users have their throughputs increased as a result of this optimisation. The cumulative throughput of all the femto users in the femtocell network before optimisation was 237.54 Mbps. The cumulative throughput of all the femto users in the femtocell network after optimisation is 378.19 Mbps. Hence the overall increase in the throughput of the whole femtocell network as a result of this optimisation based on the genetic algorithm is 140.65 Mbps. The simulation framework developed for this research has been able to optimise the network of femtocells in an indoor environment of the building. Optimisation based on the genetic algorithm has resulted in an overall increase of 59.21% in the throughput of all the femto users.

Figure 42 depicts the throughputs of all the femto users before and after optimisation. It can be seen clearly in Figure 42 that the throughput of most of the femto users after optimisation

shown in green is much higher than the throughput of most of the femto users before optimisation shown in yellow. It can also be observed in Figure 42 that the Femto Users FU11, FU13, FU17 and FU18 have experienced a decrease in their throughputs after optimisation.

The simulation results of Table 19 confirm that the path loss increases as the distance of femto user from its femtocell increase and decreases as the distance of femto user from its corresponding femtocell decrease. The path loss does not change linearly with the distance because of the logarithm function and penetration losses involved in the equations used to compute the path loss. A significant increase in the path loss is observed if there are any walls in between the femto user and its femtocell as seen in Table 17. Table 19 showing the comparison of the throughput and path loss of all the femto users before and after optimisation can be used for the comparative analysis of path loss of all the femto users. The optimised positioning of the distributed and additional femtocells in Figure 40 has confirmed that all the femto users are corresponding with their femtocells having no wall in between them after optimisation. Thus, the path loss of the femto users who were corresponding with their femtocells through walls before optimisation have a significant decrease in their path loss as they are not corresponding to their optimised position of femtocells through walls after optimisation. Hence, the objective to keep the path loss as minimum as possible for most of the femto users is achieved during this optimisation based on the genetic algorithm.

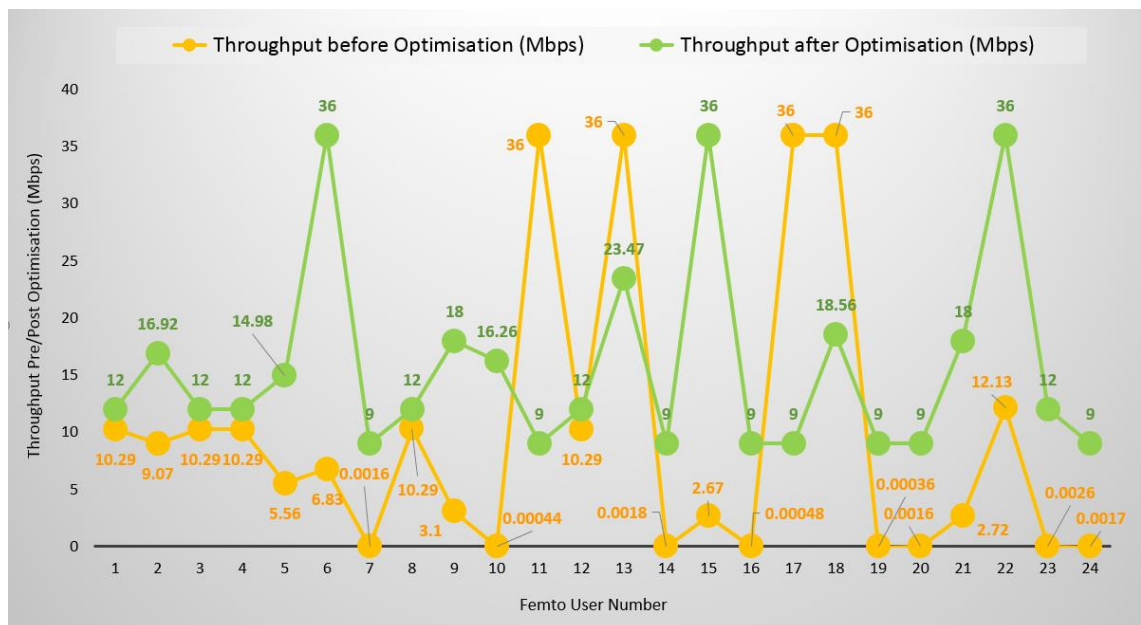


Figure 42: Throughput of the femto users before and after optimisation for Case Study 1

The path loss of most of the Femto Users FU2, FU5, FU6, FU7, FU8, FU9, FU10, FU14, FU16, FU19, FU20, FU21, FU22, FU23 and FU24 is decreased by 1.74, 8.3, 7.21, 31.81, 2.28, 15.92, 33.79, 31.86, 34.92, 37.22, 29.62, 16.13, 7.92, 29.57 and 33.5 dB each respectively. The small

decrease in the path loss of the Femto Users FU2, FU5, FU6, FU8, FU9, FU21 and FU22 is because of the decrease in their distances from their corresponding optimised positioned distributed and additional femtocells after optimisation. The path loss of the Femto Users FU2, FU5, FU6, FU8, FU9, FU21 and FU22 was 65.60, 65.49, 60.21, 65.57, 74.63, 75.29 and 69.76 dB each respectively before optimisation whereas after optimisation it has decreased to 63.86, 57.19, 53, 63.29, 58.71, 59.16 and 61.84 dB each respectively. There is a significant decrease in the path loss of the Femto Users FU7, FU10, FU14, FU16, FU19, FU20, FU23 and FU24 as they were corresponding to their respective femtocells through walls before optimisation while they are coordinating to their respective optimised positioned distributed and additional femtocells without any wall in between after optimisation and can be seen in Figure 41. The path loss of the Femto Users FU7, FU10, FU14, FU16, FU19, FU20, FU23 and FU24 have significantly reduced to 75.21, 70.76, 72.68, 75.95, 70.87, 78.39, 73.16 and 64.52 dB each respectively after optimisation while it had much higher values of the path loss as 107.02, 104.55, 104.54, 110.87, 108.09, 108.01, 102.73 and 98.02 dB each respectively before optimisation. The significant decrease in the path loss of these femto users while optimising the femtocell network in an indoor environment of the building has fulfilled the aim and objectives of this research.

An increase of 3.94, 4.54, 1.43, 2.87, 0.7, 18.21, 7.3, 2.56 and 2.5 dB each in the path loss of the Femto Users FU1, FU3, FU4, FU11, FU12, FU13, FU15, FU17 and FU18 respectively can be seen in Table 20. The path loss of the Femto Users FU1, FU3, FU4, FU11, FU12, FU13, FU15, FU17 and FU18 was 63.21, 61.48, 62.71, 68.73, 53.20, 56.24, 56.67, 60.74 and 59.96 dB each respectively before optimisation whereas after optimisation it has slightly increased to 67.15, 66.02, 64.14, 71.60, 53.90, 74.45, 63.97, 63.30 and 62.46 dB each respectively. The increase in the path loss of some of the femto users is minimal as compared to the decrease in the path loss of most of the femto users. The cumulative path loss of all the femto users in the femtocell network before optimisation was 1863.32 dB. The cumulative path loss of all the femto users in the femtocell network after optimisation is 1585.58 dB. Hence the overall decrease in the path loss of the whole femtocell network as a result of this optimisation based on genetic algorithm is 277.74 dB. The simulation framework has optimised the network of femtocells in an indoor environment of the building. Optimisation based on genetic algorithm has resulted in an overall decrease of 14.90% in the path loss of all the femto users thereby achieving the goals of this experiment.

Figure 43 depicts the path loss of all the femto users before and after optimisation. It can be clearly observed in Figure 43 that the path loss of most of the femto users after optimisation shown in green is significantly lower than the path loss of most of the femto users before

optimisation shown in yellow. It can also be deduced from Figure 43 that some of the femto users have a slight increase in their path loss after optimisation.

Table 20 shows the delta throughput i.e. the difference in the post and pre optimisation throughputs in Mbps and delta path loss i.e. the difference in the post and pre optimisation path loss in dB of all the femto users along with the simulation results of throughput and path loss of all the femto users before and after optimisation for further analysis.

The genetic algorithm developed for this optimisation aims to increase the throughput while decreasing the path loss of the femto users to be able to optimise the femtocell network. As explained earlier, the throughput of most of the femto users has increased after optimisation while the path loss of most of the femto users has decreased as a result of the optimisation. The decrease in the throughput of the 4 femto users is a trade off in this research while in comparison most of the femto users have experienced an increase in their throughputs thereby increasing the overall throughput of the whole femtocell network by 59.21%. Similarly, increase in the path loss of some of the femto users is a trade off against a substantial decrease in the path loss of most of the femto users resulting in overall decrease of the path loss of the whole femtocell network by 14.90%. Thus, the simulation framework is able to optimise the femtocell network in terms of increasing the throughput and reducing the path loss.

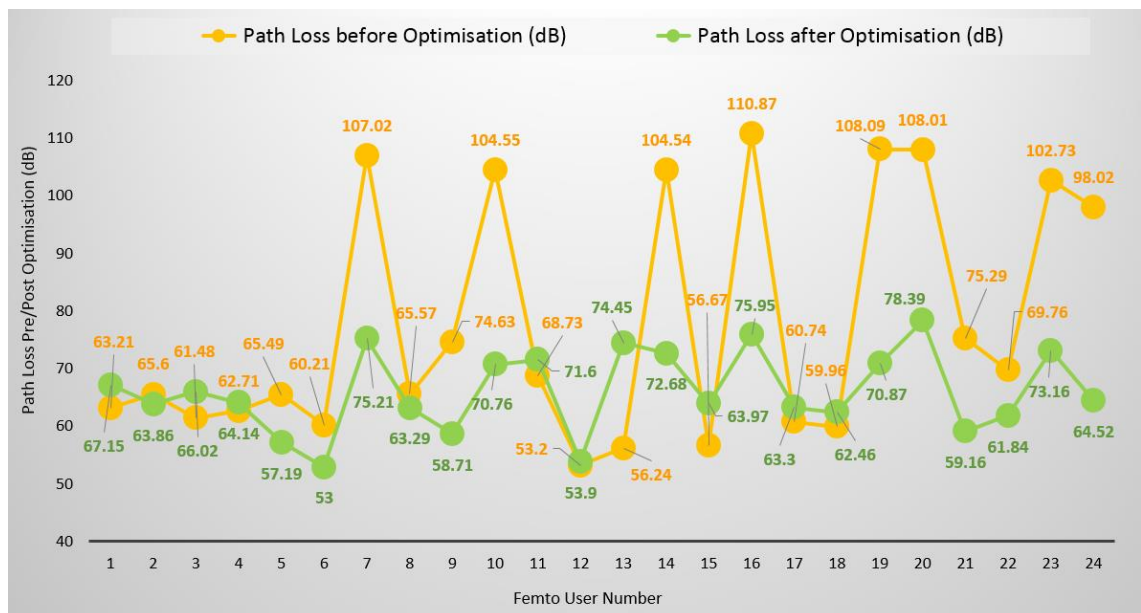


Figure 43: Path Loss of the femto users before and after optimisation for Case Study 1

Although overall throughput of the femtocell network is substantially increased and path loss is significantly reduced, it is very critical that an increase in the throughput of a femto user is not comprised for an increase in the path loss at the same time. To analyse this, the delta throughput and delta path loss of each femto user is calculated and shown in Table 20.

Most of the Femto Users FU2, FU5, FU6, FU7, FU8, FU9, FU10, FU14, FU16, FU19, FU20, FU21, FU22, FU23 and FU24 have an increase in their throughputs and at the same time decrease in their path loss after optimisation. The Femto Users FU1, FU3, FU4, FU12 and FU15 experience an increase of both the throughput and path loss as a result of optimisation. These femto users have a trade-off for an increase in throughput against an increase in path loss, but the cumulative increase in the throughput of these 5 femto users is much better than the cumulative increase in their path loss. Only the Femto Users FU11, FU13, FU17 and FU18 experience a decrease in their throughputs as well as increase in their path loss as a result of this optimisation.

Table 20: Delta Throughput and Delta Path Loss of the femto users for Case Study 1

Femto User No.	Throughput before Optimisation (Mbps)	Throughput after Optimisation (Mbps)	Delta Throughput (Post vs Pre) (Mbps)	Path Loss before Optimisation (dB)	Path Loss after Optimisation (dB)	Delta Path Loss (Post vs Pre) (dB)
1	10.29	12.00	1.71	63.21	67.15	3.94
2	9.07	16.92	7.85	65.60	63.86	-1.74
3	10.29	12.00	1.71	61.48	66.02	4.54
4	10.29	12.00	1.71	62.71	64.14	1.43
5	5.56	14.98	9.42	65.49	57.19	-8.3
6	6.83	36.00	29.17	60.21	53.00	-7.21
7	0.0016	9.00	8.9984	107.02	75.21	-31.81
8	10.29	12.00	1.71	65.57	63.29	-2.28
9	3.1	18.00	14.9	74.63	58.71	-15.92
10	0.00044	16.26	16.25956	104.55	70.76	-33.79
11	36	9.00	-27	68.73	71.60	2.87
12	10.29	12.00	1.71	53.20	53.90	0.7
13	36	23.47	-12.53	56.24	74.45	18.21
14	0.0018	9.00	8.9982	104.54	72.68	-31.86
15	2.67	36.00	33.33	56.67	63.97	7.3
16	0.00048	9.00	8.99952	110.87	75.95	-34.92
17	36	9.00	-27	60.74	63.30	2.56
18	36	18.56	-17.44	59.96	62.46	2.5
19	0.00036	9.00	8.99964	108.09	70.87	-37.22
20	0.0016	9.00	8.9984	108.01	78.39	-29.62
21	2.72	18.00	15.28	75.29	59.16	-16.13
22	12.13	36.00	23.87	69.76	61.84	-7.92
23	0.0026	12.00	11.9974	102.73	73.16	-29.57
24	0.0017	9.00	8.9983	98.02	64.52	-33.5
Sum	237.54058	378.19	140.64942	1863.32	1585.58	-277.74

Figure 44 depicts the comparison of the delta throughput and delta path loss of all the femto users. The delta throughput of all the femto users is represented by green rectangular bars while the delta path loss of all the femto users is shown by yellow rectangular bars in Figure 44. It can be seen that the throughputs of most of the femto users have increased and therefore most of the green bars are on the positive side of the axis. The path loss of most of the femto users have been reduced and consequently most of the yellow bars are on the negative side of the axis. The

higher rectangular bars correspond to the significant increase in the throughputs and substantial decrease in the path loss of the femto users. Figure 44 also illustrates that most of the femto users have an increase in their throughputs as well as a decrease in their path loss at the same time as a result of the optimisation based on the genetic algorithm.

5.3.2 Case Study 2

The simulation framework needs inputs from the end user to start the simulation i.e. the number of distributed femtocells, the number of femto users and the number of additional femtocells. The number of rooms along x and y axis are also required by the simulation framework to generate the building layout. The graphical user interface shown in Figure 33 of Case Study 1 is again utilised to set up a different building layout for Case Study 2. The simulation framework is developed in a way that simulations can be performed many times by only changing the inputs fed to the graphical user interface. It allows the flexibility of choosing the number of distributed femtocells, the number of femto users and the number of additional femtocells of user choice to be deployed in the defined layout of the building.

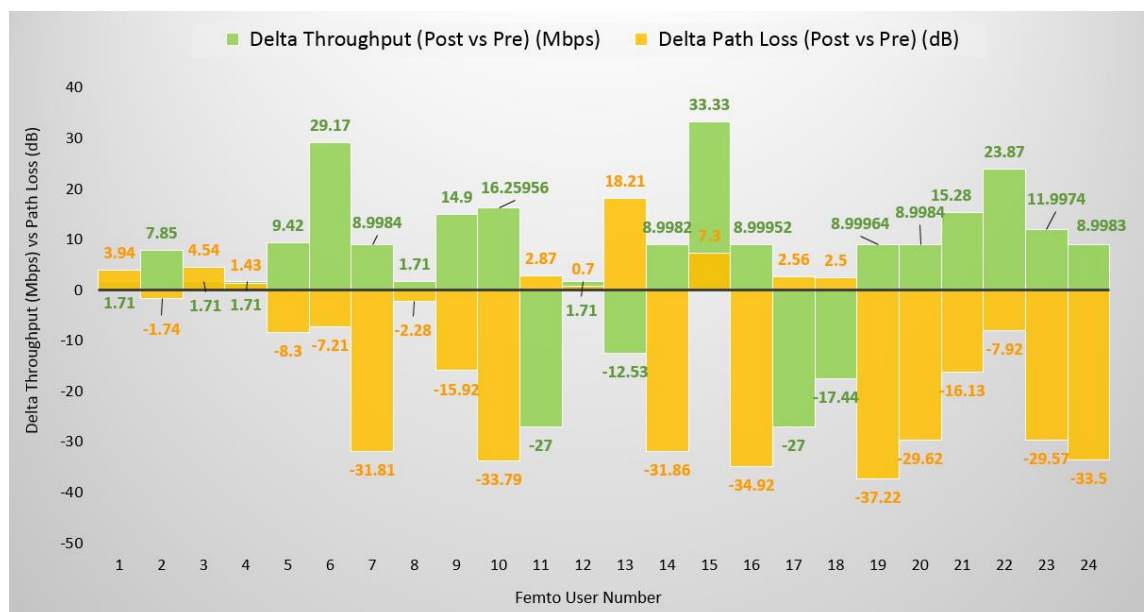


Figure 44: Delta Throughput and Delta Path Loss of the femto users for Case Study 1

For Case Study 2 unlike Case Study 1, the number of distributed femtocells selected are 9, the number of femto users selected are 40, the number of additional femtocells selected are 3 and the number of rooms along x and y axis selected are 3 each to generate a different and congested indoor environment of the building to test the capacity and capability of the designed simulation framework. Since the building layout has 9 rooms, therefore the number of distributed femtocells selected are also 9 so that each room has a distributed femtocell. The maximum number of rooms that can be selected along x and y axis are 15 each by using this simulation framework. Thus, a building layout of 225 rooms can be generated and any number of

distributed femtocells, femto users and additional femtocells can be selected. Such an indoor environment would be extremely difficult to visualise on graphical user interface; therefore, the above values are selected so that the positioning of the femto users and their distances from their corresponding distributed and additional femtocells can be seen. The positioning of the distributed and additional femtocells before and after optimisation will also be easy to visualise on graphical user interface for the values selected in Case Study 2. Figure 45 depicts the user screen once the inputs are fed in the GUI.

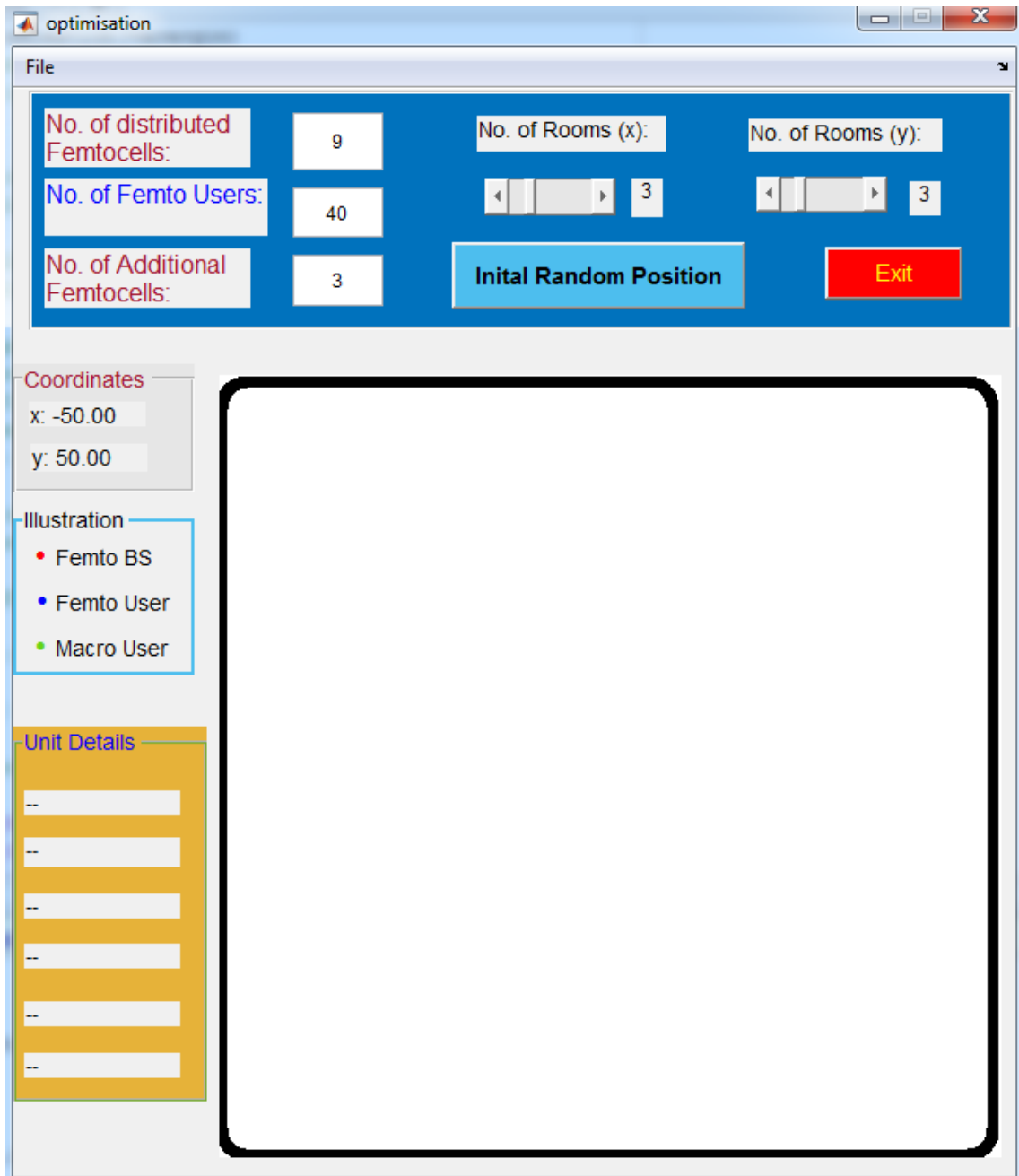


Figure 45: User screen once the inputs are fed in the Graphical User Interface for Case Study 2

All femtocell base stations operate at 20MHz/64QAM to perform optimisation in this simulation. The same process of Case Study 1 is repeated in Case Study 2 to generate the user defined topology on GUI displaying the indoor environment of the building comprising of femtocells and femto users in Figure 46.

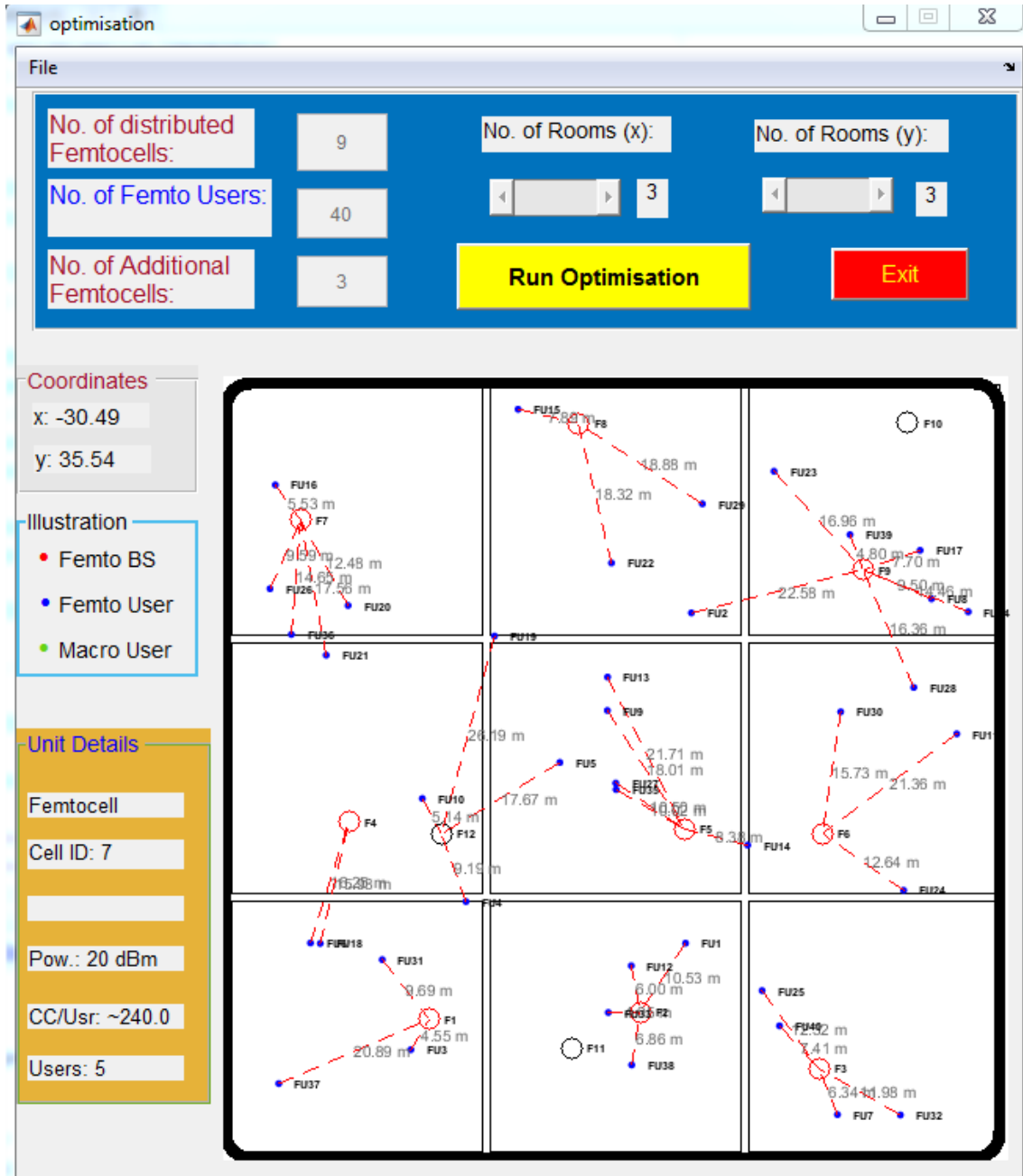


Figure 46: Graphical User Interface displaying the indoor environment of the building before optimisation for Case Study 2

The layout of the building environment before optimisation is also generated separately as shown in Figure 47. The algorithm developed for this optimisation deploys the distributed and additional femtocells according to the same criteria used in Case Study 1. The distributed femtocells are deployed uniformly while additional femtocells are deployed randomly inside the

building. Since the building layout has 9 rooms, therefore, the algorithm has deployed the 9 distributed femtocells uniformly in each room. The difference from previous Case Study 1 is the number of distributed and additional femtocells and the number of femto users deployed in this Case Study 2 and also the number of rooms along x and y axis. The red circles represent the distributed femtocells while additional femtocells are represented by pink circles in Figure 47 so that they can be easily identified. All the distributed and additional femtocells are represented by an ID number. The distributed femtocells are denoted by numbers F1 to F9 while additional femtocells are shown by numbers F10 to F12.

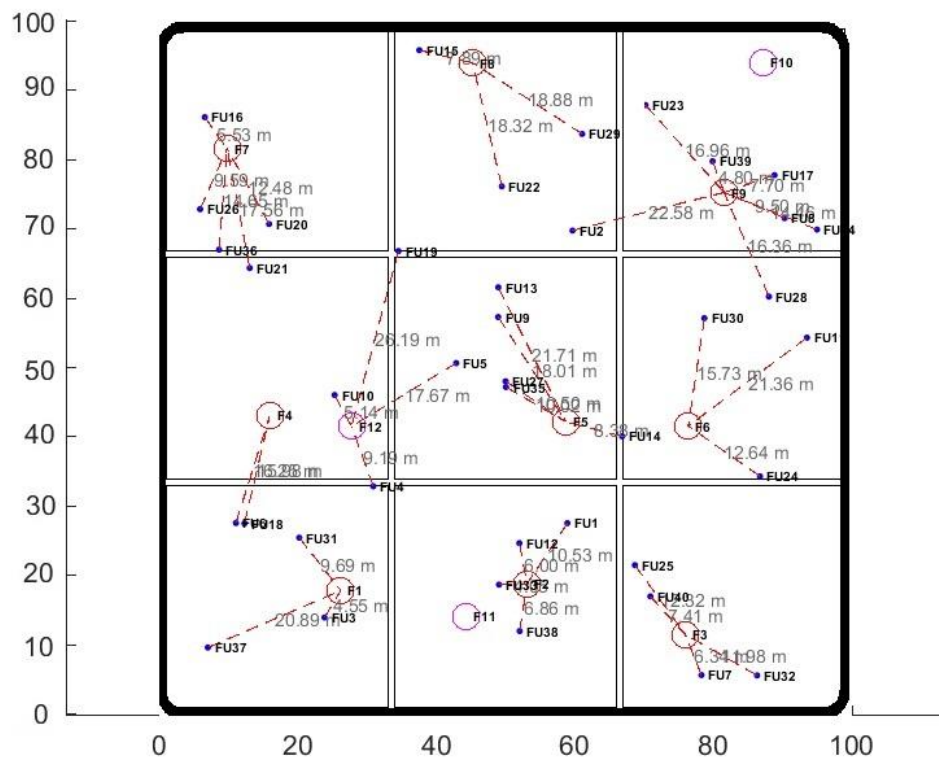


Figure 47: Layout of the building environment before optimisation for Case Study 2

The femto users are randomly distributed in different rooms of the building and are represented by blue dots in Figure 47. The femto users are connected to their nearest distributed and additional femtocells. The femto users are shown by numbers FU1 to FU40. The connection of a femto user to its corresponding femtocell is shown by a dotted red line. The distance of each femto user to its femtocell is shown in grey writing stating its value in meters (m) in Figure 47. The distance of each femto user to its corresponding femtocell is calculated according to the Pythagoras Theorem. Since the layout of the whole building is 100 x 100 m and the rooms are uniformly distributed in this layout, therefore, each room has a size of approx. 33 x 33 m.

The simulation framework calculates the throughput and path loss of all the femto users as in Case Study 1. The simulation framework automatically generates the Table 21 depicting the results of the simulation before optimisation is performed. Table 21 represents the throughput and path loss of all the femto users with respect to their distance per number of walls from their corresponding femtocells.

Table 21: Throughput and Path Loss of the femto users with respect to their distance per number of walls before optimisation for Case Study 2

Femtocell Number	Femto User Number	Throughput (Mbps)	Path Loss (dB)	Distance (m) /Number of Walls
2	1	9.35	58.91	10.53/0
9	2	0.00042	106.20	22.58/2
1	3	24	51.62	4.55/0
12	4	0.00094	97.73	9.19/2
12	5	0.00033	103.41	17.67/2
4	6	0.00078	102.68	16.25/2
3	7	18	54.51	6.34/0
9	8	8.92	58.01	9.50/0
5	9	14.4	63.57	18/0
12	10	9.63	52.69	5.14/0
6	11	24	65.29	21.36/0
2	12	11.82	54.03	6/0
5	13	14.4	65.56	21.71/0
5	14	3.12	76.93	8.38/1
8	15	24	56.40	7.89/0
7	16	14.4	53.32	5.53/0
9	17	6.56	56.19	7.70/0
4	18	0.00072	102.53	15.98/2
12	19	0.0002	128.62	26.19/3
7	20	14.4	60.39	12.48/0
7	21	0.00029	103.35	17.56/2
8	22	24	63.72	18.32/0
9	23	1.95	63.05	16.96/0
6	24	24	60.50	12.64/0
3	25	18	60.27	12.32/0
7	26	14.4	58.10	9.59/0
5	27	14.4	58.88	10.50/0
9	28	0.00036	102.74	16.36/2
8	29	24	63.98	18.88/0
6	30	24	62.39	15.73/0
1	31	24	58.19	9.69/0
3	32	18	60.03	11.98/0
2	33	7.19	50.62	4.05/0
9	34	6.40	61.66	14.46/0
5	35	14.4	58.48	10.02/0
7	36	14.4	61.77	14.65/0
1	37	24	64.93	20.89/0
2	38	3.96	55.19	6.86/0
9	39	10.29	52.08	4.80/0
3	40	18	55.86	7.41/0

Most of the femto users are connected to their femtocells without any wall in between and therefore have a reasonable throughput. The bandwidth is shared amongst femto users connected to the same femtocell. Some of the femto users have a negligible throughput because

they are located in different rooms and corresponding to their respective femtocells through walls located in other rooms being the closest femtocells available to them as seen in Figure 48. The Femto Users FU15, FU22 and FU29 all have estimated throughputs of 24 Mbps as bandwidth is shared amongst the users and they all are located in the close proximity of the distributed Femtocell F8 without any walls in between them. The Femto User FU19 has an extremely low throughput of 0.002 Mbps as it is corresponding with the additional Femtocell F12 through 3 walls thereby decreasing signal strength to almost 0. 5 Femto Users FU16, FU20, FU21, FU26 and FU36 are receiving connectivity from the distributed Femtocell F7. 4 Femto Users FU16, FU20, FU26 and FU36 all have received throughputs of 14.4 Mbps each because of no wall in between whereas the Femto User FU21 has a negligible throughput of 0.00029 Mbps because of 2 walls in between.

The simulation results of Table 21 confirm that the path loss increases as the distance of femto user from its femtocell increase and decreases as the distance of femto user from its corresponding femtocell decrease. The path loss does not change linearly with the distance because of the logarithm function and penetration losses involved in the equations used to compute the path loss. A significant increase in the path loss is observed if there are any walls in between the femto user and its femtocell. As seen in Table 21, the path loss of the Femto User FU11 is 65.29 dB with a distance of 21.36 m from its distributed Femtocell F6. In contrast, the path loss of the Femto User FU19 is 128.62 dB, although it is only 26.19 m away from its connected additional Femtocell F12 but has 3 walls in between as they are located in different rooms of the building. The path loss of the Femto User FU28 is 102.74 dB because it is connected to a distributed Femtocell F9 located in a different room and consequently path loss increases because of penetration losses due to walls in between the user and the femtocell.

Once the simulation framework has calculated the throughput and path loss of all the femto users and the results are generated in the form of Table 21, the end user has to start the optimisation process following the same methodology used in Case Study 1. Figure 48 shows the optimisation has started and is in progress.

A new Genetic Algorithm window appears as the optimisation is approaching its end showing the plot of the Fitness Value against the Generation displaying the Best and Mean values as seen in Figure 49.

A message displayed in the command window of MATLAB ‘Optimization terminated: minimum fitness limit reached’ shows the completion of the optimisation based on the genetic algorithm. The final output visualised through graphical user interface can be seen in Figure 50.

The layout of the building environment after the optimisation is completed is also generated separately as shown in Figure 51 depicting the optimised positioning of the distributed and additional femtocells.

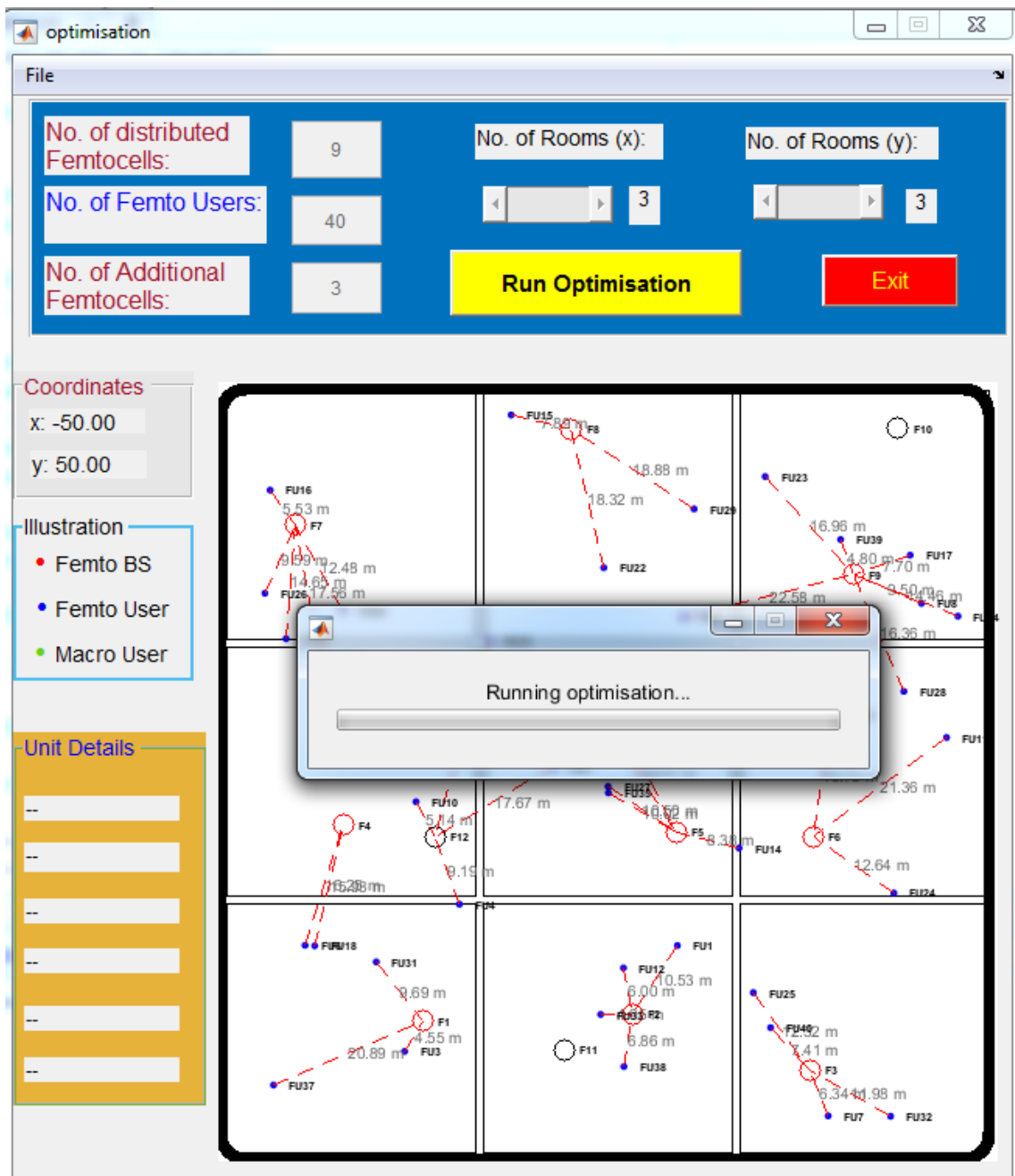


Figure 48: Graphical User Interface showing the optimisation in progress for Case Study 2

Once the distributed and additional femtocells are relocated to their new optimised positions as shown in Figure 51 at the completion of optimisation process, the simulation framework calculates the throughput and path loss of all the femto users. The simulation framework automatically generates the Table 22 depicting the results of the simulation after optimisation is

carried out. Table 22 represents the throughput and path loss of all the femto users with respect to their distance per number of walls from their corresponding optimised positioned femtocells.

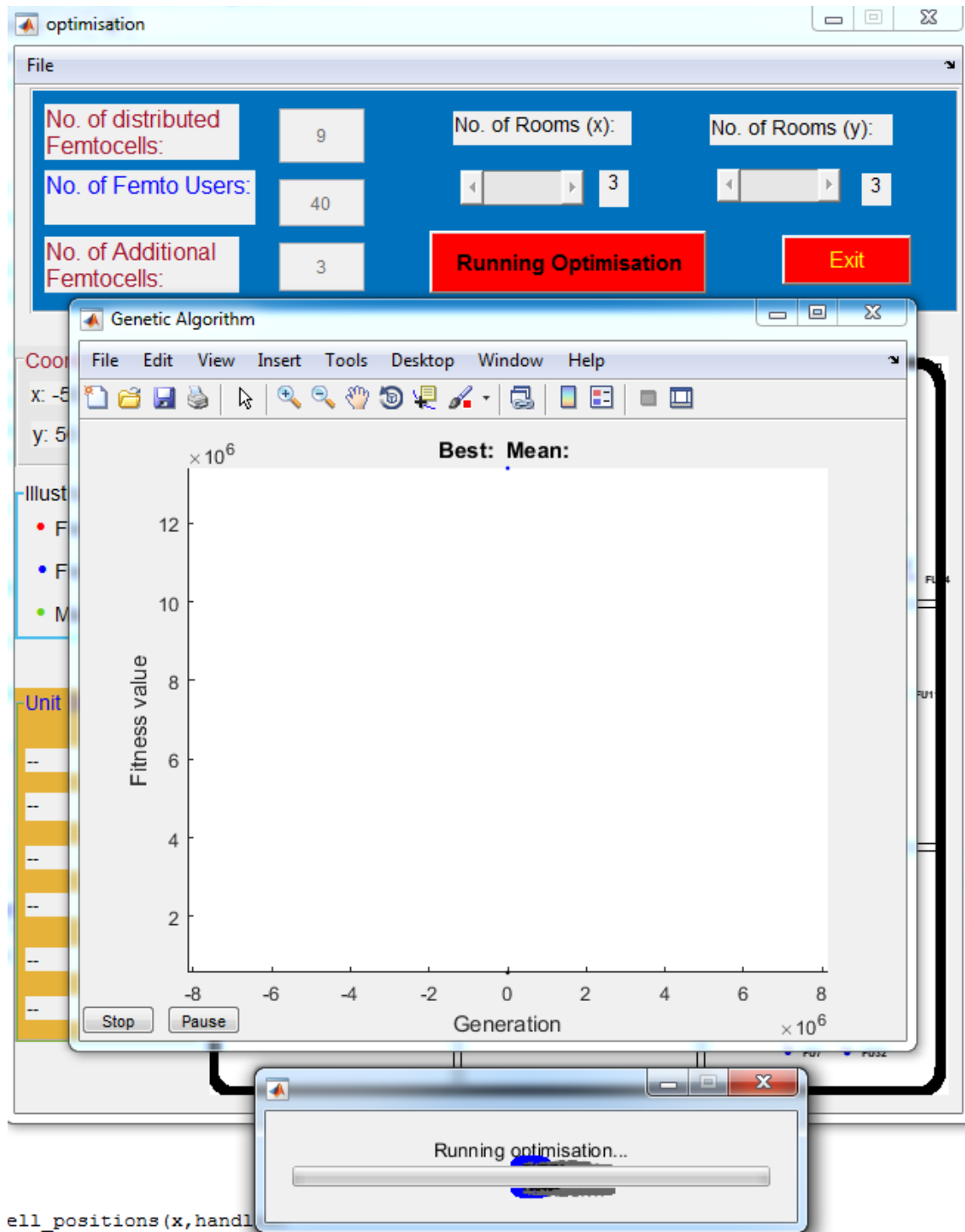


Figure 49: Graphical User Interface showing the progress of optimisation in terms of Fitness value vs Generation for Case Study 2

Since the distributed and additional femtocells are relocated to their optimised positions as a result of optimisation based on the genetic algorithm, all the femto users except the Femto User FU14 are now connected to their corresponding femtocells without any wall in between. The

Femto User FU14 being located in between the rooms as a result of the random distribution of the femto users is now connected to the optimised positioned distributed Femtocell F6 through a wall. Despite having a wall in between itself and its corresponding femtocell, the Femto User FU14 is still able to receive a reasonable throughput of 13.47 Mbps post optimisation whereas before optimisation the throughput received by the Femto User FU14 was 3.12 Mbps but at that time it was corresponding with the distributed Femtocell F5 rather than optimised positioned distributed Femtocell F6 post optimisation.

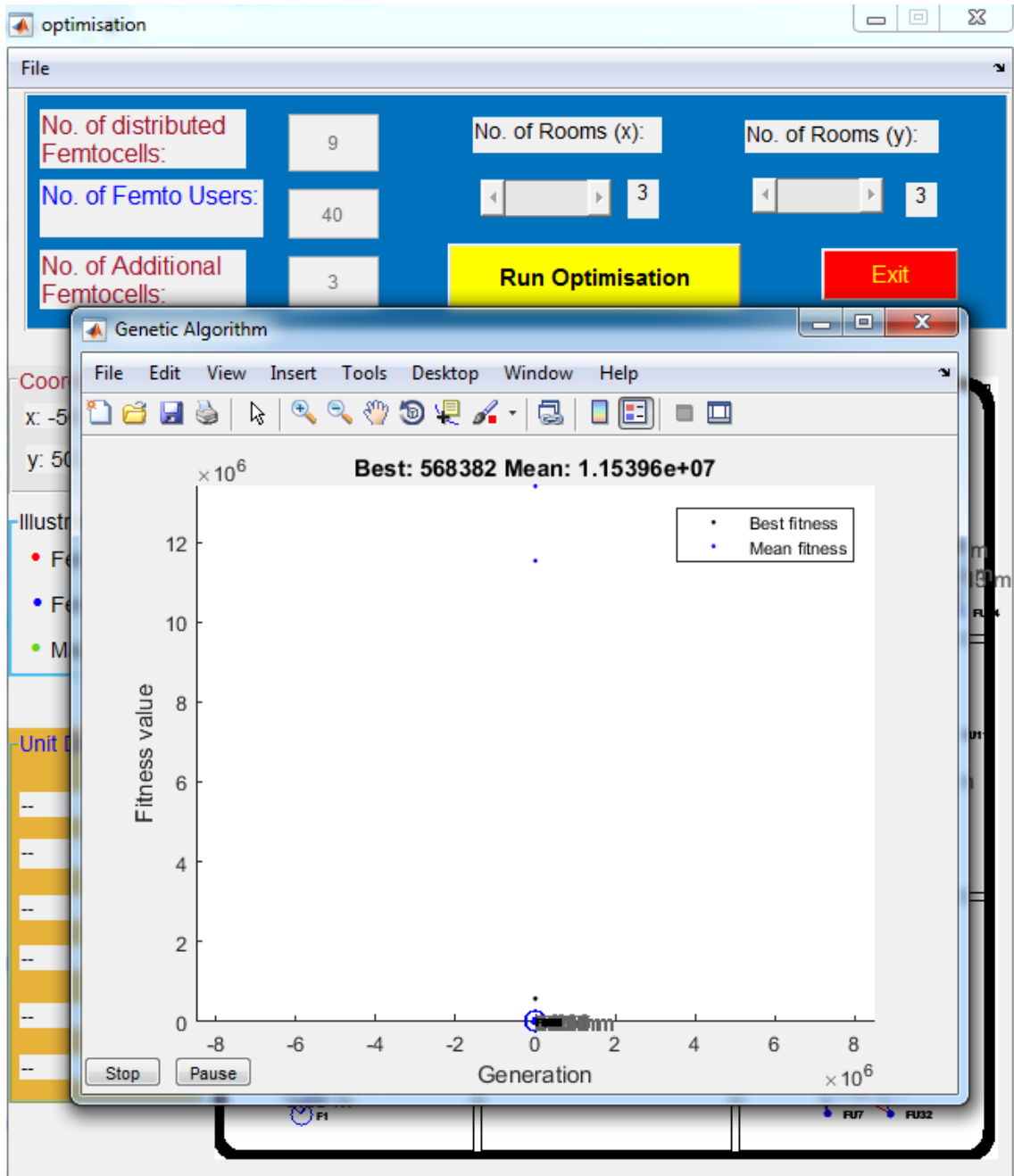


Figure 50: Graphical User Interface displaying the output once the optimisation is terminated for Case Study 2

The available bandwidth is shared amongst the femto users connected to the same femtocell. Two Femto Users FU10 and FU21 are connected to the optimised positioned distributed Femtocell F4 as seen in Figure 51 and have throughputs of 36 Mbps each because of no wall in between the users and their corresponding femtocell. 4 Femto Users FU7, FU25, FU32 and FU40 are connected to the optimised positioned distributed Femtocell F3. There is no wall in between and bandwidth is shared amongst all the femto users. Therefore, the achieved throughputs of all the Femto Users FU7, FU25, FU32 and FU40 are 18 Mbps each.

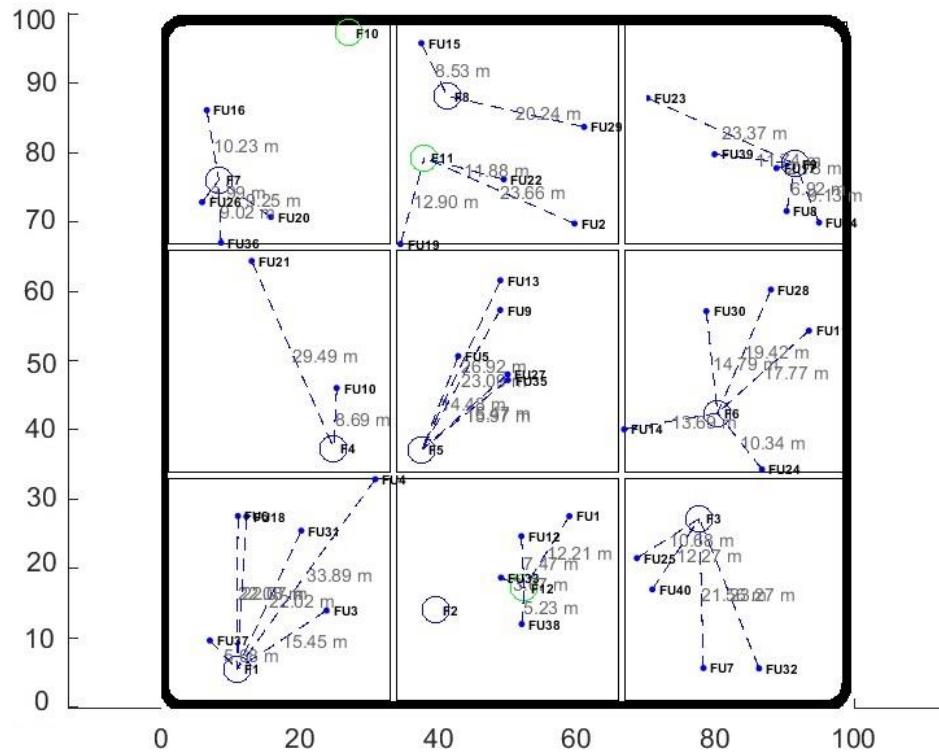


Figure 51: Layout of the building environment after optimisation for Case Study 2

As seen in Table 22, the path loss of the Femto User FU4 is 72.83 dB with a distance of 33.89 m from its optimised positioned distributed Femtocell F1 whereas the path loss of the Femto User FU17 is 47.35 dB and it is only 2.78 m away from its connected optimised positioned distributed Femtocell F9. This decrease in path loss is due to the decrease in distance of femto user from its femtocell. The path loss of the Femto User FU14 is 81.19 dB because it is connected to an optimised positioned distributed Femtocell F6 through a wall and consequently path loss increases because of penetration losses due to wall in between the user and the femtocell. The layout of the building environment displaying rooms along x and y axis and the positioning of the distributed and additional femtocells pre and post optimisation can be visualised together in Figure 52. Figure 52 shows the layouts of the building environment before and after optimisation together for comparative analysis. The blue circles represent the new

optimised positioning of the distributed femtocells unlike before optimisation where they were represented by red circles. Since boundary of the walls of each room was set as a bound for each distributed femtocell, the genetic algorithm developed for this optimisation has made sure that each distributed femtocell has found the new optimised position in the same room as seen clearly in Figure 52. Figure 52 shows that the distributed femtocells represented by numbers F1 to F9 shown in red pre optimisation have been relocated to the new optimised positions post optimisation shown in blue. All distributed femtocells were serving femto users pre optimisation whereas post optimisation the distributed Femtocell F2 is not serving any femto user.

Table 22: Throughput and Path Loss of the femto users with respect to their distance per number of walls after optimisation for Case Study 2

Femtocell Number	Femto User Number	Throughput (Mbps)	Path Loss (dB)	Distance (m) /Number of Walls
12	1	11.78	60.20	12.21/0
11	2	5.57	66.96	23.66/0
1	3	12	62.24	15.45/0
1	4	12	72.83	33.89/0
5	5	14.4	61.68	14.48/0
1	6	12	65.84	22.08/0
3	7	18	65.45	21.56/0
9	8	14.4	55.26	6.92/0
5	9	14.4	66.57	23.09/0
4	10	36	57.24	8.69/0
6	11	14.4	63.45	17.77/0
12	12	11.99	55.93	7.47/0
5	13	14.4	69.07	26.92/0
6	14	13.47	81.19	13.69/1
8	15	19.76	57.08	8.53/0
7	16	15.19	58.66	10.23/0
9	17	14.4	47.35	2.78/0
1	18	12	65.82	22.07/0
11	19	9.51	80.67	12.90/0
7	20	18	57.78	9.25/0
4	21	36	70.56	29.49/0
11	22	5.82	59.95	11.88/0
9	23	14.4	66.76	23.37/0
6	24	14.4	58.75	10.34/0
3	25	18	59.03	10.68/0
7	26	18	50.47	3.99/0
5	27	14.4	62.79	16.47/0
6	28	14.4	64.22	19.42/0
8	29	9.78	64.59	20.24/0
6	30	14.4	61.86	14.79/0
1	31	12	65.79	22.02/0
3	32	18	66.69	23.27/0
12	33	18	49.75	3.67/0
9	34	14.4	57.67	9.13/0
5	35	14.4	62.52	15.97/0
7	36	18	57.57	9.02/0
1	37	12	53.55	5.68/0
12	38	13.89	52.84	5.23/0
9	39	14.4	59.85	11.74/0
3	40	18	60.24	12.27/0

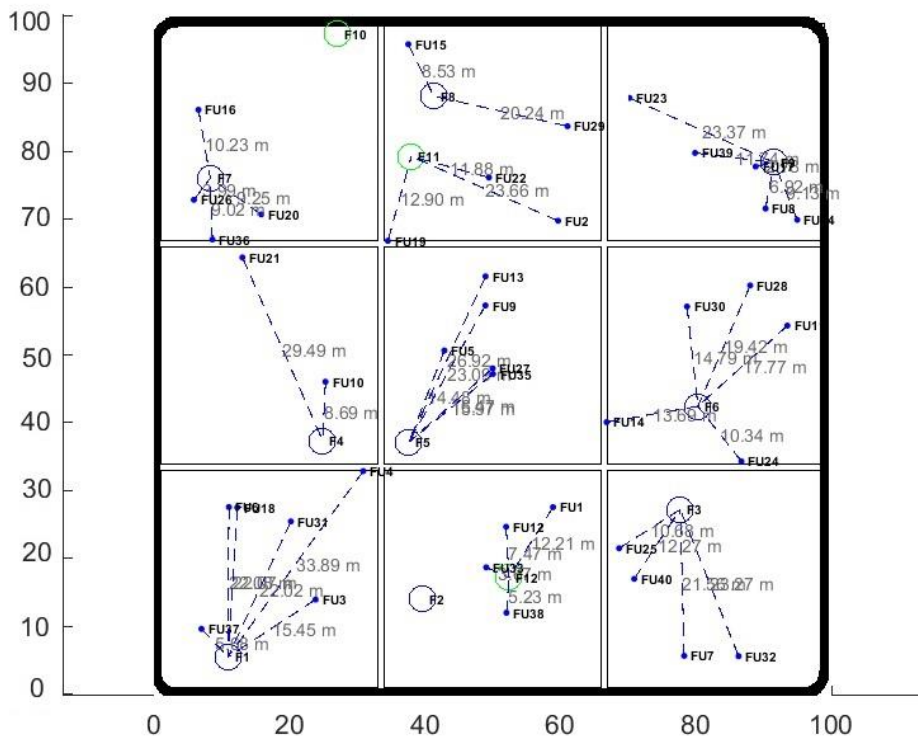
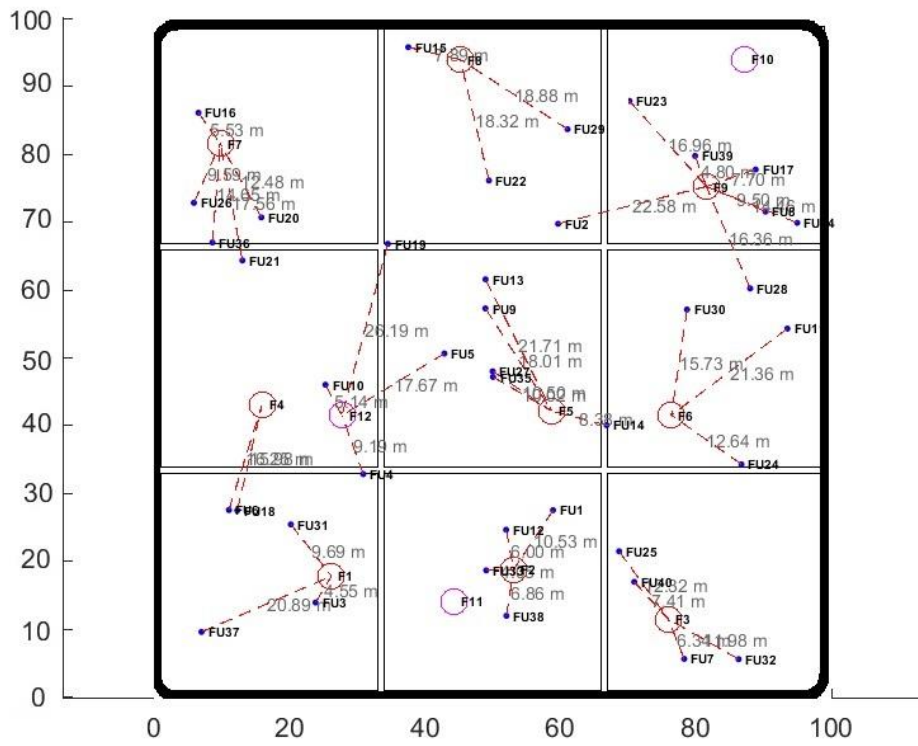


Figure 52: Layout of the building environment before and after optimisation for Case Study 2

The new optimised positioning of the additional femtocells is represented by green circles unlike before optimisation where they were represented by pink circles as shown in Figure 52. The aim of using 4 different colours is to distinguish between the positioning of the distributed and additional femtocells pre and post optimisation. Since additional femtocells were deployed randomly inside the building, therefore boundary of the entire building was set as a bound for each additional femtocell. As the purpose of additional femtocells is to ease the burden on the already serving overloaded femtocells, therefore they can move in any room of the building to accommodate the users, thereby increasing the overall throughput of the whole femtocell network. It can be seen in Figure 52 that the additional Femtocells F10 to F12 are relocated to the new optimised positions post optimisation shown in green from their previous positions pre optimisation shown in pink. Only additional Femtocell F12 was serving femto users pre optimisation whereas additional Femtocells F11 and F12 are serving femto users post optimisation.

Since the users were already randomly distributed, their positions are not changed as the objective function taken to optimise this femtocell network is the positioning of the femtocells. They are represented by same blue dots but are now connected to the optimised positioned femtocells as shown in Figure 52. For example, the Femto User FU18 was connected to the distributed Femtocell F4 shown in red pre optimisation while it is now connected to the optimised positioned distributed Femtocell F1 shown in blue post optimisation. It can also be seen clearly in Figure 52 that the Femto Users FU1, FU12, FU33 and FU38 were communicating with the distributed Femtocell F2 shown in red pre optimisation while they are now communicating with the optimised positioned additional Femtocell F12 shown in green post optimisation. The connection of a femto user to its corresponding femtocell post optimisation is shown by a dotted blue line unlike pre optimisation where it was represented by a dotted red line. The optimised distance of each femto user to its corresponding femtocell is again displayed in grey writing.

Table 23 states the calculated values of the throughput and path loss of all the femto users before and after optimisation for comparative analysis. The simulated results of Case Study 2 represented in Table 23 has achieved the desired objective of increasing the throughput while keeping the path loss as minimum as possible for most of the femto users as a result of the optimisation performed on the basis of the genetic algorithm.

The throughput of most of the femto users have increased as a result of the optimisation as seen in the simulated results of Table 23. The throughput of the Femto Users FU7, FU9, FU13, FU25, FU27, FU32, FU35 and FU40 is same pre and post optimisation. There is no increase in their throughputs before and after optimisation. The Femto Users FU7, FU25, FU32 and FU40

have throughputs of 18 Mbps each pre and post optimisation and similarly the Femto Users FU9, FU13, FU27 and FU35 have throughputs of 14.4 Mbps each before and after optimisation.

Table 23: Throughput and Path Loss of the femto users before and after optimisation for Case Study 2

Femto User Number	Throughput Pre Optimisation (Mbps)	Throughput Post Optimisation (Mbps)	Path Loss Pre Optimisation (dB)	Path Loss Post Optimisation (dB)
1	9.35	11.78	58.91	60.20
2	0.00042	5.57	106.20	66.96
3	24	12	51.62	62.24
4	0.00094	12	97.73	72.83
5	0.00033	14.4	103.41	61.68
6	0.00078	12	102.68	65.84
7	18	18	54.51	65.45
8	8.92	14.4	58.01	55.26
9	14.4	14.4	63.57	66.57
10	9.63	36	52.69	57.24
11	24	14.4	65.29	63.45
12	11.82	11.99	54.03	55.93
13	14.4	14.4	65.56	69.07
14	3.12	13.47	76.93	81.19
15	24	19.76	56.40	57.08
16	14.4	15.19	53.32	58.66
17	6.56	14.4	56.19	47.35
18	0.00072	12	102.53	65.82
19	0.0002	9.51	128.62	80.67
20	14.4	18	60.39	57.78
21	0.00029	36	103.35	70.56
22	24	5.82	63.72	59.95
23	1.95	14.4	63.05	66.76
24	24	14.4	60.50	58.75
25	18	18	60.27	59.03
26	14.4	18	58.10	50.47
27	14.4	14.4	58.88	62.79
28	0.00036	14.4	102.74	64.22
29	24	9.78	63.98	64.59
30	24	14.4	62.39	61.86
31	24	12	58.19	65.79
32	18	18	60.03	66.69
33	7.19	18	50.62	49.75
34	6.40	14.4	61.66	57.67
35	14.4	14.4	58.48	62.52
36	14.4	18	61.77	57.57
37	24	12	64.93	53.55
38	3.96	13.89	55.19	52.84
39	10.29	14.4	52.08	59.85
40	18	18	55.86	60.24
Sum	482.394	606.36	2744.38	2476.72
% Change		25.70		-9.75

There is a very minimal increase in the throughputs of the Femto Users FU12 and FU16 of 0.17 Mbps and 0.79 Mbps respectively as their throughputs pre optimisation were 11.82 Mbps and 14.4 Mbps respectively and post optimisation are 11.99 Mbps and 15.19 Mbps respectively. A slightly higher increase of 2.43, 5.57, 5.48, 7.84, 9.51, 3.60, 3.60, 8, 3.60, 9.93 and 4.11 Mbps each in throughputs is observed for the Femto Users FU1, FU2, FU8, FU17, FU19, FU20,

FU26, FU34, FU36, FU38 and FU39 respectively. The throughputs received by the Femto Users FU1, FU2, FU8, FU17, FU19, FU20, FU26, FU34, FU36, FU38 and FU39 pre optimisation were 9.35, 0.00042, 8.92, 6.56, 0.0002, 14.4, 14.4, 6.40, 14.4, 3.96 and 10.29 Mbps each respectively while post optimisation they are 11.78, 5.57, 14.4, 14.4, 9.51, 18, 18, 14.4, 18, 13.89 and 14.4 Mbps each respectively.

The Femto Users FU4, FU5, FU6, FU14, FU18, FU23, FU28 and FU33 have a substantial increase in their throughputs of 12, 14.40, 12, 10.35, 12, 12.45, 14.40 and 10.81 Mbps each respectively. The throughputs received by the Femto Users FU4, FU5, FU6, FU14, FU18, FU23, FU28 and FU33 pre optimisation were 0.00094, 0.00033, 0.00078, 3.12, 0.00072, 1.95, 0.00036 and 7.19 Mbps each respectively whereas post optimisation the received throughputs of these Femto Users are 12, 14.4, 12, 13.47, 12, 14.4, 14.4 and 18 Mbps each respectively. The Femto Users FU4, FU5, FU6, FU18 and FU28 had extremely low throughputs pre optimisation but post optimisation they have considerable throughputs as a result of the optimised positioning of the distributed and additional femtocells.

A substantial increase of 26.37 Mbps and 36 Mbps can be seen in the throughputs of the Femto Users FU10 and FU21 respectively. The throughputs received by the Femto Users FU10 and FU21 pre optimisation were 9.63 Mbps and 0.00029 Mbps respectively whereas post optimisation their received throughputs have considerably increased to 36 Mbps each respectively. 36 Mbps is the maximum calculated throughput received by any femto user after optimisation. Thus, the Femto Users FU10 and FU21 are receiving maximum throughputs as a result of the optimised positioning of the distributed and additional femtocells.

In contrast, a decrease in the throughputs of the Femto Users FU3, FU11, FU15, FU22, FU24, FU29, FU30, FU31 and FU37 can be seen in the simulated results of Table 23. The most decrement is observed in the throughput of the Femto User FU22 and its received throughput post optimisation has been decreased to 5.82 Mbps. The minimum throughput received by any femto user post optimisation is 5.57 Mbps which is quite a reasonable throughput considering that some of the femto users have almost 0 throughput pre optimisation.

For Case Study 2, the cumulative throughput of all the femto users in the femtocell network pre optimisation was 482.394 Mbps. The cumulative throughput of all the femto users in the femtocell network post optimisation is 606.36 Mbps. Hence the overall increase in the throughput of the whole femtocell network as a result of this optimisation based on the genetic algorithm is 123.97 Mbps. The simulation framework developed to perform the optimisation has resulted in an overall increase of 25.70% in the cumulative throughput of this femtocell network.

Figure 53 represents the throughputs of all the femto users pre and post optimisation. The trend in Figure 53 along the axis starting from Femto User Number 1 till 40 clearly shows that the throughput of most of the femto users post optimisation denoted by green dots is much higher than the throughput of most of the femto users pre optimisation denoted by yellow dots. It can also be observed in Figure 53 that the maximum throughput achieved by any user pre optimisation was 24 Mbps whereas post optimisation it has reached to 36 Mbps. The leader lines are used on the graph to denote the values of the throughput pre and post optimisation to avoid congestion.

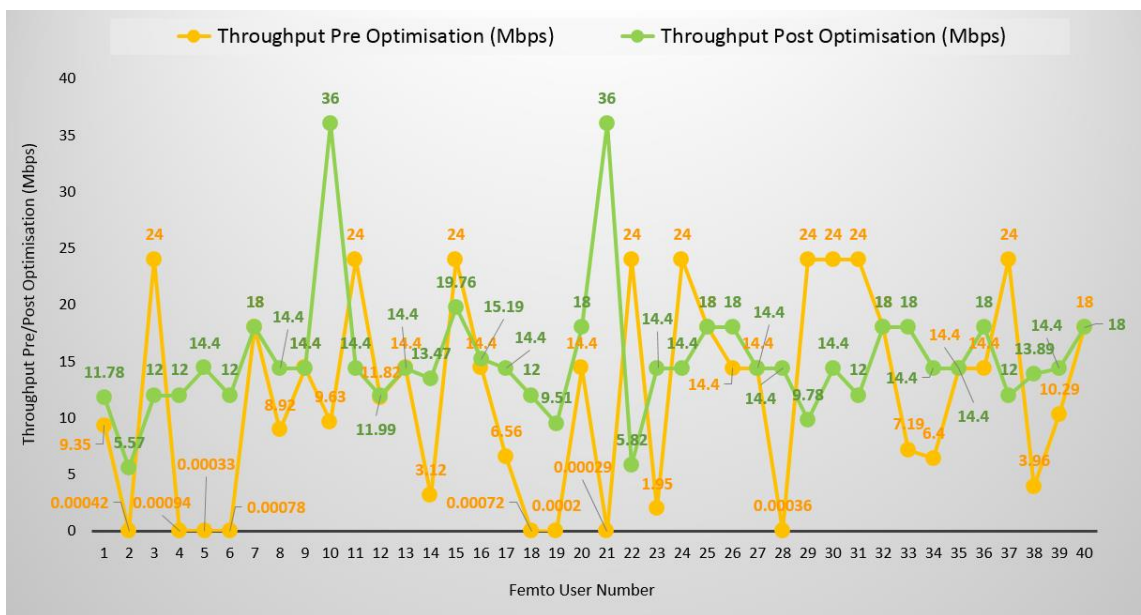


Figure 53: Throughput of the femto users before and after optimisation for Case Study 2

The simulated results of Table 23 confirm that the path loss increases or decreases as the distance of femto user from its corresponding femtocell increase or decrease. The path loss increases significantly if there are any walls in between the femto user and its femtocell as seen in Table 21. Table 23 showing the comparison of the throughput and path loss of all the femto users pre and post optimisation can be used for the comparative analysis of path loss. The path loss of the femto users who were connected to their femtocells pre optimisation through walls have a significant decrease in their path loss because most of them except FU14 are now coordinating with their optimised positioned distributed and additional femtocells without any wall in between them and their corresponding femtocells. Hence, the objective to keep the path loss as minimum as possible for most of the femto users is achieved as a result of this optimisation.

There is a substantial decrease of 39.24, 24.90, 41.73, 36.84, 36.71, 47.95, 32.79, 38.52 and 11.38 dB each in the path loss of the Femto Users FU2, FU4, FU5, FU6, FU18, FU19, FU21,

FU28 and FU37 respectively. The path loss of these Femto Users was 106.20, 97.73, 103.41, 102.68, 102.53, 128.62, 103.35, 102.74 and 64.93 dB each respectively pre optimisation whereas post optimisation it has significantly decreased to 66.96, 72.83, 61.68, 65.84, 65.82, 80.67, 70.56, 64.22 and 53.55 dB each respectively. There is a small decrease in the path loss of the Femto Users FU8, FU11, FU17, FU20, FU22, FU24, FU25, FU26, FU30, FU33, FU34, FU36 and FU38 by 2.75, 1.84, 8.84, 2.61, 3.77, 1.75, 1.24, 7.63, 0.53, 0.87, 3.99, 4.20 and 2.35 dB each respectively because of the decrease in their distances from their corresponding optimised positioned distributed and additional femtocells post optimisation. The path loss of these Femto Users pre optimisation was 58.01, 65.29, 56.19, 60.39, 63.72, 60.50, 60.27, 58.10, 62.39, 50.62, 61.66, 61.77 and 55.19 dB each respectively whereas post optimisation it has decreased to 55.26, 63.45, 47.35, 57.78, 59.95, 58.75, 59.03, 50.47, 61.86, 49.75, 57.67, 57.57 and 52.84 dB each respectively. An increase in the path loss of some of the femto users is also observed post optimisation. The maximum increase of 10.94 dB is noticed in the path loss of the Femto User FU7 whereas the maximum decrease of 47.95 dB is observed in the path loss of the Femto User FU19.

For Case Study 2, the cumulative path loss of all the femto users in the femtocell network pre optimisation was 2744.38 dB. The cumulative path loss of all the femto users in the femtocell network post optimisation is 2476.72 dB. Hence the overall decrease in the path loss of the whole femtocell network as a result of this optimisation based on the genetic algorithm is 267.66 dB. The simulation framework developed to perform the optimisation on a network of femtocells in an indoor environment of the building has resulted in an overall decrease of 9.75% in the cumulative path loss of the femto users in this femtocell network.

Figure 54 represents the path loss of all the femto users pre and post optimisation. The trend in Figure 54 along the axis starting from Femto User Number 1 till 40 clearly shows that the path loss of most of the femto users post optimisation denoted by green dots is much lower than the path loss of most of the femto users pre optimisation denoted by yellow dots. It can also be observed in Figure 54 that the maximum path loss of a femto user pre optimisation was 128.62 dB whereas post optimisation it is 81.19 dB. The leader lines are used on the graph to denote the values of the path loss pre and post optimisation to avoid overlapping of values.

In addition to the simulation results of the throughput and path loss of all the femto users pre and post optimisation, Table 24 also shows the delta throughput i.e. the difference in the post and pre optimisation throughputs in Mbps and delta path loss i.e. the difference in the post and pre optimisation path loss in dB of all the femto users in an indoor environment of the building for further analysis.

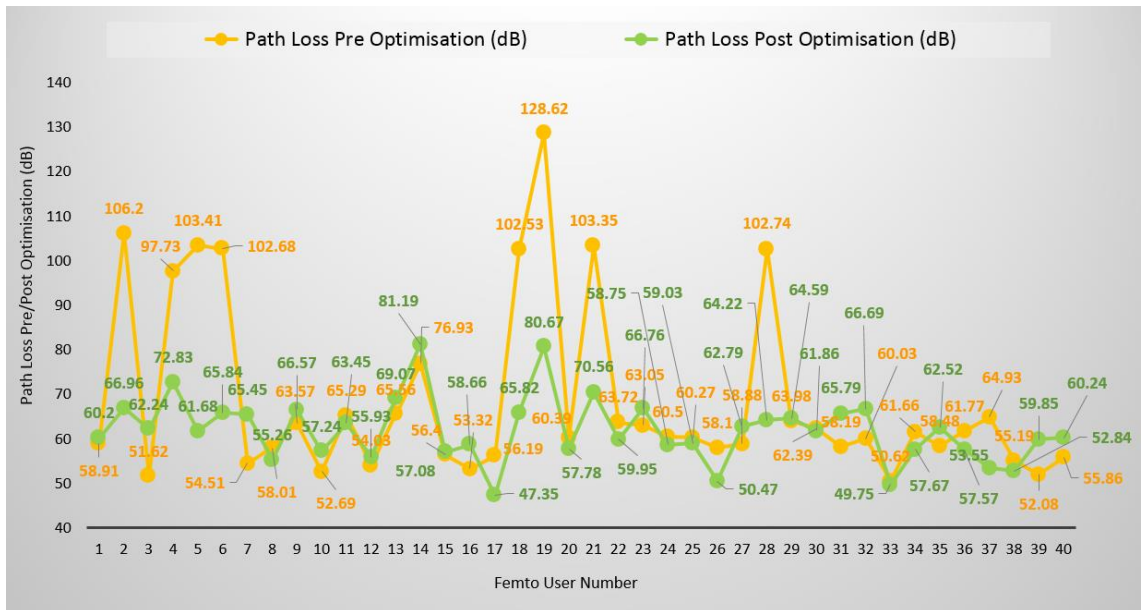


Figure 54: Path Loss of the femto users before and after optimisation for Case Study 2

The genetic algorithm developed to perform the optimisation aims to increase the throughput while decreasing the path loss of the femto users to be able to optimise the femtocell network. As evident from the simulation results of Table 24, the throughput of most of the femto users have increased while the path loss of most of the femto users have decreased post optimisation. The decrement in the throughput of the few femto users is a trade off against an increment in the throughput of most of the femto users thereby increasing the overall throughput of the whole femtocell network by 25.70%. Similarly, increase in the path loss of some of the femto users is a trade off against a substantial decrease in the path loss of most of the femto users resulting in an overall decrease of the path loss of the whole femtocell network by 9.75%. Thus, the simulation framework is able to optimise the femtocell network in terms of increasing the throughput and reducing the path loss.

As seen in Table 24, the Femto Users FU2, FU4, FU5, FU6, FU8, FU17, FU18, FU19, FU20, FU21, FU26, FU28, FU33, FU34, FU36 and FU38 have an increase in their throughputs and at the same time decrease in their path loss post optimisation. The throughput of the Femto User FU25 does not change but has a decrease in its path loss while the throughputs of the Femto Users FU7, FU9, FU13, FU27, FU32, FU35, FU40 also do not change but they have an increase in their path loss post optimisation. Although the path loss of the Femto Users FU1, FU10, FU12, FU14, FU16, FU23 and FU39 have decreased but the cumulative increase in their throughputs is more than the cumulative decrease in their path loss post optimisation. Similarly, the throughputs of the Femto Users FU11, FU22, FU24, FU30 and FU37 have decreased but it is a trade off against a decrease in their path loss. Only the Femto Users FU3, FU15, FU29 and

FU31 experience a decrease in their throughputs as well as an increase in their path loss as a result of this optimisation.

Table 24: Delta Throughput and Delta Path Loss of the femto users for Case Study 2

Femto User No.	Throughput Pre Optimisation (Mbps)	Throughput Post Optimisation (Mbps)	Delta Throughput (Post vs Pre) (Mbps)	Path Loss Pre Optimisation (dB)	Path Loss Post Optimisation (dB)	Delta Path Loss (Post vs Pre) (dB)
1	9.35	11.78	2.43	58.91	60.20	1.29
2	0.00042	5.57	5.57	106.20	66.96	-39.24
3	24	12	-12.00	51.62	62.24	10.62
4	0.00094	12	12.00	97.73	72.83	-24.90
5	0.00033	14.4	14.40	103.41	61.68	-41.73
6	0.00078	12	12.00	102.68	65.84	-36.84
7	18	18	0.00	54.51	65.45	10.94
8	8.92	14.4	5.48	58.01	55.26	-2.75
9	14.4	14.4	0.00	63.57	66.57	3.00
10	9.63	36	26.37	52.69	57.24	4.55
11	24	14.4	-9.60	65.29	63.45	-1.84
12	11.82	11.99	0.17	54.03	55.93	1.90
13	14.4	14.4	0.00	65.56	69.07	3.51
14	3.12	13.47	10.35	76.93	81.19	4.26
15	24	19.76	-4.24	56.40	57.08	0.68
16	14.4	15.19	0.79	53.32	58.66	5.34
17	6.56	14.4	7.84	56.19	47.35	-8.84
18	0.00072	12	12.00	102.53	65.82	-36.71
19	0.0002	9.51	9.51	128.62	80.67	-47.95
20	14.4	18	3.60	60.39	57.78	-2.61
21	0.00029	36	36.00	103.35	70.56	-32.79
22	24	5.82	-18.18	63.72	59.95	-3.77
23	1.95	14.4	12.45	63.05	66.76	3.71
24	24	14.4	-9.60	60.50	58.75	-1.75
25	18	18	0.00	60.27	59.03	-1.24
26	14.4	18	3.60	58.10	50.47	-7.63
27	14.4	14.4	0.00	58.88	62.79	3.91
28	0.00036	14.4	14.40	102.74	64.22	-38.52
29	24	9.78	-14.22	63.98	64.59	0.61
30	24	14.4	-9.60	62.39	61.86	-0.53
31	24	12	-12.00	58.19	65.79	7.60
32	18	18	0.00	60.03	66.69	6.66
33	7.19	18	10.81	50.62	49.75	-0.87
34	6.40	14.4	8.00	61.66	57.67	-3.99
35	14.4	14.4	0.00	58.48	62.52	4.04
36	14.4	18	3.60	61.77	57.57	-4.20
37	24	12	-12.00	64.93	53.55	-11.38
38	3.96	13.89	9.93	55.19	52.84	-2.35
39	10.29	14.4	4.11	52.08	59.85	7.77
40	18	18	0.00	55.86	60.24	4.38
Sum	482.394	606.36	123.97	2744.38	2476.72	-267.66

Figure 55 depicts the comparison of the delta throughput and delta path loss of all the femto users along the axis starting from Femto User Number 1 till 40. The leader lines are used to denote some values to avoid overlapping. The delta throughput of all the femto users is represented by green rectangular bars while the delta path loss of all the femto users is shown by

yellow rectangular bars as seen in Figure 55. It can be seen that the throughputs of most of the femto users have increased as desired and therefore most of the green bars are on the positive side of the axis. The path loss of most of the femto users have reduced as desired and consequently most of the yellow bars are on the negative side of the axis. The long rectangular bars correspond to the significant increase in the throughputs and substantial decrease in the path loss of the femto users. Figure 55 also illustrates that most of the femto users have an increase in their throughputs as well as a decrease in their path loss as a result of the optimisation based on the genetic algorithm.

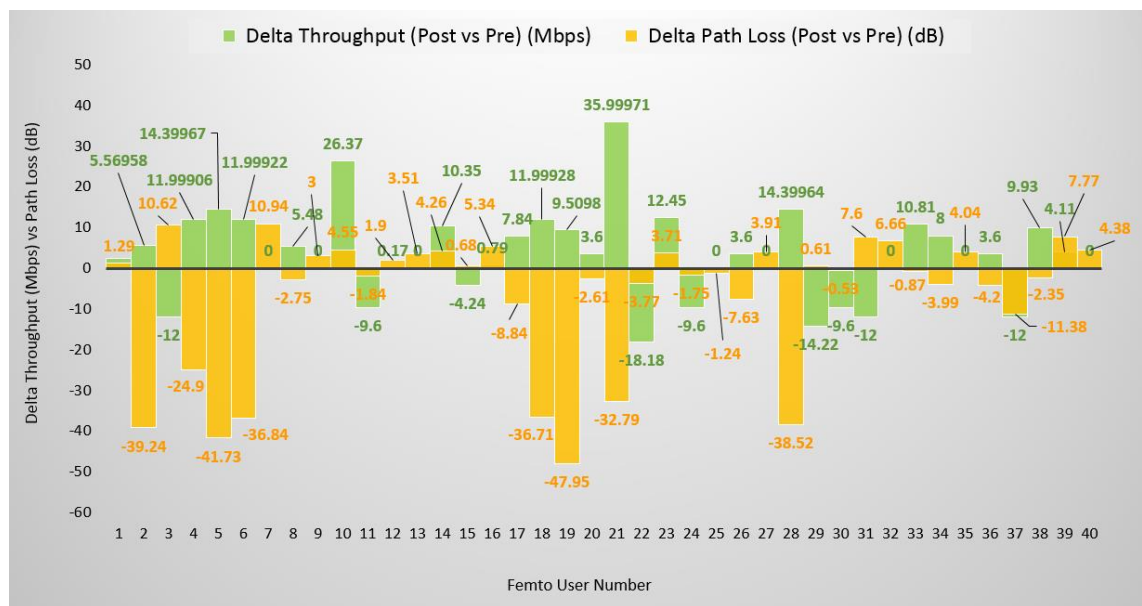


Figure 55: Delta Throughput and Delta Path Loss of the femto users for Case Study 2

5.4 Conclusion

The simulation framework developed for optimising femtocell networks has been described in detail. The framework is able to optimise the whole femtocell network for both case studies by finding the optimised positioning of the distributed and additional femtocells based on the genetic optimisation algorithm. The end user can provide the inputs of the desired network topology to the simulation framework through graphical user interface. The throughput and path loss of all the femto users are calculated before and after optimisation. The simulation results are generated in the form of tables before and after optimisation for comparison and analysis. The layouts depicting the indoor environment of the building before and after optimisation can be seen and analysed through graphical user interface developed as a part of this simulation framework. Two case studies were defined and described to show how the simulation framework can be used to identify the optimum positions of femtocells under different configurations of room designs and number of users that represent contrasting loads on the network. In first Case Study, there was a less load on the network as 4 distributed and 2

additional femtocells were deployed to accommodate 24 users in 4 rooms each of size 50 x 50 m of the building. Post optimisation results have shown that overall throughput of the femtocell network was increased by 59.21% and at the same time overall path loss of the femtocell network was decreased by 14.90%. In second Case Study, the load on the network was increased as 9 distributed and 3 additional femtocells were deployed to accommodate 40 users in 9 rooms each of size approx. 33 x 33 m of the building. A congested indoor environment was created to overload some of the femtocells in Case Study 2 to test the capacity and capability of the developed simulation framework. Post optimisation results of Case Study 2 have shown that the simulation framework was still able to optimise the femtocell network by increasing the overall throughput of the femtocell network by 25.70% and at the same time reducing the overall path loss of the femtocell network by 9.75%. Any desired network topology can be created and analysed on the basis of throughput and path loss by using this simulation framework developed to optimise the femtocell networks in an indoor environment of the building. Since genetic algorithms can cater for multiple problems at one time through multi-objective genetic algorithms, path loss or any other parameter can also be taken as an objective function along with throughput to optimise the femtocell networks by using this simulation framework as part of the future work. Some codes of the whole simulation package used to carry out the optimisation in this chapter are shared in Appendix B.

Chapter 6: Conclusion of the Thesis

This chapter concludes the thesis with the summary of the findings from all chapters and presents the contribution to knowledge. It also discusses suggestions for further work that could arise from the findings but are outside the scope of this research.

6.1 Summary of the findings of the Thesis

The aim and objectives of the research were defined in Chapter 1 including the research questions and the thesis methodology. The aim of this research was to develop the simulation framework to be able to optimise the femtocell networks for indoor communication. The remaining chapters worked towards achieving this aim following the research methodology described in Chapter 1.

In Chapter 2, the advancements in the mobile communication systems from 1G to 5G have been discussed. 2G was the first digital mobile communication network planned for better coverage. 3G was planned for voice considering data and some multimedia. 4G truly constitutes mobile broadband allowing voice, data and video access wirelessly possible anywhere. To reduce the burden on main base stations due to the substantial increase in the number of users, small cells including femtocells have been introduced in the hierarchy of networks to provide coverage to homes, offices and metropolitan areas in a cost and energy efficient way. The literature review established that research into femtocells was an active research area and provided insights about the range of research activities involving femtocells. Femtocells operate in the licensed spectrum and act as a main base stations to the users they are connected. Femtocells were identified as a crucial way to the delivery of the increased demands. The history of the femtocells was also discussed in this chapter including its origin and development over time. This chapter provided insights about the range of research activities involving femtocells and illustrated how femtocells fit in with the development of mobile networks. Femtocells could bridge the gap from operations, administration and maintenance to optimised networks. The research and recent advancements have shown that femtocells can manage the expected demand of real time traffic with dense heterogeneous networks and enable the end users to experience uninterrupted connectivity to the network. This chapter provided some background and reviewed literature that suggested optimising the location of femtocells would improve the efficiency of mobile networks.

In order to achieve the aim and objectives of the research, it was necessary to understand which specific set of parameters could be used together to carry out the allocation of resources in an efficient way and to offload the heavy traffic from already heavily loaded macrocells to lightly loaded femtocells. For this purpose, in Chapter 3, a survey of the literature was conducted to examine the parameters different authors have used to optimise the network. Methodologies and

approaches used for optimising femtocell networks were discussed. Based on the findings, throughput and path loss were selected as performance parameters for inclusion in the simulation framework used to perform the experiments and to analyse the performance of a two-tier LTE-A system having femtocell overlays. The identification of the parameters to investigate the performance of a two-tier LTE-A system with femtocell overlays and then to find the optimised positioning of the femtocells by using the simulation framework is unique to this research. The comparison of approaches and the aspects they were trying to improve was discussed in Table 3. Chapter 3 drew attention to how the different themes and approaches (mixture of parameters) had developed and changed over time. The claimed improvement in the performances of the networks was compared with the emphasis on different parameters.

Chapter 4 described the simulation framework and presented the results of set of experiments performed to analyse the performance which formed the basis to help identify the optimised positioning of the femtocells of a two-tier LTE-A system in which a macrocell remained in the top tier while femtocells worked in the lower tier of the network. The graphical user interface of the simulation framework allows the flexibility to set up the desired two-tier network topology. It calculates the throughput and path loss of all the femto and macro users for all the supported bandwidths of an LTE-A system using different modulation schemes. A series of tests were carried out to calculate the maximum throughput and path loss for the described scenarios. The experiments were run several times for different values and the simulation results were evaluated in terms of throughput and path loss. The bandwidth and modulation schemes were varied initially for simulation in Case Study 1 to analyse the effect they had on the throughput and path loss of the femto users. The simulation framework was able to analyse the performance and showed that for any bandwidth of an LTE-A system with femtocell overlays, the throughput of a femto user was increased two times for 16QAM modulation scheme as compared to QPSK. The throughput was increased to three times for 64QAM as compared to QPSK. The simulation results also confirmed that the path loss is independent of the modulation scheme. Case Study 1 used minimal load on the network because the aim was to analyse the change in throughput and path loss with respect to the change in modulation scheme for each LTE-A supported bandwidth. In Case Study 2, the load on the network was increased to test the capacity and capability of the simulation framework as the number of femtocells were increased and additional femto and macro users were added to the network. The aim was to examine the effect of walls on the throughput and path loss of the users and the effect of additional users on the throughput and path loss of the users connected to the same femtocells. In Case Study 3, the type of modulation scheme and LTE supported bandwidth was kept constant and positioning of the femtocells was changed for each scenario inside the buildings to analyse the performance. The aim was to analyse the effect of changing the positions of the femtocells only on the

throughput and path loss of the femto users if all other parameters are kept constant. The results of all these experiments contributed to define the objective function described in detail in Chapter 5 to be able to optimise the femtocell network and find the optimised positioning of the femtocells. The simulation framework was able to identify the extent to which the signal strength was reduced. The simulation results were able to validate the following key points:

- The throughput of the femto users is maximum if they are the only users in the coverage areas of their femto base stations with no wall in between them and their femto base stations
- The bandwidth is shared amongst the femto users if they all are connected to the same femtocell. Hence, the optimised location is placing the femtocell in the middle of a room or office so that the users in the corner still have reasonable throughput
- The throughputs are significantly decreased for the femto users having walls in between them and their corresponding femto base stations. It is shown that if a user is located in the close proximity of a femtocell but there is a wall in between, the signal strength reduces to a great extent and consequently the user suffers low bandwidth. In places such as corridors etc., users sometime end up with almost no connectivity. Therefore, it is important to make sure that femtocells are placed separately in corridors to mitigate the effect of walls thus preventing the degradation of signals for the users
- The path loss increases as the distance of femto or macro user from its base station increase and decreases as the distance of femto or macro user from its corresponding base station decrease
- The path loss does not change linearly with the distance because of the logarithm function and penetration losses involved in the equations used to compute the path loss
- A significant increase in the path loss is observed if there are any walls in between the user and its base station

The simulation framework incorporating two-tier mobile network is able to verify that the simulations accurately result in what is expected as a result of testing various scenarios in different case studies. The simulation framework can calculate the throughput at every point in the working environment of the LTE-A system having both a macrocell and femtocells working together. These results were used and the simulation framework was further developed as described in Chapter 5 to be able to find the optimised positioning of the femtocells in different room layouts of the building which was the main aim of this project.

In places like offices etc. with large number of people and where number of users also change constantly, the genetic optimisation algorithm needed to be incorporated in the simulation framework discussed in Chapter 4 to find the optimised positioning of the femtocells and

therefore discussed in detail in Chapter 5. The simulation framework developed for optimising femtocell networks is able to optimise the whole femtocell network by finding the optimised positioning of the distributed and additional femtocells based on the genetic optimisation algorithm. The end user can provide the inputs of the desired network topology to the simulation framework through graphical user interface. The throughput and path loss of all the femto users are calculated before and after optimisation. The simulation results are generated in the form of tables before and after optimisation for comparison and analysis. The layouts depicting the indoor environment of the building before and after optimisation can be seen and analysed through graphical user interface developed as a part of this simulation framework. Two case studies were defined and described to show how the simulation framework can be used to identify the optimum positions of femtocells under different configurations of room designs and number of users that represent contrasting loads on the network. In first Case Study, there was a less load on the network as 4 distributed and 2 additional femtocells were deployed to accommodate 24 users in 4 rooms each of size 50 x 50 m of the building. Post optimisation results have shown that overall throughput of the femtocell network was increased by 59.21% and at the same time overall path loss of the femtocell network was decreased by 14.90%. In second Case Study, the load on the network was increased as 9 distributed and 3 additional femtocells were deployed to accommodate 40 users in 9 rooms each of size approx. 33 x 33 m of the building. A congested indoor environment was created to overload some of the femtocells in Case Study 2 to test the capacity and capability of the developed simulation framework. Post optimisation results of Case Study 2 have shown that the simulation framework was still able to optimise the femtocell network by increasing the overall throughput of the femtocell network by 25.70% and at the same time reducing the overall path loss of the femtocell network by 9.75%. Thus, the simulation framework developed for this research has been able to meet the aim and objectives of this research defined in Chapter 1 and able to optimise the positioning of the femtocells and consequently able to optimise the network of femtocells in an indoor environment by increasing the throughput and at the same time decreasing the path loss of the network. Hence, the optimised network of femtocells has significantly improved the performance of the network as compared to the unoptimised scenarios or the scenarios in which femtocells are placed randomly inside the building.

6.2 Comparison of the results with the Literature

It is not possible to make direct comparisons of the results of experiments conducted for this research with the results described in the existing literature because of the use of different parameters and difference in the aims of their research. The comparison of some of the papers discussed in the literature most relevant to the research conducted for this PhD is described in the following section.

Amine and Syla (2017) were able to increase the network coverage of an indoor environment by 13.6% using the genetic algorithm to optimise the location of femtocells in order to minimise the number of femtocells required. They did not report the effect their algorithm had on throughput and path loss but designed their algorithm to keep the distance between femtocells within a set radius. This research follows a similar approach of using genetic algorithms but builds on the results of Amine and Syla (2017) by using the genetic algorithm to find the optimal balance of maximising throughput and reducing path loss. The measures of performance are not the same but the results show that the use of the genetic algorithms is successful in finding an optimum solution that improves network performance in both case studies. Likewise, to address the issues of indoor deployment of femtocells as part of the LTE-A heterogeneous network, an efficient optimisation technique based on the genetic algorithm is applied on large selection of sample buildings under various conditions in (Badra and Figueras 2018). A set of applicable guidelines for the optimal deployment of femtocells is obtained as a result of joint optimisation of average downlink throughput and outage probability. This work is able to address the issues associated with the indoor deployment of femtocells and consequently provide guidelines to deploy femtocells in optimised locations. The results in Chapter 4 are able to provide the guidelines while Chapter 5 has been able to show the increase in throughput and decrease in path loss at the same time for most of the femto users before and after optimisation for comparative analysis and hence able to demonstrate the improvement in performance as a result of optimisation based on the genetic algorithm.

The hierarchical agglomerative original algorithms were modified by taking into account the path loss influenced by various obstructions such as doors, windows and different types of walls to address the issue of indoor coverage in (Ibrahim et al. 2018). The simulation framework developed for this research has taken only walls into account but has used genetic algorithm. The objective function is defined on the basis of throughput but able to optimise the location of femtocells in terms of both throughput and path loss. The performance in (Ibrahim et al. 2018) is measured in terms of maximising SINR and reducing the number of femtocells deployed in an indoor environment. The proposed algorithm is able to reduce the cost while the simulation framework developed for this research has been able to significantly improve the performance of the whole network of femtocells in terms of throughput and path loss thereby increasing quality of service for most of the femto users. To achieve the full coverage in the building has always been a complicated issue. (Nassiri and Borujeni 2020) has computed the optimised location of femtocells using the genetic algorithm on the basis that the number of handovers is minimal while in the simulation framework developed for this research, the optimised location of femtocells is found using the genetic algorithm on the basis that the throughput is maximum and path loss is minimum for each femto user deployed inside the building. The concept of

considering the assumptions and limitations to carry out the process of optimisation for this research (as described in Section 5.2 of Chapter 5) is also taken from (Nassiri and Borujeni 2020). The experimental results of (Nassiri and Borujeni 2020) have indicated the reduction in the number of handovers up to 30% with almost complete coverage while the simulation framework developed for this research is able to improve the performance of network by 59.21% in terms of throughput and the same time in terms of path loss by 14.90% for Case Study 1 in the simulated results of Chapter 5. A case study was performed in (Deb et al. 2017) to illustrate the most suitable path loss model for an indoor scenario depending on the building structure, floor types, frequency range and wall types. Hence, same case studies of Chapter 5 could be used to find the optimised positioning of the femtocells based on Particle Swarm Optimisation, Fmincon Optimisation etc, and results can be compared with genetic algorithms for more extensive analysis as part of the future work.

(Alotaibi and Angelides 2017) in their work have predicted the number of femtocells required for successful deployment to provide coverage for indoor environment on the basis of two factors: the femtocell access point radius in the target area and the area size. Their indoor deployment plan outperformed its equivalent outdoor plan and multipath loss was amongst the various factors they have measured to improve the coverage and enhance the quality of service. Thus, femtocells are able to provide much higher high data rates in an indoor environment of the building. Path loss is also a performance measuring parameter for the research conducted for this PhD and the simulated results have shown that decrease in the path loss of the femto users have improved the performance of the femtocell network in an indoor environment of the building. The issue of jointly optimising the placement of femtocell base station and power control in commercial building environments is addressed in (Liu et al. 2012). A mathematical model with ability to capture the unique features of building (building size, structure, layout and floor/wall separation) is proposed. An effective global optimisation algorithm is suggested on the basis of convex relaxation of the formulated Mix Integer Convex Program (MICP) within a branch and bound framework resulted in prolong battery lives of mobile headsets and offered useful insights to deploy femtocells in commercial buildings. The path loss modelling is also presented in this paper. Since partitions in building environments vary drastically in their electrical and physical characteristics, it is very difficult to accurately derive and measure a general path loss model. Therefore, path loss model already exists in the literature is used in the simulation framework developed for this research (as described in Section 4.2 of Chapter 4) to conduct the experiments in order to find the optimised positioning of the femtocells inside the building. Hence, the results of the scenarios simulated for the simulation framework developed for optimising femtocell networks have improved on the performance of existing networks. This research has been able to address all the research questions stated in Section 1.4 of Chapter 1.

This research has shown that a simulation framework can be developed to optimise the network of femtocells for indoor communication. It is also able to justify that an optimised femtocell network can improve the performance of existing networks.

6.3 Contribution to Knowledge

The main contribution to knowledge of this thesis is the development of the simulation framework to find the optimised positions of the femtocells and consequently optimise the femtocell networks based on the genetic optimisation algorithm. A user friendly simulation framework is able to optimise the network of femtocells in an indoor environment of the building consisting of different configurations of room designs and number of users that represent contrasting loads on the network by increasing the throughput and decreasing the path loss of the network at the same time. The end user can provide the inputs of the desired network topology to the simulation framework through graphical user interface. The layouts depicting the indoor environment of the building before and after optimisation can be seen and analysed through graphical user interface developed as a part of this simulation framework. Initially, the simulation framework adapted from Bouras et al. (2012) was used to incorporate two-tier mobile network to verify that the simulations accurately result in what is expected as a result of testing various scenarios in different case studies. The simulation framework was able to calculate the throughput and path loss of all the femto and macro users in the working environment of the LTE-A system having both macrocell and femtocells working together. These results were used and the simulation framework was further developed to be able to find the optimised positioning of the femtocells in different room layouts of the building which was the main aim of this project. The developed simulation framework has the capacity and capability to optimise any network of femtocells. The framework allows the flexibility of defining any desired environment to perform the experiments. Any number of femto cells and femto users can be selected to be deployed in different locations of the rooms inside the building. The criteria to carry out the optimisation process based on the genetic algorithm is described in detail. Each step of the simulation process can be seen and analysed through graphical user interface. Any combination of Bandwidth/Modulation used in LTE-A systems can be selected through graphical user interface. Any number of buildings along x and y axis are selected. A very large number of values would be difficult to visualise on graphical user interface but the framework would still be able to simulate, optimise and produce output. The values of the parameters used in the simulation framework are defined. The framework also allows the end user to vary the values of the parameters which makes this developed simulation framework unique. To conclude, the development of a user friendly simulation framework to be able to find the optimised location of femtocells in an indoor environment based on the genetic optimisation algorithm in order to optimise the whole femtocell network by using a unique mix

of parameters, that is, throughput and path loss is a novel contribution of this research thesis and has not been done before in the literature to the best of author's knowledge.

6.4 Limitations of the Work and Future Work

Although, any desired network topology can be created and analysed by using this simulation framework developed to optimise the femtocell networks in an indoor environment of the building, there are some limitations in the simulation framework which could be improved as part of the future work. The walls can only be defined along x and y axis through the graphical user interface of this simulation framework and consequently the rooms generated are always uniformly distributed inside the building. The graphical user interface can be further developed to create buildings with different rooms layouts and designs to enhance the capacity of the simulation framework. Similarly, the thickness of the walls is kept constant in all the experiments whereas the walls of different buildings may have variable thickness. In addition, different materials used to construct the walls have different effects on the signal strength. Hence, the thickness and the material used to build the walls may pose different challenges and could be addressed as part of the future work. Since genetic algorithms can cater multiple problems at a time through multi-objective genetic algorithms, path loss or any other parameter can also be taken as an objective function along with throughput to optimise the femtocell networks by using this simulation framework as part of the future work. This simulation framework can also be used to implement other optimisation techniques such as Particle Swarm Optimisation, Fmincon Optimisation etc., but due its ability of fast convergence and to stick on local and global optimum points, a genetic algorithm was implemented as an optimisation technique for this research. Hence, same case studies could be used to find the optimised positioning of the femtocells based on Particle Swarm Optimisation etc. and results can be compared with genetic algorithms for more extensive analysis. It may happen that a particular optimisation technique gives best results of all the optimisation techniques for a particular scenario. This could also be investigated as part of the future work. The femto users were randomly deployed inside the building since the users working in an office or building are randomly distributed. But the locations of the users were not changed pre and post optimisation while positions of the femtocells were optimised. Hence, the users were considered to be static. The simulation framework can be modified by optimising the positioning of the femtocells for mobile users. It means that optimised positions of the femtocells would keep on changing if users constantly change their locations.

References

- Abbas, S. and Hameed, A., 2018. Power and Coverage Based Performance Analysis for Femtocells Network.
- Adi, P. D. P. and Kitagawa, A., 2019. ZigBee Radio Frequency (RF) performance on Raspberry Pi 3 for Internet of Things (IoT) based blood pressure sensors monitoring. *International Journal of Advanced Computer Science and Applications (IJACSA)*, 10 (5), 63.
- Agiwal, M., Kwon, H., Park, S. and Jin, H., 2021. A Survey on 4G-5G Dual Connectivity: Road to 5G Implementation. *IEEE Access*, 9, 16193-16210.
- Aguilar-Garcia, A., Barco, R. and Fortes, S., 2016a. Coordinated location-based self-optimization for indoor femtocell networks. *Computer Networks*, 106, 1-16.
- Aguilar-Garcia, A., Fortes, S., Duran, A. F. and Barco, R., 2016b. Context-Aware Self-Optimization: Evolution Based on the Use Case of Load Balancing in Small-Cell Networks. *IEEE Vehicular Technology Magazine*, 11 (1), 86-95.
- Aguilar-Garcia, A., Fortes, S., Garrido, A., Fernandez-Duran, A. and Barco, R., 2016c. Improving load balancing techniques by location awareness at indoor femtocell networks. *EURASIP Journal on Wireless Communications and Networking*, 2016 (1), 201.
- Ahmad, I., 2011. 3GPP Long Term Evolution, *10 th Research Seminar Series Workshop*.
- Akinlabi, O. and Joseph, M., 2016. Signal behaviour in an indoor environment: Femtocell over macrocell, *Environment and Electrical Engineering (EEEIC), 2016 IEEE 16th International Conference on* (pp. 1-5): IEEE.
- Al-Khafaji, H. M. and Majdi, H. S., 2018. A High Throughput Architecture for 5G Wireless Backhaul Networks, *2018 IEEE International Conference on Electrical Engineering and Photonics (EExPolytech)* (pp. 9-12): IEEE.
- Alnoman, A. and Anpalagan, A., 2017. Towards the fulfillment of 5G network requirements: technologies and challenges. *Telecommunication Systems*, 65 (1), 101-116.
- Alnoman, A., Sharma, S. K., Ejaz, W. and Anpalagan, A., 2019. Emerging edge computing technologies for distributed IoT systems. *IEEE Network*, 33 (6), 140-147.
- Alotaibi, A. A. and Angelides, M. C., 2017. Femtocell deployment plan: moving indoors, *2017 Intelligent Systems Conference (IntelliSys)* (pp. 210-216): IEEE.
- Alquhali, A. H., Roslee, M., Alias, M. Y. and Mohamed, K. S., 2020. D2D communication for spectral efficiency improvement and interference reduction: A survey. *Bulletin of Electrical Engineering and Informatics*, 9 (3), 1085-1094.
- Altman, E., Boulogne, T., El-Azouzi, R., Jiménez, T. and Wynter, L., 2006. A survey on networking games in telecommunications. *Computers & Operations Research*, 33 (2), 286-311.

- Amine, O. M. and Sylia, Z., 2017. Femtocell placement in an indoor building using NSGA II, *2017 5th International Conference on Electrical Engineering-Boumerdes (ICEE-B)* (pp. 1-7): IEEE.
- An, J., Yang, K., Wu, J., Ye, N., Guo, S. and Liao, Z., 2017. Achieving sustainable ultra-dense heterogeneous networks for 5G. *IEEE Communications Magazine*, 55 (12), 84-90.
- Andrews, J. G., Claussen, H., Dohler, M., Rangan, S. and Reed, M. C., 2012. Femtocells: Past, present, and future. *Selected Areas in Communications, IEEE Journal on*, 30 (3), 497-508.
- Arora, J. S., 2004. *Introduction to optimum design*. Elsevier.
- Arora, S., Singh, S. and Yetilmezsoy, K., 2018. A modified butterfly optimization algorithm for mechanical design optimization problems. *Journal of the Brazilian Society of Mechanical Sciences and Engineering*, 40 (1), 1-17.
- Arshad, Q. K. U. D., Kashif, A. U. and Quershi, I. M., 2019. A review on the evolution of cellular technologies, *2019 16th International Bhurban Conference on Applied Sciences and Technology (IBCAST)* (pp. 989-993): IEEE.
- Arunabha, G., Zhang, J., Andrews, J. G. and Muhamed, R., 2010. Fundamentals of LTE. *The Prentice Hall communications engineering and emerging technologies series*.
- Badra, R. E. and Figueras, G. E., 2018. Optimal LTE Femtocell Indoor Deployment Under External Intra-System Interference, *2018 IEEE Symposium on Electromagnetic Compatibility, Signal Integrity and Power Integrity (EMC, SI & PI)* (pp. 598-603): IEEE.
- Bagwari, A., Tomar, G. S. and Bagwari, J., 2018. *Advanced Wireless Sensing Techniques for 5G Networks*. CRC Press.
- Bhushan, N., Li, J., Malladi, D., Gilmore, R., Brenner, D., Damnjanovic, A., Sukhavasi, R., Patel, C. and Geirhofer, S., 2014a. Network densification: the dominant theme for wireless evolution into 5G. *Communications Magazine, IEEE*, 52 (2), 82-89.
- Bhushan, N., Li, J., Malladi, D., Gilmore, R., Brenner, D., Damnjanovic, A., Sukhavasi, R. T., Patel, C. and Geirhofer, S., 2014b. Network densification: the dominant theme for wireless evolution into 5G. *IEEE Communications Magazine*, 52 (2), 82-89.
- Bodenhofer, U., 2003. Genetic algorithms: theory and applications. *Lecture notes, Fuzzy Logic Laboratorium Linz-Hagenberg, Winter, 2004*.
- Bojadzievski, S., Kalendar, M. and Shuminoski, T., 2020. Ultra Reliable Advanced Framework for Emergency and Mission Critical Data for 5G Services.
- Boudreau, G., Panicker, J., Guo, N., Chang, R., Wang, N. and Vrzic, S., 2009. Interference coordination and cancellation for 4G networks. *IEEE Communications Magazine*, 47 (4), 74-81.

- Bouras, C., Diles, G., Kokkinos, V. and Papazois, A., 2016. Transmission optimizing on dense femtocell deployments in 5G. *International Journal of Communication Systems*, 29 (16), 2388-2402.
- Bouras, C., Kokkinos, V., Kontodimas, K. and Papazois, A., 2012. A simulation framework for LTE-A systems with femtocell overlays, *Proceedings of the 7th ACM workshop on Performance monitoring and measurement of heterogeneous wireless and wired networks* (pp. 85-90): ACM.
- Brickhouse, R. A. and Rappaport, T. S., 1996. Urban in-building cellular frequency reuse, *Proceedings of GLOBECOM'96. 1996 IEEE Global Telecommunications Conference* (Vol. 2, pp. 1192-1196): IEEE.
- Bryman, A., 2017. Quantitative and qualitative research: further reflections on their integration. *Mixing methods: Qualitative and quantitative research*. Routledge, 57-78.
- Bulbul, A. A.-M., Biswas, S., Hossain, M. B. and Biswas, S., 2017. Past, present and future of mobile wireless communication. *IOSR Journal of Electronics and Communication Engineering (IOSR-JECE, Vol. 12, Issue5, Ver. I (Sep.-Oct, 2017), 55-58, 2017. DOI: 10.9790/2834-1205015558*.
- Çakmak, M. and Albayrak, Z., 2018. A Review: Mobile Communication Past, Present Future. *Network*, 5, 28Ghz.
- Chandrasekhar, V. and Andrews, J. G., 2007. Uplink capacity and interference avoidance for two-tier cellular networks, *IEEE GLOBECOM 2007-IEEE Global Telecommunications Conference* (pp. 3322-3326): IEEE.
- Chandrasekhar, V. and Andrews, J. G., 2009a. Spectrum allocation in tiered cellular networks. *IEEE transactions on communications*, 57 (10), 3059-3068.
- Chandrasekhar, V. and Andrews, J. G., 2009b. Uplink capacity and interference avoidance for two-tier femtocell networks. *IEEE transactions on wireless communications*, 8 (7), 3498-3509.
- Chandrasekhar, V., Kountouris, M. and Andrews, J. G., 2009. Coverage in multi-antenna two-tier networks. *IEEE Transactions on Wireless Communications*, 8 (10), 5314-5327.
- Chen, C., Zhang, Y., Zhang, J., Chu, X. and Zhang, J., 2020. On the Performance of Indoor Multi-storey Small-cell Networks. *IEEE Transactions on Wireless Communications*.
- Cheung, W. C., Quek, T. Q. and Kountouris, M., 2012. Throughput optimization, spectrum allocation, and access control in two-tier femtocell networks. *IEEE Journal on Selected Areas in Communications*, 30 (3), 561-574.
- Chih-Lin, I., 2021. AI as an Essential Element of a Green 6G. *IEEE Transactions on Green Communications and Networking*, 5 (1), 1-3.

- Choi, D., Monajemi, P., Kang, S. and Villasenor, J., 2008. Dealing with loud neighbors: The benefits and tradeoffs of adaptive femtocell access, *IEEE GLOBECOM 2008-2008 IEEE Global Telecommunications Conference* (pp. 1-5): IEEE.
- Cisco, U., 2020. Cisco annual internet report (2018–2023) white paper.
- Claussen, H., 2007. Performance of macro-and co-channel femtocells in a hierarchical cell structure, *2007 IEEE 18th International Symposium on Personal, Indoor and Mobile Radio Communications* (pp. 1-5): IEEE.
- Claussen, H., 2008. Co-channel operation of macro-and femtocells in a hierarchical cell structure. *International Journal of Wireless Information Networks*, 15 (3-4), 137-147.
- Claussen, H., Ho, L., Karimi, H., Mullany, F. and Samuel, L., 2006. I, base station: Cognisant robots and future wireless access networks, *CCNC 2006. 2006 3rd IEEE Consumer Communications and Networking Conference, 2006.* (Vol. 1, pp. 595-599): IEEE.
- Claussen, H., Ho, L. T. and Samuel, L. G., 2008a. Self-optimization of coverage for femtocell deployments, *Wireless Telecommunications Symposium, 2008. WTS 2008* (pp. 278-285): IEEE.
- Claussen, H., Ho, L. T. and Samuel, L. G., 2008b. Self-optimization of coverage for femtocell deployments, *2008 Wireless Telecommunications Symposium* (pp. 278-285): IEEE.
- Claussen, H. and Pivit, F., 2009. Femtocell coverage optimization using switched multi-element antennas, *2009 IEEE International Conference on Communications* (pp. 1-6): IEEE.
- Dahiya, M., 2017. 5G-Upcoming of Mobile Wireless Communication. *International Journal of Electrical Electronics & Computer Science Engineering*, 4 (3), 7-9.
- Das, D. and Ramaswamy, V., 2008. On the reverse link capacity of a CDMA network of femto-cells, *2008 IEEE Sarnoff Symposium* (pp. 1-5): IEEE.
- Deb, P., Mukherjee, A. and De, D., 2017. Study of indoor path loss computational models for femtocell based mobile network. *Wireless Personal Communications*, 95 (3), 3031-3056.
- Dhifallah, K., Gourhant, Y., Senouci, S.-M. and Morand, L., 2018. Small cells placement for crowd networks, *2018 IEEE International Conference on Communications (ICC)* (pp. 1-6): IEEE.
- Dohler, M., Heath, R. W., Lozano, A., Papadias, C. B. and Valenzuela, R. A., 2011. Is the PHY layer dead? *IEEE Communications Magazine*, 49 (4), 159-165.
- dos Santos, B. N., Rossi, R. G., Rezende, S. O. and Marcacini, R. M., 2020. A two-stage regularization framework for heterogeneous event networks. *Pattern Recognition Letters*, 138, 490-496.
- Drucker, E. H., 1988. Development and application of a cellular repeater, *38th IEEE Vehicular Technology Conference* (pp. 321-325): IEEE.

- ElSawy, H., Hossain, E. and Kim, D. I., 2013. HetNets with cognitive small cells: user offloading and distributed channel access techniques. *Communications Magazine, IEEE*, 51 (6), 28-36.
- Faruque, S., 2019. Time division multiple access (TDMA). *Radio Frequency Multiple Access Techniques Made Easy*. Springer, 35-43.
- Feng, S. and Seidel, E., 2008. Self-organizing networks (SON) in 3GPP long term evolution. *Nomor Research GmbH, Munich, Germany*, 20.
- Frenzel, L., 2013. An Introduction to LTE-Advanced: The Real 4G. *Electronic design*.
- Garcia, L. G., Pedersen, K. I. and Mogensen, P. E., 2009. Autonomous component carrier selection: interference management in local area environments for LTE-advanced. *IEEE Communications Magazine*, 47 (9), 110-116.
- Garcia, L. G. U., Kovács, I. Z., Pedersen, K. I., Costa, G. W. and Mogensen, P. E., 2012. Autonomous component carrier selection for 4G femtocells—A fresh look at an old problem. *IEEE Journal on Selected Areas in Communications*, 30 (3), 525-537.
- Gawas, A. U., 2015. An overview on evolution of mobile wireless communication networks: 1G-6G. *International Journal on Recent and Innovation Trends in Computing and Communication*, 3 (5), 3130-3133.
- Ge, X., Cheng, H., Guizani, M. and Han, T., 2014a. 5G wireless backhaul networks: challenges and research advance. *arXiv preprint arXiv:1412.7232*.
- Ge, X., Cheng, H., Guizani, M. and Han, T., 2014b. 5G wireless backhaul networks: challenges and research advances. *Network, IEEE*, 28 (6), 6-11.
- Golaup, A., Mustapha, M. and Patanapongpibul, L. B., 2009. Femtocell access control strategy in UMTS and LTE. *IEEE Communications Magazine*, 47 (9), 117-123.
- Goldberg, D. E. and Holland, J. H., 1988. Genetic algorithms and machine learning.
- Goudar, S. I., Hassan, S. and Habbal, A. M. M., 2017. 5G: The next wave of digital society challenges and current trends. *Journal of Telecommunication, Electronic and Computer Engineering*, 9 (1-2), 63-66.
- Goyal, J., Singla, K. and Singh, S., 2019. A Survey of Wireless Communication Technologies from 1G to 5G, *International Conference on Computer Networks and Inventive Communication Technologies* (pp. 613-624): Springer.
- Goyal, P. and Sahoo, A. K., 2019. A roadmap towards connected living: 5G mobile technology. *Int. J. Innov. Technol. Explor. Eng*, 9 (1), 1670-1685.
- Gran, A., Lin, S.-C. and Akyildiz, I. F., 2017. Towards wireless infrastructure-as-a-service (WlaaS) for 5G software-defined cellular systems, *2017 IEEE International Conference on Communications (ICC)* (pp. 1-6): IEEE.

- Guvenc, I., Jeong, M.-R., Watanabe, F. and Inamura, H., 2008. A hybrid frequency assignment for femtocells and coverage area analysis for co-channel operation. *IEEE Communications Letters*, 12 (12), 880-882.
- Harada, T. and Alba, E., 2020. Parallel genetic algorithms: a useful survey. *ACM Computing Surveys (CSUR)*, 53 (4), 1-39.
- Hegarty, C. J., 2017. The global positioning system (GPS). *Springer Handbook of Global Navigation Satellite Systems*. Springer, 197-218.
- Ho, L., Claussen, H. and Gacanin, H., 2016. Self-optimization of coverage and sleep modes of multi-vendor enterprise femtocells, *Personal, Indoor, and Mobile Radio Communications (PIMRC), 2016 IEEE 27th Annual International Symposium on* (pp. 1-7): IEEE.
- Ho, L. T. and Claussen, H., 2007. Effects of user-deployed, co-channel femtocells on the call drop probability in a residential scenario, *2007 IEEE 18th International Symposium on Personal, Indoor and Mobile Radio Communications* (pp. 1-5): IEEE.
- Ho, L. T. W., 2003. *Self-organising algorithms for fourth generation wireless networks and its analysis using complexity metrics*. Queen Mary, University of London.
- Hoadley, J. and Maveddat, P., 2012. Enabling small cell deployment with HetNet. *IEEE Wireless Communications*, 19 (2), 4-5.
- Hossain, E., Rasti, M., Tabassum, H. and Abdelnasser, A., 2014. Evolution towards 5G multi-tier cellular wireless networks: An interference management perspective. *arXiv preprint arXiv:1401.5530*.
- Hoydis, J., Kobayashi, M. and Debbah, M., 2011. Green small-cell networks. *Vehicular Technology Magazine, IEEE*, 6 (1), 37-43.
- Ibrahim, L. F., Salman, H. and Fayed, Z., 2018. Using clustering techniques to plan indoor Femtocells layout. *IJCSNS Int J Comput Sci Netw Secur*, 18 (5), 67-74.
- Ibrahim, L. F., Salman, H. A., Taha, Z. F., Akkari, N., Aldabbagh, G. and Bamasak, O., 2019. A survey on heterogeneous mobile networks planning in indoor dense areas. *Personal and Ubiquitous Computing*, 1-12.
- Ikuno, J., Wrulich, M. and Rupp, M., 2010. 3GPP TR 36.814 V9. 0.0-Evolved Universal Terrestrial Radio Access (E-UTRA); Further advancements for E-UTRA physical layer aspects. *Tech. Rep*.
- Iliashenko, V. and Borremans, A., 2015. Iliashenko O. Yu.
- Iyer, R., Parker, J. and Sood, P., 1990. Intelligent networking for digital cellular systems and the wireless world, *[Proceedings] GLOBECOM'90: IEEE Global Telecommunications Conference and Exhibition* (pp. 475-479): IEEE.

- Jiang, Y., Lu, N., Chen, Y., Zheng, F., Bennis, M., Gao, X. and You, X., 2017. Energy-efficient noncooperative power control in small-cell networks. *IEEE Transactions on Vehicular Technology*, 66 (8), 7540-7547.
- Johnson, J. M. and Rahmat-Samii, V., 1997. Genetic algorithms in engineering electromagnetics. *IEEE Antennas and propagation Magazine*, 39 (4), 7-21.
- Jonsson, P., Carson, S., Blennerud, G., Kyohun Shim, J., Arendse, B. and Husseini, A., 2019. Ericsson mobility Report. 2019. *Ericsson: Stockholm, Sweden*.
- Joseph, M. and Akindeji, A. O., 2016. Optimizing Signal Behavior of Femtocells for Improved Network. *Transactions on Environment and Electrical Engineering*, 1 (3), 100-105.
- Joshi, S., Cheung, R. C., Monajemi, P. and Villasenor, J. D., 2009. Traffic-based study of femtocell access policy impacts on HSPA service quality, *GLOBECOM 2009-2009 IEEE Global Telecommunications Conference* (pp. 1-6): IEEE.
- Kaur, P., Sharma, T. and Singh, J., 2020. Evaluation of Internet Generations on Wireless Network: A Survey. *Journal of Technology Management for Growing Economies*, 11 (2), 55-61.
- Kazi, B. U. and Wainer, G., 2017. Handover enhancement for LTE-advanced and beyond heterogeneous cellular networks, *2017 International Symposium on Performance Evaluation of Computer and Telecommunication Systems (SPECTS)* (pp. 1-8): IEEE.
- Kim, R. Y., Kwak, J. S. and Etemad, K., 2009. WiMAX femtocell: requirements, challenges, and solutions. *IEEE Communications Magazine*, 47 (9), 84-91.
- Koohestani, B., 2020. A crossover operator for improving the efficiency of permutation-based genetic algorithms. *Expert Systems with Applications*, 151, 113381.
- Lai, W. K. and Liu, J.-K., 2018. Cell selection and resource allocation in LTE-advanced heterogeneous networks. *IEEE Access*, 6, 72978-72991.
- Lal, N., Tiwari, S. M., Khare, D. and Saxena, M., 2021. Prospects for Handling 5G Network Security: Challenges, Recommendations and Future Directions, *Journal of Physics: Conference Series* (Vol. 1714, pp. 012052): IOP Publishing.
- Liptak, B. G. and Eren, H., 2016. Process Software and Digital Networks. *Instrument Engineers Handbook (Fourth Edition)*, Volume 3 (CRC Press - Taylor and Francis Group).
- Liu, J., Kou, T., Chen, Q. and Sherali, H. D., 2012. Femtocell base station deployment in commercial buildings: A global optimization approach. *IEEE Journal on selected areas in communications*, 30 (3), 652-663.
- López-Pérez, D., Ladányi, A., Jüttner, A. and Zhang, J., 2009a. OFDMA femtocells: A self-organizing approach for frequency assignment, *2009 IEEE 20th international symposium on personal, indoor and mobile radio communications* (pp. 2202-2207): IEEE.

- López-Pérez, D., Ladányi, A., Jüttner, A. and Zhang, J., 2009b. OFDMA femtocells: A self-organizing approach for frequency assignment, *Personal, Indoor and Mobile Radio Communications, 2009 IEEE 20th International Symposium on* (pp. 2202-2207): IEEE.
- Lopez-Perez, D., Valcarce, A., De La Roche, G. and Zhang, J., 2009. OFDMA femtocells: A roadmap on interference avoidance. *IEEE communications magazine*, 47 (9), 41-48.
- Mahmoud, H. H. H., Amer, A. A. and Ismail, T., 2021. 6G: A comprehensive survey on technologies, applications, challenges, and research problems. *Transactions on Emerging Telecommunications Technologies*, e4233.
- Malini, B. and Babu, K. V., 2017. Soft frequency reuse based interference minimization technique for long term evolution-advanced heterogeneous networks, *2017 International Conference on Communication and Signal Processing (ICCSP)* (pp. 0630-0634): IEEE.
- Mao, Y., You, C., Zhang, J., Huang, K. and Letaief, K. B., 2017. A survey on mobile edge computing: The communication perspective. *IEEE Communications Surveys & Tutorials*, 19 (4), 2322-2358.
- Mitchell, M., 1998. *An introduction to genetic algorithms*. MIT press.
- Mitra, R. N. and Agrawal, D. P., 2015. 5G mobile technology: A survey. *ICT Express*, 1 (3), 132-137.
- Nassiri, M. J. and Borujeni, S. E., 2020. A Novel Approach on Femtocell Placement in the Commercial Buildings Using Genetic Algorithm.
- Network, E., 2011a. Self-configuring and self-optimizing network (SON) use cases and solutions. *Third Generation Partnership Project (3GPP) specification TR*, 36, V9.
- Network, E. U. T. R. A., 2011b. S1 Application Protocol (S1AP)(Release 10). *Technical Specification, 3GPP TS*, 36, V10.
- Nguyen, L. D., 2018. Resource allocation for energy efficiency in 5G wireless networks. *EAI Endorsed Transactions on Industrial Networks and Intelligent Systems*, 5 (14).
- Nguyen, M. T., Kwon, S. and Kim, H., 2017. Mobility robustness optimization for handover failure reduction in LTE small-cell networks. *IEEE Transactions on Vehicular Technology*, 67 (5), 4672-4676.
- Ni, W., Collings, I. B., Wang, X. and Liu, R. P., 2014. Multi-hop point-to-point FDD wireless backhaul for mobile small cells. *IEEE Wireless Communications*, 21 (4), 88-96.
- Obile, W., 2016. Ericsson mobility report. Nov.
- Omar, T., Ketseoglou, T. and Naffaa, I., 2021. A novel self-healing model using precoding & big-data based approach for 5G networks. *Pervasive and Mobile Computing*, 73, 101365.
- Panwar, N., Sharma, S. and Singh, A. K., 2016. A survey on 5G: The next generation of mobile communication. *Physical Communication*, 18, 64-84.

- Patra, G. and Sharma, K., 2020. OVERVIEW OF 5G WIRELESS TECHNOLOGY AND ITS REVOLUTION.
- Pi, Z. and Khan, F., 2011. An introduction to millimeter-wave mobile broadband systems. *IEEE communications magazine*, 49 (6), 101-107.
- Ramaswamy, V. and Das, D., 2009. Multi-carrier macrocell femtocell deployment-a reverse link capacity analysis, *2009 IEEE 70th Vehicular Technology Conference Fall* (pp. 1-6): IEEE.
- Ramiro, J. and Hamied, K., 2011. *Self-organizing networks: self-planning, self-optimization and self-healing for GSM, UMTS and LTE*. John Wiley & Sons.
- Rathore, M. A., 2020. HIGH SPEED PACKET ACCESS-APRIL 2020. *Editorial Board*, 9 (5), 164.
- Ravichandran, A., Alnoman, A., Sharma, N. and Anpalagan, A., 2017. Traffic offloading problem in two-tier HetNets with D2D support for emergency communications, *2017 IEEE Canada international humanitarian technology conference (IHTC)* (pp. 128-132): IEEE.
- Rehman, M. U. and Safdar, G. A., 2018. The Road Ahead for LTE Femtocells. *LTE Communications and Networks: Femtocells and Antenna Design Challenges*, 322.
- Roth, Z. e., Goldhamer, M., Chayat, N., Burr, A., Dohler, M., Bartzoudis, N., Walker, C., Leibe, Y., Oestges, C. and Brzozowy, M., 2010. Vision and architecture supporting wireless GBit/sec/km² capacity density deployments, *2010 Future Network & Mobile Summit* (pp. 1-7): IEEE.
- Saeed, R. A., 2019. Handover in a mobile wireless communication network—A Review Phase. *International Journal of Computer Communication and Informatics*, 1 (1), 6-13.
- Sahin, M. E., Guvenc, I., Jeong, M.-R. and Arslan, H., 2009. Handling CCI and ICI in OFDMA femtocell networks through frequency scheduling. *IEEE Transactions on Consumer Electronics*, 55 (4), 1936-1944.
- Schroder, A., Lundqvist, H., Nunzi, G. and Brunner, M., 2009. User-assisted coverage and interference optimization for broadband femtocells, *2009 IFIP/IEEE International Symposium on Integrated Network Management-Workshops* (pp. 199-204): IEEE.
- Simeone, O., Erkip, E. and Shamai, S., 2009. Robust communication against femtocell access failures, *2009 IEEE Information Theory Workshop* (pp. 263-267): IEEE.
- Singh, R. K., Bisht, D. and Prasad, R., 2017. Development of 5G mobile network technology and its architecture. *International Journal of Recent Trends in Engineering & Research (IJRTER)*, 3 (10), 196-201.
- Sitorus, Z., Ganefri, G. and Jalinus, N., 2017. Using Nobile Telecommunications-2000 International for Analyzing Technology Network Era 4G-LTE.

- Sivaganesan, D., 2019. IMPROVISATION OF MESH NETWORK WITH WIDEBAND CODE DIVISION MULTIPLE ACCESS. *Journal: IRO Journal on Sustainable Wireless Systems September, 2019 (03)*, 198-205.
- Sivaraj, R. and Mohapatra, P., 2017. Future radio access, Wi-Fi-LTE, LTE-advanced: the path to 5G. *Fiber-Wireless Convergence in Next-Generation Communication Networks*. Springer, 3-41.
- Solanki, V. and Rafiq, M. Q., 2015. Rethinking Interference Mitigation Spectrum Efficiency Model in Femtocell Networks using FFR. *International Journal of Computer Applications*, 123 (14), 17-27.
- Soldani, D. and Manzalini, A., 2015. Horizon 2020 and beyond: On the 5G operating system for a true digital society. *IEEE Vehicular Technology Magazine*, 10 (1), 32-42.
- Sood, R. and Garg, A., 2014. Digital society from 1G to 5G: a comparative study. *International Journal of Application or Innovation in Engineering & Management (IJAIEM)*, 3 (2), 186-193.
- SREELEKHA, D., VICTORIA, G., GOUD, J. S. and KUMAR, B. A., 2017. Comparative Study Between Space Division Multiple Access (SDMA) Vs WCDMA with BER.
- Stocker, A. C., 1984. Small-cell mobile phone systems. *IEEE Transactions on vehicular technology*, 33 (4), 269-275.
- Tsiropoulou, E. E., Vamvakas, P., Katsinis, G. K. and Papavassiliou, S., 2015. Combined power and rate allocation in self-optimized multi-service two-tier femtocell networks. *Computer Communications*, 72, 38-48.
- Valanarasu, M. R. and Christy, A., 2019. Comprehensive survey of wireless cognitive and 5G networks. *Journal of Ubiquitous Computing and Communication Technologies (UCCT)*, 23-32.
- Verdugo, D. A., Lupera, P. A. and Davydov, R. V., 2021. Analysis of the Capacity of an LTE Carrier Based on Simulation and Experimentation, *International Youth Conference on Electronics, Telecommunications and Information Technologies* (pp. 699-707): Springer.
- Verma, R., 2018. INTERNATIONAL JOURNAL OF ENGINEERING SCIENCES & RESEARCH TECHNOLOGY A COMPREHENSIVE STUDY ON 5th GENERATION MOBILE COMMUNICATION.
- Voudoukis, N., 2017. Performance Analysis, Characteristics, and Simulation of Digital QAM. *European Journal of Electrical Engineering and Computer Science*, 1 (1).
- Wang, C.-X., Haider, F., Gao, X., You, X.-H., Yang, Y., Yuan, D., Aggoune, H. M., Haas, H., Fletcher, S. and Hepsaydir, E., 2014. Cellular architecture and key technologies for 5G wireless communication networks. *IEEE communications magazine*, 52 (2), 122-130.

- Wang, H., Zhao, M. and Reed, M. C., 2010. Outage analysis for WCDMA femtocell with uplink attenuation, *2010 IEEE Globecom Workshops* (pp. 664-668): IEEE.
- Wang, W. and Zhang, Q., 2014a. Local cooperation architecture for self-healing femtocell networks. *Wireless Communications, IEEE*, 21 (2), 42-49.
- Wang, W. and Zhang, Q., 2014b. Local cooperation architecture for self-healing femtocell networks. *IEEE Wireless Communications*, 21 (2), 42-49.
- Wang, X., Vasilakos, A. V., Chen, M., Liu, Y. and Kwon, T. T., 2012. A survey of green mobile networks: Opportunities and challenges. *Mobile Networks and Applications*, 17 (1), 4-20.
- Wang, X., Zheng, W., Lu, Z., Wen, X. and Li, W., 2016. Dense femtocell networks power self-optimization: an exact potential game approach. *International Journal of Communication Systems*, 29 (1), 16-32.
- Wang, Y., Liu, W. and Fang, L., 2020. Adaptive Modulation and Coding Technology in 5G System, *2020 International Wireless Communications and Mobile Computing (IWCMC)* (pp. 159-164): IEEE.
- Williams, I., 2018. Community Based Networks and 5G Wi-Fi. *Ekonomiczne Problemy Usług*, 131 (2/2), 321-334.
- Xia, P., Chandrasekhar, V. and Andrews, J. G., 2010. Open vs. closed access femtocells in the uplink. *IEEE Transactions on Wireless Communications*, 9 (12), 3798-3809.
- Xiao, M., Shroff, N. B. and Chong, E. K., 2001. Utility-based power control in cellular wireless systems, *Proceedings IEEE INFOCOM 2001. Conference on Computer Communications. Twentieth Annual Joint Conference of the IEEE Computer and Communications Society (Cat. No. 01CH37213)* (Vol. 1, pp. 412-421): IEEE.
- Xu, Y., Wang, Z., Liu, P., Chen, J., Han, S., Yu, C. and Yu, J., 2017. Accuracy analysis and improvement of visible light positioning based on VLC system using orthogonal frequency division multiple access. *Optics Express*, 25 (26), 32618-32630.
- Yavuz, M., Meshkati, F., Nanda, S., Pokhariyal, A., Johnson, N., Raghothaman, B. and Richardson, A., 2009. Interference management and performance analysis of UMTS/HSPA+ femtocells. *IEEE communications magazine*, 47 (9), 102-109.
- Zhang, H., Jiang, C., Hu, R. Q. and Qian, Y., 2016. Self-organization in disaster-resilient heterogeneous small cell networks. *IEEE Network*, 30 (2), 116-121.
- Zhang, Q., Feng, Z. and Li, W., 2015a. Coverage self-optimization for randomly deployed femtocell networks. *Wireless Personal Communications*, 82 (4), 2481-2504.
- Zhang, X., Zhang, J., Wang, W., Zhang, Y., Chih-Lin, I., Pan, Z., Li, G. and Chen, Y., 2015b. Macro-assisted data-only carrier for 5G green cellular systems. *IEEE Communications Magazine*, 53 (5), 223-231.

- Zhou, H., Xu, W., Bi, Y., Chen, J., Yu, Q. and Shen, X. S., 2017. Toward 5G spectrum sharing for immersive-experience-driven vehicular communications. *IEEE Wireless Communications*, 24 (6), 30-37.
- Zhou, X., Zhao, Z., Li, R., Zhou, Y., Chen, T., Niu, Z. and Zhang, H., 2014. Toward 5G: when explosive bursts meet soft cloud. *Network, IEEE*, 28 (6), 12-17.

Appendix A

mainlayout.m

```
function varargout = mainlayout_modified1(varargin)

% MAINLAYOUT_MODIFIED1 MATLAB code for mainlayout_modified1.fig
%   MAINLAYOUT_MODIFIED1, by itself, creates a new
%   MAINLAYOUT_MODIFIED1 or raises the existing
%   singleton*.
%
%   H = MAINLAYOUT_MODIFIED1 returns the handle to a new
%   MAINLAYOUT_MODIFIED1 or the handle to
%   the existing singleton*.
%
%   MAINLAYOUT_MODIFIED1('CALLBACK',hObject,eventData,handles,...)
%   calls the local
%   function named CALLBACK in MAINLAYOUT_MODIFIED1.M with the
%   given input arguments.
%
%   MAINLAYOUT_MODIFIED1('Property','Value',...) creates a new
%   MAINLAYOUT_MODIFIED1 or raises the
%   existing singleton*. Starting from the left, property value
%   pairs are
%   applied to the GUI before mainlayout_modified1_OpeningFcn gets
%   called. An
%   unrecognized property name or invalid value makes property
%   application
%   stop. All inputs are passed to mainlayout_modified1_OpeningFcn
%   via varargin.
%
%   *See GUI Options on GUIDE's Tools menu. Choose "GUI allows
%   only one
%   instance to run (singleton)".
%
% See also: GUIDE, GUIDATA, GUIHANDLES

% Edit the above text to modify the response to help
mainlayout_modified1

% Last Modified by GUIDE v2.5 14-Nov-2020 19:33:49

% Begin initialization code - DO NOT EDIT
gui_Singleton = 1;
gui_State = struct('gui_Name',       mfilename, ...
                  'gui_Singleton',  gui_Singleton, ...
                  'gui_OpeningFcn', @mainlayout_modified1_OpeningFcn,
                  ...
                  'gui_OutputFcn',  @mainlayout_modified1_OutputFcn,
                  ...
                  'gui_LayoutFcn',   [], ...
                  'gui_Callback',    []);
if nargin && ischar(varargin{1})
    gui_State.gui_Callback = str2func(varargin{1});
end

if nargout
    [varargout{1:nargout}] = gui_mainfcn(gui_State, varargin{:});
```

```

else
    %varargin
    gui_mainfcn(gui_State, varargin{:});
end
% End initialization code - DO NOT EDIT

% --- Executes just before mainlayout_modified1 is made visible.
function mainlayout_modified1_OpeningFcn(hObject, eventdata, handles,
varargin)
% This function has no output args, see OutputFcn.
% hObject     handle to figure
% eventdata   reserved0 - to be defined in a future version of MATLAB
% handles     structure with handles and user data (see GUIDATA)
% varargin    command line arguments to mainlayout_modified1 (see
VARARGIN)

imshow('images/macrocell.png');

% Choose default command line output for mainlayout_modified1
handles.output = hObject;

hObject
% Update handles structure
guidata(hObject, handles);

% This sets up the initial plot - only do when we are invisible
% so window can get raised using mainlayout_modified1.
%if strcmp(get(hObject,'Visible'),'off')
%    plot(rand(5));
%end

% UIWAIT makes mainlayout_modified1 wait for user response (see
UIRESUME)
% uiwait(handles.figure1);

% --- Outputs from this function are returned to the command line.
function varargout = mainlayout_modified1_OutputFcn(hObject,
eventdata, handles)
% varargout    cell array for returning output args (see VARARGOUT);
% hObject     handle to figure
% eventdata   reserved - to be defined in a future version of MATLAB
% handles     structure with handles and user data (see GUIDATA)

% Get default command line output from handles structure
varargout{1} = handles.output;

% -----
function FileMenu_Callback(hObject, eventdata, handles)
% hObject     handle to FileMenu (see GCBO)
% eventdata   reserved - to be defined in a future version of MATLAB
% handles     structure with handles and user data (see GUIDATA)

% -----
function OpenMenuItem_Callback(hObject, eventdata, handles)
% hObject     handle to OpenMenuItem (see GCBO)
% eventdata   reserved - to be defined in a future version of MATLAB

```

```

% handles      structure with handles and user data (see GUIDATA)
file = uigetfile('*.fig');
if ~isequal(file, 0)
    open(file);
end

% -----
function PrintMenuItem_Callback(hObject, eventdata, handles)
% hObject      handle to PrintMenuItem (see GCBO)
% eventdata    reserved - to be defined in a future version of MATLAB
% handles      structure with handles and user data (see GUIDATA)
printdlg(handles.figure1)

% -----
function CloseMenuItem_Callback(hObject, eventdata, handles)
% hObject      handle to CloseMenuItem (see GCBO)
% eventdata    reserved - to be defined in a future version of MATLAB
% handles      structure with handles and user data (see GUIDATA)
selection = questdlg(['Close ' get(handles.figure1, 'Name') '?'], ...
                    ['Close ' get(handles.figure1, 'Name') '...'], ...
                    'Yes', 'No', 'Yes');
if strcmp(selection, 'No')
    return;
end

delete(handles.figure1)

% --- Executes on selection change in popupmenu1.
function popupmenu1_Callback(hObject, eventdata, handles)
% hObject      handle to popupmenu1 (see GCBO)
% eventdata    reserved - to be defined in a future version of MATLAB
% handles      structure with handles and user data (see GUIDATA)

% Hints: contents = get(hObject, 'String') returns popupmenu1 contents
as cell array
%           contents{get(hObject, 'Value')} returns selected item from
popupmenu1

% --- Executes during object creation, after setting all properties.
function popupmenu1_CreateFcn(hObject, eventdata, handles)
% hObject      handle to popupmenu1 (see GCBO)
% eventdata    reserved - to be defined in a future version of MATLAB
% handles      empty - handles not created until after all CreateFcns
called

% Hint: popupmenu controls usually have a white background on Windows.
%           See ISPC and COMPUTER.

```

```

if ispc && isequal(get(hObject,'BackgroundColor'),
get(0,'defaultUiControlBackgroundColor'))
    set(hObject,'BackgroundColor','white');
end

set(hObject, 'String', {'plot(rand(5))', 'plot(sin(1:0.01:25))',
'bar(1:.5:10)', 'plot(membrane)', 'surf(peaks)'});

% --- Executes during object creation, after setting all properties.
function axes1_CreateFcn(hObject, eventdata, handles)
% hObject    handle to axes1 (see GCBO)
% eventdata  reserved - to be defined in a future version of MATLAB
% handles    empty - handles not created until after all CreateFcns
called

% Hint: place code in OpeningFcn to populate axes1
% replace with an image of your choice
%axes(hObject, 'XLim', [0 510], 'YLim', [0 432]);
%set(hObject,'Axes','axes1');
axis([0 250*2 0 216*2]);
imshow('images/macrocell.png');
handles.axes1 = hObject;

function edit1_Callback(hObject, eventdata, handles)
% hObject    handle to edit1 (see GCBO)
% eventdata  reserved - to be defined in a future version of MATLAB
% handles    structure with handles and user data (see GUIDATA)

% Hints: get(hObject,'String') returns contents of edit1 as text
%        str2double(get(hObject,'String')) returns contents of edit1
as a double
normalizeInput(hObject);
setAttachMenu(handles);

% --- Executes during object creation, after setting all properties.
function edit1_CreateFcn(hObject, eventdata, handles)
% hObject    handle to edit1 (see GCBO)
% eventdata  reserved - to be defined in a future version of MATLAB
% handles    empty - handles not created until after all CreateFcns
called

% Hint: edit controls usually have a white background on Windows.
%        See ISPC and COMPUTER.
if ispc && isequal(get(hObject,'BackgroundColor'),
get(0,'defaultUiControlBackgroundColor'))
    set(hObject,'BackgroundColor','white');
end
femtoObject = hObject;

```



```

% --- Executes on button press in pushbutton4.
function pushbutton4_Callback(hObject, eventdata, handles)
% hObject    handle to pushbutton4 (see GCBO)
% eventdata  reserved - to be defined in a future version of MATLAB
% handles    structure with handles and user data (see GUIDATA)
drawMap(handles);
%deployFemtocells();

% --- Executes on button press in pushbutton8.
function pushbutton8_Callback(hObject, eventdata, handles)
% hObject    handle to pushbutton8 (see GCBO)
% eventdata  reserved - to be defined in a future version of MATLAB
% handles    structure with handles and user data (see GUIDATA)
if ~(strcmp(get(hObject, 'String'), 'Run Simulation'))
    drawMap(handles);
else
    drawColormap(handles);
end

function edit2_Callback(hObject, eventdata, handles)
% hObject    handle to edit2 (see GCBO)
% eventdata  reserved - to be defined in a future version of MATLAB
% handles    structure with handles and user data (see GUIDATA)

% Hints: get(hObject,'String') returns contents of edit2 as text
%        str2double(get(hObject,'String')) returns contents of edit2
as a double
normalizeInput(hObject);

% --- Executes during object creation, after setting all properties.
function edit2_CreateFcn(hObject, eventdata, handles)
% hObject    handle to edit2 (see GCBO)
% eventdata  reserved - to be defined in a future version of MATLAB
% handles    empty - handles not created until after all CreateFCns
called

% Hint: edit controls usually have a white background on Windows.
%       See ISPC and COMPUTER.
if ispc && isequal(get(hObject,'BackgroundColor'),
get(0,'defaultUicontrolBackgroundColor'))
    set(hObject,'BackgroundColor','white');
end

```

```

function edit3_Callback(hObject, eventdata, handles)
% hObject      handle to edit3 (see GCBO)
% eventdata    reserved - to be defined in a future version of MATLAB
% handles      structure with handles and user data (see GUIDATA)

% Hints: get(hObject,'String') returns contents of edit3 as text
%         str2double(get(hObject,'String')) returns contents of edit3
as a double
normalizeInput(hObject);

% --- Executes during object creation, after setting all properties.
function edit3_CreateFcn(hObject, eventdata, handles)
% hObject      handle to edit3 (see GCBO)
% eventdata    reserved - to be defined in a future version of MATLAB
% handles      empty - handles not created until after all CreateFcns
called

% Hint: edit controls usually have a white background on Windows.
%         See ISPC and COMPUTER.
if ispc && isequal(get(hObject,'BackgroundColor'),
get(0,'defaultUicontrolBackgroundColor'))
    set(hObject,'BackgroundColor','white');
end

% --- Executes on selection change in popupmenu4.
function popupmenu4_Callback(hObject, eventdata, handles)
% hObject      handle to popupmenu4 (see GCBO)
% eventdata    reserved - to be defined in a future version of MATLAB
% handles      structure with handles and user data (see GUIDATA)

% Hints: contents = cellstr(get(hObject,'String')) returns popupmenu4
contents as cell array
%         contents{get(hObject,'Value')} returns selected item from
popupmenu4

% --- Executes during object creation, after setting all properties.
function popupmenu4_CreateFcn(hObject, eventdata, handles)
% hObject      handle to popupmenu4 (see GCBO)
% eventdata    reserved - to be defined in a future version of MATLAB
% handles      empty - handles not created until after all CreateFcns
called

% Hint: popupmenu controls usually have a white background on Windows.
%         See ISPC and COMPUTER.
if ispc && isequal(get(hObject,'BackgroundColor'),
get(0,'defaultUicontrolBackgroundColor'))
    set(hObject,'BackgroundColor','white');
end

```

```

% --- Executes on selection change in popupmenu6.
function popupmenu6_Callback(hObject, eventdata, handles)
% hObject      handle to popupmenu6 (see GCBO)
% eventdata    reserved - to be defined in a future version of MATLAB
% handles      structure with handles and user data (see GUIDATA)

% Hints: contents = cellstr(get(hObject,'String')) returns popupmenu6
contents as cell array
%           contents{get(hObject,'Value')} returns selected item from
popupmenu6
%set(hObject, 'String',strcat(get(hObject,'Value'), 'MHz'));

% --- Executes during object creation, after setting all properties.
function popupmenu6_CreateFcn(hObject, eventdata, handles)
% hObject      handle to popupmenu6 (see GCBO)
% eventdata    reserved - to be defined in a future version of MATLAB
% handles      empty - handles not created until after all CreateFcns
called

% Hint: popupmenu controls usually have a white background on Windows.
%           See ISPC and COMPUTER.
if ispc && isequal(get(hObject,'BackgroundColor'),
get(0,'defaultUiControlBackgroundColor'))
    set(hObject,'BackgroundColor','white');
end
%fprintf(1,'%d\n', get(hObject,'Value'));
%set(hObject, 'String',strcat(get(hObject,'Value')(1), ' MHz'));

% --- Executes during object creation, after setting all properties.
function pushbutton4_CreateFcn(hObject, eventdata, handles)
% hObject      handle to pushbutton4 (see GCBO)
% eventdata    reserved - to be defined in a future version of MATLAB
% handles      empty - handles not created until after all CreateFcns
called

% --- Executes on mouse press over axes background.
function axes1_ButtonDownFcn(hObject, eventdata, handles)
% hObject      handle to axes1 (see GCBO)
% eventdata    reserved - to be defined in a future version of MATLAB
% handles      structure with handles and user data (see GUIDATA)

% --- Executes during object creation, after setting all properties.
function slider1_CreateFcn(hObject, eventdata, handles)

```

```

% hObject    handle to slider1 (see GCBO)
% eventdata  reserved - to be defined in a future version of MATLAB
% handles    empty - handles not created until after all CreateFcns
called

% Hint: slider controls usually have a light gray background.
if isequal(get(hObject,'BackgroundColor'),
get(0,'defaultUiControlBackgroundColor'))
    set(hObject,'BackgroundColor',[.9 .9 .9]);
end

% --- Executes during object creation, after setting all properties.
function slider2_CreateFcn(hObject, eventdata, handles)
% hObject    handle to slider1 (see GCBO)
% eventdata  reserved - to be defined in a future version of MATLAB
% handles    empty - handles not created until after all CreateFcns
called

% Hint: slider controls usually have a light gray background.
if isequal(get(hObject,'BackgroundColor'),
get(0,'defaultUiControlBackgroundColor'))
    set(hObject,'BackgroundColor',[.9 .9 .9]);
end

% --- Executes on slider movement.
function slider1_Callback(hObject, eventdata, handles)
% hObject    handle to slider1 (see GCBO)
% eventdata  reserved - to be defined in a future version of MATLAB
% handles    structure with handles and user data (see GUIDATA)

% Hints: get(hObject,'Value') returns position of slider
%        get(hObject,'Min') and get(hObject,'Max') to determine range
of slider
set(handles.text10,'String',int2str(uint16(get(hObject,'Value'))));
set(handles.text10,'Value',get(hObject,'Value'));

% --- Executes on slider movement.
function slider2_Callback(hObject, eventdata, handles)
% hObject    handle to slider2 (see GCBO)
% eventdata  reserved - to be defined in a future version of MATLAB
% handles    structure with handles and user data (see GUIDATA)

% Hints: get(hObject,'Value') returns position of slider
%        get(hObject,'Min') and get(hObject,'Max') to determine range
of slider

```

```

set(handles.text11, 'String', int2str(uint16(get(hObject, 'Value'))));
set(handles.text11, 'Value', get(hObject, 'Value'));

% --- Executes on slider movement.
function slider3_Callback(hObject, eventdata, handles)
% hObject    handle to slider3 (see GCBO)
% eventdata  reserved - to be defined in a future version of MATLAB
% handles    structure with handles and user data (see GUIDATA)

% Hints: get(hObject, 'Value') returns position of slider
%         get(hObject, 'Min') and get(hObject, 'Max') to determine range
of slider
set(handles.text14, 'String', strcat(num2str(get(hObject, 'Value'),
'%.1f'), 'm'));
set(handles.text14, 'Value', get(hObject, 'Value'));

% --- Executes during object creation, after setting all properties.
function slider3_CreateFcn(hObject, eventdata, handles)
% hObject    handle to slider3 (see GCBO)
% eventdata  reserved - to be defined in a future version of MATLAB
% handles    empty - handles not created until after all CreateFcns
called

% Hint: slider controls usually have a light gray background.
if isequal(get(hObject, 'BackgroundColor'),
get(0, 'defaultUiControlBackgroundColor'))
    set(hObject, 'BackgroundColor', [.9 .9 .9]);
end

% --- Executes during object creation, after setting all properties.
function text10_CreateFcn(hObject, eventdata, handles)
% hObject    handle to text10 (see GCBO)
% eventdata  reserved - to be defined in a future version of MATLAB
% handles    empty - handles not created until after all CreateFcns
called

% --- Executes on mouse motion over figure - except title and menu.
function figure1_WindowButtonMotionFcn(hObject, eventdata, handles)
% hObject    handle to figure1 (see GCBO)
% eventdata  reserved - to be defined in a future version of MATLAB
% handles    structure with handles and user data (see GUIDATA)
axis equal;
setCurrentCoordinates(handles);

```

```

function figure1_WindowButtonUpFcn(hObject, eventdata, handles)
% hObject    handle to figure1 (see GCBO)
% eventdata  reserved - to be defined in a future version of MATLAB
% handles    structure with handles and user data (see GUIDATA)
axis equal;
setCurrentCoordinates(handles);

% --- Executes on button press in radiobutton1.
function radiobutton1_Callback(hObject, eventdata, handles)
% hObject    handle to radiobutton1 (see GCBO)
% eventdata  reserved - to be defined in a future version of MATLAB
% handles    structure with handles and user data (see GUIDATA)

% Hint: get(hObject,'Value') returns toggle state of radiobutton1

% --- Executes on button press in radiobutton2.
function radiobutton2_Callback(hObject, eventdata, handles)
% hObject    handle to radiobutton2 (see GCBO)
% eventdata  reserved - to be defined in a future version of MATLAB
% handles    structure with handles and user data (see GUIDATA)

% Hint: get(hObject,'Value') returns toggle state of radiobutton2

% --- Executes during object creation, after setting all properties.
function popupmenu7_CreateFcn(hObject, eventdata, handles)
% hObject    handle to popupmenu7 (see GCBO)
% eventdata  reserved - to be defined in a future version of MATLAB
% handles    empty - handles not created until after all CreateFcns
called

% Hint: popupmenu controls usually have a white background on Windows.
%       See ISPC and COMPUTER.
if ispc && isequal(get(hObject,'BackgroundColor'),
get(0,'defaultUiControlBackgroundColor'))
    set(hObject,'BackgroundColor','white');
end

% --- Executes on selection change in popupmenu7.
function popupmenu7_Callback(hObject, eventdata, handles)
% hObject    handle to popupmenu7 (see GCBO)
% eventdata  reserved - to be defined in a future version of MATLAB
% handles    structure with handles and user data (see GUIDATA)

```

```

% Hints: contents = cellstr(get(hObject,'String')) returns popupmenu7
contents as cell array
%         contents{get(hObject,'Value')} returns selected item from
popupmenu7
if strcmp(get(handles.pushbutton8, 'String'), 'Run Simulation')
    if (get(hObject, 'Value') == 1)
        set(handles.pushbutton8, 'Enable', 'off');
    else
        set(handles.pushbutton8, 'Enable', 'on');
    end
end
end

% --- Executes on button press in togglebutton4.
function togglebutton4_Callback(hObject, eventdata, handles)
% hObject     handle to togglebutton4 (see GCBO)
% eventdata   reserved - to be defined in a future version of MATLAB
% handles     structure with handles and user data (see GUIDATA)

% Hint: get(hObject,'Value') returns toggle state of togglebutton4

% --- Executes on button press in pushbutton10.
function pushbutton10_Callback(hObject, eventdata, handles)
% hObject     handle to pushbutton10 (see GCBO)
% eventdata   reserved - to be defined in a future version of MATLAB
% handles     structure with handles and user data (see GUIDATA)
credits_display();

% --- Executes on button press in pushbutton11.
function pushbutton11_Callback(hObject, eventdata, handles)
% hObject     handle to pushbutton11 (see GCBO)
% eventdata   reserved - to be defined in a future version of MATLAB
% handles     structure with handles and user data (see GUIDATA)
mainlayout_modified;

% --- Executes during object creation, after setting all properties.
function text21_CreateFcn(hObject, eventdata, handles)
% hObject     handle to text21 (see GCBO)
% eventdata   reserved - to be defined in a future version of MATLAB
% handles     empty - handles not created until after all CreateFcns
called
defaultBackground = get(0, 'defaultUicontrolBackgroundColor');
set(hObject, 'BackgroundColor', defaultBackground);

% --- Executes during object creation, after setting all properties.
function text20_CreateFcn(hObject, eventdata, handles)
% hObject     handle to text20 (see GCBO)
% eventdata   reserved - to be defined in a future version of MATLAB

```

```

% handles    empty - handles not created until after all CreateFcns
called
defaultBackground = get(0, 'defaultUicontrolBackgroundColor');
set(hObject, 'BackgroundColor', defaultBackground);

% --- Executes during object creation, after setting all properties.
function text25_CreateFcn(hObject, eventdata, handles)
% hObject    handle to text25 (see GCBO)
% eventdata  reserved - to be defined in a future version of MATLAB
% handles    empty - handles not created until after all CreateFcns
called
defaultBackground = get(0, 'defaultUicontrolBackgroundColor');
set(hObject, 'BackgroundColor', defaultBackground);

% --- Executes during object creation, after setting all properties.
function pushbutton8_CreateFcn(hObject, eventdata, handles)
% hObject    handle to pushbutton8 (see GCBO)
% eventdata  reserved - to be defined in a future version of MATLAB
% handles    empty - handles not created until after all CreateFcns
called

% --- Executes during object creation, after setting all properties.
function uipanel15_CreateFcn(hObject, eventdata, handles)
% hObject    handle to uipanel15 (see GCBO)
% eventdata  reserved - to be defined in a future version of MATLAB
% handles    empty - handles not created until after all CreateFcns
called

% --- Executes during object creation, after setting all properties.
function text3_CreateFcn(hObject, eventdata, handles)
% hObject    handle to text3 (see GCBO)
% eventdata  reserved - to be defined in a future version of MATLAB
% handles    empty - handles not created until after all CreateFcns
called

```


Appendix B

Code for Performing Optimisation

```
function perform_optimisation(handles)

waitbar_h = waitbar(0, 'Running optimisation...');

set(handles.pushbutton8, 'String', 'Running Optimisation');

set(handles.pushbutton8, 'BackgroundColor', [1.0 0 0]);

set(handles.pushbutton8, 'Enable', 'off');

coordVectors = get(handles.figure1, 'UserData');
%numOfFemtousers=length(coordVectors.fuser_x);

x_femts = coordVectors.femt_x;
y_femts = coordVectors.femt_y;

numOfFemtocells = length(x_femts);

initial_cell_IDs = coordVectors.att_cell;

create_performance_table(handles, 'table before optimisation.xlsx');

%save_current_position_image(handles, 'plot before optimisation.png',
1);

in_val = [x_femts, y_femts];

building_IDs = coordVectors.cells_building_ID;

building_number_x = coordVectors.buildings_count(1);
building_number_y = coordVectors.buildings_count(2);

x_lim = coordVectors.x_lim;
y_lim = coordVectors.y_lim;

[building_lower_bounds, building_upper_bounds] =
get_lower_and_upper_bounds(building_number_x, x_lim ,
building_number_y, y_lim, 3);

femto_lower_x_bounds = zeros(1, numOfFemtocells);
femto_lower_y_bounds = zeros(1, numOfFemtocells);
femto_upper_x_bounds = zeros(1, numOfFemtocells);
femto_upper_y_bounds = zeros(1, numOfFemtocells);
%}
%femto_cells_bounds = zeros(4, numOfFemtocells);

random_femto_cell_count = coordVectors.random_Femto_count;

for i = 1:numOfFemtocells-random_femto_cell_count
    building_ID = building_IDs(i);
    femto_lower_x_bounds(i) =
incrValueX(building_lower_bounds(1,building_ID), x_lim(2));
```

```

    femto_lower_y_bounds(i) =
incrValueY(building_lower_bounds(2,building_ID), y_lim(2));

    femto_upper_x_bounds(i) =
incrValueX(building_upper_bounds(1,building_ID), x_lim(2));
    femto_upper_y_bounds(i) =
incrValueY(building_upper_bounds(2,building_ID), y_lim(2));
end

for i = numOfFemtocells-random_femto_cell_count+1:numOfFemtocells

    femto_lower_x_bounds(i) = incrValueX(x_lim(1),x_lim(2));
    femto_lower_y_bounds(i) = incrValueY(y_lim(1), y_lim(2));

    femto_upper_x_bounds(i) = incrValueX(x_lim(2), x_lim(2));
    femto_upper_y_bounds(i) = incrValueY(y_lim(2), y_lim(2));
end

%for y_direction the coordinates are opposite which is why need to
swap
%upper and lower bounds

ub = [femto_upper_x_bounds(1,:) femto_lower_y_bounds(1,:)];
lb = [femto_lower_x_bounds(1,:) femto_upper_y_bounds(1,:)];

%change_femto_user_position(handles);

fun = @(x) Obj_with_given_femtocell_positions(x, handles)

%obj_value = fun(in_val);
options_particle_swarm =
optimoptions('particleswarm','SwarmSize',5,'HybridFcn',@fmincon,
'ObjectiveLimit', 3E6);

options_ga = optimoptions('ga','PlotFcn',
@gaplotbestf,'FitnessLimit', 5E6);

options_fmincon =
optimoptions('fmincon','FiniteDifferenceStepSize',5e-
2,'OutputFcn',@myOutput, 'Display','iter', 'Tolfun' , 1e-5);

history.x = [];
history.fval = [];

xval = [];

%[xsol, fval] = fmincon(fun,in_val,[],[],[],[],lb,ub,[],
options_fmincon);
%[xsol,fval,exitflag,output] =
particleswarm(fun,2*numOfFemtocells,lb,ub,options_particle_swarm)
[xsol,fval,exitflag,output] =
ga(fun,2*numOfFemtocells,[],[],[],[],lb,ub,[], options_ga);

function stop = myOutput(x,optimvalues,state)
    stop = false;
    if isequal(state, 'iter')
        xval = [xval;x];
        history.x = [history.x;x];
    end
end

```

```

        history.fval = [history.fval;optimvalues.fval];
        %searchdir = [searchdir; optimvalues.searchdirection']
    end
end

close(waitbar_h);

objec_value = fun(xsol)

drawCurrentMap(handles);

save_current_position_image(handles, 'plot after optimisation.png',
2);

%final_cell_IDs = coordVectors.att_cell

create_performance_table(handles, 'table after optimisation.xlsx');

set(handles.pushbutton8, 'String', 'Run Optimisation');

set(handles.pushbutton8, 'Enable', 'on');

set(handles.pushbutton8, 'BackgroundColor', [1.0 1.0 0]);

end

function f1 = Obj_with_given_femtocell_positions(x, handles);

coordVectors = get(handles.figure1, 'UserData');

numOfFemtocells = length(coordVectors.femt_x);

if length(x) ~= 2* numOfFemtocells
    error('the provided position data are not enough');
end

coordVectors.femt_x = x(1,1:numOfFemtocells);
coordVectors.femt_y = x(1,numOfFemtocells+1:numOfFemtocells*2);

random_femto_cell_count = coordVectors.random_Femto_count;

building_ID_for_cells = coordVectors.cells_building_ID;

x_lim = coordVectors.x_lim;
y_lim = coordVectors.y_lim;

building_labels = coordVectors.buildings_count;

for i = numOfFemtocells-random_femto_cell_count+1:numOfFemtocells

    [xval,yval] = realCoordinates([x(i), x(i+numOfFemtocells)]);

    building_ID_for_cells(i) = find_building_ID_for_split(xval,
building_labels(1), x_lim, yval, building_labels(2), y_lim);

```

```
end

coordVectors.cells_building_ID = building_ID_for_cells;

set(handles.figure1, 'UserData', coordVectors);

f1 = femto_objective(handles);

drawCurrentMap(handles);

end
```

Optimisation Code

```
function varargout = optimisation(varargin)
% OPTIMISATION MATLAB code for optimisation.fig
%     OPTIMISATION, by itself, creates a new OPTIMISATION or raises
the existing
%     singleton*.
%
%     H = OPTIMISATION returns the handle to a new OPTIMISATION or
the handle to
%     the existing singleton*.
%
%     OPTIMISATION('CALLBACK',hObject,eventData,handles,...) calls
the local
%     function named CALLBACK in OPTIMISATION.M with the given input
arguments.
%
%     OPTIMISATION('Property','Value',...) creates a new OPTIMISATION
or raises the
%     existing singleton*. Starting from the left, property value
pairs are
%     applied to the GUI before optimisation_OpeningFcn gets called.
An
%     unrecognized property name or invalid value makes property
application
%     stop. All inputs are passed to optimisation_OpeningFcn via
varargin.
%
%     *See GUI Options on GUIDE's Tools menu. Choose "GUI allows
only one
%     instance to run (singleton)".
%
% See also: GUIDE, GUIDATA, GUIHANDLES

% Edit the above text to modify the response to help optimisation

% Last Modified by GUIDE v2.5 27-Dec-2020 19:41:30

% Begin initialization code - DO NOT EDIT
gui_Singleton = 1;
gui_State = struct('gui_Name',       mfilename, ...
                  'gui_Singleton',  gui_Singleton, ...
                  'gui_OpeningFcn', @optimisation_OpeningFcn, ...
                  'gui_OutputFcn',  @optimisation_OutputFcn, ...
                  'gui_LayoutFcn',  [] , ...
                  'gui_Callback',    []);
if nargin && ischar(varargin{1})
    gui_State.gui_Callback = str2func(varargin{1});
end

if nargout
    [varargout{1:nargout}] = gui_mainfcn(gui_State, varargin{:});
else
    %varargin
    gui_mainfcn(gui_State, varargin{:});
end
% End initialization code - DO NOT EDIT

% --- Executes just before optimisation is made visible.
```

```

function optimisation_OpeningFcn(hObject, eventdata, handles,
varargin)
% This function has no output args, see OutputFcn.
% hObject    handle to figure
% eventdata  reserved0 - to be defined in a future version of MATLAB
% handles    structure with handles and user data (see GUIDATA)
% varargin   command line arguments to optimisation (see VARARGIN)

axis([0 100 0 100]);

I = imread('images/building.png');

image('XData',[0 100],'YData',[0 100],'CData',I)

% Choose default command line output for optimisation
handles.output = hObject;

hObject
% Update handles structure
guidata(hObject, handles);

% This sets up the initial plot - only do when we are invisible
% so window can get raised using optimisation.
%if strcmp(get(hObject,'Visible'),'off')
%    plot(rand(5));
%end

% UIWAIT makes optimisation wait for user response (see UIRESUME)
% uiwait(handles.figure1);

% --- Outputs from this function are returned to the command line.
function varargout = optimisation_OutputFcn(hObject, eventdata,
handles)
% varargout  cell array for returning output args (see VARARGOUT);
% hObject    handle to figure
% eventdata  reserved - to be defined in a future version of MATLAB
% handles    structure with handles and user data (see GUIDATA)

% Get default command line output from handles structure
varargout{1} = handles.output;

% -----
function FileMenu_Callback(hObject, eventdata, handles)
% hObject    handle to FileMenu (see GCBO)
% eventdata  reserved - to be defined in a future version of MATLAB
% handles    structure with handles and user data (see GUIDATA)

% -----
function OpenMenuItem_Callback(hObject, eventdata, handles)
% hObject    handle to OpenMenuItem (see GCBO)
% eventdata  reserved - to be defined in a future version of MATLAB
% handles    structure with handles and user data (see GUIDATA)
file = uigetfile('*.fig');
if ~isequal(file, 0)
    open(file);

```

end

```
% -----  
function PrintMenuItem_Callback(hObject, eventdata, handles)  
% hObject    handle to PrintMenuItem (see GCBO)  
% eventdata  reserved - to be defined in a future version of MATLAB  
% handles    structure with handles and user data (see GUIDATA)  
prindlg(handles.figure1)
```

```
% -----  
function CloseMenuItem_Callback(hObject, eventdata, handles)  
% hObject    handle to CloseMenuItem (see GCBO)  
% eventdata  reserved - to be defined in a future version of MATLAB  
% handles    structure with handles and user data (see GUIDATA)  
selection = questdlg(['Close ' get(handles.figure1, 'Name') '?'], ...  
                    ['Close ' get(handles.figure1, 'Name') '...'], ...  
                    'Yes', 'No', 'Yes');  
if strcmp(selection, 'No')  
    return;  
end
```

```
delete(handles.figure1)
```

```
% --- Executes on selection change in popupmenu1.  
function popupmenu1_Callback(hObject, eventdata, handles)  
% hObject    handle to popupmenu1 (see GCBO)  
% eventdata  reserved - to be defined in a future version of MATLAB  
% handles    structure with handles and user data (see GUIDATA)  
  
% Hints: contents = get(hObject, 'String') returns popupmenu1 contents  
as cell array  
%         contents{get(hObject, 'Value')} returns selected item from  
popupmenu1
```

```
% --- Executes during object creation, after setting all properties.  
function popupmenu1_CreateFcn(hObject, eventdata, handles)  
% hObject    handle to popupmenu1 (see GCBO)  
% eventdata  reserved - to be defined in a future version of MATLAB  
% handles    empty - handles not created until after all CreateFcns  
called
```

```
% Hint: popupmenu controls usually have a white background on Windows.  
%       See ISPC and COMPUTER.  
if ispc && isequal(get(hObject, 'BackgroundColor'),  
get(0, 'defaultUiControlBackgroundColor'))  
    set(hObject, 'BackgroundColor', 'white');  
end
```

```

set(hObject, 'String', {'plot(rand(5))', 'plot(sin(1:0.01:25))',
'bar(1:.5:10)', 'plot(membrane)', 'surf(peaks)'});

% --- Executes during object creation, after setting all properties.
function axes1_CreateFcn(hObject, eventdata, handles)
% hObject    handle to axes1 (see GCBO)
% eventdata  reserved - to be defined in a future version of MATLAB
% handles    empty - handles not created until after all CreateFcns
called

% Hint: place code in OpeningFcn to populate axes1
% replace with an image of your choice
%axes(hObject, 'XLim', [0 510], 'YLim', [0 432]);
%set(hObject, 'Axes', 'axes1');
axis([0 250*2 0 216*2]);
imshow('images/macrocell1.png');
handles.axes1 = hObject;

function edit1_Callback(hObject, eventdata, handles)
% hObject    handle to edit1 (see GCBO)
% eventdata  reserved - to be defined in a future version of MATLAB
% handles    structure with handles and user data (see GUIDATA)

% Hints: get(hObject, 'String') returns contents of edit1 as text
%        str2double(get(hObject, 'String')) returns contents of edit1
as a double
normalizeInput(hObject);
%setAttachMenu(handles);

% --- Executes during object creation, after setting all properties.
function edit1_CreateFcn(hObject, eventdata, handles)
% hObject    handle to edit1 (see GCBO)
% eventdata  reserved - to be defined in a future version of MATLAB
% handles    empty - handles not created until after all CreateFcns
called

% Hint: edit controls usually have a white background on Windows.
%        See ISPC and COMPUTER.
if ispc && isequal(get(hObject, 'BackgroundColor'),
get(0, 'defaultUicontrolBackgroundColor'))
    set(hObject, 'BackgroundColor', 'white');
end
femtoObject = hObject;

```



```

% --- Executes on button press in pushbutton4.
function pushbutton4_Callback(hObject, eventdata, handles)
% hObject    handle to pushbutton4 (see GCBO)
% eventdata  reserved - to be defined in a future version of MATLAB
% handles    structure with handles and user data (see GUIDATA)
axes(handles);
%deployFemtocells();

% --- Executes on button press in pushbutton8.
function pushbutton8_Callback(hObject, eventdata, handles)
% hObject    handle to pushbutton8 (see GCBO)
% eventdata  reserved - to be defined in a future version of MATLAB
% handles    structure with handles and user data (see GUIDATA)

disable_options(handles);

if ~(strcmp(get(hObject, 'String'), 'Run Optimisation'))
    drawMap1(handles);
else
    %change_femto_user_position(handles);
    perform_optimisation(handles);
    %objec_value = femto_objective(handles)
end

function edit2_Callback(hObject, eventdata, handles)
% hObject    handle to edit2 (see GCBO)
% eventdata  reserved - to be defined in a future version of MATLAB
% handles    structure with handles and user data (see GUIDATA)

% Hints: get(hObject,'String') returns contents of edit2 as text
%        str2double(get(hObject,'String')) returns contents of edit2
as a double
normalizeInput(hObject);

% --- Executes during object creation, after setting all properties.
function edit2_CreateFcn(hObject, eventdata, handles)
% hObject    handle to edit2 (see GCBO)
% eventdata  reserved - to be defined in a future version of MATLAB
% handles    empty - handles not created until after all CreateFcns
called

% Hint: edit controls usually have a white background on Windows.
%       See ISPC and COMPUTER.
if ispc && isequal(get(hObject, 'BackgroundColor'),
get(0, 'defaultUiicontrolBackgroundColor'))
    set(hObject, 'BackgroundColor', 'white');
end

```

```

function edit3_Callback(hObject, eventdata, handles)
% hObject      handle to edit3 (see GCBO)
% eventdata    reserved - to be defined in a future version of MATLAB
% handles      structure with handles and user data (see GUIDATA)

% Hints: get(hObject,'String') returns contents of edit3 as text
%         str2double(get(hObject,'String')) returns contents of edit3
as a double
normalizeInput(hObject);

% --- Executes during object creation, after setting all properties.
function edit3_CreateFcn(hObject, eventdata, handles)
% hObject      handle to edit3 (see GCBO)
% eventdata    reserved - to be defined in a future version of MATLAB
% handles      empty - handles not created until after all CreateFcns
called

% Hint: edit controls usually have a white background on Windows.
%         See ISPC and COMPUTER.
if ispc && isequal(get(hObject,'BackgroundColor'),
get(0,'defaultUicontrolBackgroundColor'))
    set(hObject,'BackgroundColor','white');
end

% --- Executes on selection change in popupmenu4.
function popupmenu4_Callback(hObject, eventdata, handles)
% hObject      handle to popupmenu4 (see GCBO)
% eventdata    reserved - to be defined in a future version of MATLAB
% handles      structure with handles and user data (see GUIDATA)

% Hints: contents = cellstr(get(hObject,'String')) returns popupmenu4
contents as cell array
%         contents{get(hObject,'Value')} returns selected item from
popupmenu4

% --- Executes during object creation, after setting all properties.
function popupmenu4_CreateFcn(hObject, eventdata, handles)
% hObject      handle to popupmenu4 (see GCBO)
% eventdata    reserved - to be defined in a future version of MATLAB
% handles      empty - handles not created until after all CreateFcns
called

% Hint: popupmenu controls usually have a white background on Windows.
%         See ISPC and COMPUTER.
if ispc && isequal(get(hObject,'BackgroundColor'),
get(0,'defaultUicontrolBackgroundColor'))
    set(hObject,'BackgroundColor','white');
end

```

```

% --- Executes on selection change in popupmenu6.
function popupmenu6_Callback(hObject, eventdata, handles)
% hObject    handle to popupmenu6 (see GCBO)
% eventdata  reserved - to be defined in a future version of MATLAB
% handles    structure with handles and user data (see GUIDATA)

% Hints: contents = cellstr(get(hObject,'String')) returns popupmenu6
contents as cell array
%         contents{get(hObject,'Value')} returns selected item from
popupmenu6
%set(hObject, 'String',strcat(get(hObject,'Value'), 'MHz'));

% --- Executes during object creation, after setting all properties.
function popupmenu6_CreateFcn(hObject, eventdata, handles)
% hObject    handle to popupmenu6 (see GCBO)
% eventdata  reserved - to be defined in a future version of MATLAB
% handles    empty - handles not created until after all CreateFcns
called

% Hint: popupmenu controls usually have a white background on Windows.
%         See ISPC and COMPUTER.
if ispc && isequal(get(hObject,'BackgroundColor'),
get(0,'defaultUiControlBackgroundColor'))
    set(hObject,'BackgroundColor','white');
end
%fprintf(1,'%d\n', get(hObject,'Value'));
%set(hObject, 'String',strcat(get(hObject,'Value')(1), ' MHz'));

% --- Executes during object creation, after setting all properties.
function pushbutton4_CreateFcn(hObject, eventdata, handles)
% hObject    handle to pushbutton4 (see GCBO)
% eventdata  reserved - to be defined in a future version of MATLAB
% handles    empty - handles not created until after all CreateFcns
called

% --- Executes on mouse press over axes background.
function axes1_ButtonDownFcn(hObject, eventdata, handles)
% hObject    handle to axes1 (see GCBO)
% eventdata  reserved - to be defined in a future version of MATLAB
% handles    structure with handles and user data (see GUIDATA)

% --- Executes during object creation, after setting all properties.

```

```

function slider1_CreateFcn(hObject, eventdata, handles)
% hObject    handle to slider1 (see GCBO)
% eventdata  reserved - to be defined in a future version of MATLAB
% handles    empty - handles not created until after all CreateFcns
called

% Hint: slider controls usually have a light gray background.
if isequal(get(hObject,'BackgroundColor'),
get(0,'defaultUicontrolBackgroundColor'))
    set(hObject,'BackgroundColor',[.9 .9 .9]);
end

% --- Executes during object creation, after setting all properties.
function slider2_CreateFcn(hObject, eventdata, handles)
% hObject    handle to slider1 (see GCBO)
% eventdata  reserved - to be defined in a future version of MATLAB
% handles    empty - handles not created until after all CreateFcns
called

% Hint: slider controls usually have a light gray background.
if isequal(get(hObject,'BackgroundColor'),
get(0,'defaultUicontrolBackgroundColor'))
    set(hObject,'BackgroundColor',[.9 .9 .9]);
end

% --- Executes on slider movement.
function slider1_Callback(hObject, eventdata, handles)
% hObject    handle to slider1 (see GCBO)
% eventdata  reserved - to be defined in a future version of MATLAB
% handles    structure with handles and user data (see GUIDATA)

% Hints: get(hObject,'Value') returns position of slider
%         get(hObject,'Min') and get(hObject,'Max') to determine range
of slider
set(handles.text10,'String',int2str(uint16(get(hObject,'Value'))));
set(handles.text10,'Value',get(hObject,'Value'));

% --- Executes on slider movement.
function slider2_Callback(hObject, eventdata, handles)
% hObject    handle to slider2 (see GCBO)
% eventdata  reserved - to be defined in a future version of MATLAB
% handles    structure with handles and user data (see GUIDATA)

% Hints: get(hObject,'Value') returns position of slider

```

```

%         get(hObject,'Min') and get(hObject,'Max') to determine range
of slider
set(handles.text11,'String',int2str(uint16(get(hObject,'Value'))));
set(handles.text11,'Value',get(hObject,'Value'));

```

```

% --- Executes on slider movement.
function slider3_Callback(hObject, eventdata, handles)
% hObject     handle to slider3 (see GCBO)
% eventdata   reserved - to be defined in a future version of MATLAB
% handles     structure with handles and user data (see GUIDATA)

% Hints: get(hObject,'Value') returns position of slider
%         get(hObject,'Min') and get(hObject,'Max') to determine range
of slider
set(handles.text14,'String',strcat(num2str(get(hObject,'Value'),
'%.1f'), 'm'));
set(handles.text14,'Value',get(hObject,'Value'));

```

```

% --- Executes during object creation, after setting all properties.
function slider3_CreateFcn(hObject, eventdata, handles)
% hObject     handle to slider3 (see GCBO)
% eventdata   reserved - to be defined in a future version of MATLAB
% handles     empty - handles not created until after all CreateFcns
called

% Hint: slider controls usually have a light gray background.
if isequal(get(hObject,'BackgroundColor'),
get(0,'defaultUiControlBackgroundColor'))
    set(hObject,'BackgroundColor',[.9 .9 .9]);
end

```

```

% --- Executes during object creation, after setting all properties.
function text10_CreateFcn(hObject, eventdata, handles)
% hObject     handle to text10 (see GCBO)
% eventdata   reserved - to be defined in a future version of MATLAB
% handles     empty - handles not created until after all CreateFcns
called

```

```

% --- Executes on mouse motion over figure - except title and menu.
function figure1_WindowButtonMotionFcn(hObject, eventdata, handles)
% hObject     handle to figure1 (see GCBO)
% eventdata   reserved - to be defined in a future version of MATLAB
% handles     structure with handles and user data (see GUIDATA)
axis equal;
setCurrentCoordinates(handles);

```

```

function figure1_WindowButtonUpFcn(hObject, eventdata, handles)
% hObject    handle to figure1 (see GCBO)
% eventdata  reserved - to be defined in a future version of MATLAB
% handles    structure with handles and user data (see GUIDATA)
axis equal;
setCurrentCoordinates(handles);

% --- Executes on button press in radiobutton1.
function radiobutton1_Callback(hObject, eventdata, handles)
% hObject    handle to radiobutton1 (see GCBO)
% eventdata  reserved - to be defined in a future version of MATLAB
% handles    structure with handles and user data (see GUIDATA)

% Hint: get(hObject,'Value') returns toggle state of radiobutton1

% --- Executes on button press in radiobutton2.
function radiobutton2_Callback(hObject, eventdata, handles)
% hObject    handle to radiobutton2 (see GCBO)
% eventdata  reserved - to be defined in a future version of MATLAB
% handles    structure with handles and user data (see GUIDATA)

% Hint: get(hObject,'Value') returns toggle state of radiobutton2

% --- Executes during object creation, after setting all properties.
function popupmenu7_CreateFcn(hObject, eventdata, handles)
% hObject    handle to popupmenu7 (see GCBO)
% eventdata  reserved - to be defined in a future version of MATLAB
% handles    empty - handles not created until after all CreateFcns
called

% Hint: popupmenu controls usually have a white background on Windows.
%       See ISPC and COMPUTER.
if ispc && isequal(get(hObject,'BackgroundColor'),
get(0,'defaultUiControlBackgroundColor'))
    set(hObject,'BackgroundColor','white');
end

% --- Executes on selection change in popupmenu7.
function popupmenu7_Callback(hObject, eventdata, handles)
% hObject    handle to popupmenu7 (see GCBO)
% eventdata  reserved - to be defined in a future version of MATLAB

```

```

% handles      structure with handles and user data (see GUIDATA)

% Hints: contents = cellstr(get(hObject,'String')) returns popupmenu7
contents as cell array
%           contents{get(hObject,'Value')} returns selected item from
popupmenu7
if strcmp(get(handles.pushbutton8, 'String'), 'Run Simulation')
    if (get(hObject, 'Value') == 1)
        set(handles.pushbutton8, 'Enable', 'off');
    else
        set(handles.pushbutton8, 'Enable', 'on');
    end
end
end

% --- Executes on button press in togglebutton4.
function togglebutton4_Callback(hObject, eventdata, handles)
% hObject      handle to togglebutton4 (see GCBO)
% eventdata    reserved - to be defined in a future version of MATLAB
% handles      structure with handles and user data (see GUIDATA)

% Hint: get(hObject,'Value') returns toggle state of togglebutton4

% --- Executes on button press in pushbutton10.
function pushbutton10_Callback(hObject, eventdata, handles)
% hObject      handle to pushbutton10 (see GCBO)
% eventdata    reserved - to be defined in a future version of MATLAB
% handles      structure with handles and user data (see GUIDATA)
credits_display();

% --- Executes on button press in pushbutton11.
function pushbutton11_Callback(hObject, eventdata, handles)
% hObject      handle to pushbutton11 (see GCBO)
% eventdata    reserved - to be defined in a future version of MATLAB
% handles      structure with handles and user data (see GUIDATA)
delete(handles.figure1)
optimisation;

% --- Executes during object creation, after setting all properties.
function text21_CreateFcn(hObject, eventdata, handles)
% hObject      handle to text21 (see GCBO)
% eventdata    reserved - to be defined in a future version of MATLAB
% handles      empty - handles not created until after all CreateFcns
called
defaultBackground = get(0, 'defaultUicontrolBackgroundColor');
set(hObject, 'BackgroundColor', defaultBackground);

% --- Executes during object creation, after setting all properties.
function text20_CreateFcn(hObject, eventdata, handles)

```

```

% hObject      handle to text20 (see GCBO)
% eventdata    reserved - to be defined in a future version of MATLAB
% handles      empty - handles not created until after all CreateFcns
called
defaultBackground = get(0, 'defaultUicontrolBackgroundColor');
set(hObject, 'BackgroundColor', defaultBackground);

% --- Executes during object creation, after setting all properties.
function text25_CreateFcn(hObject, eventdata, handles)
% hObject      handle to text25 (see GCBO)
% eventdata    reserved - to be defined in a future version of MATLAB
% handles      empty - handles not created until after all CreateFcns
called
defaultBackground = get(0, 'defaultUicontrolBackgroundColor');
set(hObject, 'BackgroundColor', defaultBackground);

% --- Executes during object creation, after setting all properties.
function pushbutton8_CreateFcn(hObject, eventdata, handles)
% hObject      handle to pushbutton8 (see GCBO)
% eventdata    reserved - to be defined in a future version of MATLAB
% handles      empty - handles not created until after all CreateFcns
called

% --- Executes during object creation, after setting all properties.
function uipanel15_CreateFcn(hObject, eventdata, handles)
% hObject      handle to uipanel15 (see GCBO)
% eventdata    reserved - to be defined in a future version of MATLAB
% handles      empty - handles not created until after all CreateFcns
called

% --- Executes during object creation, after setting all properties.
function text3_CreateFcn(hObject, eventdata, handles)
% hObject      handle to text3 (see GCBO)
% eventdata    reserved - to be defined in a future version of MATLAB
% handles      empty - handles not created until after all CreateFcns
called

function edit6_Callback(hObject, eventdata, handles)
% hObject      handle to edit6 (see GCBO)
% eventdata    reserved - to be defined in a future version of MATLAB
% handles      structure with handles and user data (see GUIDATA)

% Hints: get(hObject, 'String') returns contents of edit6 as text
%        str2double(get(hObject, 'String')) returns contents of edit6
as a double
normalizeInput(hObject);

% --- Executes during object creation, after setting all properties.
function edit6_CreateFcn(hObject, eventdata, handles)
% hObject      handle to edit6 (see GCBO)

```



```
% eventdata reserved - to be defined in a future version of MATLAB
% handles empty - handles not created until after all CreateFcns
called

% Hint: edit controls usually have a white background on Windows.
% See ISPC and COMPUTER.
if ispc && isequal(get(hObject,'BackgroundColor'),
get(0,'defaultUicontrolBackgroundColor'))
    set(hObject,'BackgroundColor','white');
end
```